# Demountable buildings

## Maintaining structural robustness while building for demountability

Stijn Mouw

Delft University of Technology

TU Delft

# Demountable buildings

## Maintaining structural robustness while building for demountability

by

Stijn Mouw

| Student name | Student number |
|---|---|
| Stijn Mouw | 4602161 |

| | |
|---|---|
| Committee: | Ir. S. Pasterkamp |
| | Dr. F. Kavoura |
| | Ir. A. C. B. Schuurman |
| | Ir. M. Smith |
| Project Duration: | May, 2024 - June, 2024 |
| Faculty: | Faculty of Civil Engineering, Delft |

| | |
|---|---|
| Cover: | Building d(emountable): example project circularity (L. van der Wee) |
| Style: | TU Delft Report Style |

TU Delft ARCADIS

# Preface

*This thesis presents my research on maintaining structural robustness while designing for demountability. It is written as a final requirement to obtain the Master of Science degree in Civil Engineering from Delft University of Technology.*

*Throughout this research, I had the opportunity to explore the balance between structural integrity and circular construction, a topic that aligns with my interest in sustainable engineering solutions. The challenge of ensuring robustness while promoting demountability has been both complex and rewarding, allowing me to deepen my understanding of structural design principles and innovative construction methods.*

*This journey has been both challenging and fulfilling but no acadamic work is done alone, therefore, I wanna thank some people*

*First of all, I would like to thank the company Arcadis for the opportunity to graduate at a consultancy firm among many knowledgeable people. Special thanks go to my supervisor at Arcadis, ir. Meint Smith. His support and guidance during my graduation are greatly appreciated. The practical knowledge and experience he provided helped me during the moments when I was stuck in research. His sharp questions and comments to keep me on track have been very helpful.*

*I would also like to express my gratitude to my committee. First, to ir. S. (Sander) Pasterkamp, whose knowledge of construction technology and input on research questions have been valuable. Additionally, I would like to thank ir. A.C.B. (Marco) Schuurman for his expertise and practical experience. His practice-oriented approach greatly helped me determine the direction of my research and set clear boundaries. Lastly, I would like to thank Dr. F. (Florentia) Kavoura for her contributions during meetings and her knowledge of steel connections. She also assisted in finding relevant literature on the subject which really helped me in understanding the subject.*

*Lastly, I would like to thank my family, who have always supported me during my studies and beyond. My parents, whom I can always call in both good and bad times. Besides, visiting their place always makes me feel relax and reloaded me for another period of studying. I also want to thank my girlfriend, Anna, for her patience, love, and pride. Thanks to their unwavering support, I have been able to successfully complete my studies.*

*Stijn Mouw*
*Delft, March 2025*

# Summary

*The construction sector, which is generating 36% of the greenhouse gas emissions, is expected to transition to carbon neutrality by 2050 to combat climate change. Achieving this requires the use of green technology and sustainable construction practices. Demountable constructions are one such approach. Reuse of components may be a solution, although it poses challenges in maintaining structural robustness and integrity.*

*Integrating disassembly can compromise structural robustness, reducing stability and collapse resistance. Ensuring structural integrity under adverse conditions is crucial. Although much is studied in the case of individual demountable connections, a complete study of the overall behavior and strength of the building structures is lacking. Addressing this gap is vital to ensure safety, reliability, and compliance with building regulations.*

*The research begins with a literature review on structural robustness, focusing on progressive collapse and its causes, including impact loads, explosions, and initial failure effects. It includes the reasons behind progressive collapse, e.g., impact loads, explosions, and initial failure effects, as illustrated in the case examples of Ronan Point and the World Trade Center. The literature review then continues to explain Eurocodes' views on progressive collapse, for example, consequence classes and design philosophies such as redundancy, tie forces, and alternate load path analysis. The design philosophies (indirect and direct) are explained with their limit and advantage.*

*The literature review then considers the interrelation between structure circularity and construction resilience, focusing on the relevance of demountable structures for sustainability. It presents the Building Circularity Index (BCI), a tool to measure compliance with the principles of circular economy by investigating material reuse and the life cycle footprint. Furthermore, the Disassembly Index is presented as a quantitative method for evaluating the disassembly potential of buildings based on various parameters, facilitating comparisons across different designs.*

*The third section of the literature review considers the failure modes in bolted steel connections. The shear failure, bolt failure, and thread stripping failure modes are emphasized, citing calculations according to the steel code (Eurocode 3). The zip-locker effect, a sequential bolt failure process, is also cited. The chapter emphasizes maintaining structural redundancy and ductility to avert progressive collapse.*

*Subsequent sections outline the methodology for assessing the relationship between structural robustness and demountability. A model building is developed and analyzed under various accidental loading scenarios using the Arcadis Building Structural Design Tool. Different structural configurations are evaluated through unity checks to identify critical failure points.*

*Subsequently, the report highlights the method used to investigate the relationship between structural robustness and demountability in building constructions. A model building is developed to simulate and analyze structural behavior in various accidental loading scenarios. Unity checks have been performed to choose the beams in the main direction (HEB300 or HEB400) for single-span beams and continuous beams. The Eurocode rotational stiffness diagram was used to classify three types of connection: hinged, semi-rigid, or rigid.*

*Then, the structural robustness of various beam configurations has been compared. IDeaStatiCa software analyzes ductility, failure modes, and connection robustness due to point loading from a removed column. The analysis confirms column removal at an abrupt step and confirms single-span, double-span, and Gerber beam behavior. The structural response of all configurations under accidental loading is investigated by identifying critical failure points and the influence of the connection type. The results indicate that continuous beams provide 100% of the required load redistribution (350 kN in the model building used) as well as the single span beams that were rigidly connected. The flexural action works best and the catenary action is not feasible.*

*Catenary action has been shown to not contribute adequately to the resilience of demountable structures. In conventional buildings, catenary action is a predominant alternative path for loads; however, it demands relatively stiff connections and high ductility, two characteristics not widely prevalent in demountable structures. The inability to achieve long-term tension-resistant connections inhibits catenary force activation and therefore requires alternative forms of reinforcement to gain stability following a column removal event.*

*The last section of building analysis investigates the disassembly potential of the different structural configurations and their components based on the Disassembly Index. The type of connection, accessibility, independence, and geometry of the edge of the product influence the ease of disassembly. A fully demountable connection where all elements remain intact is assigned a score of 1.00, while non-demountable connections (elements are wasted and cannot be preserved) are assigned a score of 0.00. This resulted in a comparison in which single-span scenarios had a disassembly potential of 0.57, 0.39, and 0.37 for a hinged, semi-rigid, and rigid connection. The double span and Gerber beam scenarios have disassembly potentials of 0.51 and 0.53, respectively, demonstrating a better balance between robustness and reusability.*

*Demountable structures are a viable choice for sustainable construction, but the question is how to achieve the strength of a structure without sacrificing high disassembly capacity. Double-span beams provide a higher load redistribution capacity compared to single-span beams. The lowest disassembly potential (0.37) is observed in rigid single-span beams, while double-span and Gerber configurations improve disassembly potential by 38% and 44%, respectively.*

*Variation in beam span affects the disassembly and structural robustness. Shorter spans reduce bending moments and hence promote robustness, but decreases the disassembly of the structure. Since the costs of the connections in the system are now correlated with the shadow costs at the end of the building's lifespan, it can be stated that a full disassembly calculation is not necessarily required, as the costs already indicate whether a building is demountable or not.*

*Finally, it can be concluded that continuous beams, especially Gerber systems, provide the best compromise between strength and disassembly. Catenary action alone is ineffective in single-span beams, with flexural action and rigid connections offering better robustness. The study also links the disassembly potential with the environmental impact, showing that while a higher DP improves material reuse, it does not guarantee overall sustainability. However, the principle of disassembly can still be used in the design, as it influences the final shadow costs at the end of a building's design lifespan.*

*By integrating these strategies, the construction industry can achieve sustainability without compromising structural robustness, contributing to a reduced-carbon built environment.*

# Contents

# List of Figures

# List of Tables

# Nomenclature

## Abbreviations

| Abbreviation | Definition |
|---|---|
| ALP | Alternate Load Path |
| ALPA | Alternate Load Path Analysis |
| BCI | Building Circularity Index |
| CC | Consequence Class |
| CE | Circular Economy |
| CLT | Cross Laminated Timber |
| DAF | Dynamic Amplification Factor |
| DfD | Design for Deconstruction |
| DPc | Disassembly Potential of the Connection |
| DPcp | Disassembly Potential of the Composition |
| DPp | Disassembly Potential Product or Element |
| DPb | Disassembly Potential of the Building |
| ECI | Environmental Cost Indicator |
| EOL | End Of Life |
| FEA | Finite Element Analysis |
| FEM | Finite Element Method |
| GHG | Greenhouse Gas |
| PC | Precast Concrete |
| RC | Reinforced Concrete |
| SLS | Serviceability Limit State |
| TF | Tie Forces |
| ULS | Ultimate Limit State |
| VBI | VBI Hollow Core Slab |

## Symbols

| Symbol | Definition | Unit |
|---|---|---|
| $A$ | Area | [m$^2$] |
| $F$ | Force | [kN] |
| $h$ | Height | [m] |
| $I$ | Moment of Inertia | [m$^4$] |
| $L$ | Span or length | [m] |
| $st$ | Tie spacing | [m] |
| $V$ | Volume | [m$^3$] |
| $w$ | Width | [m] |
| $\alpha$ | Angle | [rad] |
| $\gamma$ | Partial safety factor | [-] |
| $\rho$ | Density | [kg/m$^3$] |
| $\sigma$ | Stress | [Pa] |
| $\phi$ | Diameter | [mm] |
| $\omega$ | Excitation frequency | [Hz] |
| $\omega_n$ | Natural frequency | [Hz] |
| $\zeta$ | Damping ratio | [-] |

| Symbol | Definition | Unit |
|---|---|---|
| $r$ | Frequency ratio | [-] |

# 1

# Introduction

This chapter presents an overview of the research context, problem, objectives, scope, and questions. It will also provide the theoretical framework and structure.

## 1.1. Research context

The building sector is a significant contributor to carbon emissions worldwide, responsible for more than a third of global emissions (Figure 1.1). New rules will transform the EU building stock into a zero-emission building stock by 2050, and from 2030, all new buildings should already be zero-emission buildings [1]. The immense environmental footprint is largely due to the widespread application of energy-intensive building materials and manufacturing, transportation, and assembly processes. Critical materials like steel and concrete, which are extensively used in buildings, are essential to contemporary structures but have high carbon intensity. Manufacturing these materials involves raw material extraction, energy use in manufacturing, and transport emissions. The embodied carbon of building materials contributes 11 percent of the world's greenhouse gas (GHG) emissions [2]. Therefore, it is crucial to reduce the usage and creation of new materials and begin reusing already available materials.

To reduce embodied carbon waste, building with a focus on demountability has gained attention in recent years. The concept of demountability facilitates the dismantling or deconstruction of a structure at the end of its life cycle for reuse, recycling, or repurposing. Demountable buildings offer benefits such as enhanced flexibility for relocation and adaptation to new uses or locations, reduced material waste, and a lower environmental impact through the reuse and recycling of building components. In addition, they offer faster construction times and potential cost savings compared to traditional building methods.

The risk of designing for demountability is that a demountable connection can lead to structural instability more quickly. Although the approach of building for disassembly can be effective for the building circularity, the removal of a column, for example, may necessitate the activation of an alternative load path, potentially causing issues. Therefore, maintaining a balance between demountability/circular constructions and structural robustness is crucial to prevent a progressive collapse.

## 1.2. Research analysis

When demountable components are included in building design, the demountability potential increases. This also equates to the fact that there is more room for more of the connections within the building to act as hinges, which would undermine the supply of a secondary load path. If there are a lot of hinges, it is simple to undermine the robustness of the building. Although wind braces and similar features can contribute to stability, the building must also resist progressive collapse. It can be difficult to do so when the connections are deliberately designed for disassembly.

It is a structural requirement to ensure structural integrity in response to accidental loads, such as an impact on a vehicle or a gas explosion. A building lacking adequate robustness may collapse like a

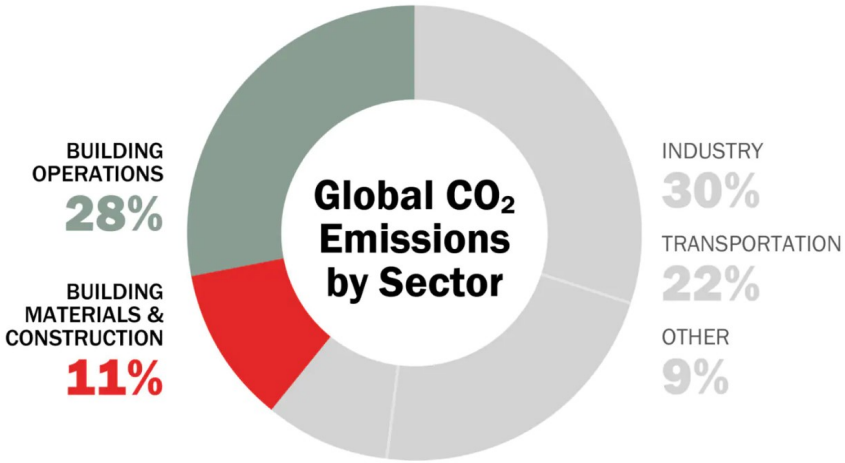


**Figure 1.1:** Contribution of the construction industry to carbon emissions [2]

house of cards; therefore, ensuring sufficient robustness is vital.

One of the key challenges in the field of demountable construction is the limited understanding of the structural behavior and robustness of such systems. Although significant research has been conducted on various demountable connections for different building materials such as timber, concrete, steel, or their composites, knowledge gaps persist. Most of the research so far has looked at creating and testing individual demountable connections. However, focusing on things like their weight and their structural performance in a system lacks some research. More research on connections and how they behave as a whole needs to be done.

It is important to understand the overall structural behavior of demountable structures to maintain their safety, reliability, and compliance with building codes and standards. A check on the strength of the structures must be made in order to identify the weaknesses and come up with strategies to prevent such unexpected occurrences.

## 1.3. Research objectives

This work investigates how robustness can be ensured while maintaining high building demountability. Its goal is to identify a strategy to ensure robustness in spite of demountability. Specifically, the research goals are:

- Develop a demountability score for various connections, assigning a demountability score between 0 and 1 for comparative analysis. Evaluate connections based on their demountability performance to identify the most efficient connection and determine which properties influence the demountability score the most.
- Investigate how the strategies outlined in Eurocode 1991-1-7 to prevent structural robustness influence the demountability of buildings with the aim of understanding their impact on disassembly possibilities.
- Analyze the structural behavior of buildings that are made for demountability. Apply accidental actions on the building to see where the critical points are. See if the critical points of the structural failure are related to the connections.
- Formulate and implement comprehensive strategies that ensure the structural integrity and robustness of buildings while simultaneously prioritizing and enhancing their demountability.

## 1.4. Research questions and outline

The main question of this report is:

*"What strategies and design principles can be employed to maintain structural robustness while aiming for a high demountability of connections in a building construction?"*

To address the main research question, a series of sub-questions were formulated and examined according to the outline presented below.

**Part I - Theoretical background**

**Chapter 2: Structural Robustness**

- *What are the primary failure mechanisms that lead to progressive collapse and how do current building codes and design standards address these risks in relation to demountability?*

**Chapter 3: Circularity**

- *Sub-question: How can the principles of the circular economy be effectively integrated into building design to enhance demountability while ensuring the necessary level of structural performance and minimizing environmental impact?*

**Chapter 4: Connection types and design standards**

- What types of connections and design standards currently exist that facilitate both structural robustness and high demountability in building construction?

**Chapter 5: Failure mechanisms**

- *What are the most common failure mechanisms in different types of connections (e.g., bolted steel connections), and how can these be mitigated through design and material selection while maintaining high demountability?*

**Part II - Building model study**

**Chapter 6: Methodology and framework for the case study**

- *How can a building model be effectively designed and used to study the interaction between structural robustness and demountability?*

**Chapter 7: Beam case studies**

- *How do different beam configurations affect the structural robustness of a building construction?*

**Chapter 8: Disassembly potential of case study situations**

- *How do different structural configurations score on disassembly and what factors influence the disassembly potential of various connection types?*

**Part III - Research outcome**

**Chapter 9: Discussion**

- *What are the key design trade-offs and interdependencies between connection types, beam configurations, structural robustness, and demountability based on the findings from the building model studies?*

**Chapter 10: Conclusion**

- *What design strategies and principles, based on the research findings, are most effective in maximizing structural robustness while simultaneously achieving high demountability of connections in building construction, and what further research is needed in this area?*

## 1.5. Research methodology

This section summarizes how the specific objectives of the study will be achieved and how the study questions will be answered. The objective of this study is to investigate the degree of interrelationship between the two concepts of demountability and structural robustness in building construction. A blended approach consisting of both qualitative and quantitative work will be used to enable adequate

comprehension and integration of all pragmatic and theoretical issues. There are several key stages of the research.

**Literature review**
There is little literature that specifically targets the robustness of modular and demountable buildings in relation to progressive collapse. There is literature on the robustness of traditional steel, concrete and timber buildings and demountable connections. To respond to the sub-questions on the interface of demountability and robustness, an attempt has been made to answer the broad question of what the existing literature on structural robustness offers. Some of these works provide answers to how progressive collapse is treated in design guides such as the Eurocodes and how robustness can be achieved in circular construction contexts.

In addition, the review of the literature focuses on the design aspects that are necessary to ensure structural integrity in demountable buildings. This includes, but is not limited to, an evaluation of specific design norms and an examination of partially collapsed structures to determine the complex systems or reinforcements that existed to render a design effective or to determine the reasons behind robust measures failing. From this, one can learn how to resolve the requirements and objectives of designing demountable connections that have both the required flexibility and strength.

**Case study**
For the purpose of acquiring high demountability and strength values, a model building is used first. A new model structure, which was developed by Arcadis, is used as a building design tool for a load bearing structure. The tool helps to form a fundamental framework, representing the proportionality of structural element sizes by performing required calculations such as load cases. With the help of this method, the study can acquire quick results. Because the topic of this research is progressive collapse, forces on various members of structures are a critical input. Input of proposed member weights into the software makes analysis easier, as it gives an immediate preview of the potential beam configurations. However, changing the span lengths and connections can also alter the beam configuration. Thus, further checks are required.

The second step focuses on analyzing the system behavior. Finite element analysis (FEA) with IDeaStatiCa will be applied at both the connection and the element levels. The software can be applied to assist in determining the structural behavior of the connections under varying loading conditions. It also provides detailed information on the ductility, failure mechanisms of different types, and overall performance of different types of connections, enhancing understanding of the robustness of the structural system. Using this FEA, structural models can be simulated to assess their response and durability through the quantification of uncontrolled loading conditions. The structural ductility and failure mechanisms in the connections are analyzed in detail to quantify their impact on structural durability.

Assessment based on the disassembly index is carried out quantitatively, taking into account the ease of disassembly of the structural building components. The Disassembly Potential (DP) scores various structural systems and connection types from 0 to 1, in which a higher value signifies more disassembly potential. The scores enable other designs to be compared on an equal basis, equally weighting demountability and resource efficiency.

For the purpose of ensuring a balanced assessment, the two parameters, disassembly potential and robustness, are combined into a list of requirements. The structural robustness is measured through the quantification of the degree to which a system resists any random loading without collapsing, and the disassembly potential is measured through the system's ability to be disassembled and reused later on. This evaluation offers awareness of correlations and trade-offs between demountability and structural robustness, and hence the possibility of finding the most effective design.

The explorations from the assessment of the robustness and disassembly potential scores have been checked against the case study building. This includes evaluating the performance of different configurations of the structures in progressive collapse and evaluating the disassembly operations. This achievement provides the basis for the design principles and strategies which would strike the desired balance.

## 1.6. Research scope

Buildings and structures are made of all kinds of materials, sizes, and shapes. Therefore, in this research, the following limits apply:

- Only office buildings will be taken into account. Residential buildings are outside the scope of this research.
- The height of the building will be limited to a minimum of 3 floors and a maximum of 15 floors.
- Only the structural part of the building will be examined. This means the floor system, the steel beams and the column.
- In this study only steel structures with a concrete core will be examined.
- The forces, outline and grid sizes of the buildings will remain the same for the all case studies to ensure a good comparison.
- The building that will be used is in 3D but the analytical calculations and modelling will be mainly done in 2D except from the IDeaStatiCa FEM models.
- The dynamic behavior of the building and the dynamic amplification factor will be beyond the scope of this research.

## 1.7. Research structure

In this section the structure of the report and the research chapters will be outlined.

**chapter 1 - Introduction**
The introduction of this report highlights the significance of the research and provides a concise problem statement. In addition, it delineates the goals and research objectives. To fulfill these objectives, it presents both primary and secondary research questions. The scope is provided to concentrate the study's focus. Finally, the research methodology describes the methods employed to collect data.

**Part I - Theoretical background**

**chapter 2 - Structural robustness**
Discusses structural robustness, its causes (impact loads, explosions, etc.), and how it is addressed in relevant building codes (Eurocodes). Analyze existing design strategies for mitigating progressive collapse, such as redundancy, tie forces, and alternate load paths. This section should highlight the challenges of balancing robustness with demountability.

**chapter 3 - Circularity**
Explore the principles of circular economy in relation to the construction industry. It defines and explains the Building Circularity Index (BCI) and the Disassembly Index, detailing their application in assessing building sustainability and ease of disassembly. Discuss the importance of demountable connections and their role in achieving circularity.

**chapter 4 - Connection types and design standards**
This section describes the development and validation of the building model used in the research. It explains the model's parameters (e.g., dimensions, materials, connection types). Justify the choice of parameters and their relevance to the research objectives. Detail the loading scenarios applied to the model and how the forces were calculated.

**chapter 5 - Failure mechanisms**
Examines common failure mechanisms in steel connections and in case of column removal. Mentioned are the bolt, welt and plate failure methods and the zip-locker effect.

**Part II - Building model**

**chapter 6 - Methodology and framework for the case study**
This part details the approach to simulate a building structure, which can be used to compare different scenarios.

**chapter 7 - Beam case studies**
This section investigates how different beam configurations behave in case of a sudden column re-

moval and how they score in terms of structural robustness. In addition, the failure mechanisms are highlighted.

**chapter 8 - Disassembly potential of case study situations**
This chapter analyzes the factors influencing the disassembly potential of various configurations. In addition, it mentions and compares the values that influence the disassembly potential.

**Part III - Research outcome**

**chapter 9 - Discussion**
Summarizes key findings, discusses the trade-offs between demountability and robustness, and explores the implications of the results.

**chapter 10 - Conclusion**
Concludes with strategies and principles for maximizing robustness while achieving high demountability. In addition, it includes recommendations for future research and the building industry.

# Part I

# Theoretical background

# 2

# Structural robustness

Progressive collapse occurs when a small localized failure in a structure triggers a chain reaction, ultimately causing the entire system to collapse. The damage spreads from one part of the structure to another, leading to a failure much larger than the initial issue. Unlike typical structural failures, which remain confined to the initial failure zone, progressive collapse spreads throughout the structure, leading to dangerous situations. Part of the chain reaction must be interrupted to prevent progressive collapse. In this chapter, possible causes for progressive collapse will be described, accidental actions in the Eurocode will be looked into, and design methods to prevent progressive collapse will be elaborated.

## 2.1. Causes of progressive collapse

A specific event always precedes the collapse of a structure or structure. This event could, for example, be a special load, material error, or design or implementation error. The chance that one of these events occurs is small, and the event itself often occurs suddenly. The consequence of the event is that local collapse may occur, after which a chain reaction occurs, and the structure collapses. The causes of collapses are explained here. These failures are typically caused by impact loads, explosions, or fires. The initiating cause is the failure of a major load-carrying element (e.g., column or beam). If one initial support element fails, the surrounding elements receive extra stress, and so on, until additional elements fail.

### 2.1.1. Impact loads

Impact loads should be taken into account when designing a building structure. When an object traveling at a specific speed collides with a structure, an impact load is created; an example can be a car or plane crashing into a column. The kinetic energy of the object that causes the impact is transformed into the deformation energy during the collision. To prevent progressive collapse, the object or structure should absorb this deformation energy.

The impact load can be categorized into two categories. A hard collision occurs when the object absorbs the deformation energy (car in the creases), while a soft collision is when the structure absorbs the impact. The structural component in a soft collision model needs to have sufficient ductility, or the ratio of maximal elastic deformation to total deformation, to allow for deformation. Large columns and walls often result in a decreasing load bearing capacity. Because colliding items tend to deform first due to the stiffer nature of structural sections, it is commonly assumed that a severe impact is necessary for safety.

### 2.1.2. Explosions

Another type of load that can cause progressive collapse is an explosion. Building explosions can occur for various reasons, but can only occur when they meet the three critical components simultaneously, often referred to as the explosion triangle Figure 2.1. The first is an ignition source, such as a flame or spark, which provides the energy that is needed to start the explosion. Secondly, there is the presence

of a combustible material, such as gas, powder, or other flammable substances. The third component is oxygen, which serves as an oxidizing agent. The Eurocode distinguishes two types of explosion: gas and dust explosions. These are described below.


**Figure 2.1:** Explosion triangle [3]

Gas explosions occur when a gas mixture, such as natural gas, comes into contact with oxygen and is ignited. The main causes of such explosions are gas leaks in homes caused by sparks or electrical appliances. However, gas leaks can cause explosions when they are hidden and create gas bubbles. Upon ignition, an explosion will occur. Incidents with gas leaks or gas stoves that are still on are rare but happen multiple times a year. Gas explosions can cause extensive damage to a building. An example is given in subsection 2.1.3.

Dust explosions are the result of the combustion of fine combustible particles, for example sawdust or flour, with air. In fact, it is caused by the accumulation of combustible dust on surfaces or in equipment. Upon being disturbed, the dust may become airborne and develop an explosive mixture. Turbulence, through examples such as the effect brought about by abrupt motions, may further distribute the particles and result in ignition. Typical examples include sawdust explosions in woodshops and flour dust explosions in bakeries.

### 2.1.3. Historic events

The initial major incident that started the need for structural robustness was at Ronan Point. This 22-story high-rise tower block in East London partially collapsed on 16 May 1968.

The catastrophe began with a gas explosion in a kitchen on the 18th floor. Although the explosion was not massive, it was strong enough to destroy the load bearing walls constructed from pre-cast concrete panels (Figure 2.2). Consequently, the southeast corner of the building progressively collapsed. The collapse resembled a domino effect, with the failure of one component precipitating the collapse of subsequent structural elements, resulting in a significant portion of the building's downfall. The design of Ronan Point used large pre-cast concrete sections that were built off-site and bolted together on-site. The failure highlighted the vulnerability of this construction method, particularly the critical role of the joints between panels. If these joints failed, as they did at Ronan Point, there was nothing to prevent progressive collapse.

The collapse of Ronan Point had a significant impact on UK building regulations. It highlighted the risks associated with large precast concrete sections and underscored the need to improve construction quality and supervision. As a result, the UK government enacted the 5th Amendment to the Building Regulations in 1970. These regulations have also been incorporated into Annex A of the Eurocode, which addresses ”Accidental Actions” [4]. They stipulate that buildings must be designed to avoid disproportionate collapse in the event of an accident. The regulations also require structural redundancy, ensuring that if one component fails, the remaining structure can support itself and avert complete collapse.

**Figure 2.2:** Progressive collapse at Ronan Point [5]

Another historic event was the progressive collapse of the World Trade Center in New York. Although they were robustly designed, progressive collapse occurred after the attack. Constructed as tube frame structures, the towers had perimeter load bearing columns on the outside acting as Vierendeel trusses (Figure 2.5f). These columns were connected with steel trusses.

An investigation by the US National Institute of Standards and Technology [6] [6] found out how the collapse could occur. When the plane crashed into the building, the heat of the fire weakened the trusses extending from the core to the facade. This forced them to deflect more than 1000 mm vertically, pulling the outer columns inward. This, in combination with a rotation of the upper part (Figure 2.3a) due to the inward-pulled columns, increased the forces on the columns even further. Eventually, the forces on the columns became so large (Figure 2.3b) they failed under buckling, leading to a progressive collapse.

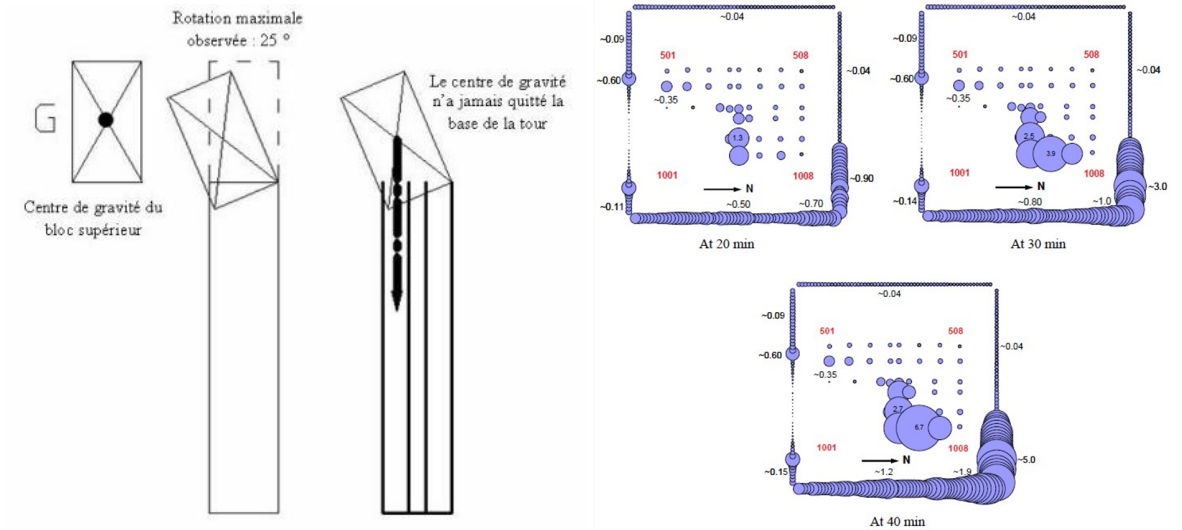


**(a)** Rotation of the top part

**(b)** Column forces 20, 30 and 40 minutes after the collapse

**Figure 2.3:** Collapse of the World Trade Center [7]

## 2.2. How to deal with progressive collapse according to the Eurocode

Standards have been established to regulate this issue to prevent progressive collapse. In the Netherlands, these standard rules are specified in the Building Decree (Bouwbesluit 2012) and the calculation standards of the Netherlands Standardization Institute (NEN).

NEN-EN 1991-1-7 [8] deals with 'general actions - accidental actions.' This includes strategies and rules for protecting structures against accidental actions such as explosions or vehicle impact. European regulations also contain relevant provisions. However, these provisions are not always clear-cut and can be subject to different interpretations by various people or institutions, and have been under discussion for quite some time. This ambiguity in interpretation can lead to the constructive coherence of structures being overlooked in design.

NEN-EN 1991-1-7+C1+A1/NB:2019 [9] is the Dutch National Annex to the Eurocode for actions on structures. It specifies the national choices from the options given in the Eurocode and sets the values for nationally determined parameters for the Netherlands. This annex ensures that construction works achieve the level of structural safety required by Dutch building regulations.

According to the code, two types of strategies can be distinguished. The first is to prevent an accidental action from happening or to reduce the action or the impact of an action. The second strategy is based on the limitation of structural collapse after an accidental action occurs.

In the Dutch code, the indicative limit for local damage in building constructions is the lesser of 100 m² or 15 % of the combined floor area of two contiguous floors Figure 2.4, resulting from the removal of any supporting column, beam, or wall. This measure is designed to ensure the structure's robustness, whether or not an extraordinary load has been considered.

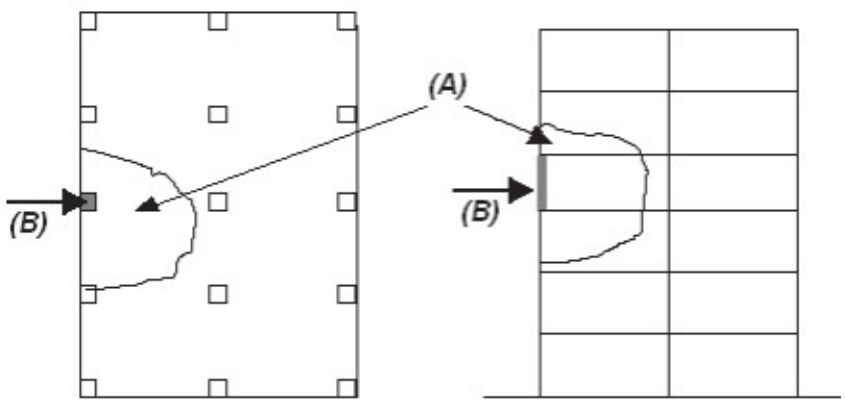


**Figure 2.4:** Recommended limit of permissible damage where (A) is the damaged area and (B) is the removed element [9]

### 2.2.1. Consequence classes

The Eurocode 1 - Actions on structures - Part 1-7: Accidental actions [8], outline the concept of "consequence classes" (CC) in the context of structural design, particularly for accidental actions. The consequence classes (CC), which are classified according to the possible consequences of structural failure, considering factors such as loss of life, injury, and economic, social, or environmental losses, are listed below.

**CC1 (Low Consequences of Failure):**

- Single occupancy houses not exceeding 4 stories
- Agricultural buildings
- Buildings that are rarely accessed by people, provided that no part of the building is located closer to another building or an area frequently accessed by people than a distance of 1.5 times the height of the building.

**CC2a (Lower Risk Group - Medium Low Consequences of Failure):**

- 5 story single occupancy houses
- Hotels not exceeding 4 stories
- Flats, apartments, and other residential buildings not exceeding 4 storeys
- Offices not exceeding 4 stories.
- Industrial buildings not exceeding 3 stories
- Retailing premises not exceeding 3 stories of less than 1,000 m2 floor area in each story
- Single-storey educational buildings
- All buildings not exceeding two stories to which the public are admitted and which contain floor areas not exceeding 2,000 m2 at each story

**CC2b (Upper Risk Group - Medium High Consequences of Failure):**

- Hotels, flats, apartments, and other residential buildings greater than 4 stories but not exceeding 15 stories
- Educational buildings greater than a single story but not exceeding 15 stories
- Retailing premises greater than 3 stories but not exceeding 15 stories
- Hospitals not exceeding 3 stories
- Offices greater than 4 stories but not exceeding 15 stories
- All buildings to which the public are admitted and which contain floor areas exceeding 2,000 m2 but not exceeding 5,000 m2 at each story
- Car parking not exceeding six stories

**CC3 (High Consequences of Failure):**

- All buildings defined above as Class 2 Lower and Upper Consequences Class that exceed the limits on area and number of stories
- All buildings to which members of the public are admitted in significant numbers
- Stadiums accommodating more than 5,000 spectators
- Buildings containing hazardous substances and/or processes

Accidental design scenarios for the various consequence classes outlined in the list above can be approached as follows.

- CC1: No specific consideration is needed for accidental actions except to comply with robustness and stability rules from EN 1990 to EN 1999.
- CC2a: Applying horizontal and vertical ties.
- CC2b: Provide an alternate load-carrying path if any supporting element fails
- CC3: Performing a systematic risk analysis in which all normal and unusual hazards are included in the analysis.

In the Dutch National Annex (NEN-EN 1990+A1+A1/C2/NB:2019, annex A1.1), the consequence class depends on the design lifetime for buildings. For a lifespan of 5 or 15 years, the calculation is based on consequence class 1 or 2, respectively. However, temporary structures, other than residential functions, with a lifespan of less than 15 years must still be designed for a minimum lifespan of 15 years for consequence classes 2 and 3 if the building type falls in that class. The class of consequences of a building, therefore, takes precedence over the lifetime of the building in the case of a reusable building.

### 2.2.2. Limitations

The Eurocodes provide general recommendations, but not specific recommendations as to how one should design against robustness. Well-established global strategies for mitigating progressive collapse, particularly for complex and high-risk structures, do currently not exist. Also, there are contradictory requirements placed on different materials; the Eurocodes have varying requirements for steel, timber, and concrete, and it becomes even more challenging in multi-material structures. Additionally,

while both ductility and redundancy are also very essential to strength, neither of these are dealt with directly under the Eurocodes. This can result in less robust structures, as these attributes are crucial to prevent progressive collapse.

## 2.3. Design methods

Several design methodologies to provide structural robustness will be described in this section. These are classified into direct and indirect design methodologies [10].

### 2.3.1. Indirect design methods

The rest of this section will discuss in more detail several design methods used to prevent or limit progressive collapse in buildings.The primary advantage of using an indirect design strategy is the speed and efficiency with which it can be implemented. A direct second-line-of-defense analysis, which involves removing each element one by one to study the impact on the structure, is a very time-consuming process. This direct method requires analyzing both the floors and the walls/columns in detail, making it impractical for many projects. Nevertheless, for unique or very large constructions, an indirect design strategy might ultimately prove to be more costly than a direct method.

#### Redundancy design

Static redundancy is the inclusion of more structural members (such as beams, columns, or braces) beyond the minimum required to support permanent and variable loads. This guarantees that if a member fails, the remaining members can still carry the load. In dynamic structures, redundancy is achieved by adding extra stiffness or damping to absorb energy from vibrations caused by winds, earthquakes, or other forces, including impact loads. Redundancy creates multiple pathways for load distribution within a structure, allowing for redistribution if one pathway fails due to damage or overload. The downside of redundancy design is the implementation of extra constructional elements. This leads to the use of extra elements and thus more material, cost, and a higher impact on the carbon footprint of the building. In addition, the implementation of more elements in a structure can lead to a higher complexity.

#### Tie Forces

Tie forces help prevent a building from collapsing progressively by redirecting loads to nearby parts of the structure. If a main load-bearing element fails, tie forces transfer the load to other parts that are still intact, stopping the collapse from spreading. This approach ensures that the structure stays stable even when some damage occurs. Continuous tying of all floor edges and all columns and walls in two perpendicular directions to the floor creates a coherent structure that should provide adequate alternative load paths (ALP). For example, if a column were to be removed, the floor ties should redistribute the column's forces. The fundamental operation of minimal tie forces is, therefore, similar to that of a catenary system [11], which will be described in Figure 2.3.2.

The application of the tie force design approach serves to improve structural integrity and reduce the likelihood of progressive collapse. This technique requires mechanical connections between structural elements to provide continuity, ductility, and ALP. By shifting loads to nearby components, tension forces are essential to prevent the progressive collapse of vertical load bearing elements. Tie forces redirect the load to intact elements in the case a primary load-bearing element fails, preventing a collapse.

The principles of the tie force design approach are integrated into European standards for structural design in EN 1991-1-7, Annex A [8]. The types of tie forces described in the Eurocode are listed below.

- **Internal tie forces:** These tie forces provide collaboration between elements and should be placed in longitudinal and transverse directions.
- **Peripheral tie forces:** These tie forces initially ensure that the loose floor slabs function as a diaphragm, effectively diverting wind loads through the floor plate to the building core. For this reason, the tie forces only need to be placed around the hollow core slabs. The tension straps should be securely anchored within the building's core structures to establish a secondary load path.
- **Vertical tie forces:** These tie forces ensure continuity in the vertical direction of the building. These tensile straps are mostly placed in the columns and in the load-bearing walls.

In annex A.5.1 of Eurocode 1: Actions on structures - Part 1-7: General actions - Accidental actions [9], the maximum tie forces are described. The formula for the internal tie forces is as given in Equation 2.1. The formula for the peripheral tie forces is as given in Equation 2.2. For load-bearing walls, different requirements regarding tie forces are applied. However, these are not considered in this study.

$$\text{Internal tie forces:} \quad H_i = 0.8(g_k + \psi q_k)s_t * L, \quad \text{or} > 75\,\text{kN} \tag{2.1}$$

$$\text{Peripheral tie forces:} \quad H_p = 0.4(g_k + \psi q_k))s_t * L, \quad \text{or} > 75\,\text{kN} \tag{2.2}$$

$$g_k \quad \text{is the characteristic permanent action, in [kN/m2]} \tag{2.3}$$

$$q_k \quad \text{is the characteristic variable action, in [kN/m2]} \tag{2.4}$$

$$s_t \quad \text{is the spacing of ties, in [m]} \tag{2.5}$$

$$L \quad \text{is the span of the tie, in [m]} \tag{2.6}$$

In NEN-EN 1992-1-1 [12], which deals with concrete structures, progressive collapse is also considered. Requirements for tie forces in the construction also apply here, but they differ from NEN-EN 1991-1-7. The tie forces in concrete structures should be as follows.

$$F_{\text{tie,int}} = 20\,\text{kN/m} \quad \text{for CC 2b and 3} \tag{2.7}$$

$$F_{\text{tie}} = \frac{(L_1 + L_2)}{2} * q_3 \leq Q_4\,\text{kN/m} \tag{2.8}$$

$$L_1, L_2 \quad \text{are the spans (in m) of the floor slabs on both sides of the beam} \tag{2.9}$$

$$q_3 = 20\,\text{kN/m} \quad \text{for CC 2b and 3} \tag{2.10}$$

$$Q_4 = 70\,\text{kN/m} \quad \text{for CC 2b and 3} \tag{2.11}$$

### 2.3.2. Direct design methods

There are three direct design methods to prevent progressive collapse. The first is to create an alternate load path analysis. If providing an ALP is not possible, critical components can be assigned as 'key elements'. The key elements must withstand a one-way pressure of 34 $\mathrm{kPa}$ ($\mathrm{kN/m^2}$) [8], based on a gas explosion [13]. The third method is segmentation; this can be utilized to inhibit the spread of collapse across the entire structure by segmenting it into isolated compartments. The alternate load path analysis will be further elaborated in the following subsection.

### Alternate load path analysis

Tie forces were previously indicated as a technique to develop a substitute load path that can be used in the event of collapse of the building and are needed in class CC2a. An Alternate Load Path Analysis (ALPA) will have to be performed for a class CC2b building. ALPAs present a system of redundancy when a failure of the principal structural element occurs (Figure 2.5). This ensures that the entire structure remains stable and does not collapse. Furthermore, ALPAs are less expensive than the conventional 'key element' method, where every load-carrying element is made to withstand an incident in specific. In ALPAs, more funds are saved. In simple terms, ALPAs create the strength of a structure against unforeseen occurrences, although encompassing random collisions or sectional breaches, but so that even when one element fails, other elements can bear the load such that the structure is still in one piece. This built-in redundancy guarantees that the structures withstand partial destruction but do not totally fail, creating an improved security feature. In contrast to the general notion of redundancy presented above in subsection 2.3.1, ALPAs also react to the particular investigation and confirmation of the performance of such redundant load paths that form the basis of the added capacity and multiple load transfer paths. Structural components such as beams, columns, and slabs must remain in sustained contact with each other to distribute forces. The most important aspect of this kind of design is probably ductility, the capacity of the materials and structural members to undergo very large deformations before failure. Ductile structures allow components to absorb energy and respond to stress without collapse. The two most important factors that have to be taken into account when designing with ductility are:

- **Selection of appropriate materials:** The use of highly ductile materials, such as steel or reinforced concrete, ensures that members of a structure can stretch and bend without fracture. Ductility assists in the absorption of energy from a sudden failure of an element.
- **Good connections designing:** Good connection design, i.e., beam-column joints, must be ensured. They must be able to resist some movement, that is, rotation or deformation upon column failure.

This emphasizes the importance of continuity in reinforcement and ductile detailing to enhance the structure's ability to develop alternative load paths. Provide guidelines for detailing connections and reinforcement to ensure that loads can be redistributed in the event of localized failure.

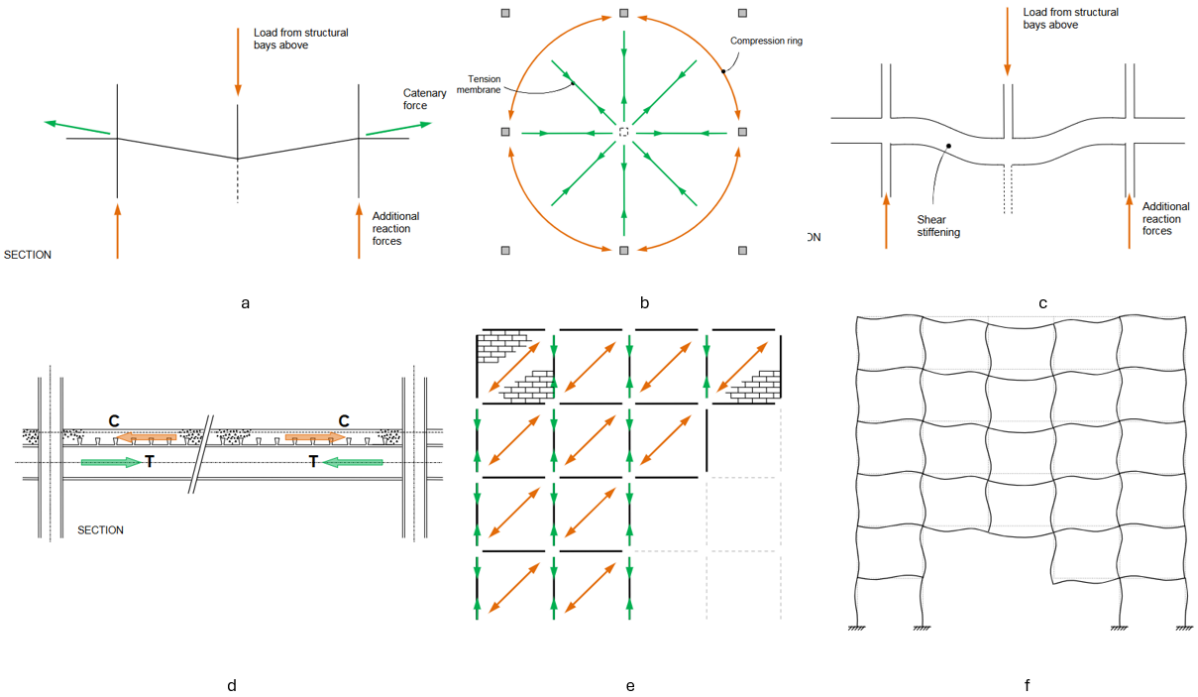


**Figure 2.5:** Alternative load paths: (a) catenary action, (b) membrane action, (c) flexural action, (d) arching action, (e) compressive strut action, and (f) Vierendeel action [14]

### Constructive cohesion

It is important to understand that structural cohesion differs from an alternative load path. Structural cohesion refers to how various parts of a building work together to form a unified and stable structure, which means that forces are evenly distributed across all parts of the building, avoiding weak spots. Each part of the structure helps to keep the whole building stable and strong. An ALP, on the other hand, is an additional or backup system in a structure that can take over if the primary load-bearing system fails. This safety measure helps prevent collapse in the event of damage to the main structural system.

### Catenary action

When a structure faces severe damage, such as the sudden removal of a column due to an explosion, the system is going to behave like a chain, better known as catenary action.

Catenary action (Figure 2.5a) describes the capacity of beams and slabs to withstand vertical loads by forming a mechanism similar to a catenary. Considering a suspended chain or cable, the natural curve it forms under its weight is called a catenary. In the same way, when a structure is compromised, undamaged elements can achieve a new state of equilibrium by forming a catenary configuration.

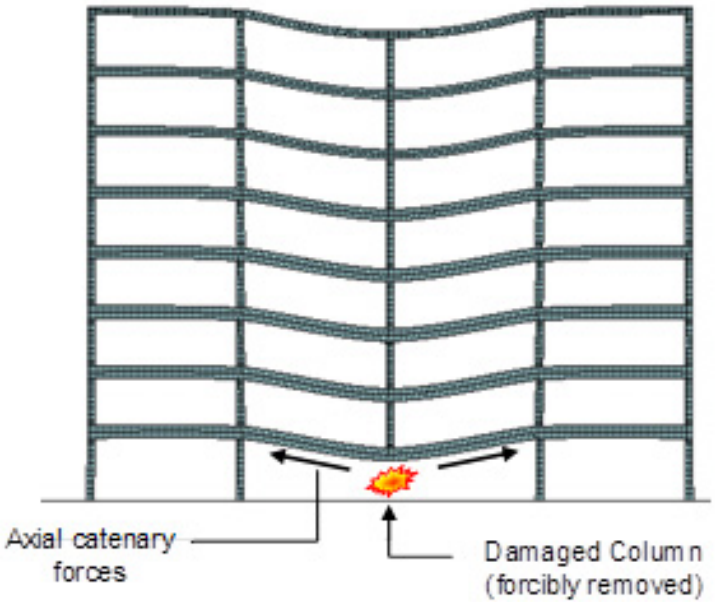


**Figure 2.6:** Catenary action due to the failure of a column[11]

As an example, a multistory building with several columns supporting the floors is given. If one of the columns fails (due to an impact load, an explosion, or fire as described in section 2.1), the load it was carrying must be redistributed to the remaining columns and beams (Figure 2.6). Subsequently, the remaining beams and slabs undergo significant deformations. These deformations allow them to form a catenary shape, which acts as a last line of defense against progressive collapse. Essentially, the structure ”hangs” from the remaining elements, transferring loads in a horizontal and vertical component (Figure 2.7). For a catenary action to occur, the joints between the structural members must exhibit high continuity and ductility. This ensures that the structure can redistribute loads effectively and maintain stability.

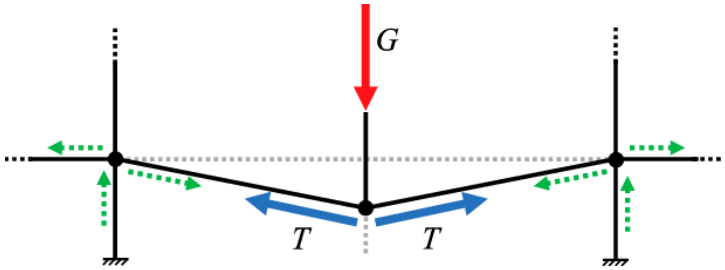


**Figure 2.7:** Force directions of catenary action due to the failure of a column, where (T) are the tie forces [15]

### 2.3.3. Ductility of connections

For structures to be not only strong but also capable of sustaining large deformations without losing much of their strength, they must be ductile. Ductility is what allows a structure to deform plastically without collapse. The capacity to deform plastically enables the structure to dissipate and absorb energy. Mathematically, ductility can be defined as the ultimate deformation to deformation in the yielding ratio. Concrete is extremely brittle and therefore not very ductile. However, once the concrete starts cracking, the reinforcing steel assumes the ductility of the reinforced concrete. Steel is more ductile by nature. This proves useful in case a column buckles because this will induce joint rotations. Such kinds of rotations can be accommodated with the help of the plasticity of the steel. Steel plastic deformation is more likely to occur in the case of an accident than elastic deformation.

## 2.4. Conclusion

This chapter has covered the structural robustness of a building structure. Progressive collapse occurs as a result of impact loads, explosions, and classic structural failures. Eurocodes were also covered, and a focus was on how they cover robustness through consequence classes, indirect and direct design methods, and ductility requirements. This information is required for this research because increasing the robustness of a building while increasing its demountability is a challenge.

# 3

# Circularity

This chapter presents the principles of the circular economy in relation to the construction industry. The Building Circularity Index (BCI) and the Disassembly Index (DI) are defined and described, elaborating on their application in evaluating building sustainability and the ease of building disassembly. The importance of demountable connections and their role in reaching circularity are also presented.

## 3.1. Building circularity index

The building and construction industry is one of the major consumers of natural resources and a significant source of environmental impacts worldwide. Building and construction activities in the European Union produce 36% (Figure 1.1) of solid waste, most of which is down-cycled at the End of Life [2]. Traditionally, buildings are designed for a singular purpose without considering disassembly and deconstruction at the EOL. Policymakers have pointed out that the building industry has to reduce resource depletion, greenhouse gas emissions, and carbon footprints. Solutions for sustainable use of construction resources are proposed here; The problems of economic, social and environmental constraints of the linear economic cycle should be changed to a Circular Economy (CE).

CE is ”an economic system that is restorative and regenerative by design and aims to keep products, components, and materials at their highest utility and value at all times” [16]. In the ’take-make-dispose’ approach, which includes waste disposal and increasing demand for new resources, CE has a different model of closing material loops. CE has been adopted as a national policy in various countries; for example, construction and building are included in the EU Circular Economy Action Plan as one of the five priority sectors. The Building Circularity Index (BCI) is an indicator developed to date to determine the level at which a building design can adhere to CE principles [17]. Some variables considered will include material reuse, possible disassembly, and the impact on the lifecycle of the construction materials applied. The BCI can be integrated into building design and assessment processes so that stakeholders can have a better view of the sustainability and circularity levels of their projects, ensuring a resource-efficient built environment.

### 3.1.1. Standards for reusing structural steel

Remelting of steel requires a lot of energy; therefore, it is much more beneficial to the environment to reuse steel elements. To link this to reasonable regulations, NTA 8713 has been created [18]. The NTA 8713 is a Dutch technical agreement dealing with the reusing of structural steel. The objective of this standard is to stimulate the reuse of steel structures so that the environmental impact of steel is minimal. The agreement describes procedures and material properties for steel elements that are retrieved from a so-called donor structure and will be reused. It also deals with the safety features of reusing the steel members and the liabilities of all parties involved.

## 3.2. Disassembly index

The disassembly index is a measurement method to determine the ease of disassembling a building or its components. This methodology was developed by the consortium of Alba Concepts, DGBC, RVO, and W/E Advisors [19] to help architects and engineers to make environmentally responsible and resource-efficient decisions.

### 3.2.1. Goal and definition

Developing the disassembly index involves reviewing practices and procedures to create a framework that includes qualitative and quantitative measures of circularity. The analysis involves the life cycle of a building, material selection, and design through construction methods, operational performance, and end-of-life management. The step in which the construction industry can be guided is a resilient and sustainable building climate with the pointing of the disassembly index. The disassembly index (DI) aims to guide the construction industry towards a more resilient and sustainable building environment.

### 3.2.2. Measurement method

A disassembly potential measuring method should indicate how much a building and its components can be disassembled. The design of a building greatly affects its disassembly potential. Process and financial guarantees must be secured for the successful development of a circular building. The disassembly of a product or a building depends on various aspects. In the technical design aspect, a decision is made on whether the products and elements can be physically dismantled. On the other hand, process-related aspects pertain to controlling the design and construction process in a way that secures the possibility of disassembly at the end of the building's life. The financial feasibility of developing and disassembling a building can be secured by the value of the product or element being greater than the cost of disassembly.

In total, 25 factors have been identified (Figure 3.1), grouped into technical, financial, and process-related aspects, all influencing the degree to which an object can be disassembled. By analysis, these factors are narrowed down to the 14 most important ones, 7 of which are technical. Although 25 factors have been identified, this report addresses only the technical disassembly potential. This explains how products and components can be physically disassembled.

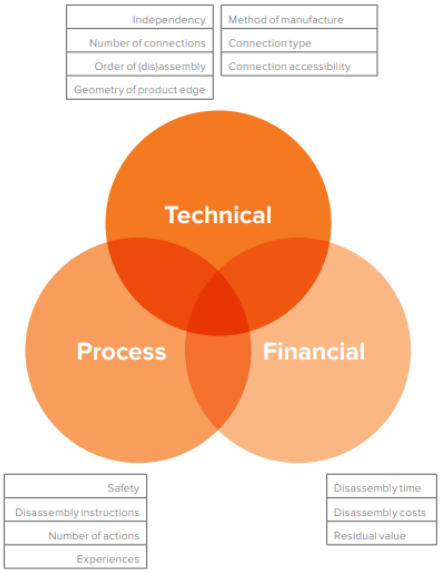


**Figure 3.1:** Overview of aspects of disassembly potential [19]

The Disassembly Potential of the Connection (DPc), is the possibility of a product or an element being disassembled at the end of a building's life, basically representing the reverse order of construction. Factors influencing DPc include the type of connection and its accessibility.

The disassembly potential of the composition (DPcp) expresses the ease of disassembling a product in interim scenarios such as renovation or repairs. Here, the independent factors are the independence and the geometry of the product's edges.

Every product or element analyzed by this measurement technique is assigned a disassembly potential based on both DPc and DPcp added together to give an overall score regarding the disassembly feasibility.

The four parameters influencing the disassembly potential of a product or component are provided below, and their arrangement can be viewed in Figure 3.2.

- Connection Type (CT): Several types of connection are used to connect the objects. When the disassembly potential is evaluated, preference is given to dry connections, connections with added elements, and direct integral connections over soft and hard chemical connections. Table D.1 elaborates on these categories, including the most widely used fasteners in the construction industry.
- Connection Accessibility (CA): The essence of the "connection accessibility" characteristic is the physical accessibility of the connecting elements and the amount of damage induced on surrounding objects in accessing them. High accessibility-where the connecting element can be reached without destroying parts of a building surrounding it increases the disassembly potential of the product (Table D.2). The accessibility assessment is similar to that of connection type.
- Independency (ID): "Independency" refers to the degree to which products or elements are intertwined or integrated (see Table D.3). Consequently, disassembly of such products or elements at the end of their useful life will involve more operations. This becomes more complicated when the life spans of the products involved are different and, thus, intermediate replacements and salvage of adjacent products or elements are required.
- Geometry of Product Edge (GPE): This factor refers to the orientation of products in an open or closed structure. It is linked to the physical boundaries or "edges" of an element or product (see Table D.4). Encasement or restriction by other objects implies consideration of the product edge geometry, which can hinder disassembly unless performed in the reverse order of assembly. What is important in this case is the geometry of the edge of a product, primarily for products contained within the structure as a single unit, in terms of accessibility, ease of maintenance, possible repair, or replacement. The interrelation of a product's shape, size, and placement within a structure determines its functionality and lifespan. Therefore, it is important to optimize and know the geometry of the edges of products to maintain proper design, usability, and sustainability of the overall system or environment.

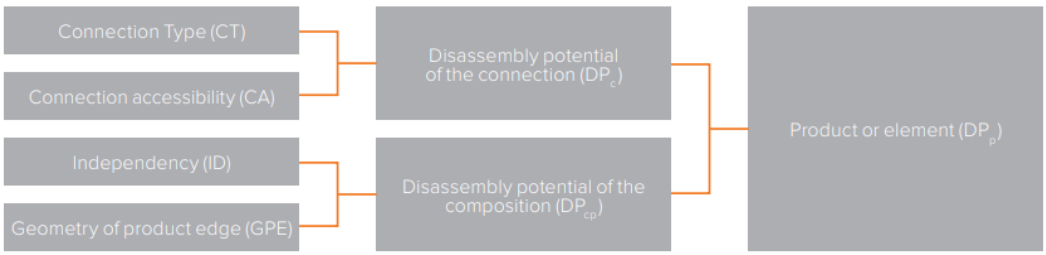


**Figure 3.2:** Step-by-step plan for assessing the disassembly potential of a product or element [19]

Although many more factors affect a building's disassembly potential, they are not considered within the measurement method. Optionally, this measurement method enables the determination of the disassembly potential per building layer. In other words, different types of products and layers (Figure 3.3) in a building can have different disassembly difficulties, offering more detailed information to users. This measurement method aims to embed the principles of disassembly potential in sustainability tools so that other buildings can be compared regarding their disassembly feasibility. This comparison is brought about by the total Disassembly Potential of the Building.


**Figure 3.3:** Disassembly potential layers [19]

## 3.3. Conclusion

This chapter on circular economy principles in construction focuses on the Building Circularity Index (BCI), the Circular Economy (CE) and the Disassembly Index (DI). It also examines the potential for the reuse of steel elements, its environmental benefits, and regulatory frameworks such as the NTA 8713 standard.

The findings in this chapter support the research since they show how important building circularity and disassembly are. It sets up the quantitative tools like BCI and DI that are used later to compare the environmental and structural impact of different types of connection.

# 4

# Connection types and design standards

This chapter addresses different types of connections in construction, such as design requirements and standards. General connection principles are addressed, with considerations for strength, stiffness, ductility, and fatigue resistance, along with special connections for floor systems and column-beam connections, together with their benefits and drawbacks.

## 4.1. Connections in general

Connections between elements are important to ensure stability, load transfer, and robustness. The following are some design considerations that should be taken into account when designing connections.

- **Strength**: The first requirement for any connection is that it must withstand applied loads without failure. This includes all types of loads, such as permanent loads, live loads, wind loads, and seismic loads. The connection must be designed to support the highest expected load with a safety factor to account for uncertainties in material properties, load estimates, and other issues. Doing so will guarantee that the connections continue to hold in normal and adverse conditions.
- **Stiffness**: The flexibility of a connection helps to establish global deflection behavior and structural stiffness throughout the world. Excessive flexibility in a connection can cause aberrant deflections with attendant impacts on performance and structural serviceability. However, overly rigid connections can cause stress concentrations.
- **Ductility**: Ductility, as in subsection 2.3.3, is defined as the extent to which a material can stretch in severe plastic deformation before breaking. In ductile connections, there is a warning of failure in the form of visible deformation, allowing intervention or repair before the connection has completely failed.
- **Fatigue Resistance**: Fatigue is a local weakening due to alternating loading and unloading. In preventing fatigue failure, expected load cycles and the magnitude of fluctuating stresses must be taken into account.

## 4.2. Connecting floor systems to beams

Two floor systems that are widely used and can act great in terms of disassembly will be discussed in this section. Among the two types considered are the hollow core slab and the steel-concrete composite floor system.

### 4.2.1. Hollow core slab floors

In the construction of buildings, a hollow core slab floor system with hollow core tends to be used due to its simplicity in installation. Concrete slabs that contain voids along their length tend to have a typical

width of 1200 mm and can be supplied in lengths up to 18 meters. The voids reduce the weight of the slab, minimize the cost of materials, and create space for services (electrical wiring and plumbing). Because they are prefabricated and can be easily installed, they are often used in buildings. The slabs are used in both domestic and office structures. Hollow core slabs have are pretensioned concrete, in which the high-strength steel bars are pretensioned prior to casting the concrete. Upon hardening of the concrete, the tension is relaxed, squeezing the concrete and giving it substantial strength.

The slabs can also act as diaphragms, which distribute lateral loads such as wind or seismic loads to vertical stabilizing elements of the building. The continuity of the hollow cores may also provide a certain degree of torsional stiffness, which generally contributes to the stability of the structure. Hollow core slabs can be produced in a wide variety of depths and spans with regard to special design needs. This flexibility allows to optimize the design for both load-bearing capacity and material efficiency. The use of these slabs can result in thinner floor profiles, allowing greater floor-to-ceiling heights or more floors within a given building height. Figure 4.1 gives an overview of an often used configuration.

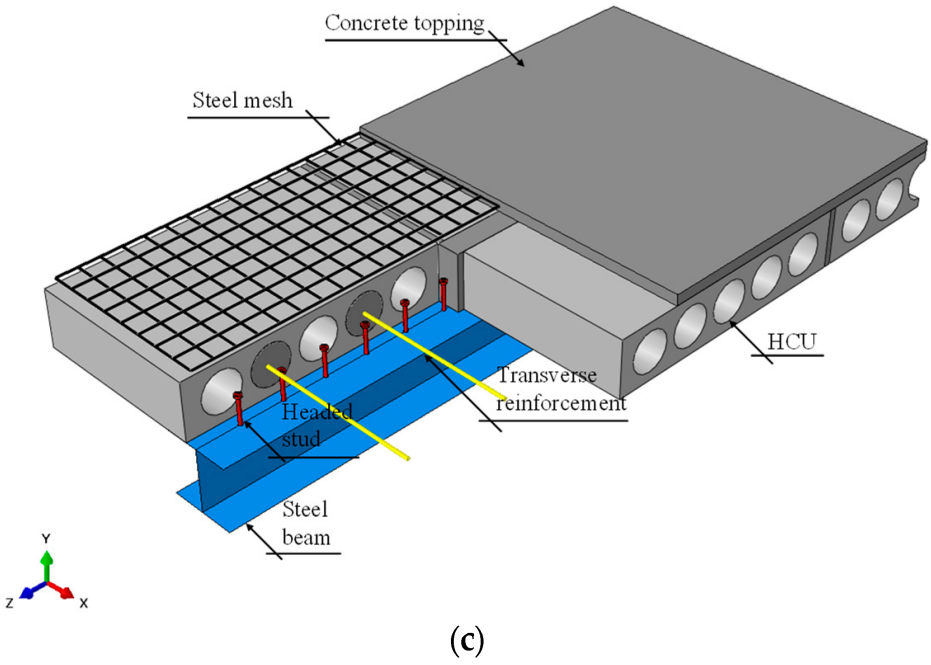


**Figure 4.1:** Steel beam to concrete hollow core slab connection [20]

### Screed floor systems without a monolithic layer

The system for hollow core slabs is widely used in buildings for residential and office purposes for some beneficial reasons. Pre-fabricated elements can speed up the process by allowing construction completion up to 7 weeks earlier than solid concrete floors, thereby facilitating faster project delivery [21]. The so called DoorStapelSysteem (DSS) allows for pre-fabricated construction without the need for edge formwork and edge beams and integrates wall and floor systems in a seamless way to improve efficiency and design flexibility. Floors are also more sustainable because they use fewer raw materials because of their air channels, do not require an additional top layer, and are reusable and able to be demountable to support sustainable building practices. In addition, less labor is required to install hollow core slab floors using the dry assembly process, making the building process safer and reducing construction costs, which promises to be economical for apartment buildings. In summary, these features make hollow core slab floors fast, durable, and cost-effective, hence quite popular in building construction.

A significant advancement in disassembly technology is the remountable floor system developed by Verband Beratender Ingenieure e.V. (VBI) [22] (Figure 4.2). A key guideline for demountable construction is to forego the use of a structural compression layer. VBI has engineered a flooring system that eliminates the need for this layer. Construction without compression layers is an essential step to

promote disassembly. The traditional reinforced compression layer, which is often used in floor construction, is eliminated. By not using a compression layer, $CO_2$ is immediately saved because the printing layer material is no longer needed. In addition, the lack of a compression layer is a prerequisite for high-quality reuse of building elements.

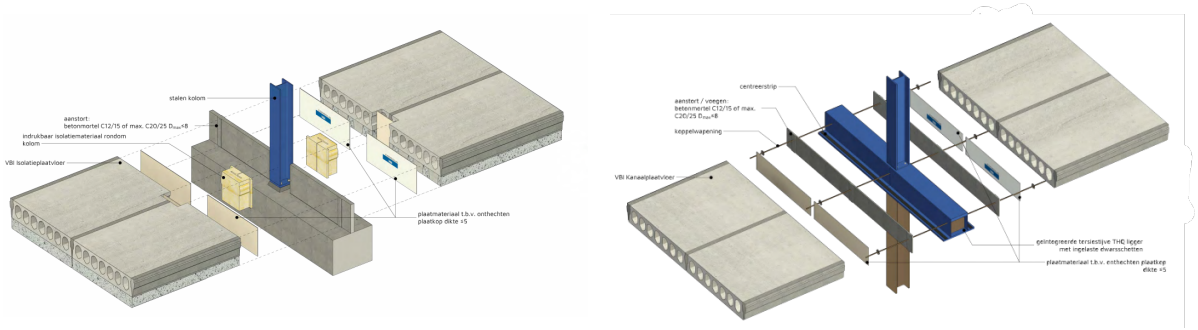


(a) Demountable floor system ground floor.

(b) Demountable floor system on a steel beam, VBI.

**Figure 4.2:** Detail demountable floor systems by VBI [22]

The primary drawback of the VBI (Vibration-Based Inspection) system is the necessity of installing tie forces. In buildings classified in CC2, tie forces must be installed in both orthogonal directions to provide an alternative load-bearing path. When a compression layer is not utilized, reinforcement can only be applied along the longitudinal axis of the hollow core slabs. Typically, reinforcement in the transverse direction is integrated within the compression layer. Consequently, an effective solution is required to facilitate horizontal force transfer perpendicular to the hollow core slabs, ensuring structural integrity and stability.

A clear distinction should be taken into account between residential buildings and non-residential buildings. These two types of building vary in several requirements in relation to structural requirements.

Residential buildings typically experience lower live loads, such as occupants, furniture, and appliances, compared to non-residential structures, which often have higher live loads due to equipment, machinery, and storage. Design considerations for residential buildings prioritize comfort, aesthetics, and functionality for occupants, while non-residential structures focus on functionality, efficient space utilization, and specialized requirements like clear spans for warehouses and column spacing for offices.

Non-residential buildings in the Netherlands, such as offices, factories, and stores, have different requirements for sound insulation. The general requirements for non-residential buildings are laid out in the Dutch building regulations and codes [23]. The codes address airborne sound transmission (such as noise from surrounding rooms) and structure borne noise (transmitted vibration through the building elements). The minimum value for wall soundproofing against airborne sound pollution in residential rooms is 52 dB.

### Compression layer

A compression layer is often applied as standard in constructions as it has various functions, such as load distribution, increasing load bearing capacity and span, improving stiffness, improving shear behavior, and sound insulation. In addition, the compression layer often serves as a finishing floor. However, a compression layer has a significant drawback. It causes the entire floor field to be cast together. As a result, the precast concrete slab cannot be disassembled without damage, thus losing its value for future reuse in new projects.

In contrast, according to experts, it is not usually necessary to have a compression layer [24]. In normal office buildings, high point loads or torsion due to uneven loading of floor areas are generally not an issue. The required disc action can often be solved by calculating the joints and adding dowels. A tension belt pressure arch system can function without a compression layer.

#### Compression layer alternative

The basis of the solution is the use of the steel structure as a tension band around the floors. This means that the steel structure acts as a kind of belt that holds the elements of the floor together. In addition to the usual steel for supporting hollow core slabs, an additional steel profile is required along the sides of the floor fields to complete the tension strip. The hollow core slabs can be secured by pouring the joints and edges. This concrete is only loaded in compression. When dismantling, the hollow-core slabs can be pulled loose, and the concrete releases again. It is important to shield the heads of the hollow core slabs to prevent a chain effect in the head joint.

### 4.2.2. Steel-Concrete Composite Floor System

In office buildings, other floor systems used are composite steel-concrete floors. These usually consist of a steel deck that serves as formwork and reinforcement, overlaid with a concrete slab. The combined action between concrete and steel provides a floor system that uses the strength of steel under tension and the strength of concrete in compression. Compared to traditional all-concrete floors, steel-concrete composite floors are lighter, easing the load on the building foundations and structural framing. The use of prefabricated steel components and concrete pouring on site reduces construction time. Since the steel deck serves as formwork, no temporary support is needed during construction.

For high structures such as skyscrapers and office buildings with multiple stories, the strength-to-weight ratio of composite floors ensures minimum dead weight while reducing the weight of the whole structure and foundation. This allows for easy construction of higher structures, thereby optimizing space. In the case of multi-unit housing such as condos and flats, composite floors translate into less sound transmission and greater fire resistance between units due to the added concrete. This results in better living conditions.

The cost effectiveness of composite structures is the result of less material cost and construction time, thus lowering the overall project costs. Composite materials enable longer unsupported spans, which reduce the number of columns and other structural elements. This results in lower material and labor costs. In addition, a better structural load distribution ensures safe performance under seismic and wind loads. Composite structures deflect and vibrate less, ensuring building stability and comfort to occupants.

#### Welded shear connectors

There are multiple solutions to connect concrete slabs to steel beams. One of the common solutions is that in composite floors, steel sheet plates (metal decking) are utilized as permanent formwork to the concrete slab. The decking carries the wet concrete and cooperates with the concrete once it has hardened to create a composite slab with load-carrying capacity. To ensure composite action between the steel decking and the concrete slab, shear connectors are used, as can be seen in Figure 4.3. These shear connections are important to ensure an effective interaction between the composite slabs and steel beams.

**Figure 4.3:** Steel composite floor deck detail [25]

### Demountable shear connectors

One of the disadvantages of composite concrete floors is that they have little potential for disassembly. The joining of steel and concrete provides a strong and durable structure, but in the process, dismantling or changing it is complex and time-consuming. This then translates into higher expenses and time when adjustments are needed.

Existing studies try to improve these connections to make them robust, durable, and more accessible, addressing issues such as ensuring consistent load transfer and simplifying construction and demolition [26] [27] [28]. One solution to provide better disassembly is to use bolted connectors instead of welded bolts. These can be combined with a steel plate underneath where the concrete is poured on site or with pre-cast plates, which are attached to the structure with demountable bolts. Examples can be found in Figure 4.4.

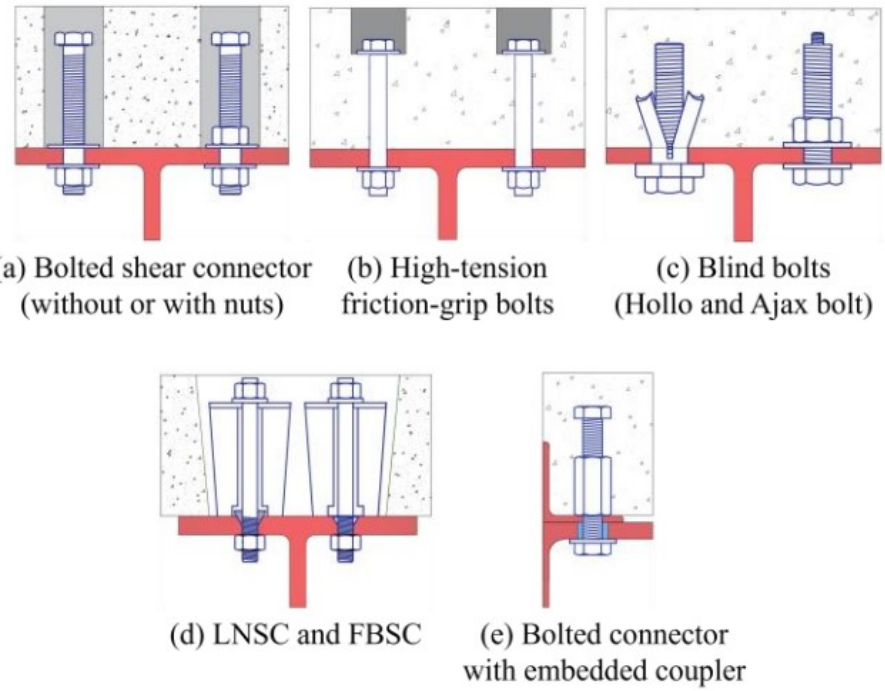


**Figure 4.4:** Schematic diagram of main demountable connectors [27]

The same principle as in Figure 4.4 can also be applied to connect steel members with timber plates or timber members [26].

## 4.3. Beam to column connections in steel

Structural integrity and stability in buildings are essential. In achieving this, the beam-to-column connection plays a very important role. They are designed to resist different types of load, including vertical forces from the weight of the building and its occupants and horizontal forces from wind or seismic activity, among other dynamic forces. Numerous research studies have been conducted on the demountability of beam-column connections. Bolted steel connections are ideal for the circular economy because they offer benefits such as improved durability, flexibility, and ease of maintenance. They are well suited for disassembly as well, as they can be assembled and dismantled with ordinary tools, making the separation of structural elements possible without any sophisticated equipment. This will save a lot of time during both assembly and disassembly, saving time in the construction process, and increasing productivity.

Unlike welded connections, which are usually permanent and not easy to dismantle without damaging them, bolted connections can be disassembled without destroying the structural members. This allows the possibility of reusing steel components in other structures, saving the need for new materials, and

supporting sustainable construction practices. Bolted connections provide great design flexibility. Not only are they modified or extended easily with new members, but the existing ones can also be reconfigured without any major structural overhauls. Another advantage of these is that bolted connections are easy to maintain. These can be inspected for wear and tear, while the bolts can easily be replaced when needed, thus making maintenance easy and accessible to further prolong the life and reliability of structures. The main characteristics of bolted connections include reliability and safety. Hence, they are quite suitable for demountable construction. Modern bolts and nuts are strong and reliable, which ensures that the connections can carry heavy loads under different environmental conditions. It is also easier to inspect the quality of the bolted connections and to ensure that at the assembly there is a higher standard of construction safety. In the final analysis, bolted connections can significantly reduce costs. Due to easier assembly and disassembly, they have lower labor costs, and in some cases, even the steel parts may be reused. Thus, they are overall cost-effective.

## 4.4. Types of bolted connections

For this research, three types of bolted connections between beams and columns will be considered. Namely hinged connections, rigid connections, and semi-rigid connections (Figure 4.5). They will be explained in detail below.

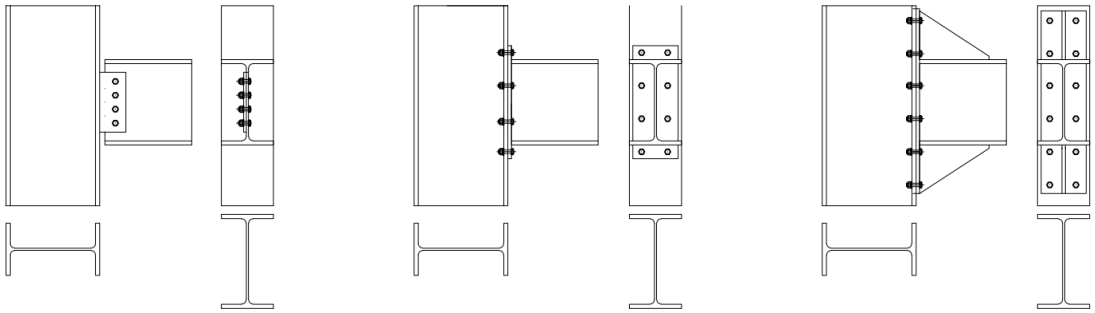

**Figure 4.5:** Three types of bolted connections: a hinged connection, a semi-rigid connection and a rigid connection

### 4.4.1. Hinged joint

Hinged connections allow rotational motion between connected members while restricting translational motion. Unlike rigid or fixed connections, which resist both moments and shear forces, hinged connections enable rotation about a defined axis without generating significant bending moments at the joint, thus making them useful in applications where flexibility or controlled motion is desired. Hinges are usually used to simplify the analysis of the structure and eliminate any internal stresses; they also offer differential movements due to changes in temperature, loading, or settlement. Allowing rotation between connected members and hinged connections can prevent any undesired stress concentrations, and hence a failure that might arise in fully fixed connections.

Another important consideration is that hinged connections are relatively more straightforward in construction and maintenance, giving them practical advantages from an engineering application point of view. Therefore, they are more economical and may be applied in structures for which resistance to lateral loads is not a major requirement. Such connections are easier to use and allow for more demountability, since they are flexible. However, they usually need more bracing or shear walls to be stable, mainly in cases where high structural performance is required. The choice of connection type is always a compromise between structural integrity, cost, design flexibility, and adaptability to future changes. Structures that allow for ease of disassembly and reconfiguration in the future may employ hinged connections, provided that the additional bracing required for stability is taken into account. On the other hand, Moment frame connections, which are more expensive and complex up-front, are generally favored over other types of connections when long-term strength and resistance to lateral loads are a concern. The two connection types will be compared to their structural behavior. This will be done using a hand calculation based on the catenary system and the forces in the structure due to the catenary and with the help of finite element modeling.

### 4.4.2. Rigid connection

Rigid connections do not provide relative rotation between connected members. Rigid connections in traditional steel structures can be made with welded or bolted connections, usually with incorporated stiffeners or moment-resistant frames. These connections cause beams and columns to function together, redistributing loads more evenly and offering more resistance to lateral loads such as wind and seismic forces. The rigid connection design must pay close attention to the load paths, the connection geometry, and the material properties to offer the required strength and stiffness. Moment frame connections are appropriate for structures that require high resistance to lateral loads. They are capable of imparting structural strength because of the existence of many load paths and high deformations. They are, however, expensive, complicated, and have increased maintenance requirements. Rigidity in moment frame connections also hinders demountability, hence future modification or dismantling will be challenging.

### 4.4.3. Semi-rigid connection

The semi-rigid connections have the peculiar characteristic of offering only partial rotational restraint, and hence are capable of transmitting some portion of the bending moments while still allowing for a slight rotation. In actual practice, semi-rigid connections represent the middle ground sought after strength and flexibility. They are commonly used in structural designs that benefit from flexibility, such as frameworks designed to absorb dynamic loads or to allow differential movements without loss of overall stability. Implementations could be, among others, partially restrained bolted or welded joints, in which the connection details are well thought out and engineered to attain the desired level of stiffness. The application of semi-rigid connections demands a more sophisticated method of structural analysis and design. The unique properties of the connections, like their stiffness and moment-rotation curves, need to be considered to provide a good prediction of the behavior of the structure. Semi-rigid connections have been very slowly gaining recognition for the optimization of material use, improvement in structural resilience, and finding their place as an integral part of modern steel structure design. In developing effective, flexible, and resilient steel structures, knowledge of the principles and applications of semi-rigid connections becomes more important.

### 4.4.4. Joint classification

In steel constructions, a fully hinged connection is rarely realized in practice because it is difficult to make a connection that does not offer any resistance to rotation. Although a hinged joint theoretically allows unlimited rotation without any resistance (which is often assumed to be an ideal situation in calculations), in reality, this is difficult to achieve due to the properties of the materials and the way connections are made.

In contrast, a steel bolted connection will behave as a nonlinear rotational spring due to the interaction between various elements of the connection, including bolts, plates, and friction between contacting surfaces. This behavior is often seen in beam-column connections, where the connection resists rotation by both elastic and plastic deformation and friction and slip between the elements.

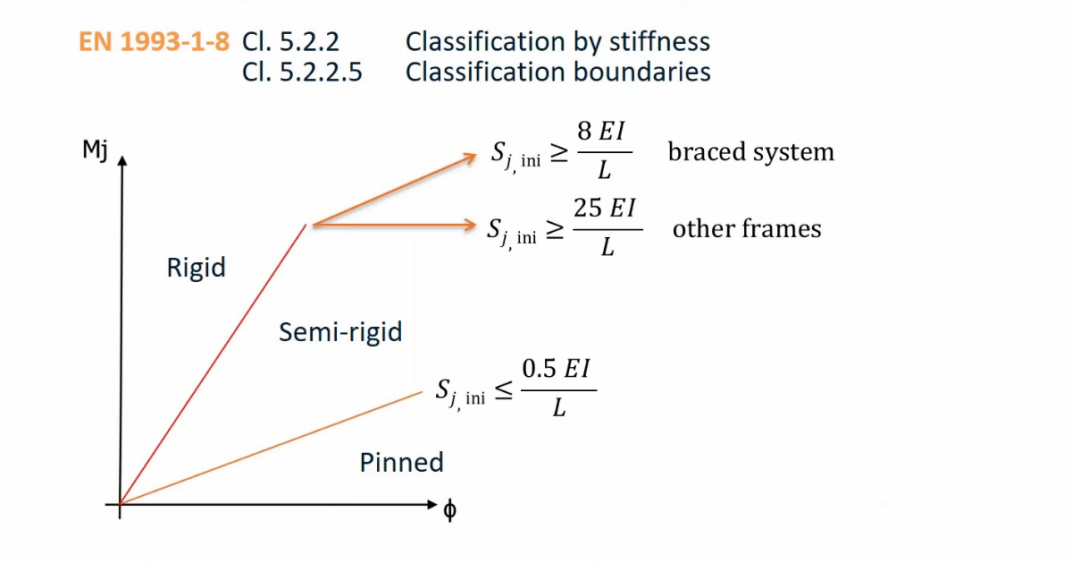


**Figure 4.6:** Type of connection based on the rotational stiffness curve [29]

The classification of joints is based on the initial stiffness of the joint ($S_{j,ini}$), the theoretical length of the analyzed member ($L_b$), Young's modulus of elasticity ($E$), and the moment of inertia of the analyzed member ($I_b$) [30]. This is also visualized in Figure 4.6.

Rigid joints have an insignificant change in the original angles between members. They are defined by the following conditions:

$$\frac{S_{j,ini}L_b}{EI_b} \geq k_b \tag{4.1}$$

Where $k_b$ is a constant that depends on the bracing system:

- $k_b = 8$ for frames where the bracing system reduces horizontal displacement by at least 80%.
- $k_b = 25$ for other frames.

Semi-rigid joints provide a dependable and known degree of flexural restraint. They are defined by:

$$0.5 < \frac{S_{j,ini}L_b}{EI_b} < k_b \tag{4.2}$$

Pinned joints do not develop bending moments and are defined by:

$$\frac{S_{j,ini}L_b}{EI_b} \leq 0.5 \tag{4.3}$$

Parameters:

- $S_{j,ini}$: Initial stiffness of the joint.
- $L_b$: Theoretical length of the analyzed member.
- $E$: Young's modulus of elasticity.
- $I_b$: Moment of inertia of the analyzed member.
- $k_b$: Constant based on the bracing system.

## 4.5. Connecting steel columns to the foundation

A solution to connect the steel column to the foundation is the common base plate method. This is a base plate fixed to the bottom of the steel column; then, this plate is anchored to the concrete foundation with anchor bolts or some other kind of fastener (Figure 4.7a). This technology is widely used in construction because it more efficiently distributes forces in a steel column, spreading them to a larger area at the base of the column. The pressure that passes through the concrete foundation is less than that allowed, which protects it from damage or failure. Among the benefits associated with using a base plate is the simplicity in installing and implementing a column. The base plate may also be prefabricated and welded directly to the steel column. The flexibility imparted by the anchor bolts allows for perfectly leveled and positioned steel columns when installation occurs. Another big advantage is strength and stability. The way the base plate helps distribute the load is to avoid any form of concentrated stress points, which may result in cracking or any other kind of damage to the concrete foundation [31]. The result is a strong and durable connection that will support heavy loads and most environmental conditions. The connection of the steel column to the concrete foundation can be hinged, stiff, or flexible, depending on the design requirements (Figure 4.7b).

The base plate method also has some drawbacks. One of them is that it must be manufactured and aligned with the anchor bolts with a high degree of precision, otherwise misalignment will result. Secondly, the base plate method can have a greater susceptibility to corrosion, particularly in environments of high humidity or chemicals. The risk can be minimized with proper protection, e.g., galvanizing or the use of special corrosion-resistant coatings.

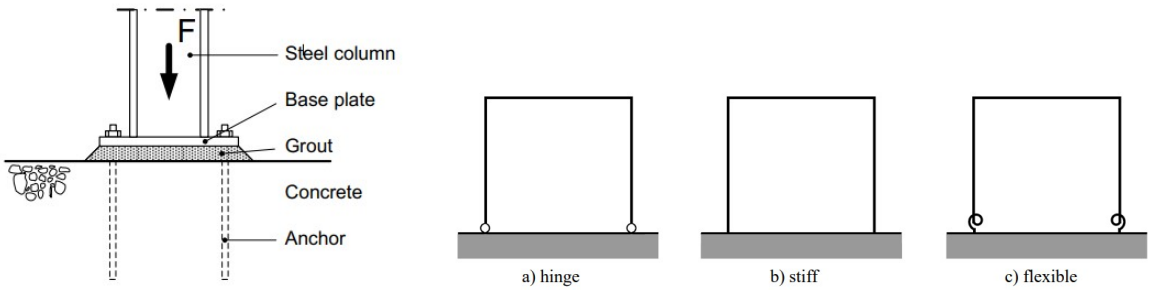


**(a)** Typical detail of a column base plate connection **(b)** Possibilities for the schematization of the connection

**Figure 4.7:** Column base plate connections [32]

## 4.6. Conclusion

Steel structures are more simple to disassemble naturally than concrete in several key ways. First, it is simple to weld or bolt the separate component steel pieces together, so construction and deconstruction can be simple, without any of the materials getting damaged; thus, the steel pieces can be recycled for use in another project, therefore avoiding waste and improving sustainability. In addition, steel has a favorable strength-to-weight ratio and structural members are easy to transport and maneuver when dismantling. In contrast to concrete, which can need to be demolished in the demolition process, steel structures can be easily dismantled without affecting the integrity of the components. The above considerations make steel the preferred material when flexibility, reusability, and sustainability are the priorities.

# 5

# Failure mechanisms of steel connections

Common failure modes of steel joints and column removal are addressed in this chapter. Specific failure modes such as bolt failure, weld failure, and plate failure, along with the zip-locker effect, are explained.

## 5.1. Steel bolted connection

Although steel bolted connections are used in construction, various failure mechanisms can take place in such connections. Some of these failure mechanisms are summarized in Table 5.1 below. For a better and more reliable structure design, the possibility of a number of failure mechanisms in the bolted connection must be considered.

| Failure Mechanism | Description |
|---|---|
| **Slip** | Occurs when the connection is subject to shear forces, and friction in a preloaded bolt connection is insufficient to prevent movement. |
| **Bolt Shear Failure** | Happens when the shear force exceeds the bolt's shear resistance, causing the bolt to fail. |
| **Bolt Tension Failure** | Occurs when tensile forces exceed the bolt's tensile resistance, leading to fracture. |
| **Bearing Failure** | Takes place when high bearing stress between the bolt and the plate results in local yielding or deformation. |
| **Block Shear Failure** | Involves a combination of shear and tension failure in the plate material surrounding the bolt holes. |
| **Net Section Fracture** | Happens when the net cross-section of the plate at the bolt holes fails in tension. |
| **Plate Yielding** | Occurs when excessive stress causes plastic deformation in the plate, leading to loss of strength. |
| **Plate Rupture** | Failure due to excessive tension in the plate, particularly near bolt holes. |
| **Prying Action** | Additional forces develop due to bending of the plate in bolted connections, increasing bolt tension and potentially leading to failure. |
| **Corrosion and Environmental Degradation** | Long-term exposure to environmental conditions can weaken bolts and plates, reducing structural integrity. |

**Table 5.1:** Failure mechanisms in steel bolt connections according to NEN-EN 1993 [33]

**Design strength of the bolt in tension**:
The design strength $F_{\text{Rd}}$ of the bolt is determined by the tensile strength $f_u$ and a partial safety factor $\gamma_{M2}$.

$$F_{\text{Rd}} = \frac{f_u \cdot A}{\gamma_{M2}} \tag{5.1}$$

**Design strength of the bolt in shear**:
The design strength $V_{\text{Rd}}$ of the bolt is determined by the shear strength $f_v$ and a partial safety factor $\gamma_{M2}$.

$$V_{\text{Rd}} = \frac{f_v \cdot A}{\gamma_{M2}} \tag{5.2}$$

The ultimate strength of a bolt is higher than the design strength of the bolt. During any accidental occurrence, it is necessary to understand what load a bolt can withstand. The ultimate strength is not the same as the design strength. For the M20 bolt, the ultimate shearing load would be approximately 200 kN [34] based on how much the threaded section sticks out on the plates. The calculated shear force according to the code is 117.6 kN Equation 6.45.

## 5.2. Zip-locker effect

The "zip-locker effect" is a critical phenomenon in bolted steel connections. This failure mechanism resembles the action of a zipper, where a crack rapidly propagates along the line of bolts due to the stress concentration around the bolt holes. As one bolt hole fails, the load shifts to neighboring bolts, escalating their stress and potentially triggering a chain reaction of failures. Research [35] and [36] indicates that the maximum vertical force of a connection is achieved when the first bolt fails. Though this force is then reached multiple times, it never goes beyond the initial force, yet displacement on the vertical plane and angular deflection do occur.

The zip-locker effect is a phenomenon that occurs under extreme loading conditions and is indicated by two distinct phases of resisting load: the flexural action and the catenary action. In the initial stage, the joint resists the load primarily due to resistance against the bending moment, and the bolts and plates transmit the force. With an increase in the load, the bolt is also subjected to higher stress, leading to the failure of the most heavily loaded bolt. This failure loads the other bolts, further loading them and producing a chain of sequential bolt failures. Now, the flexural action becomes a catenary action as the growing number of bolts starts to fail, as can be seen in Figure 5.1. At this point, the remaining bolts and plates begin to behave like a hanging chain, where the load is carried predominantly by tensile forces rather than bending. As can be seen in the figure, the load is at its maximum when the first bolt fractures. The deformation will still increase, but the forces that can be taken up by the system do not improve in this particular case.

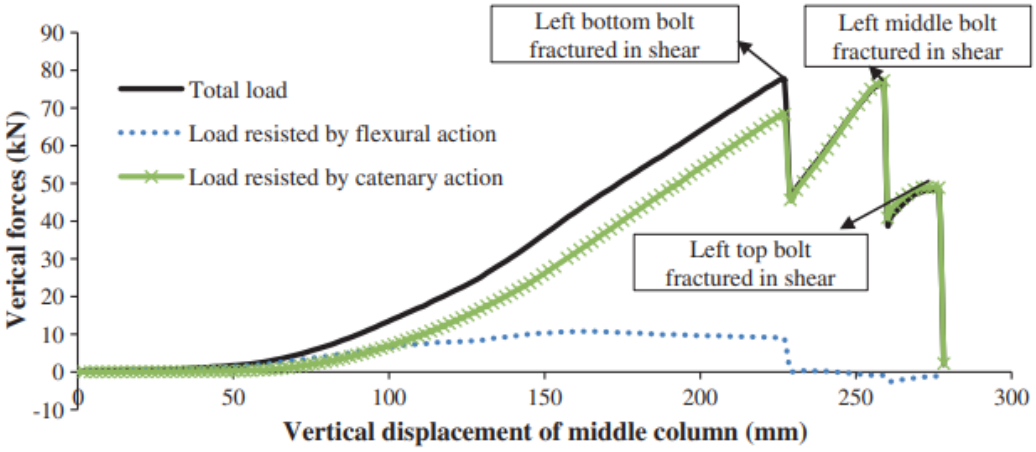


**Figure 5.1:** Maximum load on a test configuration. Single spans and finplate shear connectors are used. [36]

As said, the resistance of the connection can be divided into two stages (Figure 5.3): resistance when catenary action is initiated ($F_c$) and the ultimate resistance of the connection ($F_u$). The distinction between a load resisted by catenary action and a load resisted by flexural action is in the mechanisms and conditions under which they operate [36]. The flexural action, or bending action, is the process by which a beam or a slab bends under loading. The resistance of the material to bending moments is the main resistance. The beam or slab curves when it deforms in flexural action. This kind of behavior is most typical in the early stages of loading, where the structure is elastic and the load is resisted by the bending strength of the material.

If a connection has a higher bending stiffness, it will take longer for the catenary action to be activated, and the flexural action will take longer. In that case, the delta y in Figure 5.3 will shift further to the right, and the Fc (force where the catenary action is activated) will move further upward. In catenary action, the structure significantly deforms and the load is carried through axial tension rather than bending. This action is mobilized when the structure experiences large displacements and the flexural capacity is exceeded.

$$F_c = \sum \frac{4M_p}{L} \quad \text{(see Figure 5.2)} \tag{5.3}$$

$$F_u = \sin(\theta_u) \times \min\left(\sum f_y(A_{st} + A_{fl}), \sum f_{y,w}(A_{st,w} + A_{fl,w})\right) \tag{5.4}$$

$$\delta_c = L \times \tan(\theta_c) \tag{5.5}$$

$$\delta_u = L \times \tan(\theta_u) \tag{5.6}$$

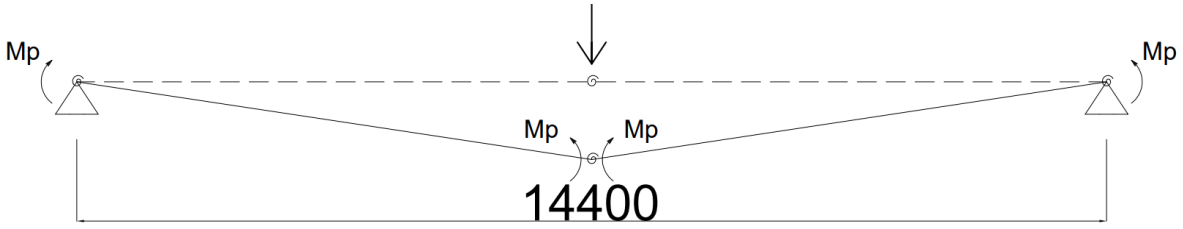


**Figure 5.2:** Moments action on the beam configuration

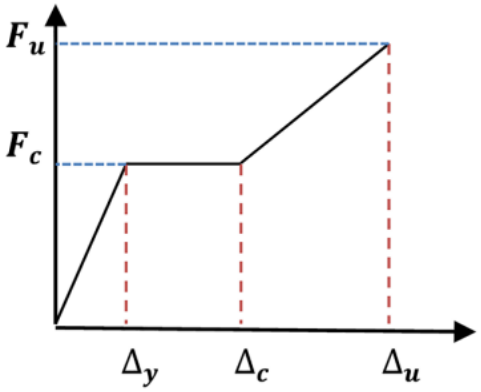


**Figure 5.3:** Load versus deflection simplified [36]

## 5.3. Ultimate strain of steel

Another failure mechanism occurs when the ultimate limit strain has been reached and a steel element is fractured. The ultimate limit strain is the maximum strain value that a material can withstand before failure. In the context of an accidental limit state, the ultimate limit strain has to be clearly understood so that the failure of steel beams can be predicted accurately. The ultimate limit strain for structural steel usually falls between 10% and 30% as can be seen in Figure 5.4, depending on the specific steel grade and conditions. The maximum strain used in the report will be set to 15%.

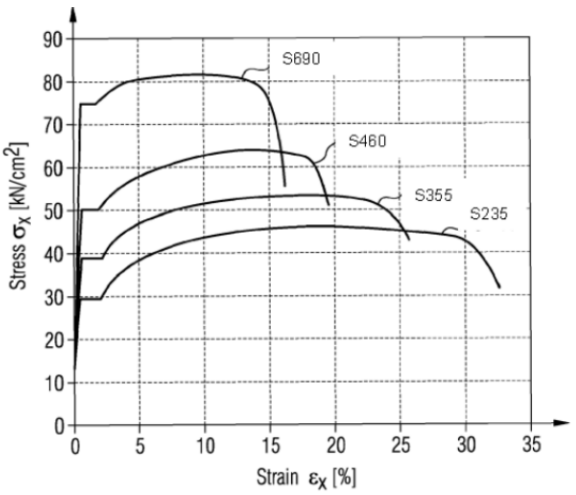


**Figure 5.4:** Stress strain curve steel for multiple steel classes [37]

## 5.4. Conclusion

This chapter discusses the most critical failure mechanisms in steel connections. All of these mechanisms must be understood when designing strong and trustworthy structures. The zip lock effect and the ultimate steel strain were also discussed, with a focus on the importance of sequential failure of the bolts and the limitation of the material to avoid fractures. Ensuring that there are robust connections that can hold loads and conditions of different types is vital to the strength and versatility of steel structures.

# Part II

# Building model study

# 6

# Methodology and framework for the case study

This chapter describes the development and validation of the building model used in the research. The model parameters, such as dimensions, materials, and connection types, are explained, with justification provided for their relevance to the research objectives. The loading scenarios applied to the model and the methods used to calculate the forces are also detailed.

This chapter details the approach to simulating a building structure for comparative analysis of different scenarios. The framework for testing various cases is outlined, and the methodology applied in this research is explained.

Three cases are considered to quantify how structural robustness can be achieved. These will be distinguished by the connection's location and the beam's length (single-span or continuous). Accordingly, three failure mechanisms will be applied to the building. These failure mechanisms are the removal of a corner column, the removal of an interior column, or the removal of a column in the facade. This is displayed in Figure 6.2 below.

The general grid size that will be used for all buildings is displayed in Figure 6.1. The heart-to-heart distance is set to be 7.2 meters. The columns' height that will be considered will be set to 3.6 meters.

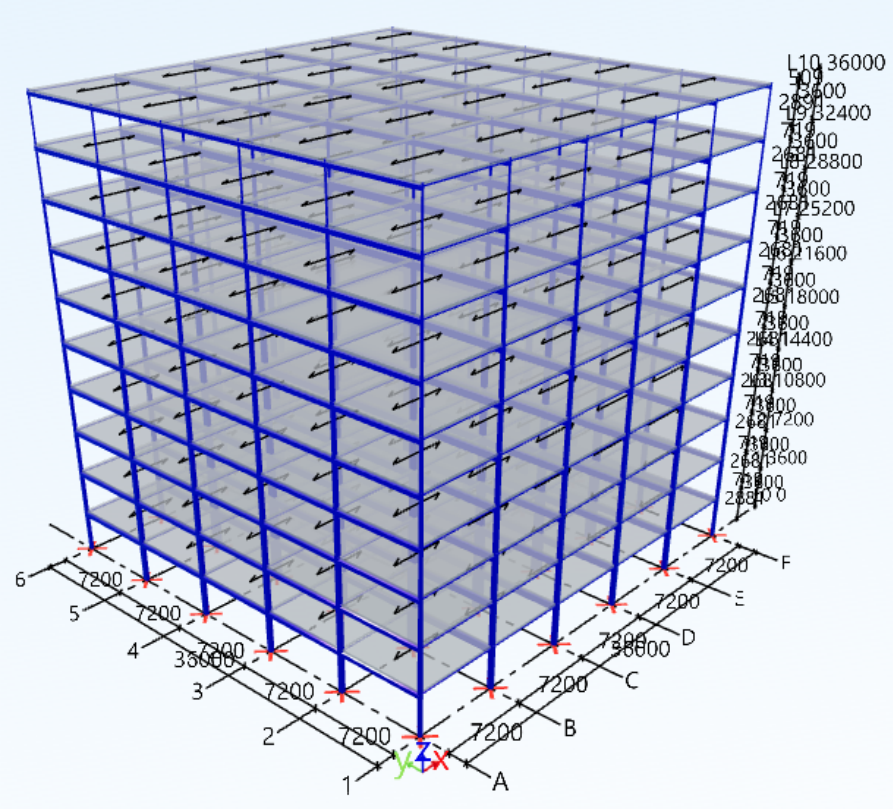


**Figure 6.1:** Model building layout

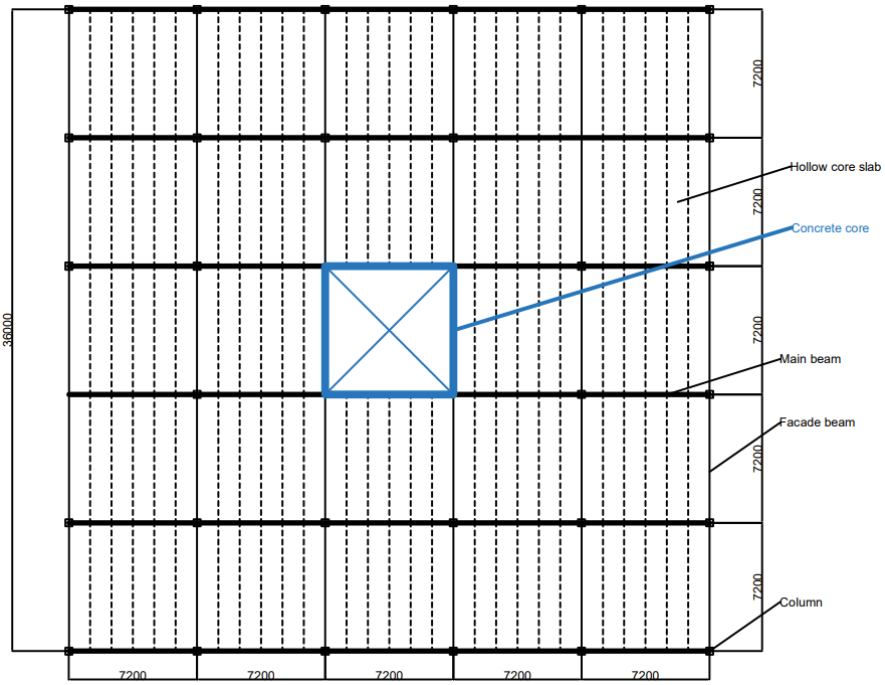


**Figure 6.2:** Floorplan of the building

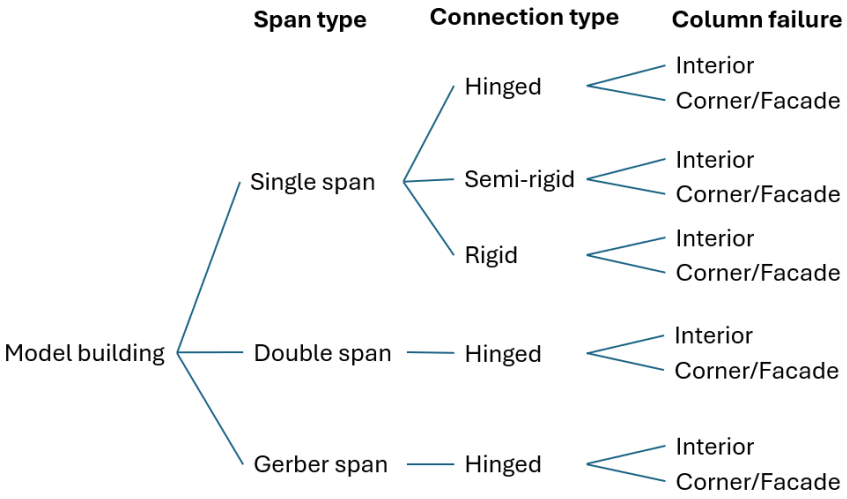


**Figure 6.3:** Possible layouts and column failure scenarios

| Scenario | Description |
|---|---|
| **1a** | **Single span, 7.2 m per beam, Hinged**: The beam-column connections are hinged, meaning they allow rotation and do not resist moments. The structure primarily resists loads through axial and shear forces, with minimal moments at the connections. |
| **1b** | **Single span, 7.2 m per beam, Semi-rigid**: The beam-column connections provide partial resistance to rotation, meaning the structure experiences a combination of axial forces, shear forces, and moments. Some moments are resisted at the connections, offering moderate rotational flexibility. |
| **1c** | **Single span, 7.2 m per beam, Rigid**: The beam-column connections are fully rigid, resisting rotation and transferring moments. The structure resists loads through axial forces, shear forces, and moments, with minimal rotational flexibility at the connections. |
| **2** | **Double Span, 14.4 m per beam**: Similar to the single-span cases, but with continuous beams spanning two columns instead of individual beams per span. This configuration allows for load redistribution and different moment behavior. |
| **3** | **Gerber Span**: This setup includes beams extending from the moment-zero point of a clamped beam, minimizing moments in the connections. The figure below illustrates the moment distribution in a clamped beam. |

**Table 6.1:** Description of building scenarios

## 6.1. Forces on the Structure

The forces that act on the building must be analyzed before a structural analysis can be performed. Both permanent and variable loads are considered. Since the forces vary with the height of the building, all three scenarios will involve a 10-story office building. The forces in the lowest layer are the most significant, which is why the forces in these elements are examined.

The permanent forces considered include the load of the structural elements and the finishing. The variable loads acting on the structure are live loads, snow loads, and wind loads. Wind load varies with building height. For reference, the city of Rotterdam will be used.

| Permanent Load | |
|---|---|
| Floor load | $G_k$ = 3.08 [kN/m$^2$] |
| Compression layer | $G_k$ = 1.2 [kN/m$^2$] |
| Total | $G_{k,tot}$ = 4.28 [kN/m$^2$] |
| **Variable Load** | |
| Live load | $Q_{k1}$ = 4 [kN/m$^2$] ($\Psi$1 = 0.5) |
| Snow load | $Q_{k2}$ = 0.56 [kN/m$^2$] ($\Psi$2 = 0.0) |
| Wind load | $Q_{k3}$ = 1.0 [kN/m$^2$] ($\Psi$2 = 0.0) |

**Table 6.2:** Loads on the structure

**Serviceability Limit State (SLS)**
Here, the calculations for the loads in case of the SLS are given.

$$\text{Permanent floor load } (G_d) = \#\text{floors} \times \gamma_G \times G_{k,tot} \tag{6.1}$$
$$= 1.0 \times (4.28) \tag{6.2}$$
$$= 4.28 \text{ kN/m}^2 \tag{6.3}$$

$$\text{Variable live load } (Q_d) = \gamma_Q \times Q_{k1} \tag{6.4}$$
$$= 1.0 \times 4 \tag{6.5}$$
$$= 4 \text{ kN/m}^2 \tag{6.6}$$

$$\text{Total Load on Column} = A \times (G_d + Q_d) \tag{6.7}$$
$$= 7.2^2 \times (4.28 + 4) \tag{6.8}$$
$$= 429 \text{ kN} \tag{6.9}$$

$$\text{Load per meter } (G_d) = \#\text{floors} \times \gamma_G \times G_{k,tot} \tag{6.10}$$
$$= 7.2 \times 1.0 \times (4.28 + 4) \tag{6.11}$$
$$= 59.6 \text{ kN/m}^2 \tag{6.12}$$

Based on the forces on the structure, the Unity check can be determined. The results for the unity checks can be found in Table 6.3 and the calculations can be found in Appendix A.

**Ultimate Limit State (ULS)**
Here, the calculations for the loads are given in the case of the ULS.

$$\text{Permanent floor load } (G_d) = \gamma_G \times G_{k,tot} \tag{6.13}$$
$$= 1.35 \times 4.28 \tag{6.14}$$
$$= 5.8 \text{ kN/m}^2 \tag{6.15}$$

$$\text{Variable live load } (Q_d) = \gamma_Q \times Q_{k1} \tag{6.16}$$
$$= 1.5 \times 4 \tag{6.17}$$
$$= 6 \text{ kN/m}^2 \tag{6.18}$$

$$\begin{aligned}\text{Total Load on Column} &= A \times (G_\text{d} + Q_\text{d}) \\ &= 7.2^2 \times (5.778 + 6) \\ &= 611 \text{ kN}\end{aligned}$$

$$\text{Load per meter} = \text{Width} \times (G_\text{d} + Q_\text{d}) \tag{6.19}$$
$$= 7.2 \text{ m} \times (5.8 + 6) \tag{6.20}$$
$$= 85 \text{ kN/m} \tag{6.21}$$

Based on the loads on the beams, the Unity Checks can be determined for both the SLS and the ULS. The results of the Unity Check can be found in Table 6.3 and the calculations can be found in Appendix A.

| Beam Type | Scenario | SLS Unity Check | ULS Unity Check |
|---|---|---|---|
| HEB400 | Single span, hinged | 0.816 | 0.580 |
| HEB300 | Single span, hinged | 1.054 | 0.745 |
| HEB400 | Single span, semi-rigid | 0.679 | 0.484 |
| HEB300 | Single span, semi-rigid | 0.878 | 0.621 |
| HEB400 | Single span, rigid | 0.544 | 0.387 |
| HEB300 | Single span, rigid | 0.702 | 0.497 |
| HEB400 | Double span, hinged | 0.815 | 0.578 |
| HEB300 | Double span, hinged | 1.048 | 0.743 |

**Table 6.3:** Unity Check Results for HEB400 and HEB300 Beams with Different Support Conditions

Based on Appendix A, it can be concluded that for a single span and the use of a (semi-)rigid girder, the beams can have an HEB300 profile. In the case of a hinged connection, an HEB400 profile will be used, which is also selected for the Gerber beam.

**Accidental Limit State (ALS)**

According to Eurocode (EN 1990), the load factors are applied as follows in case of an accidental failure situation:

**Accidental Limit State**

$$\text{Permanent floor load } (G_\text{d}) = \#\text{floors} \times \gamma_\text{G} \times G_\text{k,tot} \tag{6.22}$$
$$= 10 \times 1.2 \times 4.28 = 51.36 \text{ kN/m}^2 \tag{6.23}$$

$$\text{Variable floor load extreme } (Q_{\text{d1}}) = \#\text{floors extreme} \times \gamma_\text{Q} \times Q_\text{k1} \tag{6.24}$$
$$= 2 \times 1.5 \times 4 = 12 \text{ kN/m}^2 \tag{6.25}$$

$$\text{Variable floor load momentary } (Q_{\text{d2}}) = \#\text{floors momentary} \times \gamma_\text{Q} \times \psi_1 \times Q_\text{k1} \tag{6.26}$$
$$= 8 \times 1.5 \times 0.5 \times 4 = 24 \text{ kN/m}^2 \tag{6.27}$$

$$\text{Total Load on Column} = A \times (G_{\text{d}} + Q_{\text{d1}} + Q_{\text{d2}}) \tag{6.28}$$
$$= 7.2^2 \times (51.36 + 12 + 24) = 4529 \text{ kN} \tag{6.29}$$

$$\text{Permanent floor load } (G_{\text{d}}) = \#\text{floors} \times \gamma_{\text{G}} \times G_{\text{k,tot}} \tag{6.30}$$
$$= 10 \times 1.0 \times 4.28 = 42.8 \text{ kN/m}^2 \tag{6.31}$$

$$\text{Variable floor load extreme } (Q_{\text{d1}}) = \#\text{floors extreme} \times \gamma_{\text{Q}} \times Q_{\text{k1}} \tag{6.32}$$
$$= 2 \times 1.0 \times 4 = 8 \text{ kN/m}^2 \tag{6.33}$$

$$\text{Variable floor load momentary } (Q_{\text{d2}}) = \#\text{floors momentary} \times \gamma_{\text{Q}} \times \psi_1 \times Q_{\text{k1}} \tag{6.34}$$
$$= 8 \times 1.0 \times 0.5 \times 4 = 16 \text{ kN/m}^2 \tag{6.35}$$

$$\text{Total Load on Column} = A \times (G_{\text{d}} + Q_{\text{d1}} + Q_{\text{d2}}) \tag{6.36}$$
$$= 7.2^2 \times (42.8 + 8 + 16) = 3463 \text{ kN} \tag{6.37}$$

When the lowest of the ten columns collapses, not all the weight will rest on the lowest beams. The columns above the collapsed column will settle over the entire height. Because it settles simultaneously at all points, each floor will contribute to the load transfer of the lost column. This way, the forces from the columns can be transferred via the steel beams to the surrounding columns. For this reason, the force at the center of the span where the column has fallen will not be equal to 3463 kN. As there are ten floors, the vertical downwards force for each column will be as follows.

$$F_{\text{vertical downwards}} = 1.0 \times \frac{1}{10} \times 3463 = 346.3\text{kN} \tag{6.38}$$

To see if the designed connections meet reality, the ultimate limit state (ULS) and the serviceability limit state (SLS) need to be calculated. These calculations can be found in Appendix A.

### 6.1.1. Dynamic Amplification Factor

The Dynamic Amplification Factor (DAF) quantifies the extent to which a structure magnifies dynamic loads relative to static loads. Regarding structural robustness, the DAF is essential as it highlights the possible escalation in stresses or displacements a structure may undergo when subjected to dynamic forces, such as those from earthquakes or wind. Since the location chosen is the city of Rotterdam, earthquakes will be excluded from consideration.

$$\text{DAF} = \varphi_{dynamic} = \frac{1}{\sqrt{(1 - r^2)^2 + (2\zeta r)^2}} \tag{6.39}$$

**Where:**

$r$ $= \frac{\omega}{\omega_n}$ (frequency ratio)
$\zeta$ = damping ratio
$\omega$ = excitation frequency
$\omega_n$ = natural frequency of the system

In case of a sudden failure of a column, the impact load factor is:

$$\varphi_{\text{dyn}} = 2.0 \quad \text{(impact load, article C.2.2 [8])} \tag{6.40}$$

In the case of a very slow (static) failure, the impact load factor is:

$$\varphi_{\text{dyn}} = 1.0 \tag{6.41}$$

- **Sudden Failure**: When a column fails suddenly, the dynamic effects are significant, and the impact load factor is higher ($\varphi_{\text{dyn}} = 2.0$). This means the load experienced by the structure is effectively doubled due to the sudden impact.
- **Slow (Static) Failure**: When a column fails very slowly, the dynamic effects are minimal, and the impact load factor is lower ($\varphi_{\text{dyn}} = 1.0$). This means the load experienced by the structure is the same as the applied load, with no additional impact.

## 6.2. Structural elements and connection properties

The input of the building is as mentioned before in the intro of this chapter and section 6.1. The output can be found in Table 6.4. These results are accomplished by the structural design tool. The main beams of HEB400 was given based on single span beams which are connected by hinges. When possible are more economic beam of type HEB300 is chosen. The unity checks to see if this is possible can be found in Appendix A. Figure 6.1 gives an overview of how the structure of the building is built up.

| | |
|---|---|
| Storeys | 10 |
| Main beam | HEB300 |
| Main beam | HEB400 |
| Secondary beam | IPE240 |
| Columns | HEB450 |
| Steel class | S355 |
| Hollow core slab floors | 200 mm |
| Concrete class | C50/60 |

**Table 6.4:** Properties and dimensions of structural elements

**Steel and concrete class**
Steel of grade S355 is increasingly being used instead of the more traditional S235. This is partly due to its higher strength and more efficient material usage, and it also provides better ductility, making it particularly suitable for structures subjected to dynamic or impact loads, such as in the case of column removal. This ductility is essential for scenarios where alternate load paths or significant deformations may occur.
The VBI hollow core slabs ([21]), such as the 200 hollow core slab, are made of prestressed, pre-cast concrete. The concrete grade commonly used for these slabs is C50/60. This means that the concrete has a compressive strength of 50 MPa after 28 days. For in-situ cast concrete, C25/30 is often chosen. This lower concrete grade for a structural topping layer is frequently selected because it is cast on-site. In-situ cast concrete generally has a lower strength class than precast concrete, as the conditions on the construction site are less controlled than in a factory.

### 6.2.1. Connection properties

Boundary conditions are important when investigating different types of connections because they define the constraints and interactions between a system and its environment. The boundary conditions determine which values are not changed so that the values that do change can be better compared.

The beams and columns are already set to a standard and will be used for all cases to make sure this does not influence the results. The following values in the connections will also remain the same over all the cases. In the case of this study, the following values remain the same across different connection types. This allows for a better comparison of the connections. Rules of thumb [38] are used to simply

define the connections. They will be divided into three categories, the hinged, semi-rigid, and rigid connection, and the properties can be found in Table 6.5, Table 6.6 and Table 6.7. There is also the Gerber beam connection between the two beams. These connections will make of the properties displayed in Table 6.8.

For the hinged fin plate connection, it is of great importance that the plastic deformation comes out of the plate. For this reason, the plate should not be too large in relation to the bolts and weld seam to which the plate is connected to the column.

**Table 6.5:** Hinged connection properties by rules of thumb

| **Hinged connection** | | |
|---|---|---|
| Bolts | M20 | |
| Fin-Plate thickness | 10 [mm] | > bolt diameter / 2 |
| Welds | 8 [mm] | |

**Table 6.6:** Semi-rigid connection properties by rules of thumb

| **Semi rigid connection** | | |
|---|---|---|
| Bolts | M24 | |
| End-Plate thickness | 12 [mm] | > bolt diameter / 2 |
| Welds | 12 [mm] | Rule of thumb |

**Table 6.7:** Rigid connection properties by rules of thumb

| **Rigid connection** | | |
|---|---|---|
| Bolts | M24 | |
| End-Plate thickness | 25 [mm] | > bolt diameter |
| Welds | 18 [mm] | 0.7*26 [mm] |

**Table 6.8:** Gerber beam connection properties by rules of thumb

| **Gerber beam to beam connection** | | |
|---|---|---|
| Bolts | M24 | |
| Plate thickness | 15 [mm] | > flange tw |

To analyze the entire building structure, it is important to know the rotational stiffness capacity of the connection. As this is a nonlinear behavior, IDeaStatiCa will be used to develop the nonlinear rotation vs. moment-capacity diagram. The stiffness of the connection decides if the connection is hinged, semi-rigid or rigid. The graph in Figure 6.4 shows the beginning (up to 4 mrad) of the rotational stiffnesses of the connection that are used later on in chapter 7. These line fall within respectively the area for a rigid, semi-rigid and hinged connection (subsection 4.4.4).

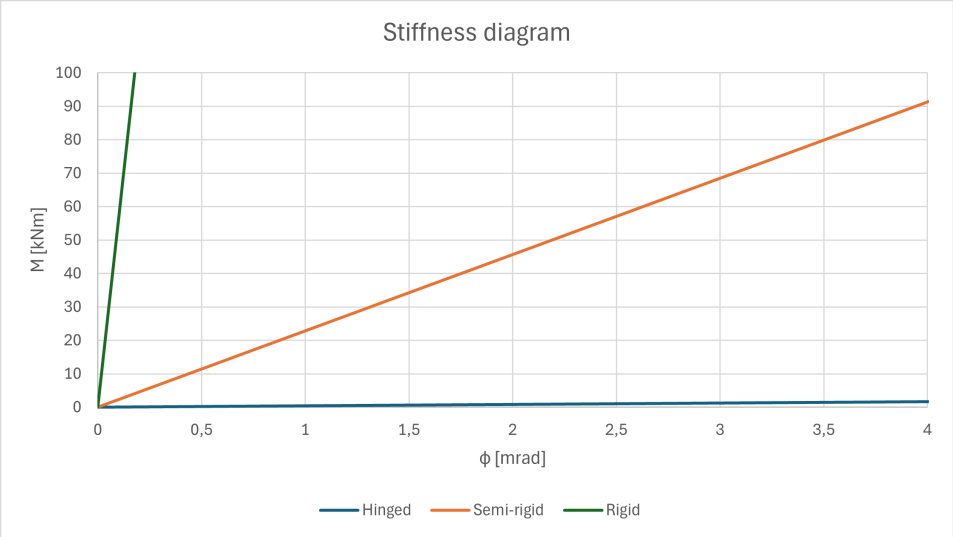


**Figure 6.4:** Rotational stiffnesses of three connections

As the angular rotation in a structural connection increases, the moment at that connection may change due to the non-linear behavior of the materials and the connection. This most often means that the rotational stiffness decreases when the rotation increases. Since both the rotational stiffness and the angular rotation are not fixed values, this relationship becomes complex and nonlinear.

### Bolt strength

For a bolt of grade 8.8 with a diameter of M20, the tension strength $F_t$ can be calculated using the formula:

$$F_t = f_u \times A_s \tag{6.42}$$

Given:

- $f_u = 800$ MPa (ultimate tensile strength)
- $A_s = 245$ mm$^2$ (tensile stress area)

Plugging in these values:

$$F_t = 800 \times 245 = 196 \text{ kN} \tag{6.43}$$

So, the tension strength $F_t$ is **196 kN**.

The shear strength can be calculated using the formula:

$$F_v = 0.6 \times f_u \times A_s \tag{6.44}$$

Where:

- $f_u$ is the ultimate tensile strength of the bolt material, which is 800 MPa for grade 8.8 bolts.
- $A_s$ is the tensile stress area of the bolt, which for an M20 bolt is approximately 245 mm$^2$.

Plugging in the values:

$$F_v = 0.6 \times 800\,\text{MPa} \times 245\,\text{mm}^2 = 117.6\,\text{kN} \tag{6.45}$$

So, the shear strength of an M20, grade 8.8 bolt is approximately 117.6 kN.

### Weld strength

Here, the calculation for the strength of the welds is given. The calculations include both the shear strength and the tensile strength of the weld. The given parameters are a weld thickness of 12 mm and a weld length of 100 mm.

Given:

- Weld thickness, $a = 12\,\text{mm}$
- Weld length, $l = 100\,\text{mm}$
- Steel grade, S355 (yield strength, $f_y = 355\,\text{MPa}$)
- Partial safety factor, $\gamma_M = 1.0$

$$\text{Allowable shear stress } \tau: \quad \tau = 0.6 \cdot f_y = 0.6 \cdot 355\,\text{MPa} = 213\,\text{MPa} \tag{6.46}$$

$$\text{Allowable tensile stress } \sigma: \quad \sigma = f_y = 355\,\text{MPa} \tag{6.47}$$

$$\text{The weld area } A: \quad A = a \cdot l = 12\,\text{mm} \cdot 100\,\text{mm} = 1200\,\text{mm}^2 \tag{6.48}$$

$$\text{The weld strength in shear } F_w: \quad F_w = \tau \cdot A = 213\,\text{MPa} \cdot 1200\,\text{mm}^2 = 255.6\,\text{kN} \tag{6.49}$$

$$\text{The weld strength in tension } F_t: \quad F_t = \sigma \cdot A = 355\,\text{MPa} \cdot 1200\,\text{mm}^2 = 426\,\text{kN} \tag{6.50}$$

Therefore, the strength of the weld for the given configuration is approximately:

- $255.6\,\text{kN}$ in shear for a weld length of 100 mm.
- $426\,\text{kN}$ in tension for a weld length of 100 mm.

**Force at an Angle** $\alpha$

$$\text{Shear component of the force } F_{\text{shear}}: \quad F_{\text{shear}} = F \cdot \cos(\alpha) \tag{6.51}$$

$$\text{Tensile component of the force } F_{\text{tension}}: \quad F_{\text{tension}} = F \cdot \sin(\alpha) \tag{6.52}$$

$$\text{Maximum shear force per meter } F_{\text{shear max}}: \quad F_{\text{shear max}} = 2556\,\text{kN/m} \tag{6.53}$$

$$\text{Maximum tensile force per meter } F_{\text{tension max}}: \quad F_{\text{tension max}} = 4260\,\text{kN/m} \tag{6.54}$$

$$\text{Maximum force at angle } \alpha: \quad F_{\text{max}} = \min\left(\frac{F_{\text{shear max}}}{\cos(\alpha)}, \frac{F_{\text{tension max}}}{\sin(\alpha)}\right) \tag{6.55}$$

## 6.3. Reinforcement of floor system

Concrete parts of the structure require reinforcement. Reinforcement bars (rebars) in concrete floors can act as tension ties, compensating for concrete's inherent weakness in tension. In the event of an accidental load, these rebars may help maintain structural integrity by absorbing and distributing tensile forces. In this section, the general reinforcement for the hollow core slab floor system will be calculated.

### 6.3.1. Hollow core slab floor

One of the floor systems used in this project is a channel plate floor with a thickness of 200 mm and a span of 7200 mm. See Figure 6.5 for a cross-section of a hollow core slab element. The complete calculation of the required strands, prestressing, and moment capacity of the cross-section falls outside the scope of this thesis and is, therefore, omitted.

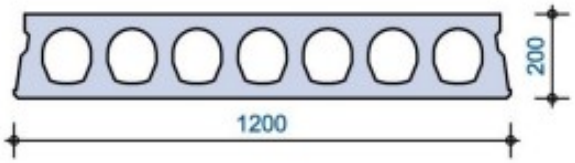


**Figure 6.5:** VBI hollow core slab floor element cross-sectional view, dimensions in mm

In practice, prestressing strands usually have a diameter of 12.5 mm, steel grade FeP1860, with at least one strand between each rib at the bottom of the channel plate. Given the substantial floor thickness of 200 mm for the span of 7.2 meters, it is assumed that the floor contains the minimum amount of prestressing strands. Thus, seven strands of 12.5 mm diameter are used.

#### Coupling reinforcement and tensile strap

To transfer horizontal wind load to the stabilizing core, the required amount of reinforcement needs to be determined. First, the horizontal coupling reinforcement will be calculated.

$$\text{Windload} = 1.0 \text{ kN/m}^2 \tag{6.56}$$

This is for the combination of wind suction and internal over-pressure, pulling on the beams surrounding the floor. This tensile load must be transferred to the floor through the connection. Since the heart-to-heart distance of the beams is 7.2 meters, the wind load is multiplied by this value to obtain the following:

$$7.2 \times 1.0 = 7.2 \text{ kN/m} \tag{6.57}$$

The choice was made to place the coupling reinforcement in the joint between the various hollow core slabs instead of in cut grooves. Therefore, the wind load is further multiplied by 1200 mm as this is the width of the hollow core slabs. This leads to a final load of:

$$7.2 \times 1.2 = 8.64 \text{ kN} \tag{6.58}$$

Since this load is considered relatively small, practical coupling reinforcement is applied in the form of a $\varnothing 12$ dowel with a spacing of 1200 mm.

The perimeter tie is determined based on Figure 6.6. This figure illustrates the situation with wind from any side, as the building is squared. The wind load for this consideration is therefore.

$$3.6 * 1.0 = 3.6 \text{ kN/m} \tag{6.59}$$

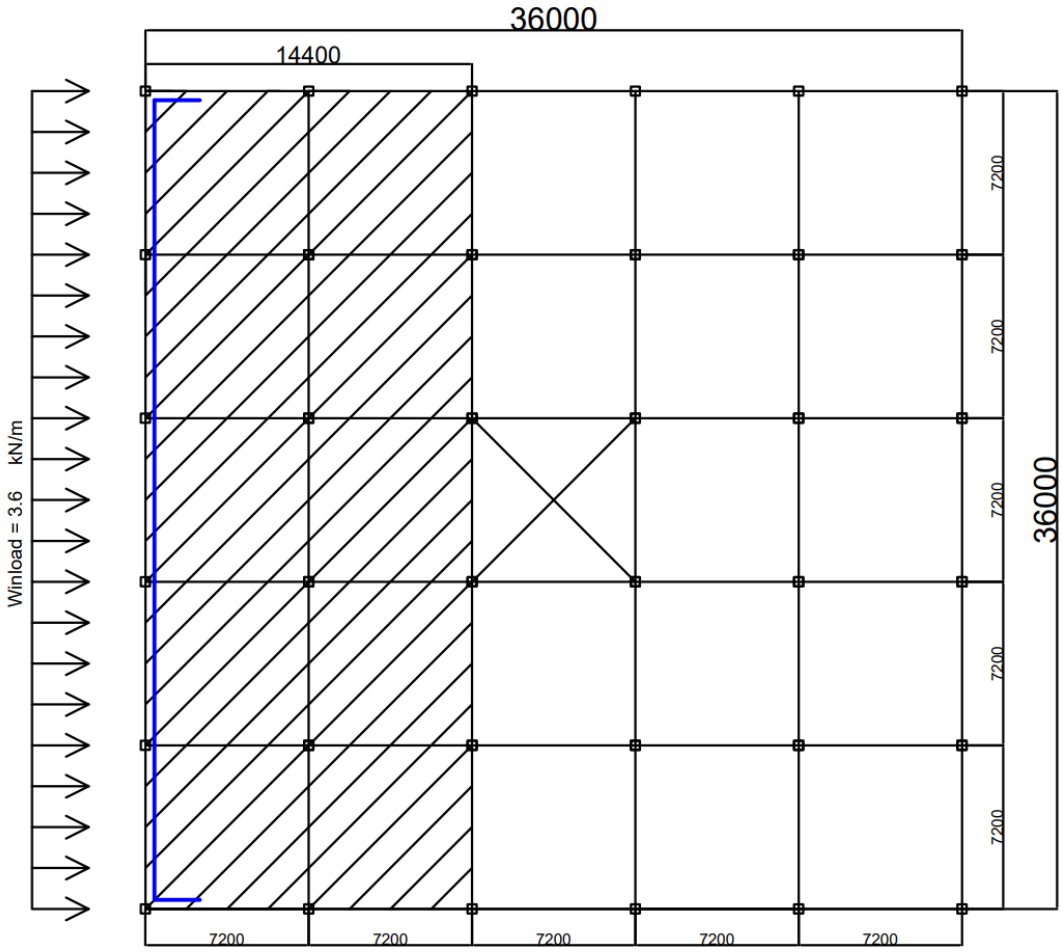


**Figure 6.6:** Wind load on the building and the floor part that has to redistribute the force to the core. Including the perimeter tie in blue.

When the wind acts from any direction, it is assumed that a horizontal beam is formed that extends the height of the field to one floor. The wind load is transferred to the stabilizing element through a cantilever that contains 4 floor fields in both the top part and the bottom part. The moment that occurs is, therefore, equal to the following:

$$M = F * L = (q * 2L) * L = (3.6 * 2 * 7.2) * 7.2 = 374\text{kNm} \tag{6.60}$$

$$F_t = \frac{M}{L} = 53 \text{ kN} \tag{6.61}$$

This creates a tensile load at the edge that the tension tie must resist. To handle this load, standard reinforcement steel is used, requiring a bar with a cross-sectional area of 120 mm$^2$, which corresponds to a $\varnothing 16$ mm bar.

# 7

# Beam case studies

This chapter investigates the behavior of different beam configurations in the event of sudden column removal, focusing on structural robustness. The failure mechanisms associated with various scenarios are highlighted.

## 7.1. Case 1: single span beams

As previously discussed, Case 1 refers to a basic building structure comprising beams with single spans and columns that span multiple floors, where the beams extend from column to column. When removing a set of columns, specifically a corner column, a facade column, and a middle column, all located on the ground floor of the building, the decision is made to evaluate the entire system.

### 7.1.1. Interior Column Removal

The process of removing a facade column mirrors that of removing an interior column with respect to the redistribution of forces within the structure. It is crucial to differentiate between a facade column that supports the main beam and a facade column that supports the secondary beam. Refer to Figure 7.1 for a floorplan that illustrates the removal of a column in the interior and a column in the facade, the column in the facade in this case located where the main beam is supported. Notably, removing a facade column generates distinct forces compared to removing an interior column, significantly affecting the horizontal equilibrium of the floor at the column's position.

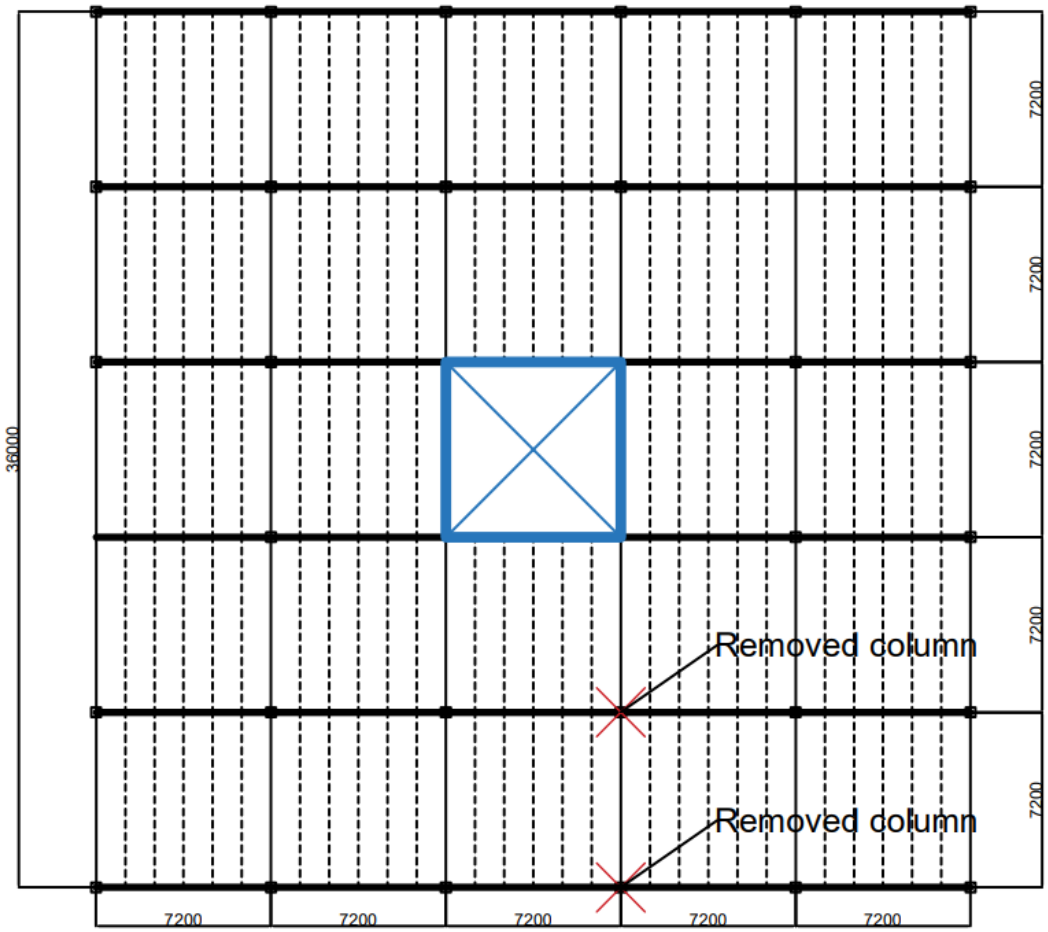


**Figure 7.1:** Floor plan including columns, the main beams (thick lines), the secondary beams (thin lines), and the removed columns

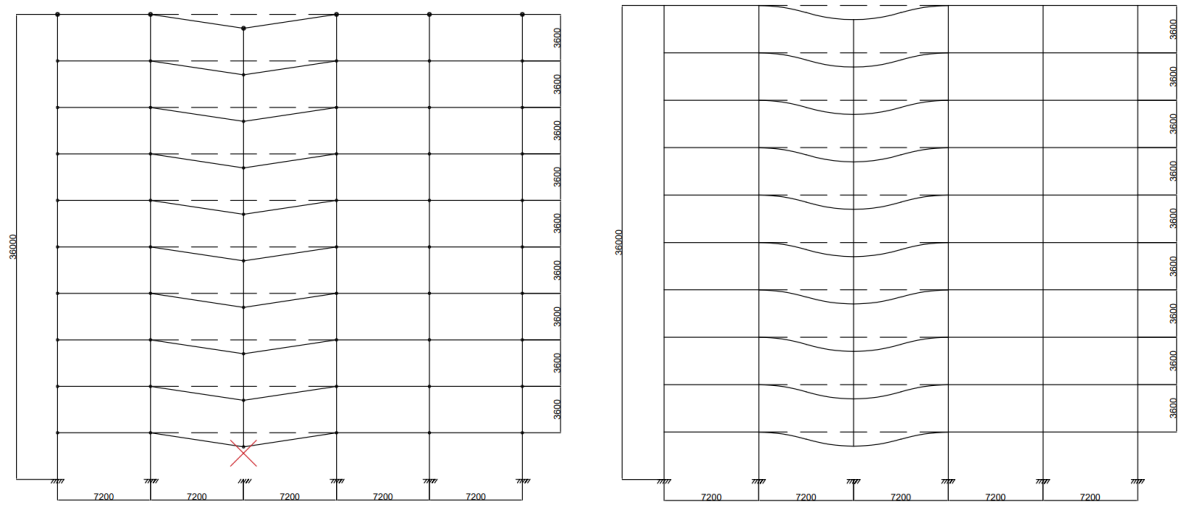


**(a)** Hinged connection

**(b)** Rigid connection

**Figure 7.2:** Side view of the building where an interior or facade column is removed. (a) Hinged connection, (b) Rigid connection

### Hinged connection

In this first situation, the beam is connected by hinges every 7.2 meters. This means that in a simplified model, it can be assumed that there is free rotation at the connection. This model is shown in Figure 7.3. The details of the connection used can be seen in Figure 7.4. With a point load on the structure, a bilinear catenary action will occur. Since the hinges are designed in such a way that they do not resist moments, the force must come from the elongation of the steel HEB400 beams and the plastic resistance of the connection. The calculation to base the elongation on the deflection within the catenary action can be found below.

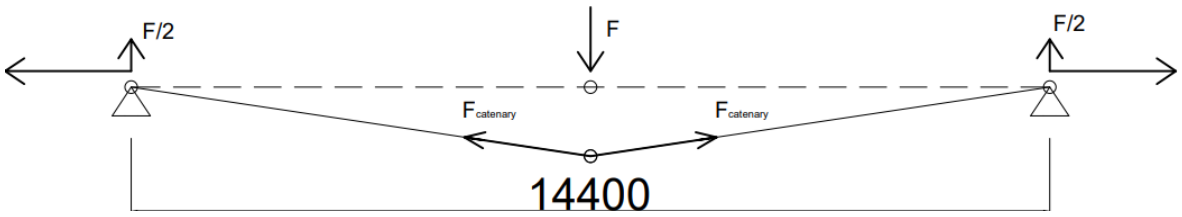


**Figure 7.3:** Interior or facade column removed, single span beams supported by hinged connections

In a standard situation, the span is 7.2 meters. With a ULS load of 85 kN/m (see Equation 6.21), the shear force taken up by the connection should be equal to 306 kN (see Equation 7.1). Given that the shear strength of each bolt is 117 kN, this requires 3 bolts.

$$85 \times 7.2 \times 0.5 = 306 \text{ kN} \tag{7.1}$$

In the case of a removed column, the forces are redistributed and make an equilibrium, including horizontal forces at the connection and vertical forces at the connection, as can be seen in Figure 7.3.

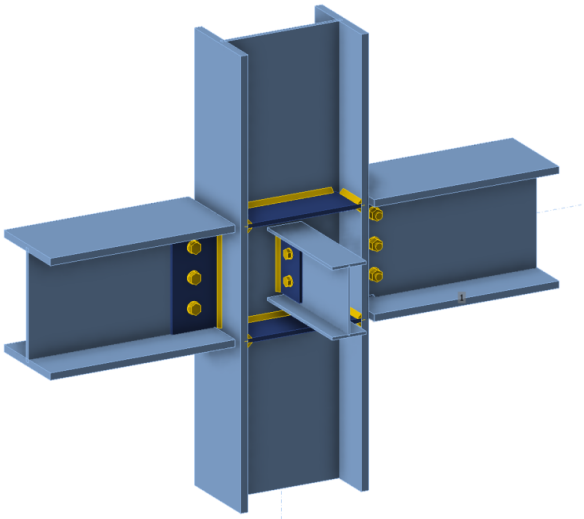

**Figure 7.4:** Detail of a hinged connection used in the model building. Column: HEB450; Main beams: HEB400; Secondary beams: IPE240. Dimension can be found in Table 6.5

Since the hinges are designed so that they do not resist moments, the force must come from the connection or the elongation of the steel HEB400 beams and the plastic resistance of the connection. The calculation to base the elongation on the deflection within catenary action can be found below.

The equilibrium equation

$$F_H * u = F_V * L \text{ and } F_V = \frac{F}{2} \quad \Rightarrow \quad \frac{F_H}{F} = \frac{1}{2}\frac{L}{u} \tag{7.2}$$

The formula of Regan for a bilinear cable shape

$$\epsilon = \frac{\Delta L}{L} \approx \frac{1}{2}\left(\frac{u}{L}\right)^2 \quad \Rightarrow \quad \frac{u}{L} \approx \sqrt{2\epsilon} \tag{7.3}$$

$$\frac{F_H}{F} = \frac{1}{2}\frac{L}{u} = \frac{1}{2}\frac{1}{\sqrt{2\epsilon}} \quad \Rightarrow \quad \epsilon = \frac{1}{8}\left(\frac{F}{F_H}\right)^2 \tag{7.4}$$

The beams allow even further elongation, transforming into a higher vertical deformation of the mid-span where the column is removed. This will also decrease the horizontal tensile forces in the construction. However, a large deformation also means that the connection has to allow such large deformations. This is difficult to achieve because there will always be a moment in the connection and it never functions as a fully hinged joint. There must also be room to get under the sagging floor/beam in an emergency. This study sets a limit for which sagging may not exceed 15% of the length. This translates into 1080 mm. This maximum sag is maintained based on a situation where there must still be enough space to walk under the sagging floor. In the case of a center-to-center floor of 3600 mm and a clearance of 3000 mm, this will mean that in the case of a drop column, the minimum passing height must still be equal to 1920 mm. In addition, studies show that such displacement of steel beams does not occur quickly because the connection has collapsed before reaching the percentage of 15% (15% is allocated by the municipality of Rotterdam, ensuring that there is still adequate passage space left)

When adhering to the force distribution in ties according to NEN-EN 1993-1-7 (section 2.2), otherwise, the strain will always exceed the allowed maximum [39].

At a maximum deflection of 15% of the span and a span length of 7.2 meters, the maximum deformation is equal to:

$$0.15 \times 7.2 = 1.08 \text{ meters} \tag{7.5}$$

$$\frac{F_H}{F} = \frac{1}{2}\frac{7.2}{1.08} = 3.33 \tag{7.6}$$

The elongation of the steel elements will then be equal to:

$$\epsilon = \frac{1}{8}\left(\frac{1}{3.33}\right)^2 = 0.01125 = 1.125\% \tag{7.7}$$

NEN-EN 1993-1-1 [33] specifies two strain limits for structural steel. The first strain limit refers to the region where necking occurs, with $A_0$ representing the initial cross-sectional area. This region is relatively short and cannot be used to determine the average strain across an entire bar. Consequently, the second criterion is adopted as the strain limit.

- The elongation at fracture, measured over a length of $5.65\sqrt{A_0}$, should be at least 15%.
- The strain at ultimate tensile strength ($f_u$) must meet the condition $\varepsilon_u \geq 15\varepsilon_y$, which translates to 1.7-2.5% for steel grades S235 and S355.

Now that it is known that steel elements can handle the strain, it is also essential to determine whether the connections can withstand the loss of a column and the associated moment capacity. A detailed description of a possible connection, a shear connection, is shown in Figure 7.4. Bolts in steel joints have some plastic power, but this is limited compared to other connecting elements, such as fin plates. Bolts are designed to work primarily in tension or shear. A fin plate, on the other hand, can allow for more plastic deformation because it has a larger surface area and often works in bending. This generally makes fin plates better able to absorb plastic deformation and dissipate energy during load.

Since many local stresses will develop around the bolts on the fin plate, a Finite Element Analysis (FEA) will be conducted. The number of bolts required to absorb this maximum rotation and force is crucial in

determining the demountability. A shear connection based on a fin plate and three bolts. In this case, the column is an HEB450 profile and the beam is an HEB400 profile.

When the middle column fails, the forces must be redistributed; this will be done via beams and columns that are still intact. Initially, the force will be transferred by means of bending forces.

The bending force describes how a construction element, such as a beam, responds to bending due to the applied forces. The resistance to bending comes from the bending capacity.

In the case of the lost column, the beams will behave as a cantilever. In this case, the hinges absorb the moments. As soon as the last connection reaches its moment capacity, the construction will switch to chain action. In this case, the moment capacity will be released and the forces will be distributed in diagonals. This means that the beams will behave more like cables under tension instead of strong beams under bending. The force is then carried by axial tensile forces in the beams.

The loss of the column causes the beams to pull on the columns, which creates horizontal forces. The structure depends on the tensile strength of the beams and the ability of the connections to transfer these forces to the columns. This transfer of these horizontal forces is crucial to maintaining the integrity of the structure after a column failure.

The structure given in Figure 7.5a was implemented in IDeaStatiCa. The code settings can be found in section E.1. The connection details according to the connection at the ends of the elements can be found in Figure 7.5b. All beam ends can freely rotate but are restricted from moving in the XYZ direction. Exceptions are the beam on the left side, which can freely translate in the X direction (direction of the beam) and the middle column, which can freely move in the Z direction (direction of the column).

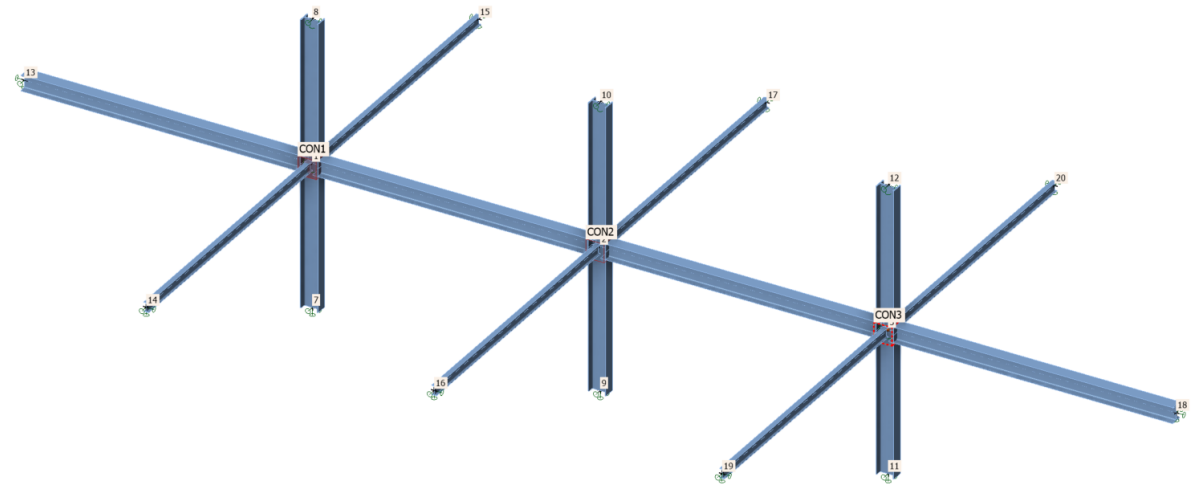


**(a)** Overview of the situation, the force is applied on the middle column, and the column is free to move in z direction

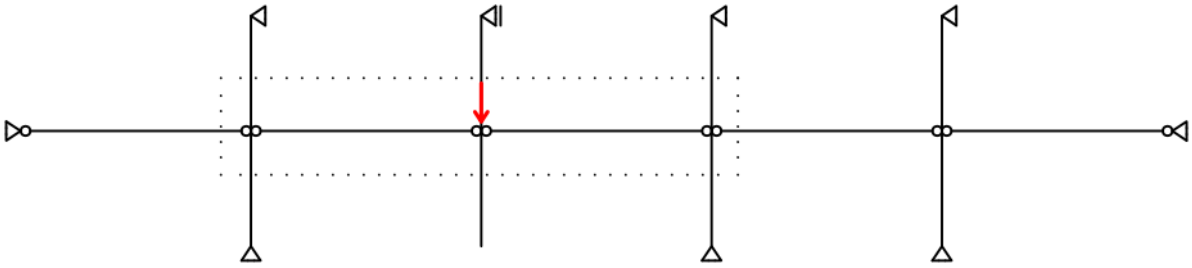

**(b)** Mechanical scheme of the system in 2D

**Figure 7.5:** Beam and column system for a 7.2-meter span and hinged connections scenario. A load is applied on the middle column

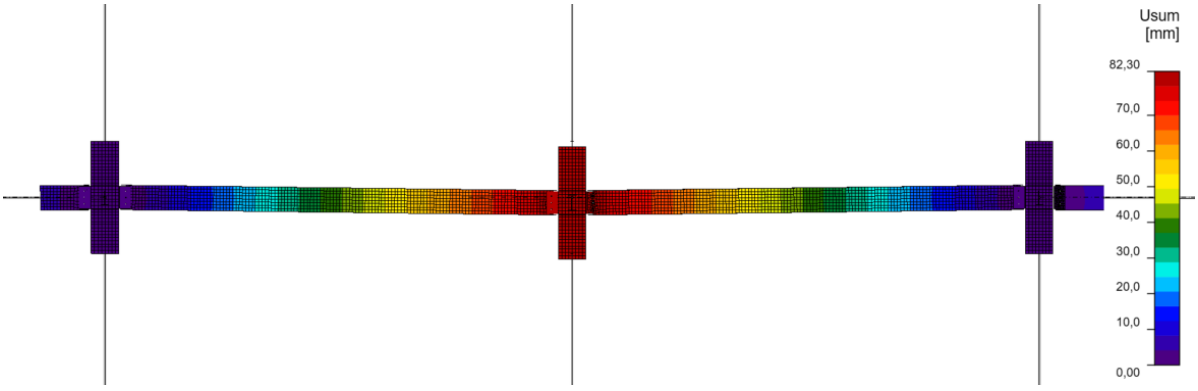


**(a)** Point load = 10 kN

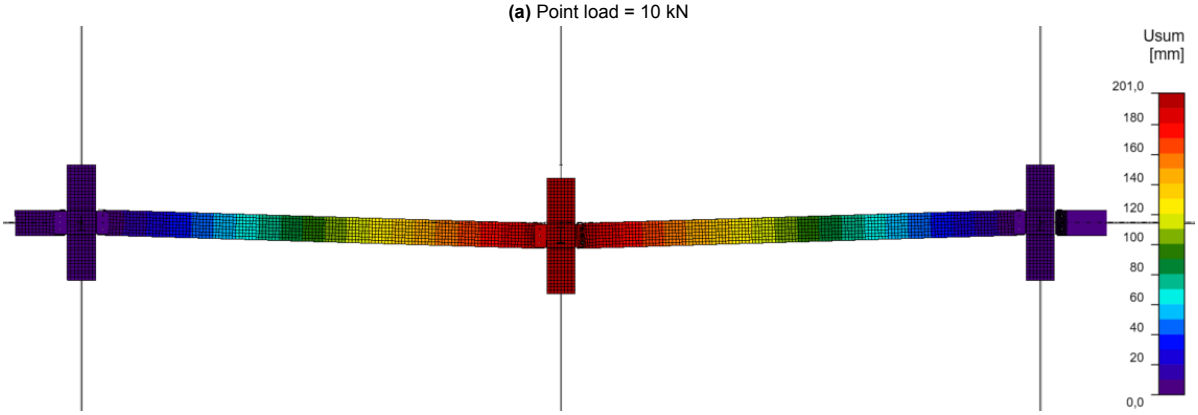


**(b)** Point load = 15 kN

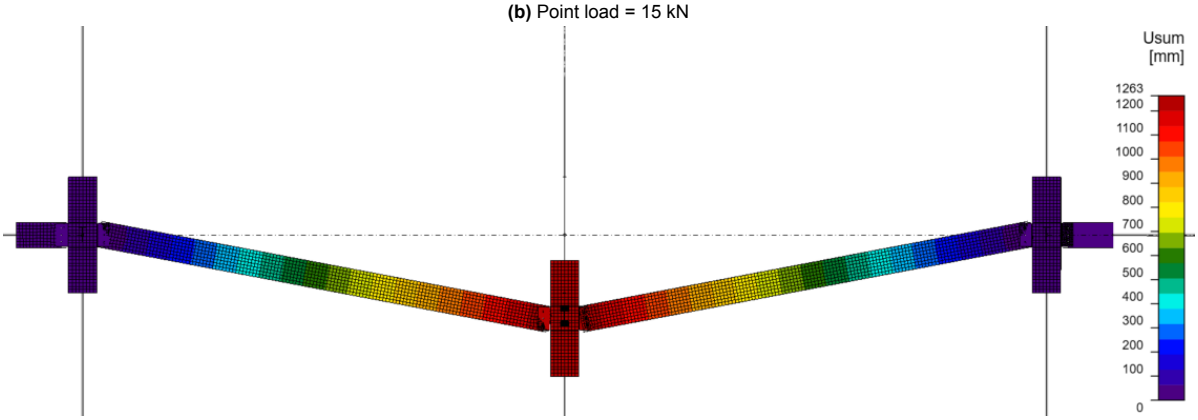


**(c)** Point load = 20 kN

**Figure 7.6:** Deformation of the structure under a point load at the middle column

The deformation of the structure under various point loads can be found in Figure 7.6. Here, it can be seen that catenary is already activated at a point load of 20 kN on the middle column. In Figure 7.7 the strain check of the elements can be found. It can be seen that the strain check of the structure is below the 15%.

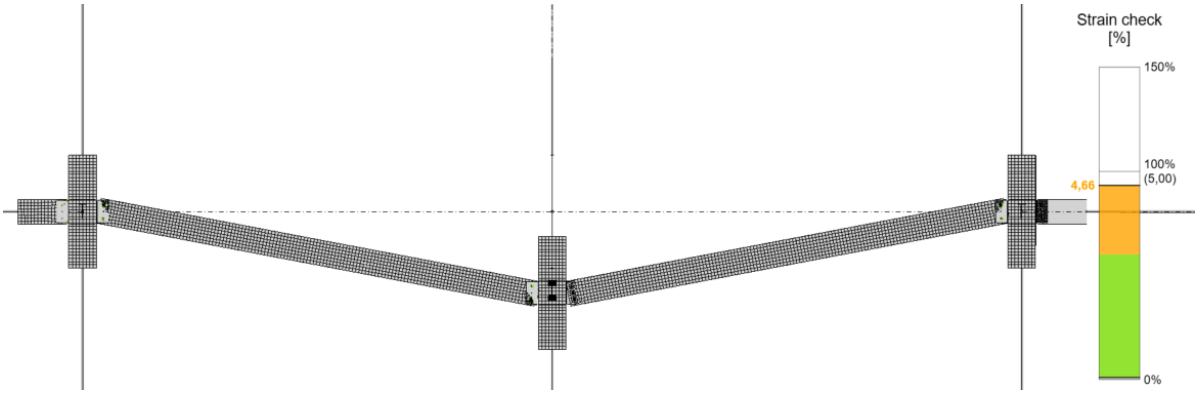


**Figure 7.7:** Strain check for the members at a load of 20 kN on the middle column (4.66%)

When the catenary action is activated, it is important to look at the connection. As high stresses occur on the bolts, the bolts will be damaged. In the example connection shown in Figure 7.4, there are three bolts. One of the potential failure modes occurs when the connection starts to rotate (Figure 7.8). In this scenario, the forces on the upper and lower bolts will be the greatest, causing one of them to fail before the middle bolt. With further rotation, another bolt, which could be either the middle bolt or the remaining upper/lower bolt, will fail. Ultimately, a full hinge will form with only one bolt left (Figure 7.9b). The shear force that this last bolt can absorb will then be critical. If this final bolt fails, the structure will collapse if it is solely based on steel connections. The maximum shear force in the bolt is 117 kN, as calculated in Equation 6.45. The ultimate strain on the bolt will be higher.

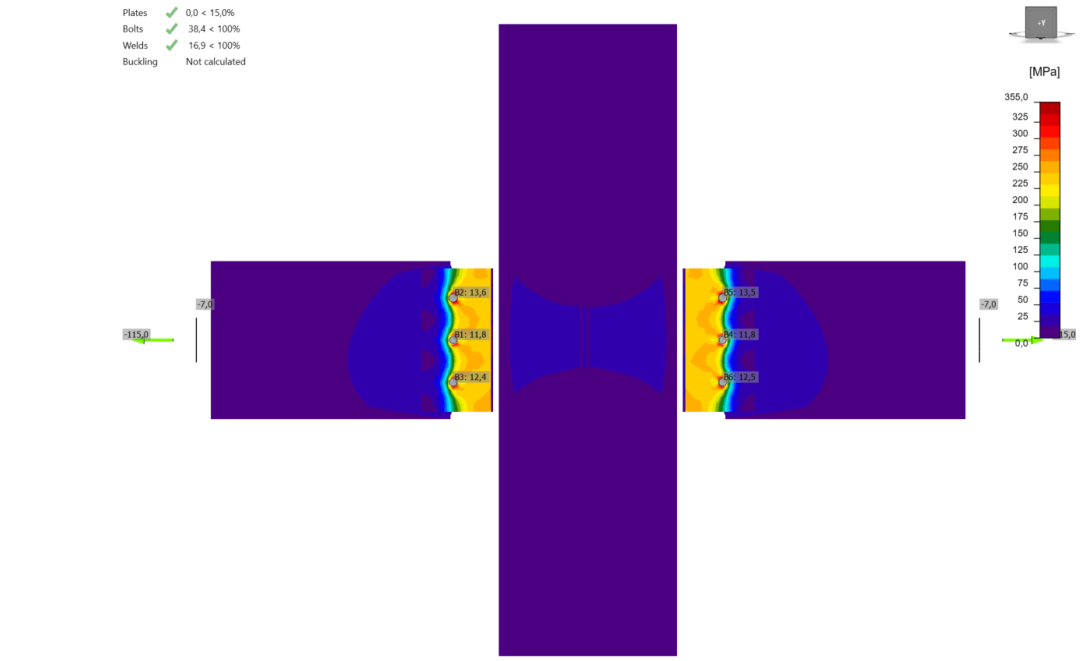


**(a)** 10 kN applied. All elements meet the requirements

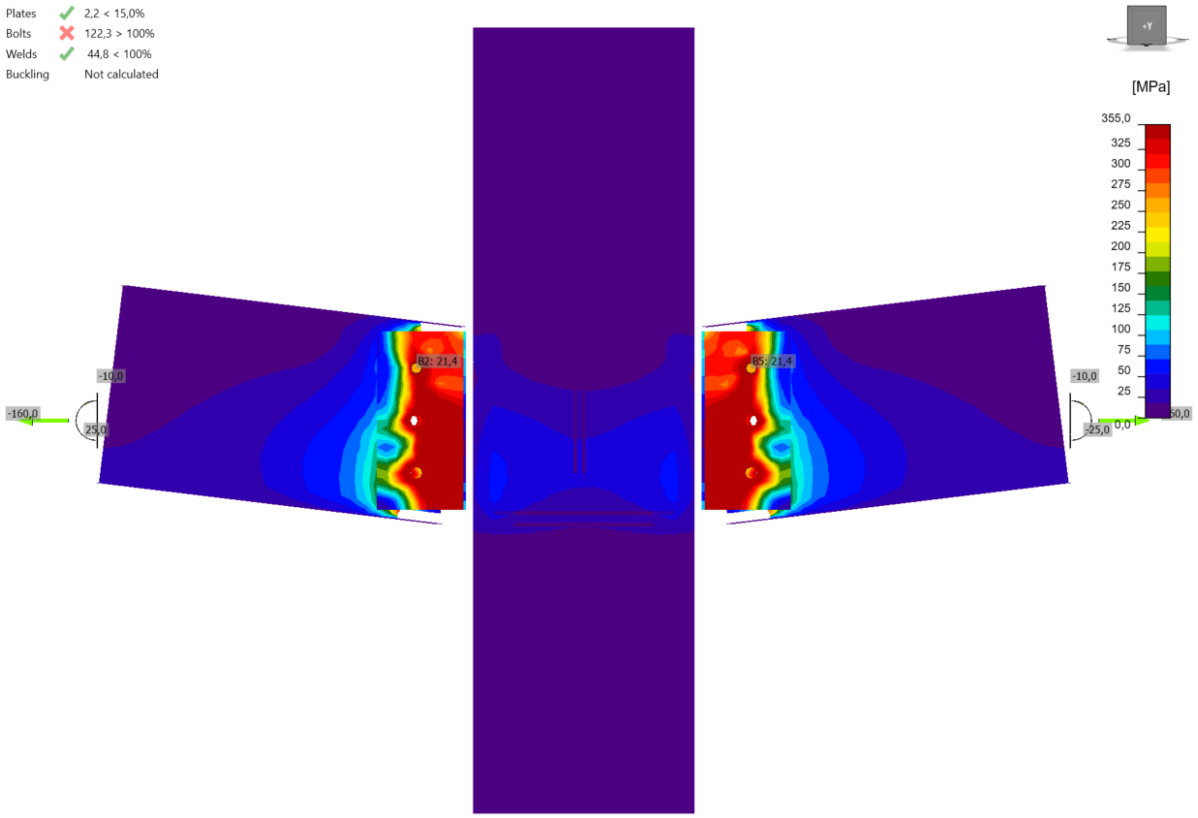


**(b)** 15 kN applied. Only one bolt intact

**Figure 7.8:** Comparison of connections under different loads

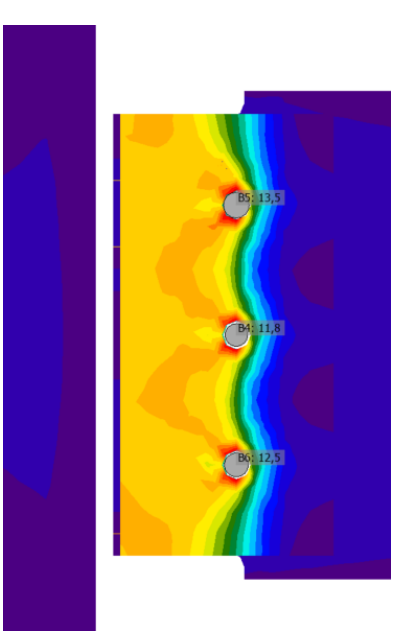


**(a)** 10 kN applied, three bolts still intact

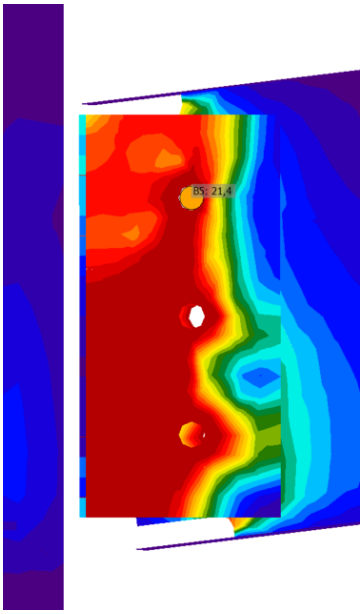


**(b)** 15 kN applied, only one bolt intact because of the large shear forces

**Figure 7.9:** Comparison of connection behavior under different loads

Assuming full catenary action and maximum deflection to minimize the horizontal force relative to the vertical force, the following applies: With a maximum deflection of 1080 mm over a span of 7200 mm, the horizontal force in a connection will always be equal to:

$$\frac{350}{2} \times \left(\frac{100}{0.15}\right) = 1167 \text{ kN} \tag{7.8}$$

$$\text{Unity check: } \frac{1167}{117} = 10.0 \gg 1.0 \tag{7.9}$$

This means the forces in the connection are way too high in case of catenary action, and a hinged connection is not suitable for loads this big.

The situation as indicated in Figure 7.10 will occur. The bolts break one by one until only one bolt remains on each side. This results in a free rotation that is twice the distance between the lower and upper bolt (Figure 7.10b). Due to a force equilibrium in the system, the force depends on this deflection. In the case of a maximum allowable sag of 15%, the sag will be equal to 1080 mm Figure 7.10c. Here, it can be seen that, in that case, the transverse force on the bolt is equal to 3.22 times the force on the column.

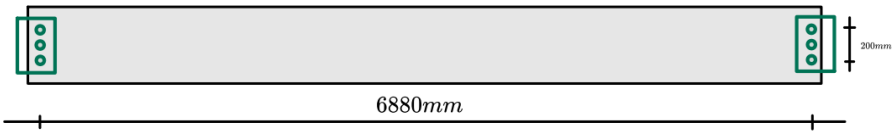


**(a)** Actual hinge to hinge distance, 7200 - 320 = 6880 mm. Distance between top and bottom bolt: 200 mm

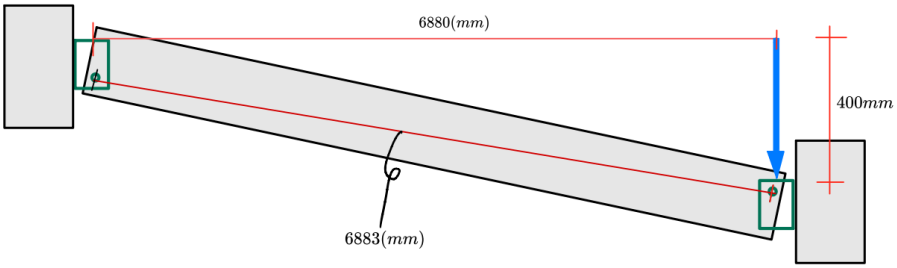


**(b)** Free deformation of the system when only one bolt is left

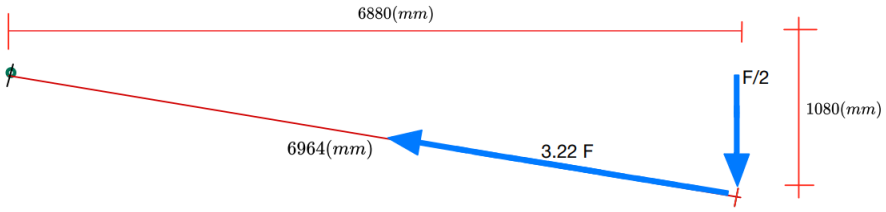


**(c)** Force distribution in case of catenary action

**Figure 7.10:** Catenary system of a single span hinged situation

The maximum shear force of an M20 bolt class 8.8 can be calculated as follows:

For a cylindrical bolt, the cross-sectional area is calculated using the formula:

$$A = \frac{\pi}{4} \times d^2 \tag{7.10}$$

where $d$ is the diameter of the bolt. For an M20 bolt, the diameter is 20 mm:

$$A = \frac{\pi}{4} \times 20^2 \approx 314\,\text{mm}^2 \tag{7.11}$$

The maximum shear force $F$ is calculated using the formula:

$$F = A \times \tau \tag{7.12}$$

where $A$ is the cross-sectional area and $\tau$ is the nominal shear strength of the bolt. The shear strength is typically 60% of the tensile strength. For a class 8.8 bolt, the nominal tensile strength is 800 N/mm², so the shear strength is:

$$\tau = 0.6 \times 800\,\text{N/mm}^2 = 480\,\text{N/mm}^2 \tag{7.13}$$

Thus, the maximum shear force is:

$$F = 314.16\,\text{mm}^2 \times 480\,\text{N/mm}^2 \approx 150.80\,\text{kN} \tag{7.14}$$

Assuming a maximum shear force of the bolt of $151$ kN and a deflection of a maximum of 1080 mm, the maximum force is ultimately calculated using the formula:

$$F_{\text{max}} = \frac{151\,\text{kN}}{3.22} \tag{7.15}$$

where 3.22 is a constant representing the ratio between the shear force and the vertical deformation (Figure 7.10c). The calculation is as follows:

$$F_{\text{max}} = \frac{150.80\,\text{kN}}{3.22} \approx 47\,\text{kN} \tag{7.16}$$

Figure 7.11 provides a very rough sketch of the flexural and catenary action in the system after the loss of a column. The results used in the graph come from IDeaStatiCa and the hand calculation. As long as all three bolts are intact, the system still benefits from the flexural action. Once two bolts are broken, the flexural action will disappear and the share of the catenary action will increase.

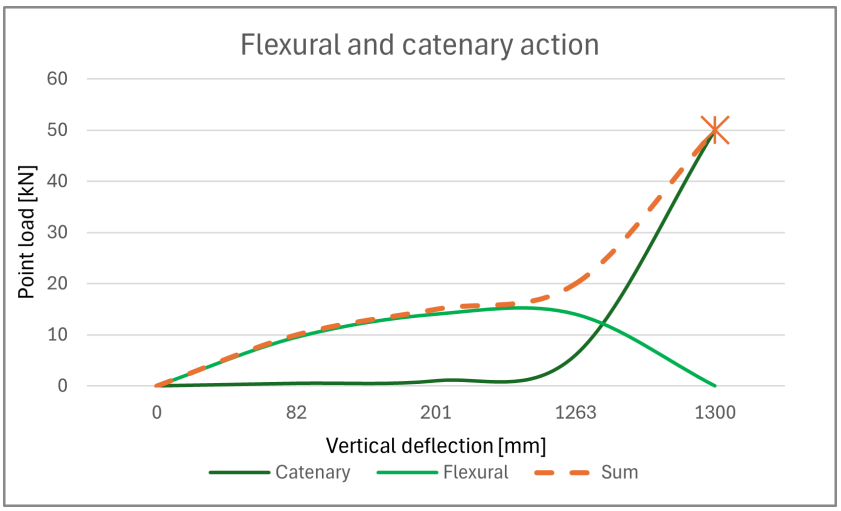


**Figure 7.11:** Catenary action and flexural action

### Rigid connection

Moment-resisting connections are not often used in spans due to their complexity and the additional costs associated with their design and construction. These connections require precise detailing and higher material strength to effectively resist moments, making them less economical for typical span applications. However, they are included in this research to provide a comprehensive comparison. By analyzing moment-resisting connections alongside other types, the study aims to highlight their performance characteristics and potential benefits, offering valuable insights for structural design and engineering. A detailed description of the connection can be found in Figure 7.12.

In the case of rigid connections, the catenary action will not be activated. The element is rigidly connected in such a way that there is minimal rotation at the location of the connection, as can be seen in Figure 7.13. The beam should absorb the forces by flexural action.

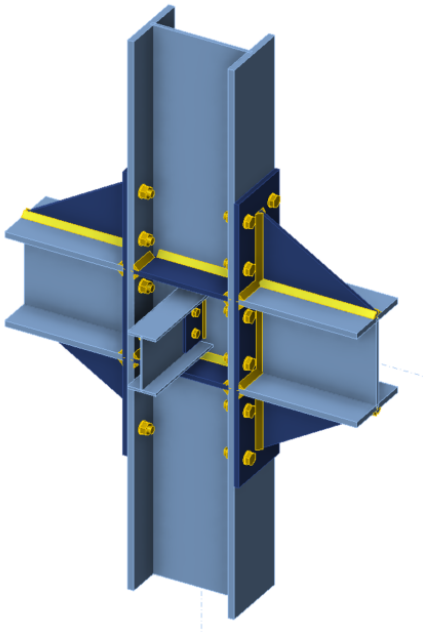

**Figure 7.12:** Detail of a rigid connection used in the model building. Column: HEB450; Main beams: HEB300; Secondary beams: IPE240 Table 6.7

This will result in a parabolic cable shape. The formula for the strain force relation can be found in Equation 7.35.

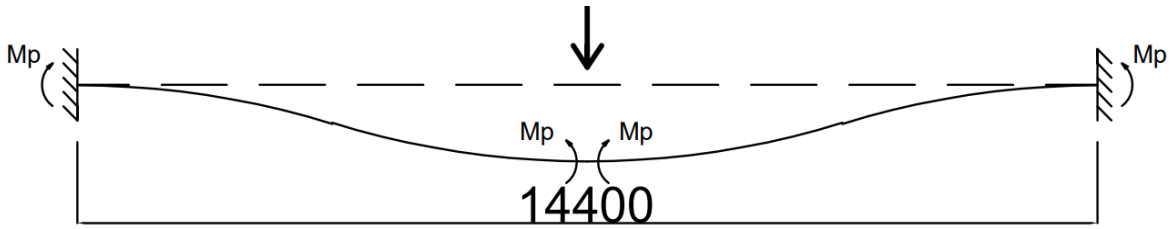


**Figure 7.13:** Interior or facade column removed, single span beams supported by rigid connections

The moment in the moment-resistant connection can be calculated using a ”forget-me-not.” This moment must then be accommodated by the connection, where the bolts, plate, and beam may undergo plastic deformation but not failure. The forget-me-not related to a pin-connected beam is:

$$\text{Moment at the supports} : T = \frac{1}{8}Fl \tag{7.17}$$

$$T = \frac{1}{8} \times 350 \times 14.4 = 630 \text{ kNm} \tag{7.18}$$

$$\text{deformation at the midspan : } w = \frac{1}{192} \cdot \frac{Fl^3}{EI} \tag{7.19}$$

The moment capacity $M$ of a connection, considering its rotational stiffness, can be expressed as:

$$M = T = k \cdot \theta \tag{7.20}$$

Where:

- $M$ is the moment capacity (in units such as N·m),
- $k$ is the rotational stiffness (in units such as N·m/rad),
- $\theta$ is the rotation angle (in radians).

As can be seen in Figure 7.14, the deformation under a point load at the middle column changes a lot when going from 400 to 500 kN. The deformation, in this case, is 124 mm when loaded by a point load of 400 kN and 1830 when loaded by a point load of 500 kN.

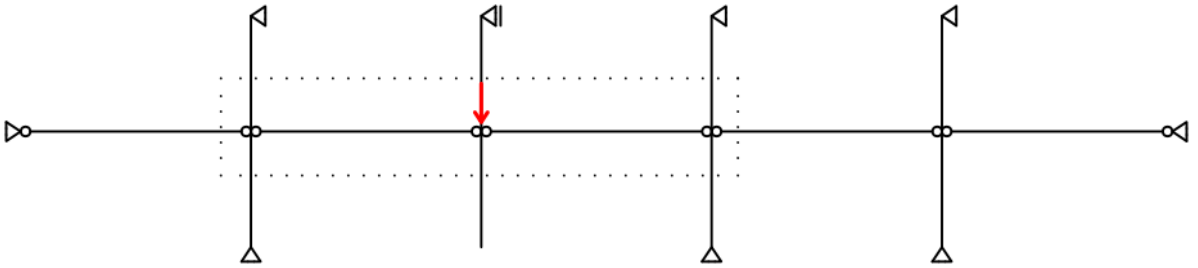

**(a)** Mechanical scheme of the system in 2D

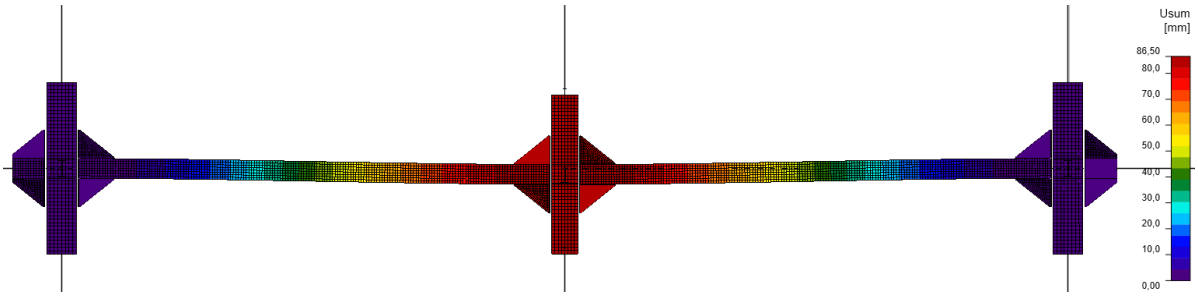


**(b)** Point load of 300 kN on the middle column

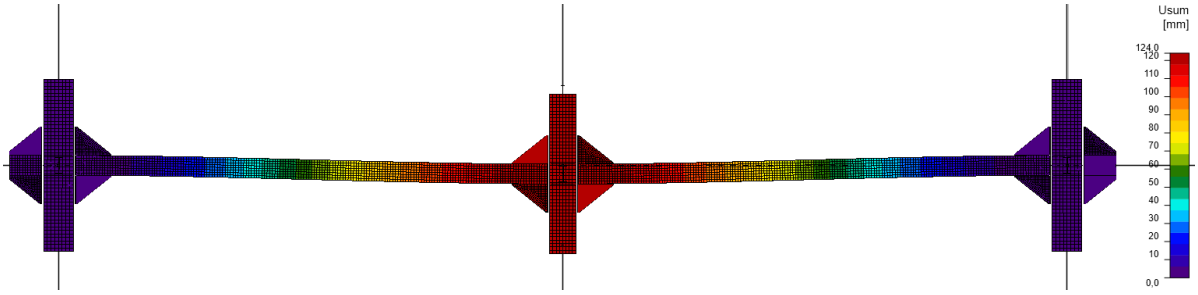


**(c)** Point load of 400 kN on the middle column

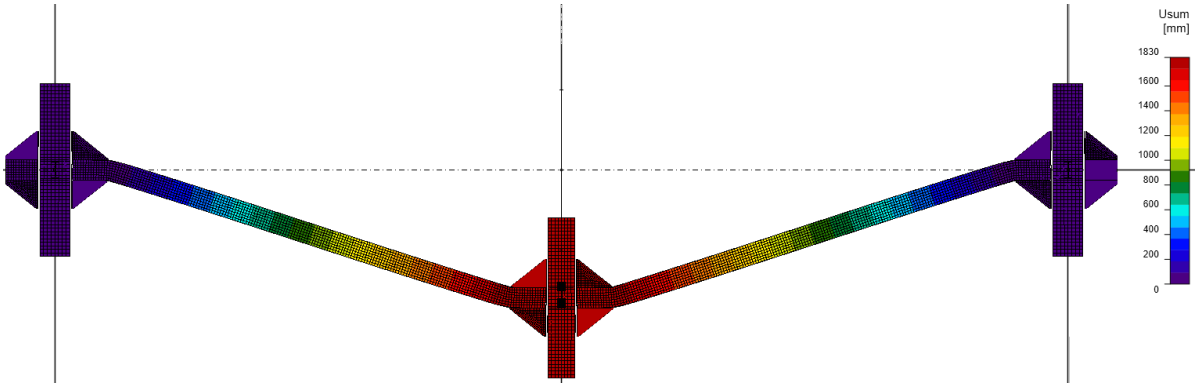


**(d)** Point load of 500 kN on the middle column

**Figure 7.14:** Rigid connection and the deformation under several point loads

This scenario fails under a point load of 500 kN as strain in the beam next to the connection becomes more than 15% in the beam next to the connection. This can be seen in Figure 7.15.

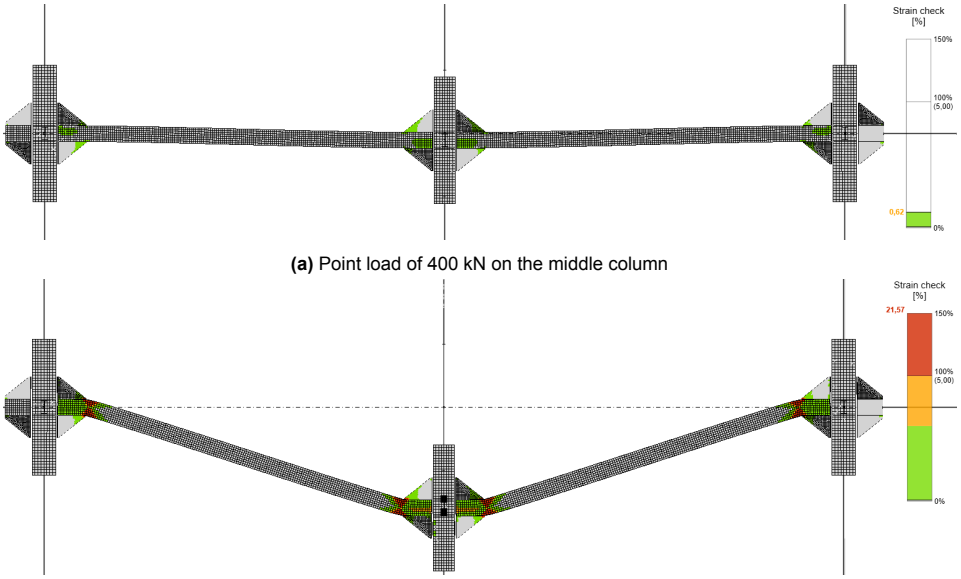


**(a)** Point load of 400 kN on the middle column

**(b)** Point load of 500 kN on the middle column

**Figure 7.15:** Rigid connection failure mechanism. Maximum strain 0.62 and 21.57 respectively

Due to the large deformation in the situation of 500 kN the forces in the bolts and the plates also become large. That the connection fails at this load can be seen in Figure 7.16b.

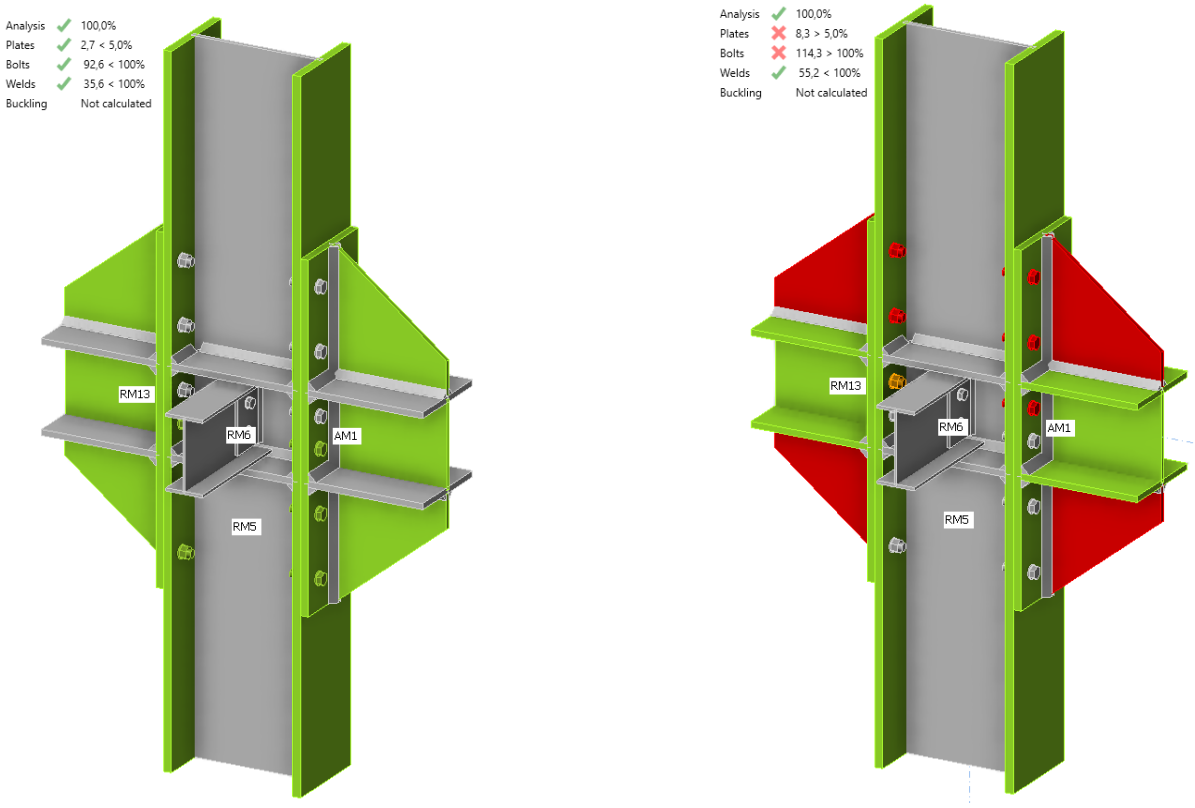


**(a)** 400 kN

**(b)** 500 kN

**Figure 7.16:** Rigid connection check of two point loads

### Semi-rigid connection

The design of semi-rigid connections must consider the balance between flexibility and strength. The connections should be capable of withstanding the moments and shear forces that arise due to the redistribution of loads.

This performance of semi-rigid connections is influenced by factors such as the type of connection (e.g., bolted or welded), the geometry of the connection, and the material properties. According to Eurocode 3 [29], the classification of semi-rigid connections is based on their moment rotation behavior. The design should ensure that the connections can accommodate the expected rotations without significant loss of strength or stiffness.

In the case of a semi-rigid connection, the forces will be partially absorbed by the connection, which acts like a spring, and partially by the bending of the beam. These two forces must be considered to determine whether the steel structure can serve as a secondary load path. A detailed description of the connection can be found in Figure 7.18.

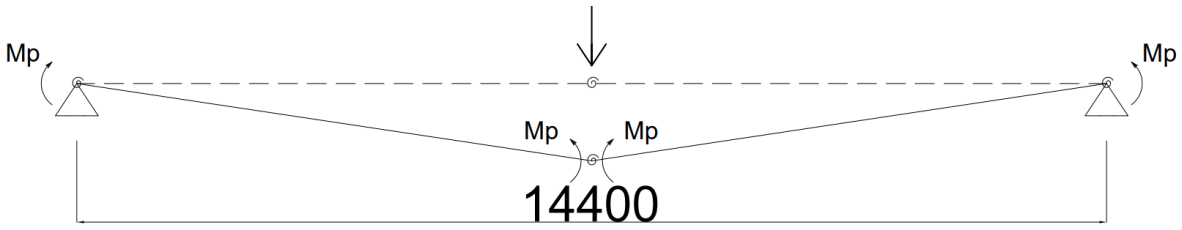


**Figure 7.17:** Interior or facade column removed, single span beams supported by semi-rigid connections

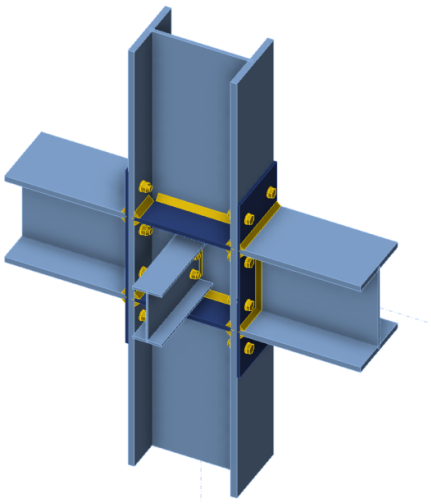

**Figure 7.18:** Detail of a semi-rigid connection used in the model building. Column: HEB450; Main beams: HEB300; Secondary beams: IPE240 connection details in Table 6.6

Catenary action is initiated when plastic hinges form in the beam, and resistance can be calculated based on the plastic bending moment of the section, which includes 4 connections, so 4 bending moments (see Figure 7.17 and Equation 5.3). In the catenary stage, the failure behavior of the frame is governed by the following two scenarios: tensile fracture of the net section of flange plates or shear tab and cleavage fracture of the welds. The corresponding displacement of the specimen can be predicted based on the rotation of the beams (Equation 5.5 and Equation 5.6). The bending moment of the steel endplate can be calculated as follows.

Given:

- Thickness of the plate, $h = 12\,\text{mm}$
- Width of the plate, $b = 300\,\text{mm}$
- Steel grade, S355 (yield strength, $f_y = 355\,\text{MPa}$)
- Partial safety factor, $\gamma_M = 1.0$

Section modulus $W$:

$$W = \frac{b \cdot h^2}{6} = \frac{300 \cdot 12^2}{6} = 7200\,\text{mm}^3 \tag{7.21}$$

Plastic bending moment $M$ of the plate:

$$M = \frac{f_y \cdot W}{\gamma_M} = \frac{355 \cdot 7200}{1} = 2{,}556{,}000\,\text{Nmm} = 2{,}556\,\text{kNm} \tag{7.22}$$

The number is $2{,}556{,}000$. Implementing the system in IDEAStatiCa gives the results as shown in Figure 7.19. A significant change can be observed when the force on the middle column increases from 200 to 250 kN. At this point, catenary action begins to take effect. In the following figure (Figure 7.20), it can be seen that the strain changes from 3.62% to 26.41% due to the force change. This latter strain exceeds the previously assumed maximum strain of 15%, so the connection will fail and can withstand a maximum of 200 kN based on the plates and beam.

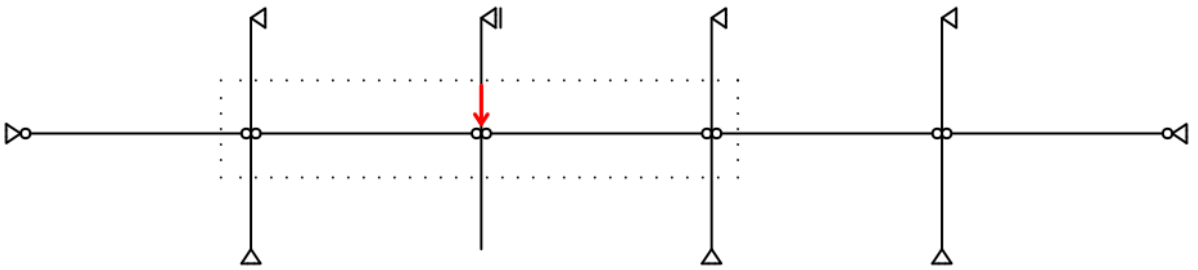

**(a)** Mechanical scheme of the system in 2D]

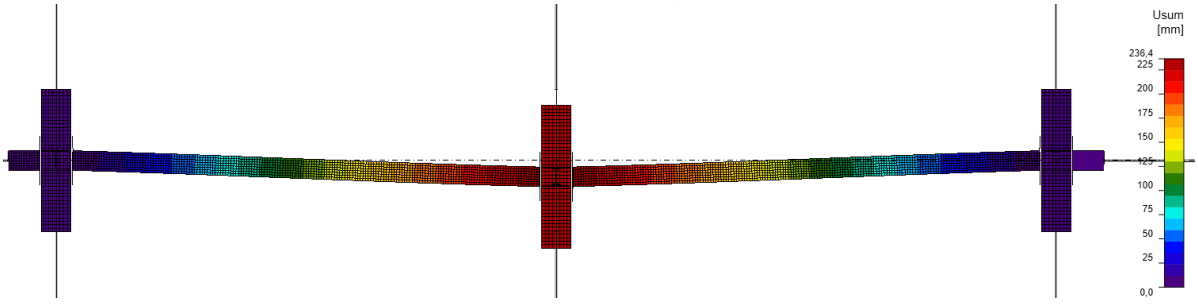


**(b)** 200 kN

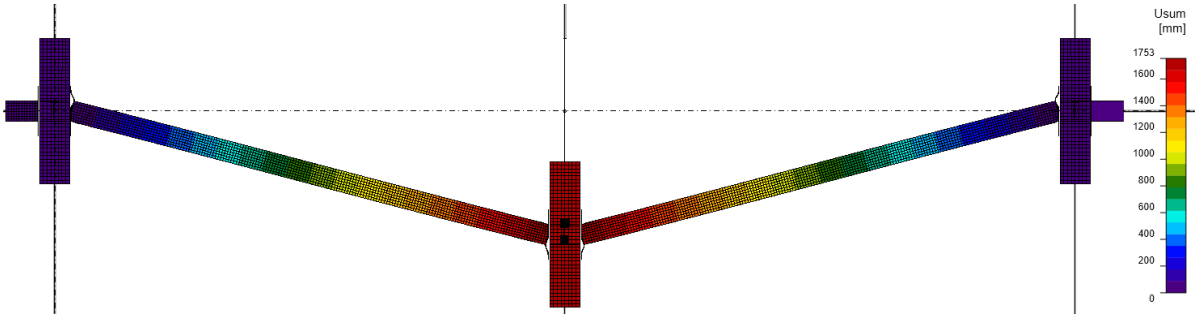


**(c)** 250 kN

**Figure 7.19:** Deformation under the point loads on the middle column

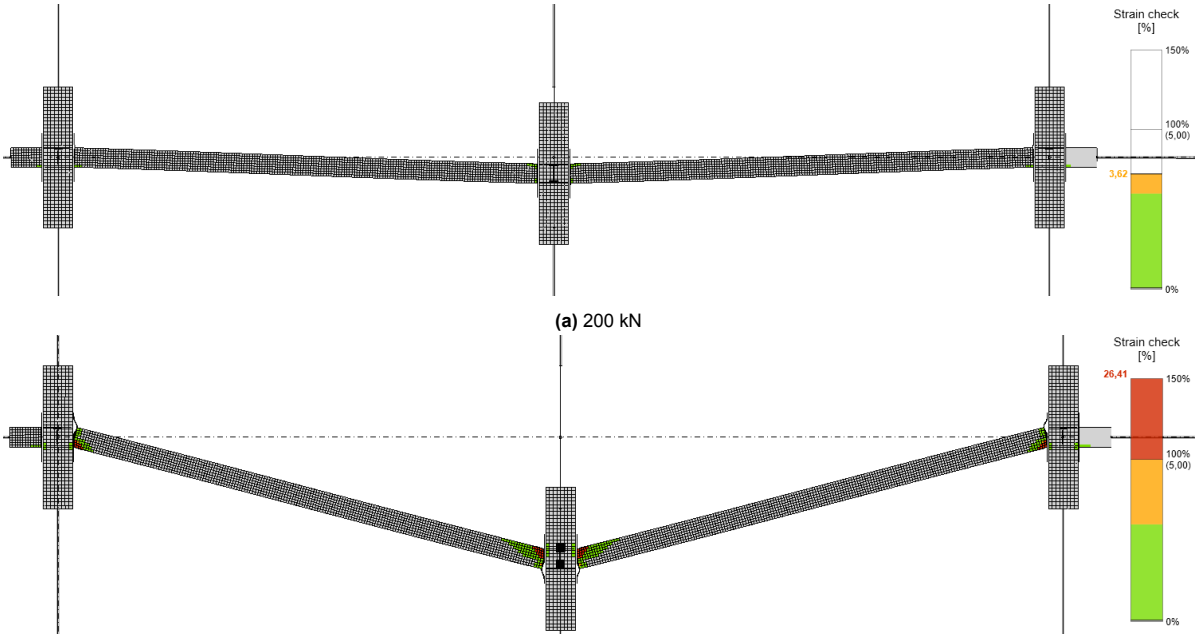


**(a)** 200 kN

**(b)** 250 kN

**Figure 7.20:** Deformation under the point loads on the middle column

Despite the plates and beams being able to withstand a force of 200 kN, this is not the case for the connection. The bolts, as shown in Figure 7.21a, can handle a maximum force of at least 50 kN, and they will fail at a force of 100 kN.

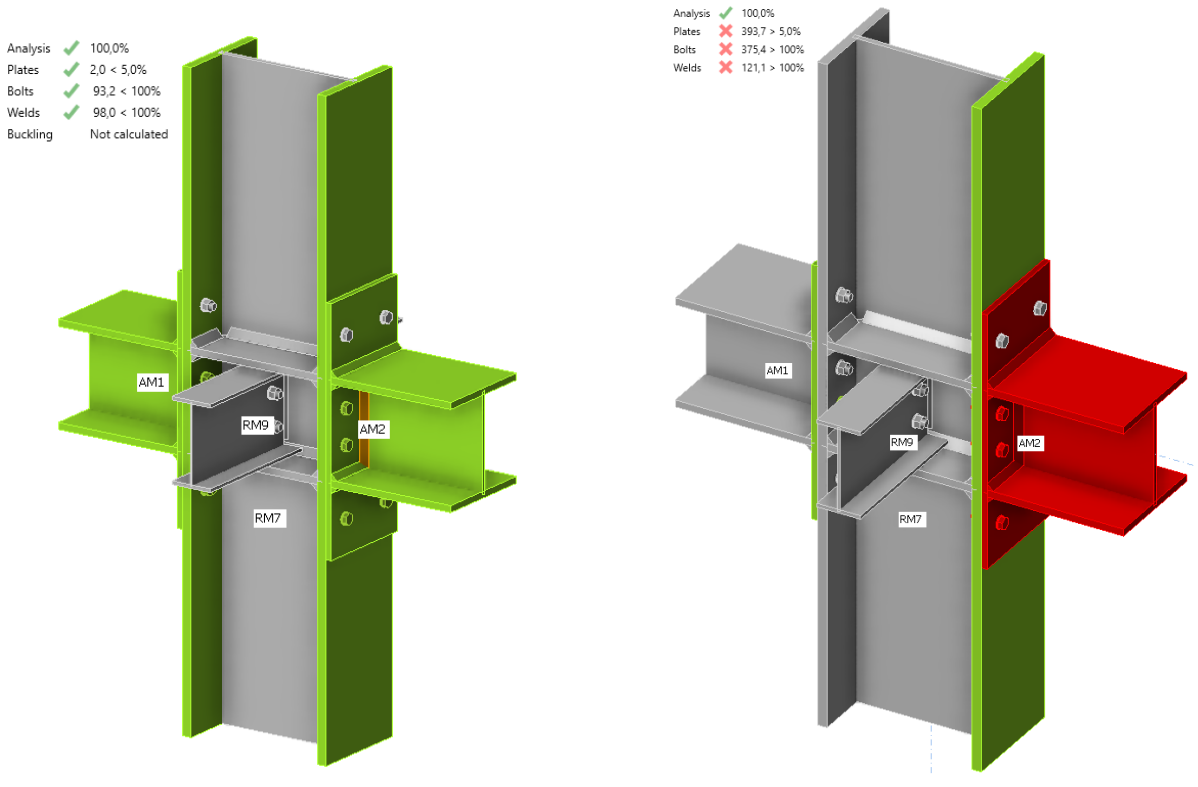


**(a)** 50 kN

**(b)** 100 kN

**Figure 7.21:** Connection check of the semi-rigid connection

Just as in the case of the hinged connection, the ziplock effect will also occur in the case of a semi-rigid connection. In the middle connection, the forces on the second lower bolt will be the greatest first, causing it to fail first. This can be seen in Figure 7.22a. Subsequently, the force will be transferred to the remaining bolts, and the middle point will sag further. In the optimal scenario, only the upper bolt will remain connected to the left and right columns Figure 7.21b. In the case of the middle column, only the upper bolt will remain. If the plate bends, the free sagging can thus be 800 mm (2 times the distance between the top and bottom bolt, see Figure 7.10b). However, the tensile force in the bolt will again become so great (Equation 7.8) that the last bolt will also fail.

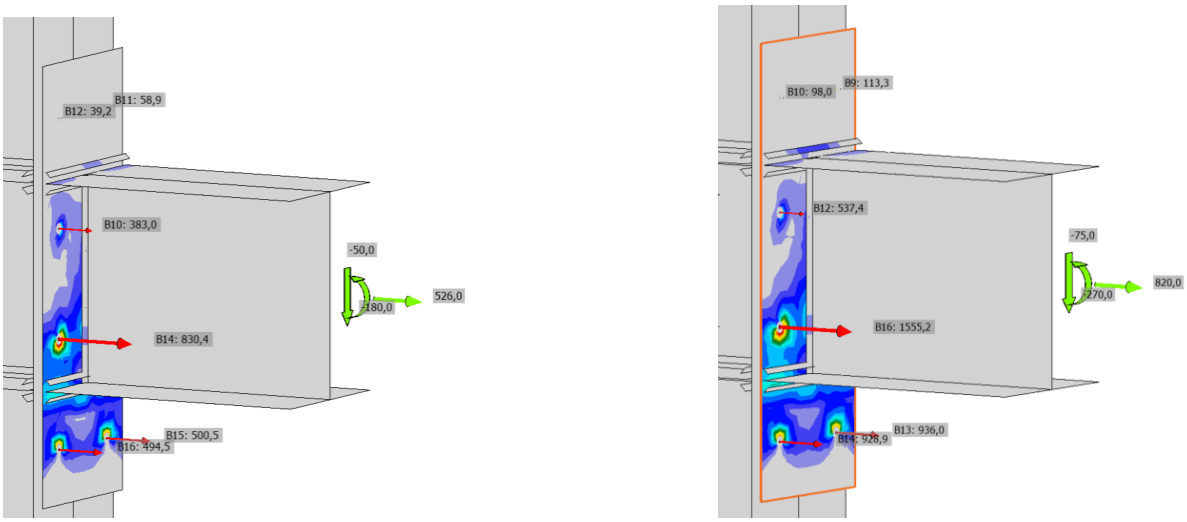


**(a)** 100 kN **(b)** 150 kN

**Figure 7.22:** FEA of the connection under two point loads, including the tensile forces on the bolts.

The maximum tensile force of an M20 bolt class 8.8 can be calculated as follows:

For a cylindrical bolt, the cross-sectional area is calculated using the formula:

$$A = \frac{\pi}{4} \times d^2 \tag{7.23}$$

where $d$ is the diameter of the bolt. For an M20 bolt, the diameter is 20 mm:

$$A = \frac{\pi}{4} \times 20^2 \approx 314\,\text{mm}^2 \tag{7.24}$$

The maximum tensile force $F$ is calculated using the formula:

$$F = A \times \sigma_t \tag{7.25}$$

where $A$ is the cross-sectional area and $\sigma_t$ is the nominal tensile strength of the bolt. For a class 8.8 bolt, the nominal tensile strength is 800 N/mm²:

$$F = 314\,\text{mm}^2 \times 800\,\text{N/mm}^2 \approx 251\,\text{kN} \tag{7.26}$$

Assuming a maximum tensile force of the bolts of $2 \times 251.33 \approx 500\,\text{kN}$ and a deflection of a maximum of 1080 mm, the maximum force is ultimately calculated using the formula:

$$F_{\text{max}} = \frac{500\,\text{kN}}{3.22} \tag{7.27}$$

where 3.22 is a constant representing the ratio between the tensile force and the vertical deformation (Figure 7.10c). The calculation is as follows:

$$F_{\text{max}} = \frac{500\,\text{kN}}{3.22} \approx 156\,\text{kN} \tag{7.28}$$

### 7.1.2. Facade or corner column removal

Unlike a mid-span, beams located at the corner or facade of a structure cannot use catenary action as a secondary load-bearing path. Catenary action depends on sufficient horizontal restraint at each end of a beam to support the tensile forces developing under loading. In case of a facade or corner column collapse, the vertical support is removed, leaving the beams unsupported on one side and making them a cantilever. Without horizontal support on the side of the collapsed column, the beams lack the necessary connection to maintain tension, and the remaining lateral restraint is unlikely to give sufficient support to the load through catenary action.

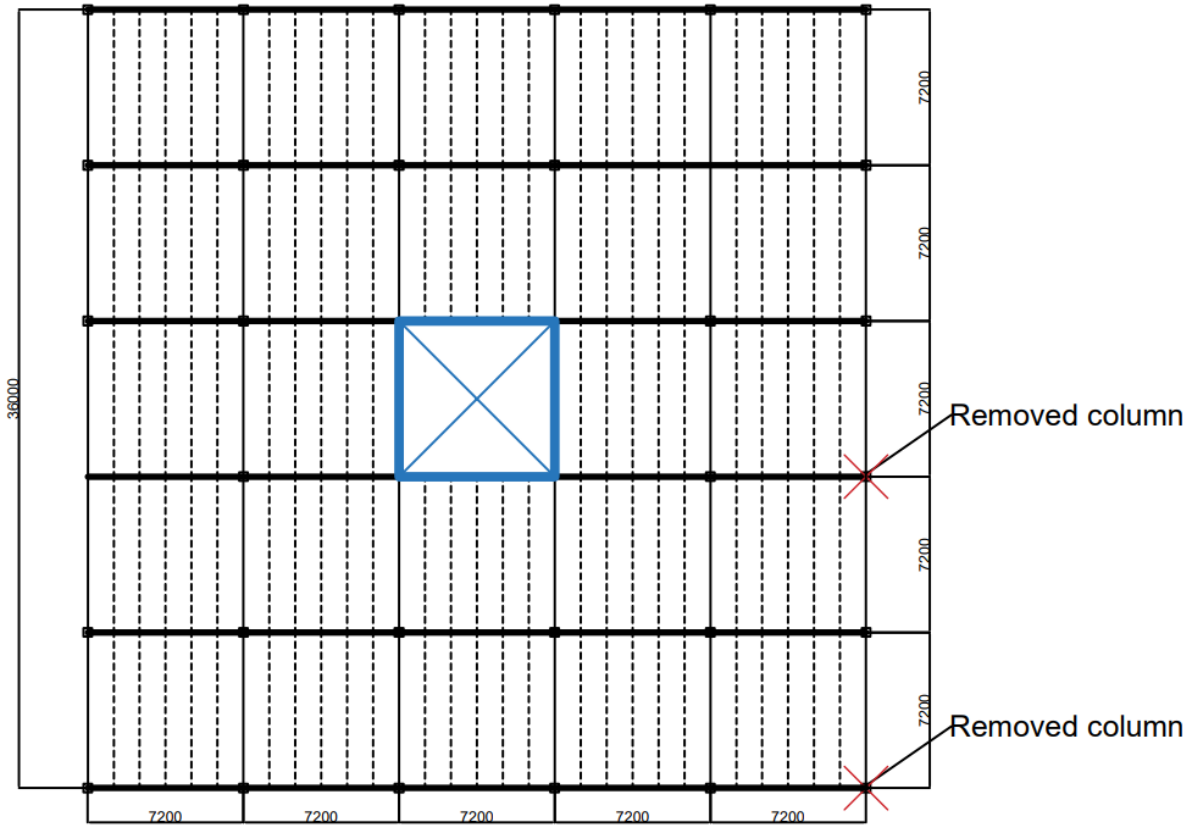


**Figure 7.23:** Floor overview where the facade or corner columnis removed

#### Hinged connection

Hinged connections cannot resist moments. For this reason, if a corner column is removed in a single-span structure, the steel frame cannot act as an alternative load path. In this case, other solutions must be employed. These alternatives are, at first, horizontal steel structures, such as wind bracing and ring beams. They can help transfer the loads that arise from the loss of a column to other parts of the building. Other solutions are diagonal ties or coupling beams. These elements can be added to transfer forces in the event of column failure. They connect various columns and can help redirect loads to other supporting structures.

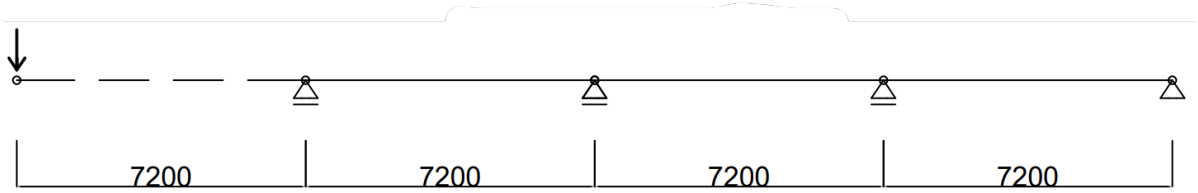


**Figure 7.24:** Corner column removed, single span beams supported by hinged connections

### Rigid connection

By using moment-resisting connections, the moment should be fully absorbed by the connection to make sure the beams act as a cantilever beam. This would then ensure that the steel connection is able to support the entire weight of the column on the end of the cantilevered beam. Additionally, the connection itself (the bolts and steel plates) must be able to withstand the moment and not fail; however, they may undergo plastic deformation. By utilizing plasticity, the structure deforms and absorbs energy. The bending strain of the steel beams is also crucial when it comes to progressive collapse.

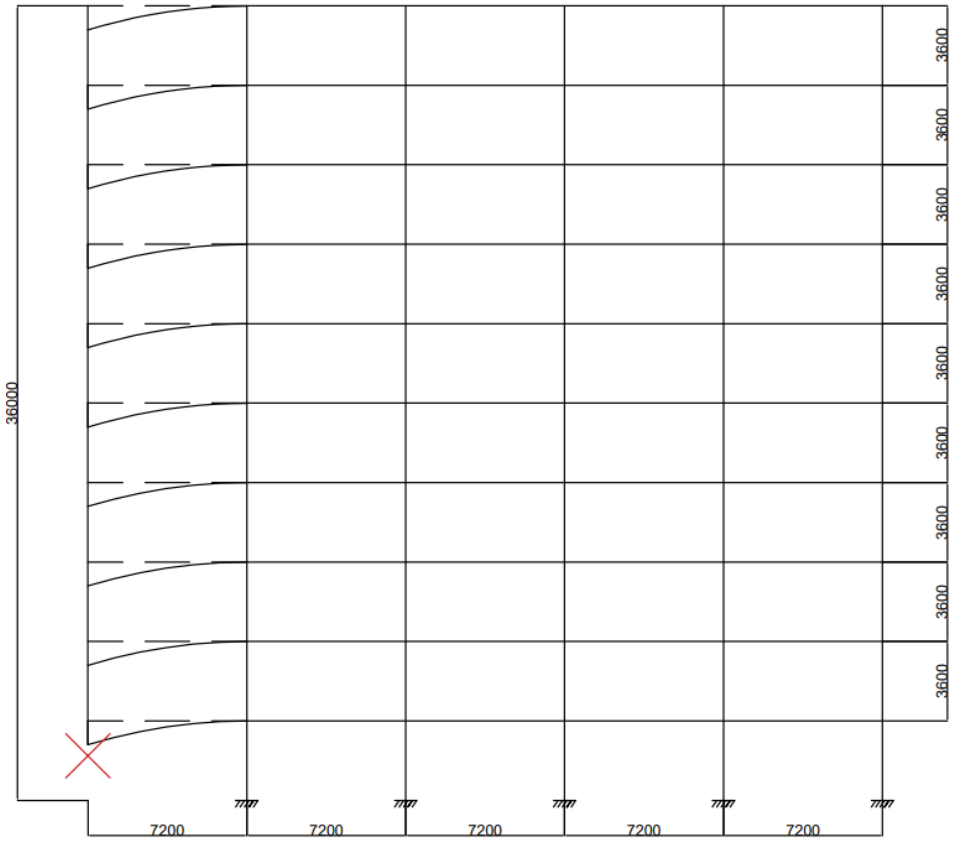


**Figure 7.25:** Side view of the building where a column is removed

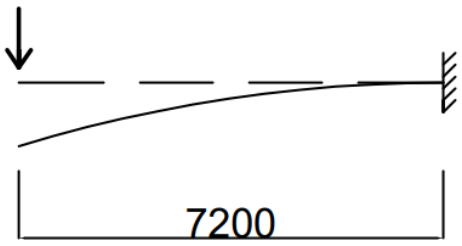


**Figure 7.26:** Corner column removed, single span beams supported by rigid connections

The moment as a product of a force on the outer end of the cantilever can be described as follows:

$$M = -P \times L \tag{7.29}$$

Given:

$$P = \frac{350}{2} = 175 \text{ kN} \tag{7.30}$$

$$L = 7.2 \text{ m} \tag{7.31}$$

Substituting the values:

$$M = -P \times L = -175 \times 7.2 = -1260 \text{ kNm} \tag{7.32}$$

Due to the Vierendeel action in the system, the forces will also be partially transferred via the outer column. How this system works can be seen in Figure 7.27. Therefore, the moment in the connection will not be equal to 1260 kNm. How the moment line shifts due to the Vierendeel action can be seen in Figure 7.28.

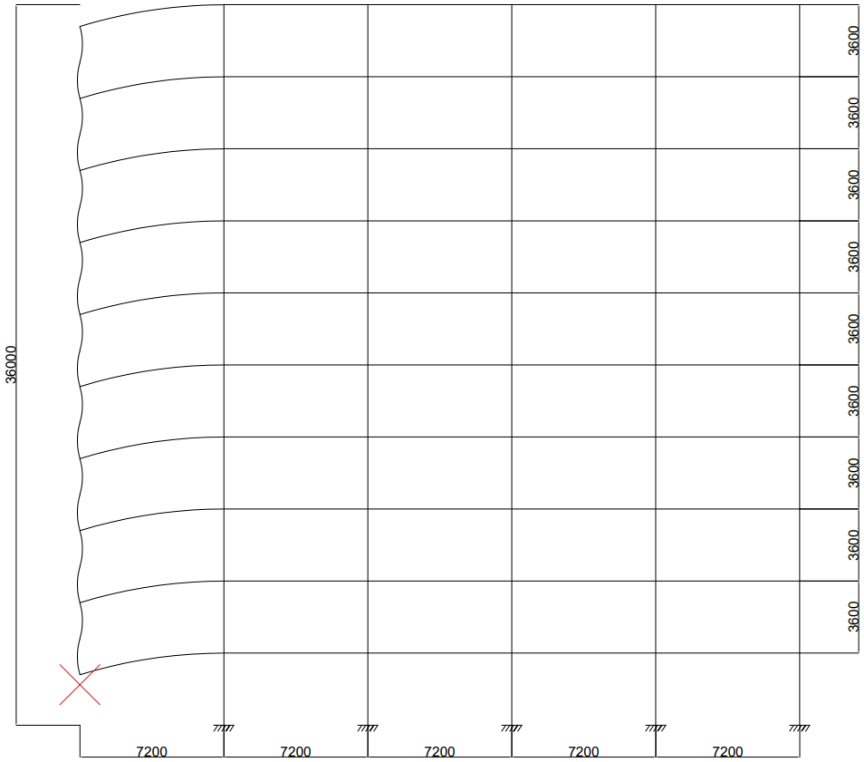


**Figure 7.27:** Vierendeelaction in the system

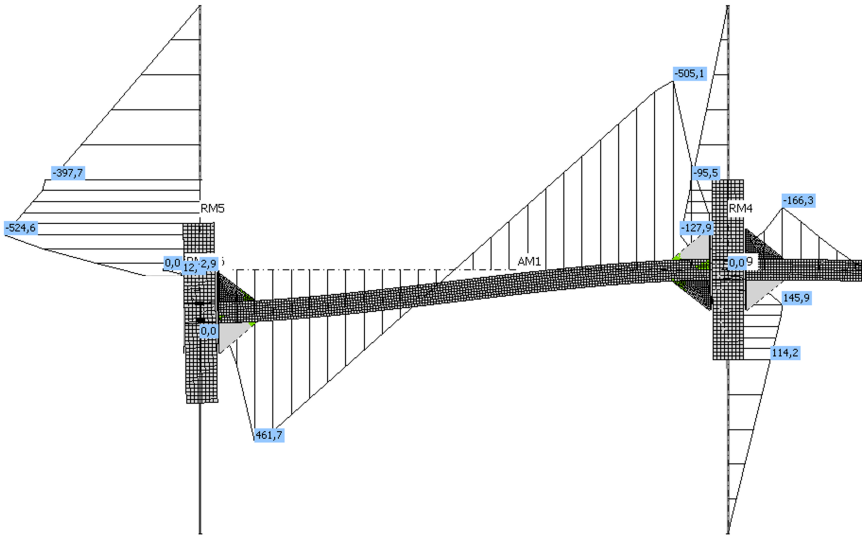


**Figure 7.28:** Moment line through the system, maximum 525 kN

Because the clamping is not completely fixed and the moment capacity decreases as the force grows, there must be a nonlinear relationship between the Moment and the rotation. This can be calculated using IDeaStatiCa. the results can be found in Figure 7.29 below.

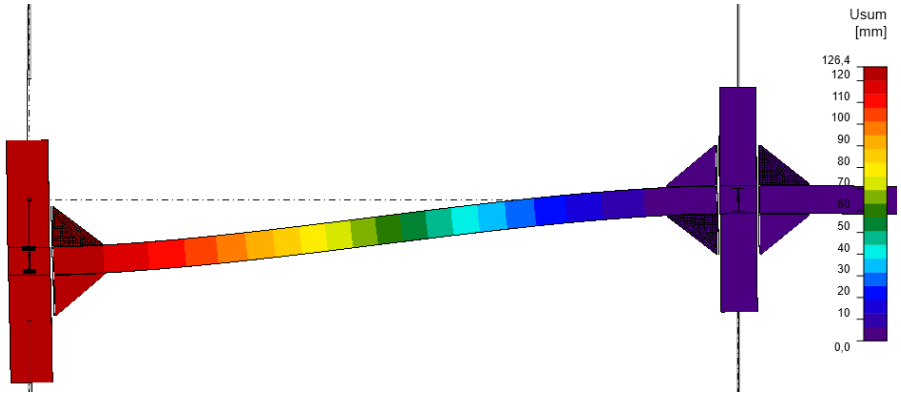


**(a)** Vertical deformation (maximum 126.4 mm)

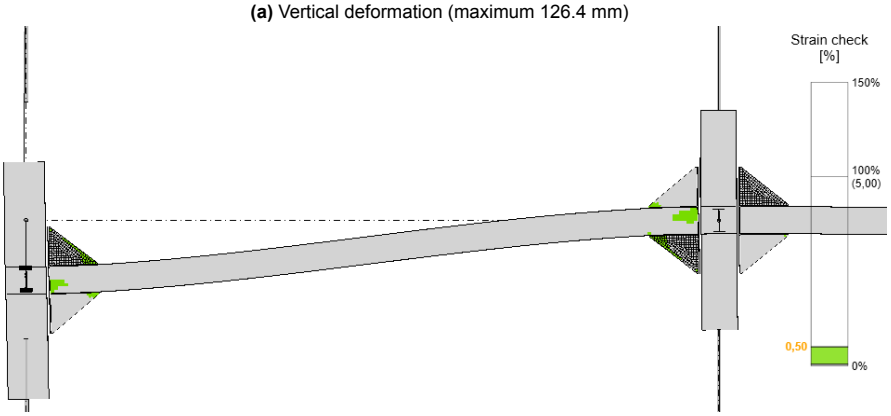


**(b)** Strain (maximum 0.5 [%])

**Figure 7.29:** Corner column removal, load of 175 kN on the left column

Figure 7.29 shows that both the deflection, which is 126 mm, and the strain of half a percent meet the requirements of 1080 mm and 15%, respectively

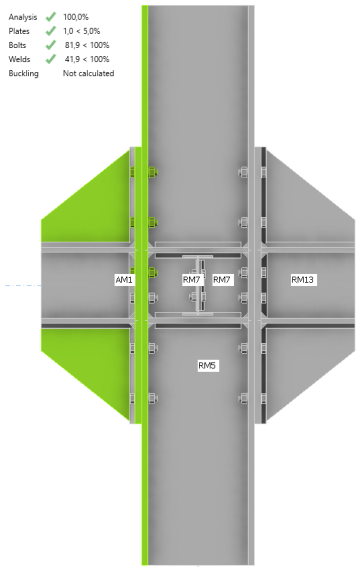


**Figure 7.30:** Moment resistant connection check in case of a corner column removal

If the forces (such as the moment from Figure 7.28) are entered into a calculation to check the connection (Figure 7.30), it can be seen that this also meets the construction requirements and can accommodate a missing column.

### Semi-rigid connection

A semi-fixed connection is between a hinged connection, which the cantilevered beam cannot support, and a fixed connection, which can support the cantilever. With a semi-fixed connection, it is therefore necessary to see whether it can handle the cantilever. The rotational stiffness of the connection is of great importance. This can be calculated with IDeaStatiCa. Figure 7.31 gives an overview of how the connection can be schematized. In this scenario, the same applies as in the previous subsection. The moment resistance of the connection should be equal to 1260 kN Equation 7.32.

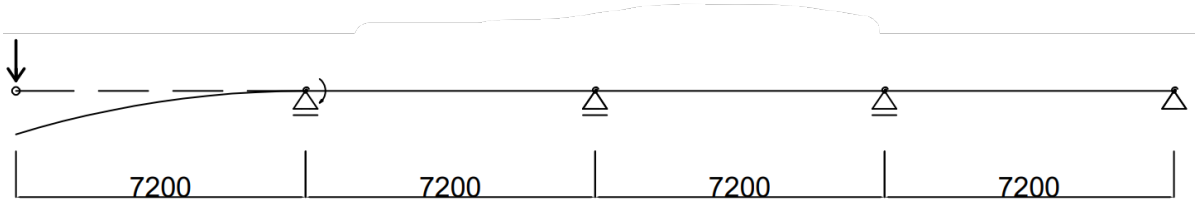


**Figure 7.31:** Corner column removed, single span beams supported by semi-rigid connections

## 7.1.3. Conclusion

When analyzing the secondary load path in various scenarios where a column fails, it appears that only moment-resisting connections are effective. In this configuration, the forces are absorbed by the beam rather than the connections. This results in a more stable and safer system, as the moments are fully transferred and the structural integrity is maintained. Hinged and semi-rigid connections provide insufficient resistance in such scenarios, which can lead to instability and potential structural damage.

Moreover, it turns out that the catenary action in these situations never actually works. The tensile forces in the connections become so large that they cannot be absorbed by the bolts, further limiting the effectiveness of this method.

One way to make the system work could be to increase the bolt cross-section or to allow the system to sag further, thereby reducing the horizontal force. A third option is to decrease the distance between the columns. These options are compared in Figure 7.32.

As shown in Figure 7.32a, a maximum shear force in the connection before the bolt shears off of 200, 300, and 400 kN is chosen, which corresponds to a bolt of type M20, M24, or M30 (class 8.8). By reducing the distance between columns, the force per column also decreases. This force is represented by the red diagonal line. It increases from 58 kN at a span of 1200 mm to a force of 350 kN on the column at a span of 7200 mm. In addition, the maximum strain of 15% must be met. This limit is indicated by the vertical red line. All points above and to the right of the vertical red line are possible. Thus, it can be seen that a span of 3000 mm is possible with an M20 bolt and a span of 4300 mm with an M30 bolt.

It should be noted that the failure mode of the situation may change in the case of a larger bolt. In these situations, the plate may fail first, so the bolt failure is no longer the leading factor.

A second possibility is a higher allowed vertical deformation of the system, where the force equilibrium changes and the horizontal forces become smaller. This option is shown in Figure 7.32b. The graph is constructed in the same way as the graph above, but due to the changing vertical displacements, the strain per system also changes. The strain per situation is indicated by a dotted line in the same color. In the graph, a vertical red line is drawn as an example for the maximum strain of 15% for the scenario where the maximum displacement is 1080 mm. The part of the blue line that is above the red diagonal and to the right of the vertical diagonal meets the strain requirement and the force requirement provided by the missing column.

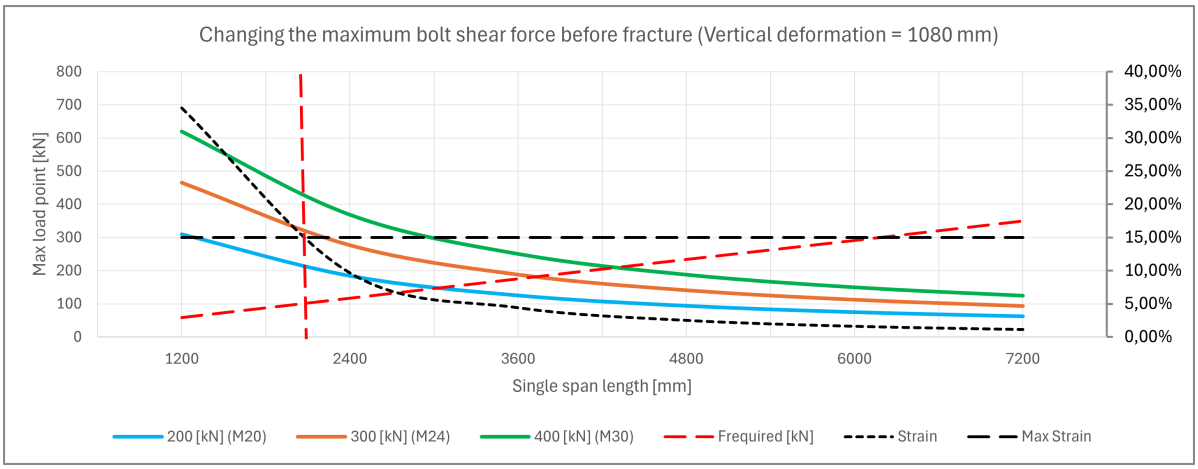


**(a)** Changing the maximum bolt shear force

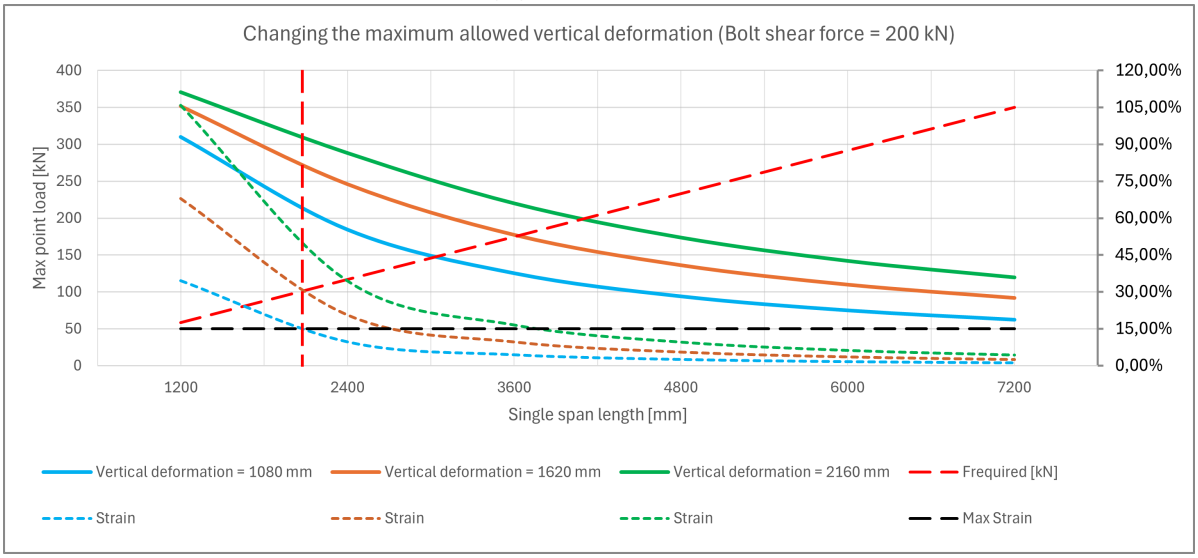


**(b)** Changing the maximum vertical deformation

**Figure 7.32:** Influence of vertical deformation and bolt strength on the maximum point load that can be applied. The design load is 350 kN

Table 7.1 shows within which margins the spans can fall to meet both the strain and the force requirements.

**Table 7.1:** Comparison of Bolt Size, Span, and Deformation Requirements

| Bolt Type (Class 8.8) | Max Shear Force (kN) | Minimum Span (mm) | Maximum Span (mm) | Allowed deformation (mm) |
|---|---|---|---|---|
| M20 | 200 | 2100 | 3100 | 1080 |
| M24 | 300 | 2100 | 3700 | 1080 |
| M30 | 400 | 2100 | 4300 | 1080 |
| **Alternative Approach: Increased Deformation** | | | | |
| M20 | 300 | 2100 | 3000 | 1080 |
| M20 | 300 | 2700 | 3600 | 1620 |
| M20 | 300 | 3800 | 4000 | 2160 |

## 7.2. Case 2: double span beams

The second case is quite similar to the first case. The difference is that the beams span two floors instead of one. This means that the beams that will be used have a length of 14.4 meters instead of 7.2 meters. A double-span steel beam offers several advantages in terms of demountability. With a double span, there are fewer connections to manage, which simplifies the disassembly process and reduces the time and effort required to dismantle the structure. In addition, they are better suited for use in other projects because longer beams can be cut to size, making them adaptable to various structural needs. The elongated beams will make the structure behave differently from the single-span beams in the case of a removed column.

### 7.2.1. Interior column removal

A double span refers to a beam that spans two columns. This concept is commonly used in construction and engineering to provide stability and distribute loads more effectively. In addition, a double span saves the number of connections, which can save money and construction time. The maximum length of beams is often limited by practical considerations, such as transport and installation. It is difficult to transport and handle very long beams on a construction site. Typically, the maximum transportable length is around 12 to 15 meters. Because the beam essentially spans over a column, there are two ways to consider the forces on the structure. In the first scenario, the force from a column will rest in the middle of the span if the column below it fails. In the second scenario, the column to which the beam is connected may fail and the force will then rest on a cantilevered beam. Both cases are discussed in more detail in the following subsection.

#### Load at midspan

When the load is at the mid-span of the beam, it can be considered as a simple single-span structure. In addition, this case can be considered as a parabolic cable shape, as can be seen in Figure 7.33. The arrow in this figure refers to the point load of the column above. The advantage arises in this situation because there are no connections in the middle of the span. The total force distribution depends solely on the fixations or hinges at both ends.

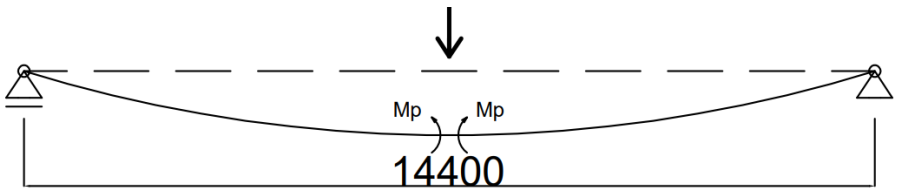


**Figure 7.33:** Interior or facade column removed at the midspan (7200 mm), beams supported by hinged connections

To calculate the elastic deformation in the beam, the formula for a parabolic cable shape under a uniform load can be derived from the principles of statics and mechanics. For a cable with a uniform load per unit length, the shape of the cable can be described by Regan's equation. The reaction forces in the horizontal and vertical directions in both connections are assumed to be F (vertical) and H (horizontal).

$$\epsilon = \frac{\Delta L}{L} \approx \frac{2}{3}\left(\frac{u}{L}\right)^2 \quad \Rightarrow \quad \frac{u}{L} \approx \sqrt{\frac{3}{2}\epsilon} \tag{7.33}$$

$$\frac{H}{F} = \frac{1}{2}\frac{L}{u} = \frac{\varphi_{\text{dyn}}}{2}\sqrt{\frac{2}{3\varepsilon}} \tag{7.34}$$

$$\frac{H}{F} = \frac{1}{2}\frac{L}{u} = \frac{1}{2}\frac{1}{\sqrt{\frac{2}{3}\epsilon}} \quad \Rightarrow \quad \epsilon = \frac{1}{6}\left(\frac{F}{H}\right)^2 \tag{7.35}$$

At a maximum deflection of 15% of the span and a span length of 7.2 meters, the maximum deformation equals:

The elongation of the steel elements will then be equal to:

$$\epsilon = \frac{1}{6}\left(\frac{1}{3.33}\right)^2 = 0.015 = 1.5\% \tag{7.36}$$

When the ends are connected with hinges, as displayed in Figure 7.33, the moment will be zero. However, this also means that the connection must be able to rotate. The connection must have sufficient rotational capacity, allowing it to deform plastically without failing. Below, the required rotational capacity of a connection in a hinged span will be calculated. This rotation can be determined using a so-called ”forget-me-nots.”

$$\theta = \frac{1}{16} \cdot \frac{Fl^2}{EI} \tag{7.37}$$

In the case of moment-resistant connections, the structure can be considered similar to a single span (column to column). However, with the double span, far fewer connections are needed to achieve the same result. How much this impacts the ease of disassembly will be calculated in chapter 8.

The IDeaStatiCa results for various point loads are given in Figure 7.34. In this figure a load of 300, 350 and 400 kN are given as point load in the middle of the span. As can be seen in the figure, the vertical deformation between 300 and 350 kN does not increase significantly. This is in contrast to the difference in vertical deformation between 350 and 400 kN.

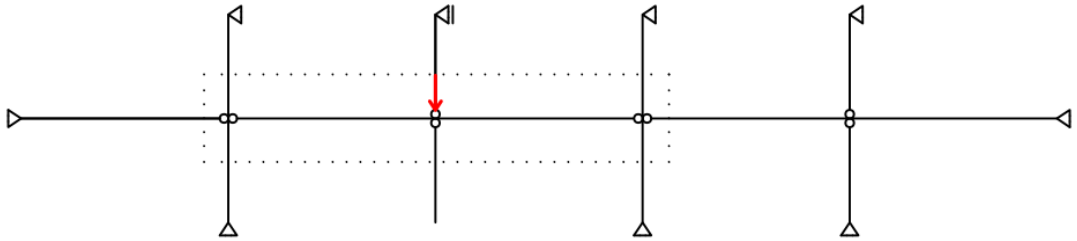

**(a)** Mechanical scheme of the situation in 2D

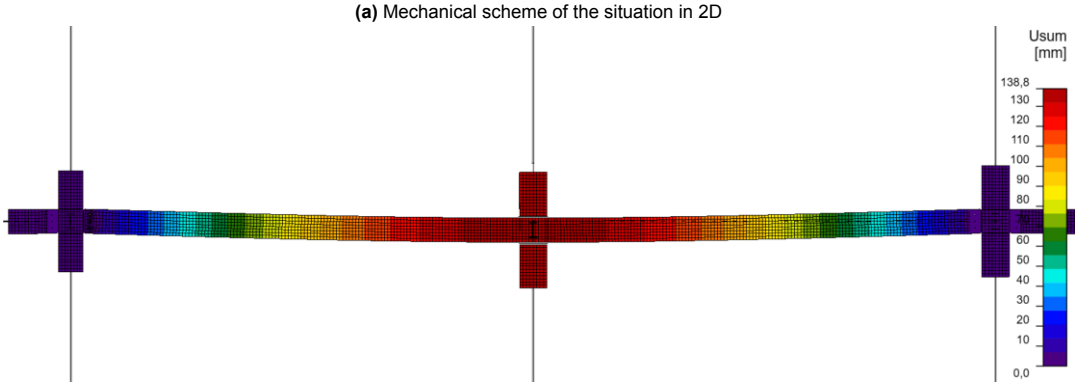


**(b)** Point load of 300 kN applied at the middle column

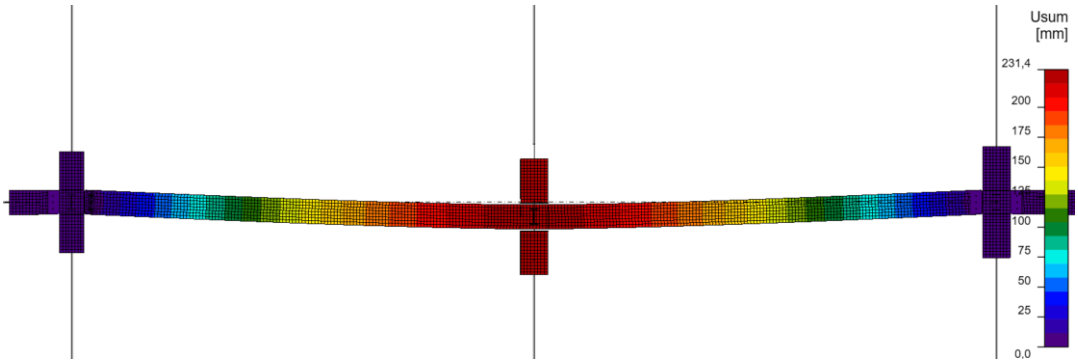


**(c)** Point load of 350 kN applied at the middle column

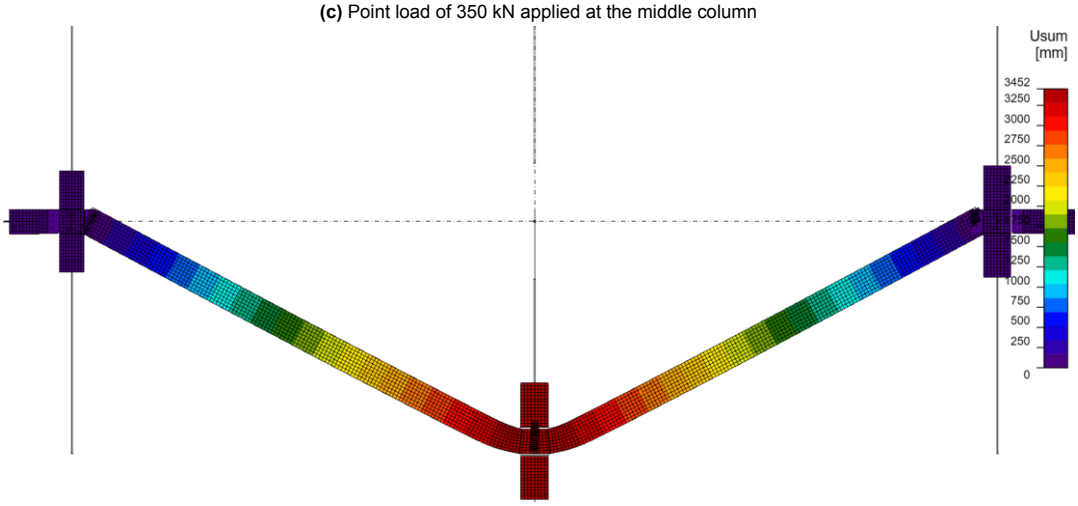


**(d)** Point load of 400 kN applied at the middle column

**Figure 7.34:** Deformation of the double span under various loads.

Zooming in on the left column (Figure 7.35), it can be seen that the bolts are not yet shown in red. This means that the top bolt (orange) is in a critical area but will not fail. The structure, as such, can withstand a force of 350 kN. In the case of 400 kN, the top bolt will fail, and the ziplocker effect, as

described in section 5.2, will occur again.

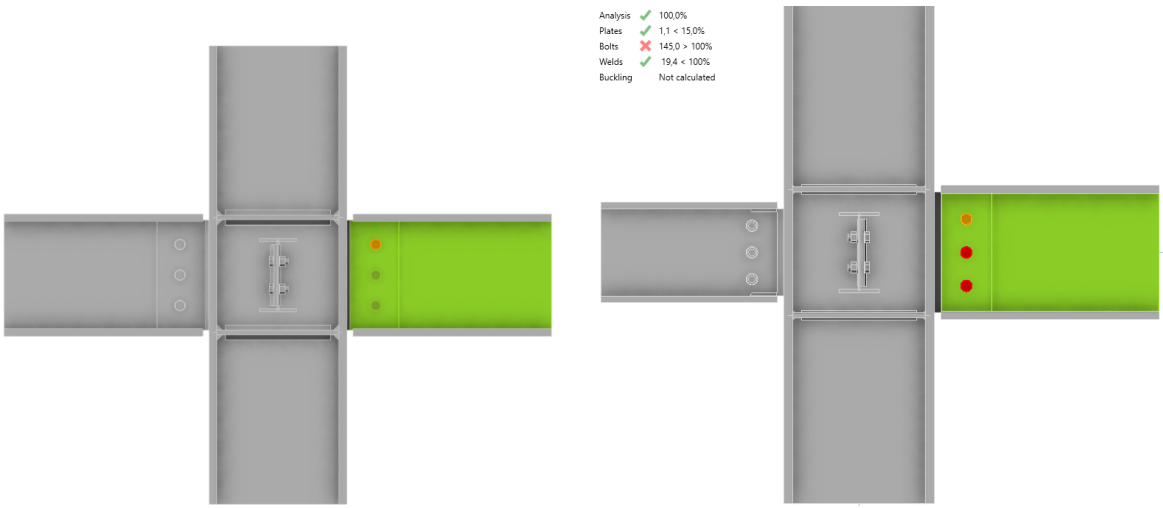


**(a)** 350 kN **(b)** 400 kN

**Figure 7.35:** Left column connection check for two forces on the middle column

### Load at location of connection

The same system as in the previous system will be used, but in this case the forces will be applied at the location of the connection(Figure 7.36). In the case of a force at the location of a hinge, a rotational moment will develop on either side at the location of the adjacent columns. In a simplified version, assuming that there is no horizontal restriction, this system can be considered as an overhanging beam. However, since some of the horizontal displacement is restricted by the connection at the location of the point load, the horizontal force on the connection will increase, along with the stresses on the bolt and the connection plates. The overall vertical deflection and the moment can be calculated using ”forget-me-nots.” The local stresses on the connection resulting from the missing column can be calculated using software. IDeaStatiCa will be used to check the connection in detail and perform the calculations on the bolts and plates.

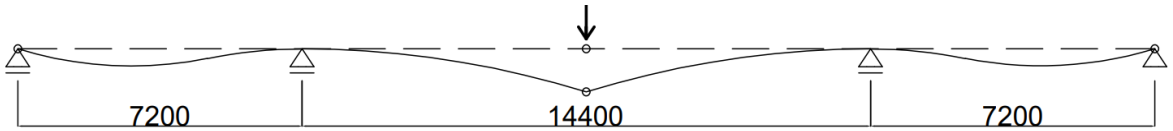


**Figure 7.36:** Interior or facade column removed, double span beams supported loaded at the hinge

The same situation as in subsection 7.2.1 was implemented in IDeaStatiCa (Figure 7.37). However, now the beam extends over the column on both the left and right sides. In this case, it can also be seen that the greatest change occurs when the force is increased from 350 to 400 kN.

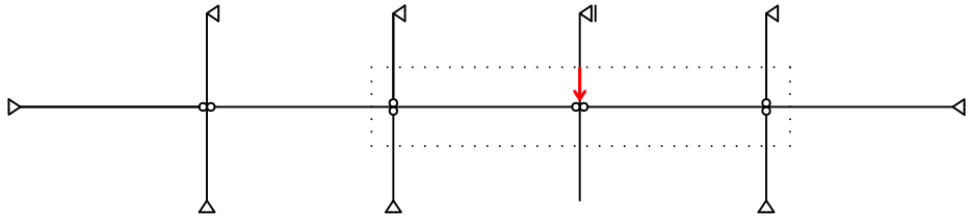

**(a)** Mechanical scheme of the situation in 2D

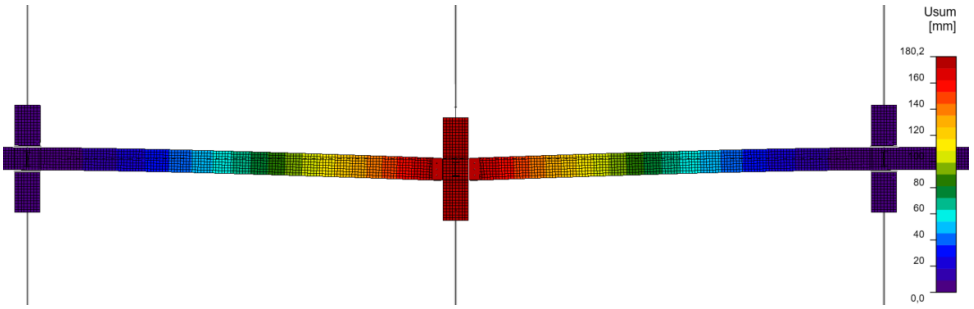


**(b)** Point load of 300 kN applied at the connection column

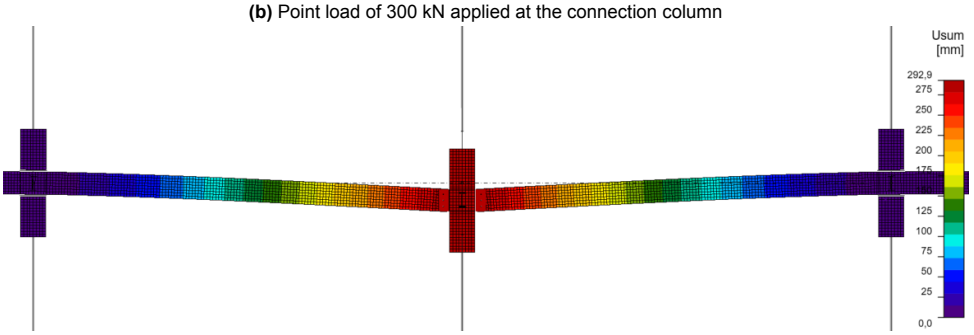


**(c)** Point load of 350 kN applied at the connection column

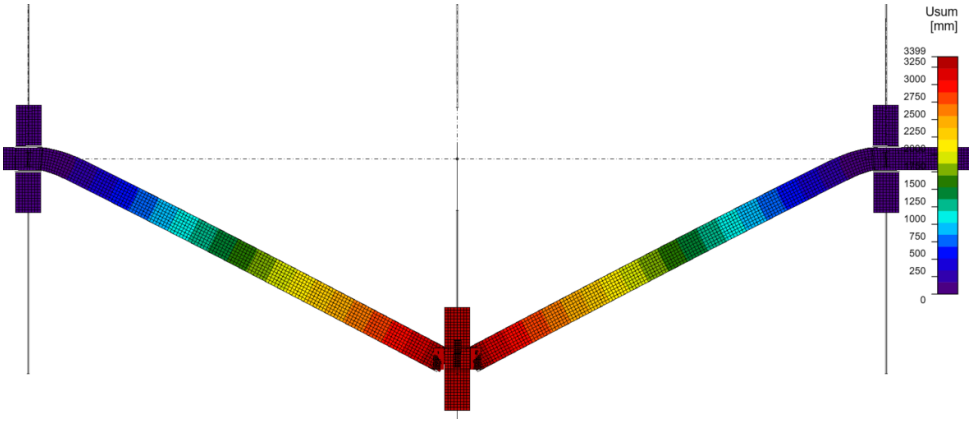


**(d)** Point load of 400 kN applied at the connection column

**Figure 7.37:** Double span situation loaded at the connection column. The beam is continuous over the left and right columns.

Zooming in on the middle connection (Figure 7.38), it can be seen that the elements of the connection are sufficient and do not exceed the limits at a force of 350 kN but fail at a force of 400 kN.

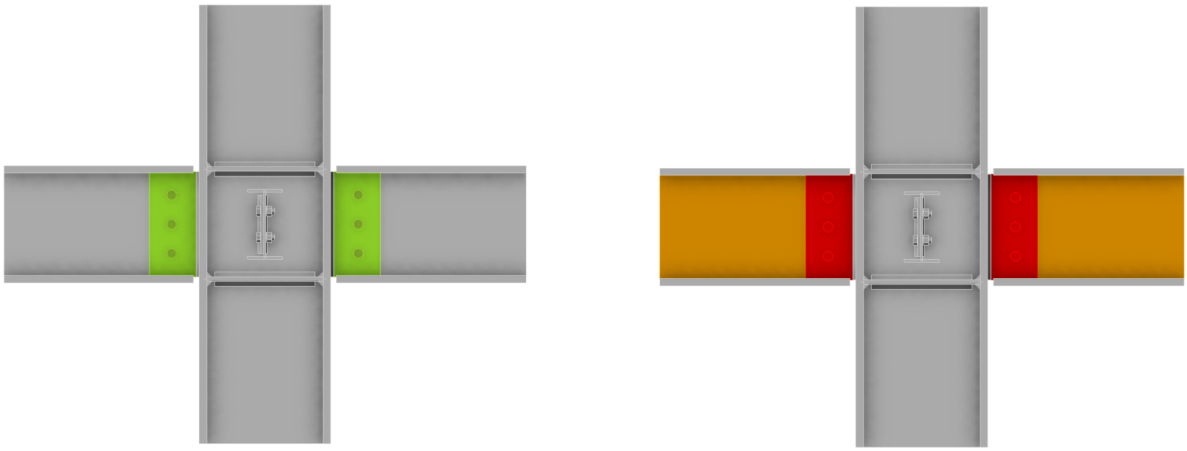

**(a)** 350 kN **(b)** 400 kN

**Figure 7.38:** Detailed overview of the connection of the middle column. Green=good, orange=warning, red=failure

### 7.2.2. Facade or corner column removal

In the case of a double span, the span must extend to the facade. If this is not the case and stops one span before the facade, an additional shorter beam must be added. If this beam is hinged, it means that the secondary load path must be achieved through the floor system (Figure 7.39).

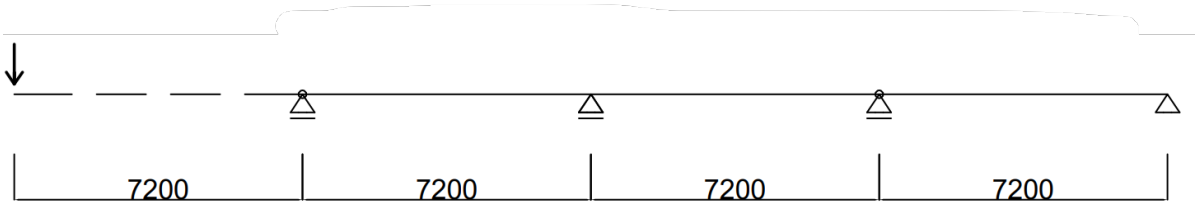


**Figure 7.39:** Corner column removed, double span beams supported by hinged connections, situation 1

In the case of a double span that ends at the facade, a support moment will occur at the adjacent columns (Figure 7.40). This configuration allows the double span to potentially provide a secondary load path.

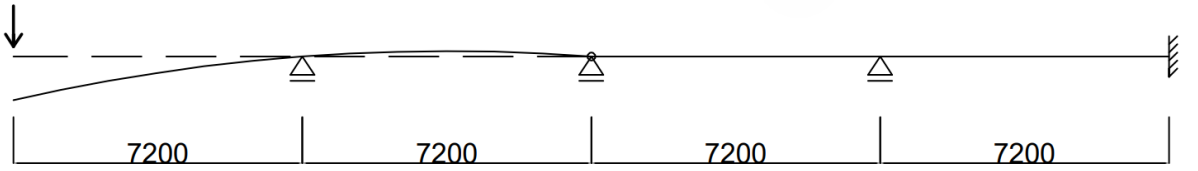


**Figure 7.40:** Corner column removed, double span beams supported by hinged connections, situation 2

$$M_{\text{middle}} = P \times 7.2\,\text{kNm} \tag{7.38}$$

In the situation of Figure 7.40 there are two situations in which the beam resists the moment in the middle of the beam. These are:

- **Simply Supported**: The middle support does not resist the moment; the beam experiences the moment as a bending moment.

- **Clamped**: The middle support resists the moment, effectively clamping the beam (by the columns) and preventing/minimizing rotation at that point.

In the clamped scenario, the beam itself must take up the moment, resulting in higher internal stresses and deflections near the clamped support.

To calculate the maximum bending moment resistance of a HEB400 beam, we use the following formula:

$$M = \frac{W_{pl} \times f_y}{\gamma_{M0}} \tag{7.39}$$

Where:

- $M$ is the maximum bending moment resistance.
- $W_{pl}$ is the plastic section modulus.
- $f_y$ is the yield strength of the material.
- $\gamma_{M0}$ is the partial safety factor for material properties.

For a HEB400 beam:

- The plastic section modulus $W_{pl}$ is $3232.35\,\text{cm}^3$ (or $3.23235 \times 10^6\,\text{mm}^3$).
- The yield strength $f_y$ for structural steel is generally $355\,\text{MPa}$.
- The partial safety factor $\gamma_{M0}$ is generally 1.0 for steel.

Plugging in these values:

$$M = \frac{3.23235 \times 10^6\,\text{mm}^3 \times 355\,\text{MPa}}{1.0} = 1147\,\text{kNm} \tag{7.40}$$

$$\text{Unity check: } \frac{1260}{1147} = 1.1 > 1.0 \tag{7.41}$$

This means the beam can not take up the bending moment according to the simple hand calculation kNm (Equation 7.32).

When we completely release the column, we will see a similar outcome in IDeaStatiCa, as shown in Figure 7.41. We can also see that the strain exceeds the maximum of 15%. However, it should be noted that the column is connected at the top. This causes the moments to shift (due to the Vierendeel action), and the system cannot be considered as a full cantilever. This also gives the results for the deflection and strain, which can be seen in Figure 7.42 and Figure 7.43.

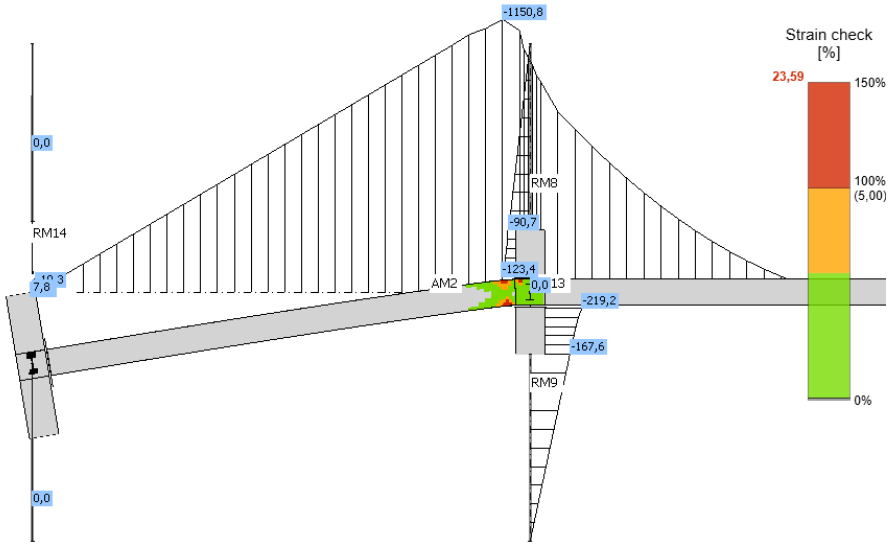


**Figure 7.41:** Clamped situation, Moment given by the line and strain given by colorpalet

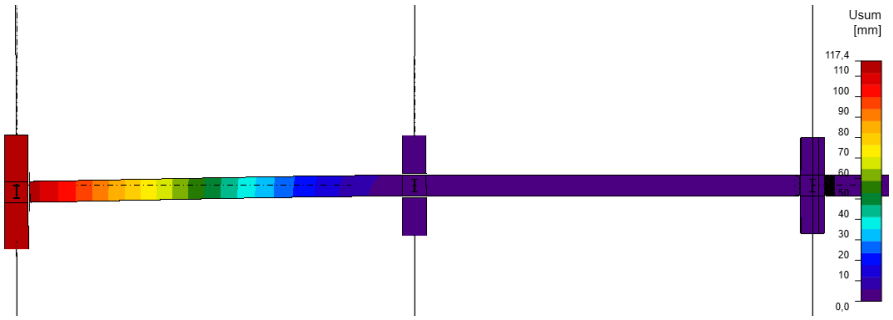


**Figure 7.42:** Total vertical deformation (maximum 117.4 mm)

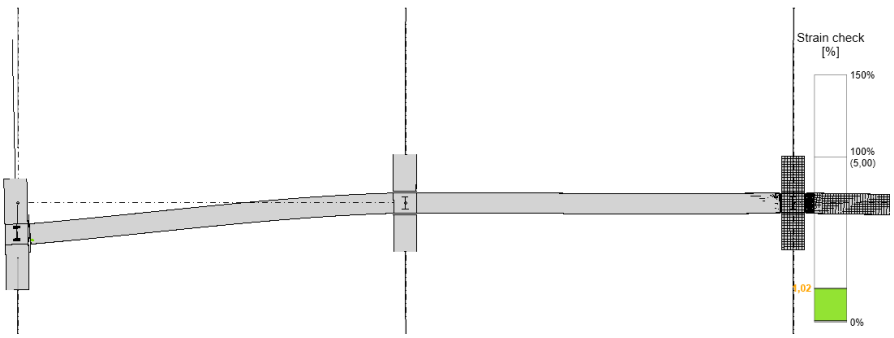


**Figure 7.43:** Strain check of the cantilever (1.02%)

### 7.2.3. Conclusion

The system using a double span proves to work very well because the forces from the missing column are mostly absorbed by the bending stiffness of the beam and not by the connections. The maximum force of a missing column that this system can handle is 350 kN, which is exactly the same as a scenario where a column falls away. Therefore, the bending stiffness of the beam works much better than the catenary action. However, the maximum length of beams and their transportation must be taken into account. As long as the beam can be transported without special modifications to the transport, using a beam over columns is a good option.

## 7.3. Case 3: Gerber beams

For a Gerber beam, unlike a normal span, the hinges are not placed at the location of the columns. By shifting the hinges, the moment in the connections is reduced. One advantage of placing the connection close to the zero-moment point is that a less robust connection is required, allowing for savings on the number of bolts. In addition, the hinge on a Gerber beam is easier to access, which is very practical for replacing a component or dismantling it.

A Gerber beam is relatively easy to assemble and disassemble because of its hinged connections. This makes it easier to remove or adjust parts of the structure without having to dismantle the entire framework. However, the shorter beams in a Gerber beam system are less easily reusable. This is because they are specifically designed for their original position and function, which can complicate their reuse in other constructions.

How the beam is divided along the length of the building can be seen in Figure 7.47. Based on the shear forces in a ULS situation provided by Technosoft, the maximum shear forces in the connection can be calculated. The span is 7.2 meters, and the hinges are located at $x = 1.8\,\text{m}$ and $x = 5.4\,\text{m}$.

$$\text{Shear force} = \frac{2 \times 235\,\text{kN}}{7.2\,\text{m}} \times 1.8\,\text{m} = 117.5\,\text{kN} \tag{7.42}$$

As can be seen in Figure 7.45 and a maximum shear force of 117 kN per bolt, two bolts need to be applied on each side of the plate of the Gerber beam connection (see Figure 7.46).

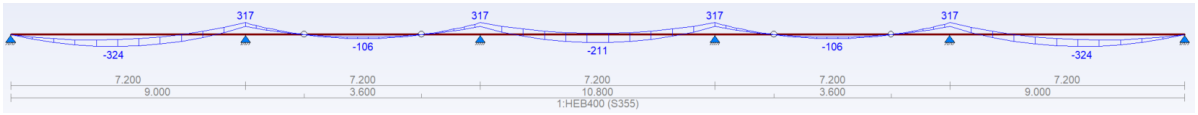


**Figure 7.44:** Gerber-beam Moment distribution under ULS load.

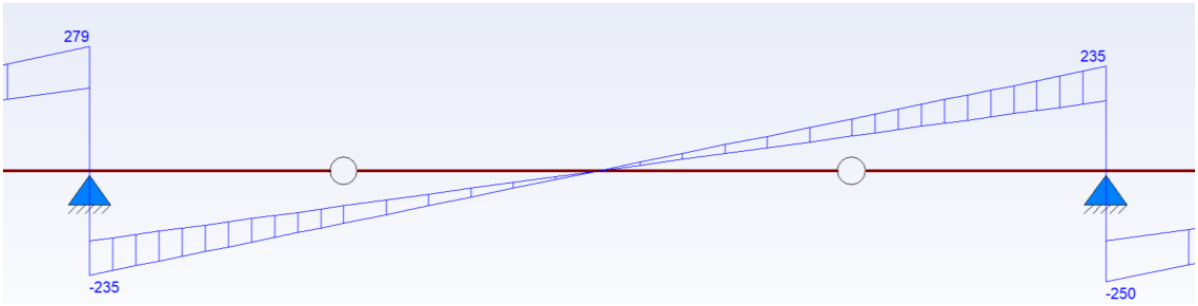


**Figure 7.45:** Shear forces Gerber beam, support to support equals 7.2 m, hinge to hinge equals 3.6 m

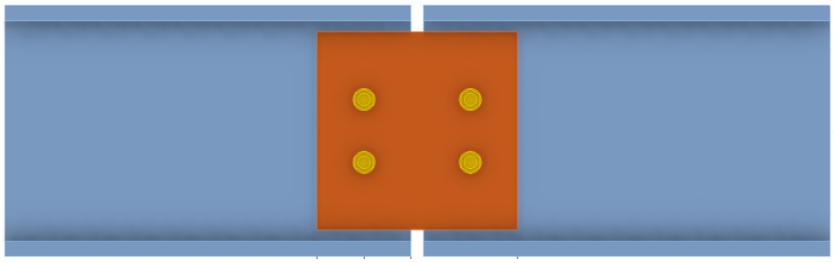

**Figure 7.46:** Connection between the beams. 4 Bolts of type M20.

The joints of the Gerber beam are designed to avoid taking up moments. However, if a column drops, these moments shift. Consequently, the hinged joints will rotate and begin to bear moments. In such a scenario, two bolts are insufficient to handle the resulting twisting.

### 7.3.1. Facade or interior column removal

The Gerber beam situation is expected to deform as given in Figure 7.47.


**Figure 7.47:** Interior or facade column removed, Gerber beams supported by hinged connections

For the Gerber situation, IDeaStatiCa is used again. As shown in Figure 7.48, there is little difference in deflection when the forces are increased from 250 to 350 to 450 kN. The highest stresses occur in the connection of the column above the point where the column has fallen away. Because the beam below does not drop straight down but bends, the column above will have to accommodate this bending.

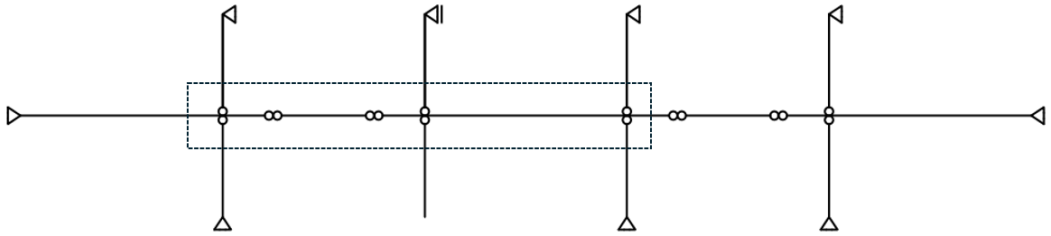

**(a)** Mechanical scheme of the Gerber situation in 2D

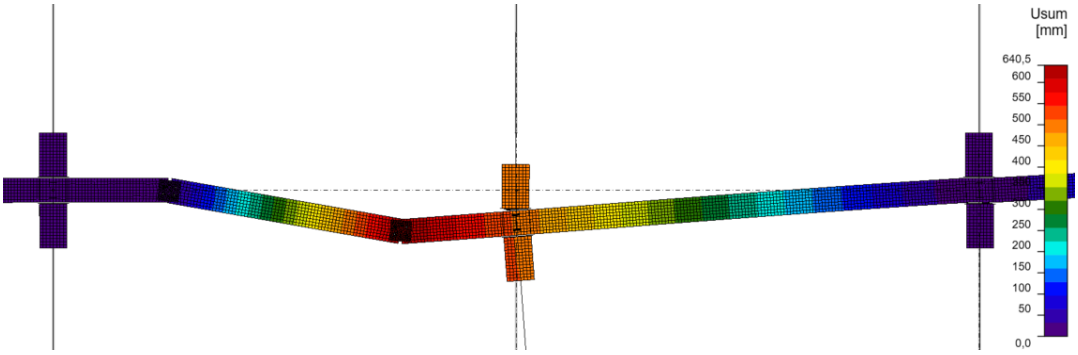


**(b)** Point load of 250 kN

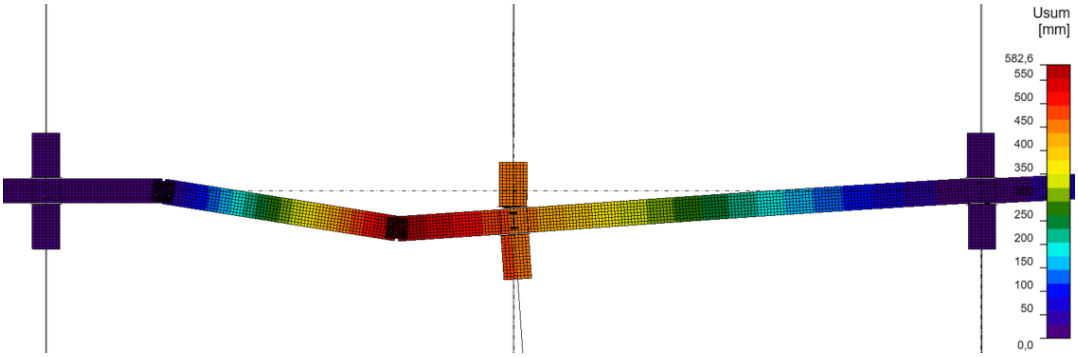


**(c)** Point load of 350 kN

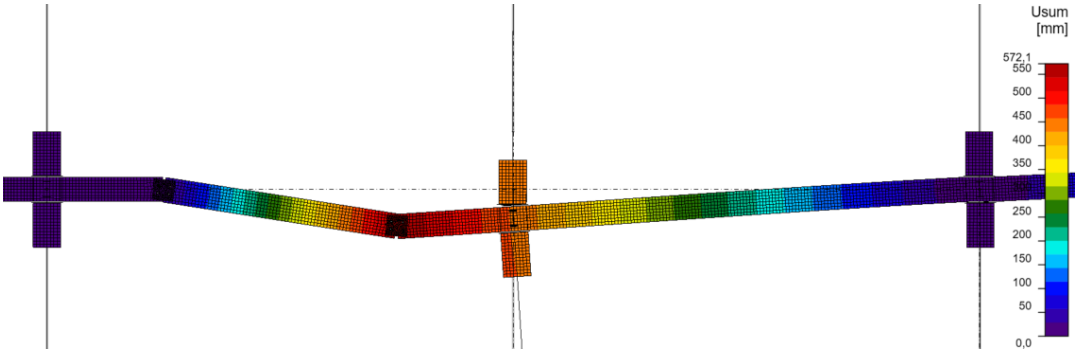


**(d)** Point load of 450 kN

**Figure 7.48:** Deformation of the Gerber-beam situation under a point load

Zooming in on the right Gerber connection, we can see that the two-bolted system is not strong enough (Figure 7.49a). Changing the connection to a situation with three bolts solves the problem and makes the connection strong enough to bear the load of 350 kN. This can be seen in Figure 7.49b

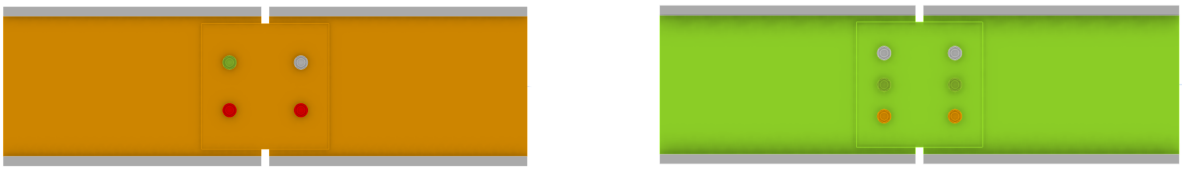

**(a)** 2 bolts on both sides

**(b)** 3 bolts on both sides

**Figure 7.49:** IDeaStatiCa results of the connection under a load of 350 kN

In case of the Gerber beam, the system that will occur is a combination of catenary action in the shorter beam in the middle and flexural action in the longer beams that are continuous. The distribution of normal foces in the beams can be found in Figure 7.50, this figure is a result after the changes made in Figure 7.57. The normal forces in the connection are somewhere equal to 100 kN. The normal force on the right side of the removed column is equal to 86 kN. The moment distribution can be found in Figure 7.51 and equals 100 around the connections. On the right side of the left column, the moment equals 220 kN. On the left side of the right column, the moment in the beam is equal to 850 kN.

In the case of a fully fixed beam of 14 meters (column edge to column edge) with a point load of 350 kN in the middle, the moments at both ends are 612.5 kNm. The sum of the moments on the left and right in that case is 1225 kNm. In the case of the Gerber beam, it can be seen that the sum of the moments in the left and right columns in Figure 7.51.

$$\frac{23}{350} = 7\% \text{ catenary action} \tag{7.43}$$

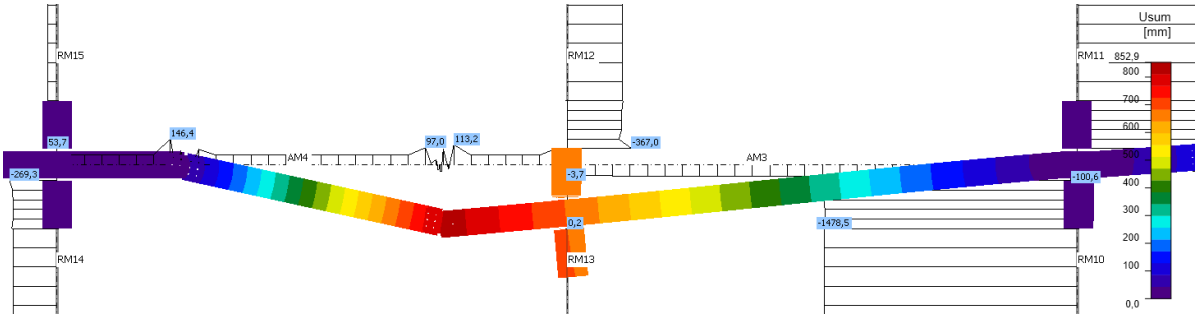


**Figure 7.50:** Normal force distribution in the Gerber beam under a column removal and a point load of 350 kN on the middle column. The normal force on the right side is 100 kN

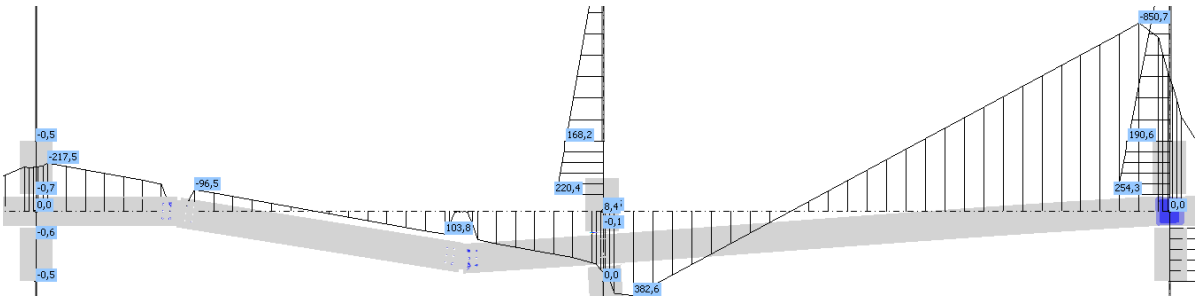


**Figure 7.51:** Moment distribution in the Gerber beam under a column removal and a point load of 350 kN on the middle column.

Figure 7.52 displays the force equilibrium in the right Gerber connection based on a force of 100 kN in the right beam of the meter. Figure 7.50. This results in a total load of 23 kN in vertical direction. Referring back to the total force of 350 kN vertical, this means that the percentage absorbed by the catenary is equal to the following.

$$\frac{23 \text{ kN}}{350 \text{ kN}} \approx 7\% \tag{7.44}$$

7% is taken up by catenary action, and 93% is taken up by the flexural action.

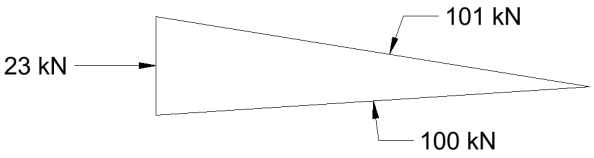


**Figure 7.52:** Force equilibrium of the right gerber connection

### 7.3.2. Corner column removal

Because a Gerber beam is not part of the standard ”forget-me-nots” of mechanics and the entire length of the structure contributes to achieving rotational stiffness and thus the deflection of the floor at the corner, Technosoft software is used.

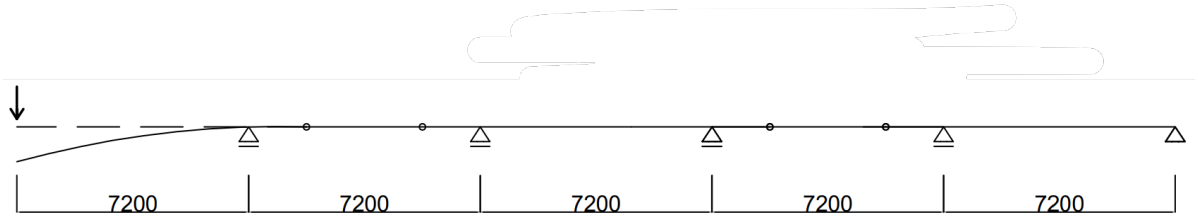


**Figure 7.53:** Corner column removed, Gerber beams supported by hinged connections

In the figure above, the connections are indicated as hinges. Because the connection consists of four bolts, it will never be fully hinged but will also take up a moment. This is necessary because otherwise, in the case of the point load, an unstable situation would arise where the left hinge is pushed up, causing the leftmost support to shift to the right. Because the connection makes the whole assembly generally rigid, this will happen less quickly.

The Gerber beam and the situation where a column in the facade falls away are also modeled in IDEAStatiCa. Under a point load of 175 kN, the beam will bend as shown in Figure 7.54 and Figure 7.55.

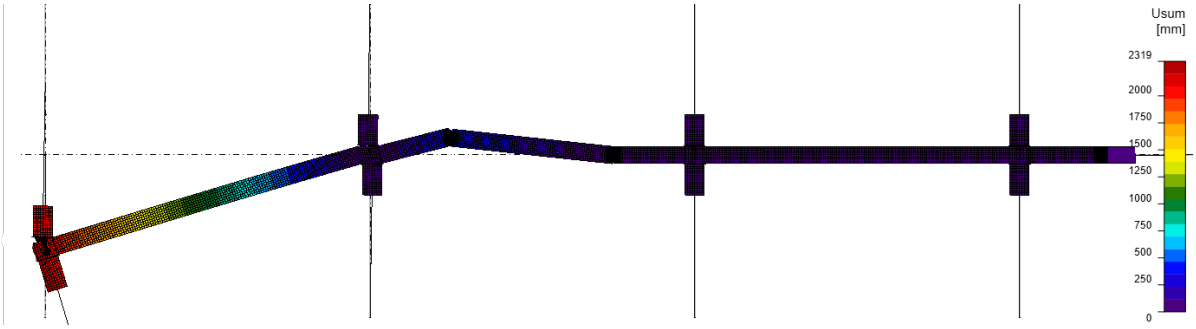


**Figure 7.54:** Total deformation of the Gerber beams under a force load 175 kN on the column.

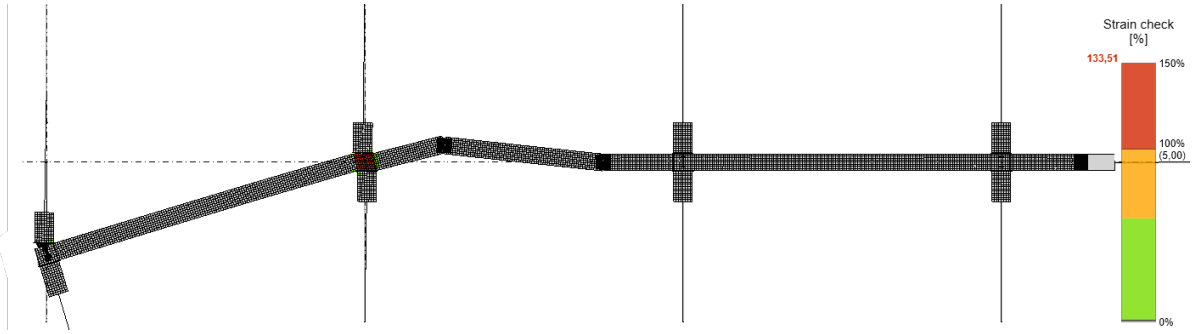


**Figure 7.55:** Strain check of the Gerber beams under a force load 90 kN on the column.

Zooming in on Figure 7.55, the areas where the strain is at its highest are visible. In Figure 7.56a, it can be seen that the maximum deformation is in the end plate of the top column. As long as the end plate is still connected to the beam in some way, a progressive collapse can be prevented. However, in Figure 7.56b, it can be seen that there are also high strains between the columns, where the beam is clamped by these columns. The strain in this part equals 21.6 %. The strain at the location of the plate is equal to 29.5 %. These values are both higher than 15 %, so they do not meet the previously stated requirement.

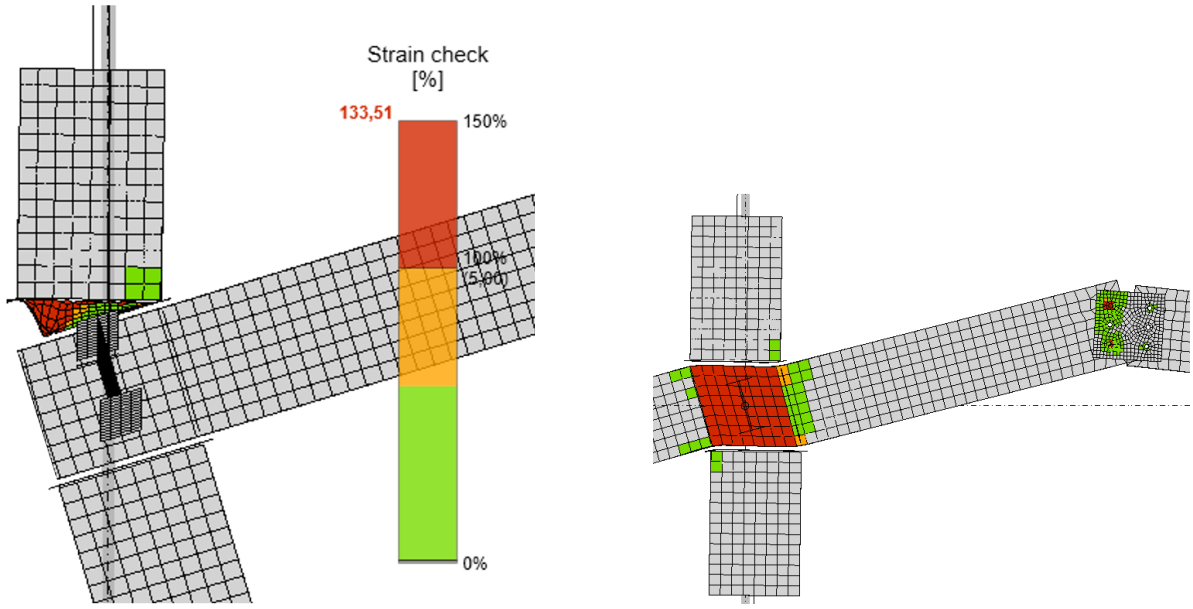


**(a)** Left column **(b)** Middle column and finplate

**Figure 7.56:** Total deformation of the Gerber beams under a force load 175 kN on the column.

An adjustment to the element needs to be made to allow the Gerber beam to function. A larger plate with more bolts could provide a solution, but this also affects the eventual disassembly of the connections and, consequently, the building. The adapted connection layout can be seen in Figure 7.57. To check if 6 bolts are sufficient, the connection was re-entered into IDeaStatiCa. It is important to keep in mind that the connection was initially chosen because it was moment-free. More bolts also mean that the connections attract more moments. However, this is necessary to make the connection stiffer and to reduce the buckling at the column.

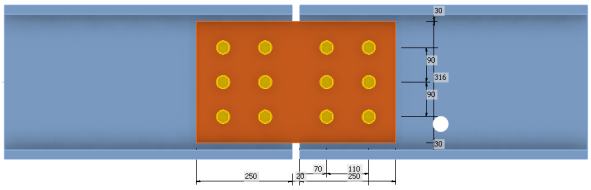


**Figure 7.57:** Adapted connection

In Figure 7.58a, the maximum deflection is noticeably reduced when using 6 bolts compared to 3. The strain in the connection remains highest in the end plate atop the left column.

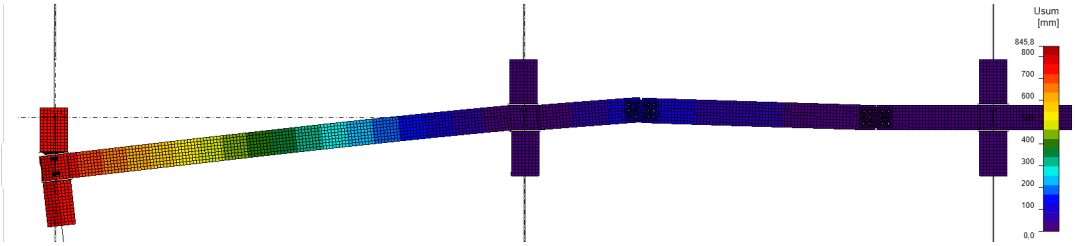


**(a)** Total deformation of the Gerber beams under a force load of 175 kN on the left column.

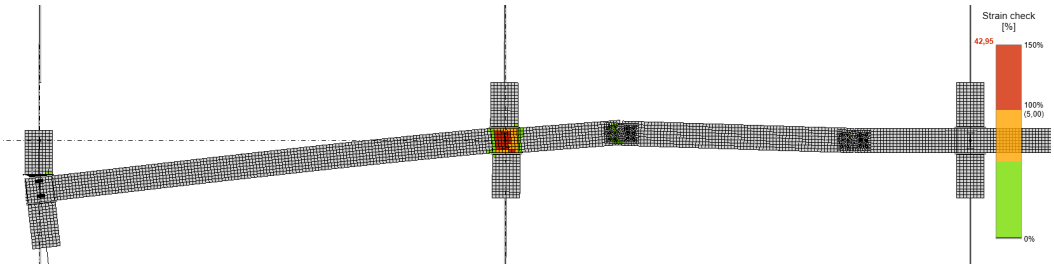


**(b)** Strain check of the Gerber beams under a force load of 175 kN on the left column.

**Figure 7.58:** Combined figures of total deformation and strain check of the Gerber beams under a force load of 175 kN on the left column.

In Figure 7.59a, you can see that the connection meets the requirements for the bolts. In Figure 7.59b, the locations of the greatest strains are shown. The maximum strain at the column is 5.7 % and at the end plate 3.0 %

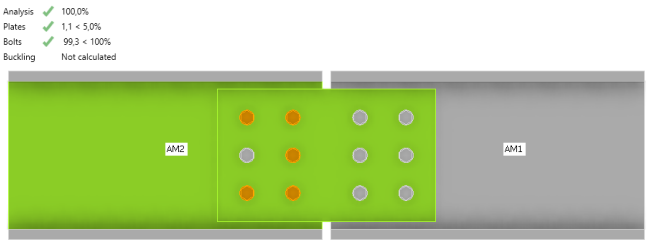


**(a)** Total deformation of the Gerber beams under a force load 175 kN on the column.

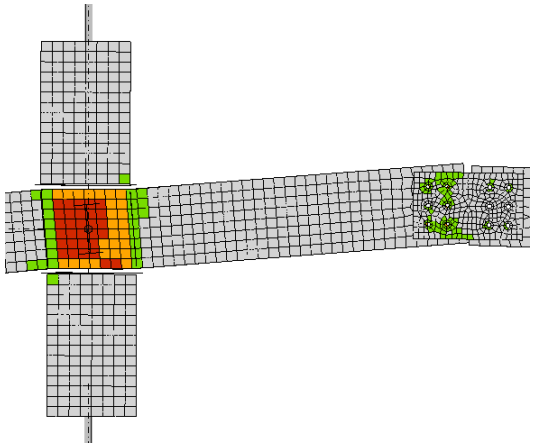

**(b)** Strain check of the Gerber beams under a force load 175 kN on the column.

**Figure 7.59:** Total deformation and strain check of the Gerber beams under a force load 175 kN on the column.

### 7.3.3. Conclusion

Due to the strategic placement of the hinges in a Gerber beam situation, a system can be developed without complex connections while still providing sufficient resistance against the loss of a column in the middle of the structure, as well as in the facade or corner.

## 7.4. Membrane action

When a column is removed from a floor system, the surrounding structure must redistribute the loads to prevent collapse. The membrane action of the concrete floor is also part of this process. Membrane action keeps the development of tensile and compressive forces within the slab. When a column is removed, the immediate area around the missing column experiences a sudden loss of support, causing the slab to deform and sag. As the slab sags, tensile forces develop in the central area of the slab, which acts like a stretched membrane to help carry the loads across the opening created by the removed column. Around the perimeter of the affected area, a compressive ring (simplified as diagonals in Figure 7.60) forms, which balances the tensile forces in the middle and provides additional stability. In some cases, especially with significant deformations, the slab may also develop a catenary action, acting like a hanging cable with tensile forces carried along the edges. The combination of tensile membrane action and the compressive ring enables the slab to redistribute the loads to adjacent columns and structural elements.

To achieve the forces in the compressive ring, the force will be divided into a force in the direction of the hollow core slab and a force perpendicular to it (Figure 7.61). The force in the longitudinal direction must be transferred through the joint between the hollow core slabs. To determine if it meets the requirements, a calculation of the shear forces in the joint can be performed.

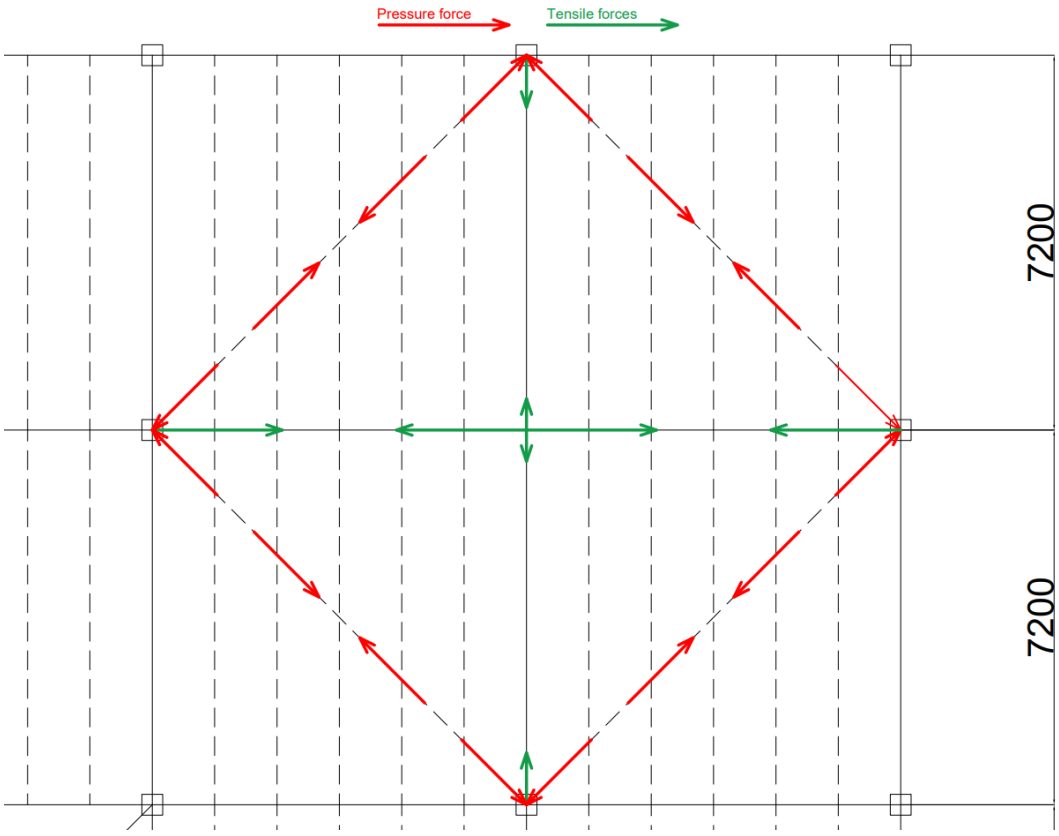


**Figure 7.60:** Membrane action due to the internal tie forces.

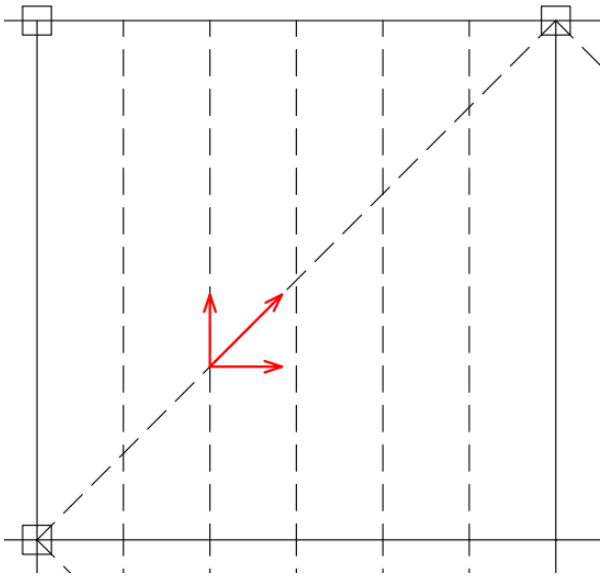

**Figure 7.61:** Membrane action (diagonal) and the resolving shear force in the joint (vertical) and a resolving horizontal force

This calculation concerns the shear capacity of pocket joints in a 200 mm thick hollow core slab with a length of 7200 mm. The shear capacity depends on the concrete strength, reinforcement, and joint filling material.

Properties:

- Concrete strength: C45/55
- Joint filling: Sand-cement mortar (C12/15)
- Reinforcement: Prestressed reinforcement
- Slab thickness: 200 mm
- Slab length: 7200 mm

The shear capacity $V_{rd}$ can be calculated using the following formula:

$$V_{rd} = \tau_{rd} \cdot A_c \tag{7.45}$$

Where:

- $\tau_{rd}$ is the design value of the shear stress, depending on the concrete strength and joint filling.
- $A_c$ is the effective area of the joint.

Given:

- $\tau_{rd,\text{concrete}} = 0.3$ MPa
- $\tau_{rd,\text{joint filling}} = 0.15$ MPa
- $A_c = \text{thickness} \times \text{length} = 200 \text{ mm} \times 7200 \text{ mm} = 1,440,000 \text{ mm}^2$

$$V_{rd,\text{concrete}} = \tau_{rd,\text{concrete}} \times A_c = 0.3 \text{ MPa} \times 1.44 \text{ m}^2 \times 1000 = 432 \text{ kN} \tag{7.46}$$

$$V_{rd,\text{joint filling}} = \tau_{rd,\text{joint filling}} \times A_c = 0.15 \text{ MPa} \times 1.44 \text{ m}^2 \times 1000 = 216 \text{ kN} \tag{7.47}$$

The total shear capacity is:

$$V_{rd,\text{total}} = 648 \text{ kN} \tag{7.48}$$

When a concrete floor absorbs membrane action due to a failed column, the forces in the diagonal of the membrane can indeed become quite high. While the middle of the floor might handle these forces well, the edges and corners can experience significant stress concentrations. At the edges and corners of the floor, stress concentrations occur naturally due to the abrupt change in geometry. This can lead to high local stresses that need to be taken into account. One way to address these high stresses is by applying additional reinforcement. Extra steel bars or meshes can be used to distribute the stresses more evenly and thereby prevent cracks. Other possible applications to distribute the high stresses include using curved or chamfered edges instead of sharp corners. Furthermore, the anchoring of the reinforcement at the edges and corners is crucial. Proper anchoring ensures that the reinforcement can effectively withstand tensile forces without shifting or failing. Finally, it is important to consider the interaction between the steel beam and the concrete floor.

## 7.5. Cost Analysis

Table 7.2 indicates estimated costs of steel connection structural members and operations from IDEA StatiCa data. The estimated costs, which are Netherlands-specific, encompass steel component cost, welding, bolt assembly, and hole drilling. This is important in evaluating the economic viability of different demountable building types. With the inclusion of cost factors in design, structural stability can be combined with economic effectiveness by engineers. This information is used as a basis for comparing various types of connections and determining their cost-effectiveness in relation to their structural stability. The default settings were used for these estimations.

| Component | Estimated Cost |
|---|---|
| Steel parts | €2.00 per kg |
| Welds | €40.00 per kg |
| Bolt assemblies | €5.00 per kg |
| Hole drilling | 30% of bolt assembly cost |

**Table 7.2:** Estimated Costs in the Netherlands/Europe

In Table 7.3, the costs of the connections are shown. The detailed cost calculations can be found in Appendix B.

| Scenario | Cost per connection | Number of connections | Total cost | Cost per $m^2$ |
|---|---|---|---|---|
| Single span, hinged | €237 | 10 | €2,384.83 | €9.22 |
| Single span, rigid | €1,675 | 10 | €16,764.86 | €64.62 |
| Single span, semi-rigid | €735 | 10 | €7,344.19 | €28.36 |
| Double span | €237 | 6 | €1,432.13 | €5.53 |
| Gerberspan | €68 | 4 | €272.16 | €1.05 |

**Table 7.3:** Total and Adjusted Cost of Connections per Square Meter with Additional Details

## 7.6. Conclusion

Comparison of five different beam configurations (Table 7.4) and their corresponding failure modes has helped to provide information on structural strength and load redistribution. The key conclusions of this work are as follows and can also be found in Table 7.5. It should be noted that a unity check of 1.00 is not realistic, and in practice, the connection should be examined more closely. In this study, a unity check of 1.0 is considered acceptable because the focus is on whether the structure can handle 350 kN. Deviations were only made if the result was significantly lower or much higher.

| Nr | Span type | Length [m] | Connection |
|---|---|---|---|
| 1a | Single span | 7.2 | Hinged |
| 1b | Single span | 7.2 | Rigid |
| 1c | Single span | 7.2 | Semi-Rigid |
| 2 | Double span | 14.4 | Hinged |
| 3 | Gerber span | 10.8/5.4 | Hinged |

**Table 7.4:** Scenarios

Hinged single-span beam connections demonstrated a high probability of connection failure at 50 kN point load. However, rigid connections supported much higher loads, up to 400 kN, with a unit control value of less than 1.0 (see Figure 7.62). Semi-rigid connections exhibited partial plastic deformation under load with a high local stress concentration. Although they redistributed some load, their failure modes had little structural strength relative to rigid connections. Adding a double span increased overall robustness, enabling local yielding without causing a successful load redistribution failure. The tests proved that a point load of 350 kN could be resisted without structural failure. The Gerber beam scenario created effective plastic hinges that provided load redistribution. The redistribution mechanism provided structural stability in failed conditions and constituted an operational trade-off between disassembly and strength. In the case of catenary action, membrane action needs to be used to provide a building's resilience upon column failure. However, areas near edges and corners possess concentrated stress, where local failure will only be hindered by secondary reinforcement.

| Scenario | Point load kN | Unity check | Failure Mode |
|---|---|---|---|
| 1a | 50 | 7.00 | Connection failure due to excessive deflection |
| 1b | 400 | 0.88 | Yielding at the connection, no collapse |
| 1c | 150 | 2.33 | Partial plastic deformation, failure due to deflection |
| 2 | 350 | 1.00 | Localized yielding, successful load redistribution |
| 3 | 350 | 1.00 | Plastic hinge formation, redistribution effective |

**Table 7.5:** Failure modes of the systems

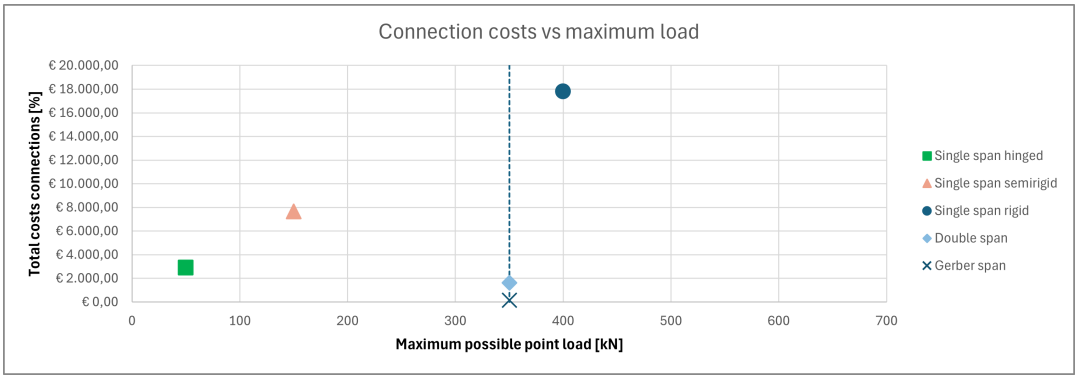


**Figure 7.62:** Total cost of the connections and maximum possible point load. The blue dotted line is the required force (350 kN

# 8

# Disassembly potential of case study situations

In this chapter, the factors influencing the disassembly potential of various configurations are analyzed. The values affecting the ease of disassembly are compared, and the potential for reuse is assessed.

To calculate the disassembly potential of the connection, several steps must be followed. The detailed numerical calculations are provided in Appendix D. This chapter describes how the values were determined and presents the results. An explanation of the disassembly index can be found in section 3.2.

## 8.1. Products

The products that apply for the various types of connection are as given in Table 8.1.

| Nr. | Product | Load-bearing connection | Structure Layer |
|---|---|---|---|
| 1 | Compression layer | Hollow core slabs | Structure |
| 2 | Grout | Hollow core slabs | Structure |
| 3 | Hollow core slab | Steel beams | Structure |
| 4 | Perimeter ties | Grout | Structure |
| 5 | Peripheral ties | Grout | Structure |
| 6 | Steel studs | Finplate/endplate | Structure |
| 7 | Steel beam 3.6 | Endplate/Finplate | Structure |
| 8 | Steel beam 7.2 | Endplate/Finplate | Structure |
| 9 | Steel beam 9.0 | Endplate/Finplate | Structure |
| 10 | Steel beam 10.8 | Endplate/Finplate | Structure |
| 11 | Steel beam 14.4 | Endplate/Finplate | Structure |
| 12 | Gerber Finplate | Steel beam (10.8/14.4) | Structure |
| 13 | Finplate | Column | Structure |
| 14 | Extended Endplate semi-rigid | Column | Structure |
| 15 | Extended Endplate rigid | Column | Structure |
| 16 | Diagonal plate | Column | Structure |
| 17 | Column | Column | Structure |

**Table 8.1:** Load-bearing Connections with Structure Layer

1. **Compression layer**: A layer applied to hollow core slabs to spread loads as much as possible throughout the structure to increase its structural stability and load bearing capabilities.
2. **Grout**: Specific grout of hollow core slab; it has compressive strength that gives rigid structural integrity.

3. **Hollow core slab**: Precast concrete slabs with cavities inside to reduce weight and material consumption, usually supported by steel beams for efficient load carrying.
4. **Perimeter ties**: Reinforcement elements are strategically used with grout to provide reinforcement and stability to the perimeter of the structure for overall structural integrity.
5. **Peripheral ties**: Similarly to perimeter ties, these components act together with grout to tie the external perimeter of the structure and hence resist external forces.
6. **Steel studs**: Vertical steel pins placed on top of steel beams provide cohesive integration between steel components and concrete for structural synergy and stability.
7. **Steel beam 3.6**: Horizontal steel members that serve as the main load carrying member.
8. **Steel beam 7.2**: Horizontal steel members that serve as the main load carrying member.
9. **Steel beam 9.0**: Horizontal steel members that serve as the main load carrying member.
10. **Steel beam 10.8**: Horizontal steel members that serve as the main load carrying member.
11. **Steel beam 14.4**: Horizontal steel members that serve as the main load carrying member.
12. **Gerber Finplate**: A special plate used with steel beams to provide continuity of spans for better load transfer and to increase strength through proper load distribution.
13. **Finplate**: A steel plate used in the connection of beams to columns.
14. **Extended Endplate semi rigid**: A variant of a longer endplate that extends beyond the beam length.
15. **Extended Endplate rigid**: A variant of a longer endplate that extends beyond the beam length.
16. **Diagonal plate**: A structural plate used in the connection of the endplates and beams; it provides diagonal bracing, which enhances the stability of the structure, increases resistance to bending, and improves general load distribution.
17. **Column**: Vertical structural members that carry loads from the beams and slabs to the foundation.

The area that will be compared is given in Figure 8.1 (green part) and has an area of 7.2 x 36 meters. The height that will be taken into account is one floor (3.6 meter). The column connections are not considered as the research focusses on beam configurations. A detailed description of a connection Figure 8.1, (orange square), and the numbered elements can be found in Figure 8.2. The figures of all the other scenarios and their elements can be found in section D.2.

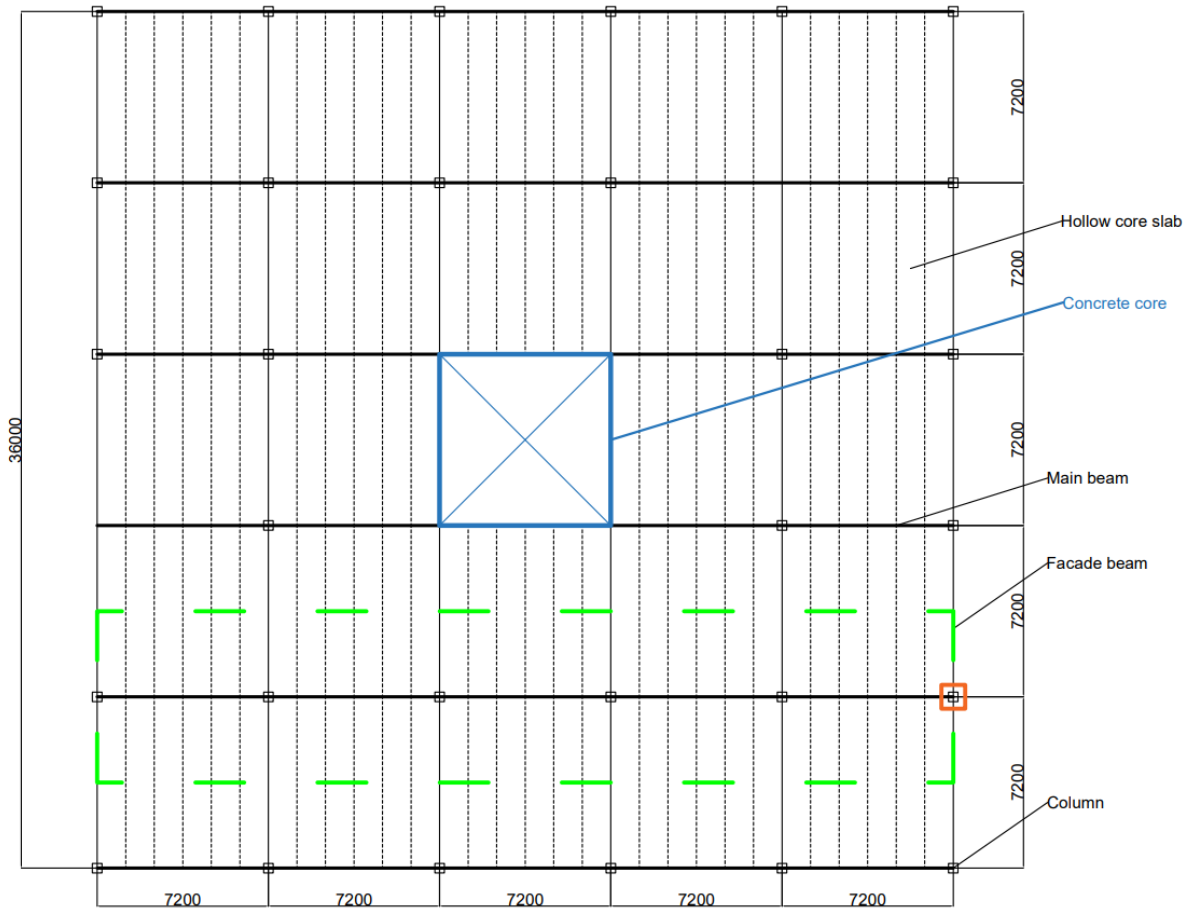


**Figure 8.1:** Green area: part for the comparison of disassembly. Orange area: connection detail as given in Figure 8.2

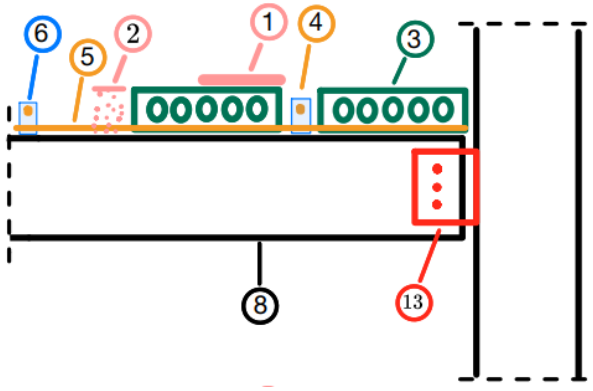


**Figure 8.2:** Detail of products in a single span hinged connection situation

## 8.2. Disassembly Potential of the Connection ($DP_c$)

The formula for determining the disassembly potential of the connection is:

$$DPc_n = \frac{2}{CT_n} + \frac{1}{CA_n} \tag{8.1}$$

Where:

- $DPc_n$ = disassembly potential of the connection of product or element $n$

- $CT_n$ = type of connection of product or element $n$
- $CA_n$ = accessibility connection of product or element $n$

### 8.2.1. Connection type (CT)

The first step to determine $DP_c$ is to analyze the type of connection used in the assembly. Each connection type ($CT$) is assigned a score which quantifies how easily the connection can be disassembled or deconstructed. The connection types can be classified into various categories depending on the materials used and the nature of the bonding. For the first 6 products, the CT is given and can be found in Table 8.2. These scores are based on the information given in Table D.1.

| Product | Load-bearing connection | Connection type | CT |
|---|---|---|---|
| Compression layer | Hollow core slabs | Structure | 0.1 |
| Grout | Hollow core slabs | Structure | 0.2 |
| Hollow core slab | Steel beams | Structure | 1.0 |
| Perimeter ties | Grout | Structure | 0.2 |
| Peripheral ties | Grout | Structure | 0.2 |
| Steel studs | Finplate/endplate | Structure | 0.1 |

**Table 8.2:** Connection Type scores for floor system products

These values are based on the type of connection, where a higher score represents greater ease of disassembly, and a lower score indicates more challenging or irreversible connections. For the floor system, the demountability is the same for all systems. Only the CT value of the compression layer can vary. If it is considered to cooperate with the floor system, it can be seen as a hard chemical connection. If it is only a finishing layer, it can be seen as a soft chemical or dry connection.

### 8.2.2. Connection Accessibility (CA)

The Connection Accessibility score centers around two key questions: Can you physically access the connecting elements, and how much damage occurs to the surrounding components during this process? If the accessibility is good, meaning the connecting elements are easy to reach without causing harm to the adjacent building parts, it positively impacts the product's potential for disassembly (see Table 8.3). The accessibility of a connection can be assessed in the same way as the type of connection. These scores are based on the information given in Table D.2.

$$CA_n = \frac{1}{A_n} \tag{8.2}$$

Where:

- $CA_n$ = accessibility of the connection of product or element $n$
- $A_n$ = accessibility factor of product or element $n$

| Product | Load-bearing connection | CA |
|---|---|---|
| Compression layer | Hollow core slabs | 0.80 |
| Grout | Hollow core slabs | 0.40 |
| Hollow core slab | Steel beams | 0.40 |
| Perimeter ties | Grout | 0.10 |
| Peripheral ties | Grout | 0.10 |

**Table 8.3:** Connection Accessibility scores for floor system products

## 8.3. Disassembly potential of the composition (DPcp)

The formula for determining the disassembly potential of the composition is:

$$DPcp_n = \frac{2}{\frac{1}{ID_n} + \frac{1}{GPE_n}} \tag{8.3}$$

Where:

- $DPcp_n$ = disassembly potential of the composition of element $n$
- $ID_n$ = independency of product or element $n$
- $GPE_n$ =product edge geometry of product or element $n$

### 8.3.1. Independency (ID)

The term “independency” refers to the complete intermingling or integration of products or elements. Consequently, disassembling a product or element at the end of its life requires more effort. This is particularly challenging when the lifetimes of the involved products vary, necessitating interim replacements while preserving the surrounding products or elements. The scores in Table 8.4 are based on the information given in Table D.3.

| Product | Load-bearing connection | ID |
|---|---|---|
| Compression layer | Hollow core slabs | 1.0 |
| Grout | Hollow core slabs | 0.4 |
| Hollow core slab | Steel beams | 1.0 |
| Perimeter ties | Grout | 1.0 |
| Peripheral ties | Grout | 1.0 |

**Table 8.4:** Independency scores for floor system products

### 8.3.2. Geometry of product edge (GPE)

The geometry of the product edge factor evaluates how products are arranged within a composition, determining if it is open or closed. This concept pertains to the physical ”edges” of the product or element. When a product is ”locked up” by surrounding products, it is referred to as product edge geometry. This arrangement makes disassembly possible only in the reverse order of construction. The product edge geometry factor is significant in two scenarios: 1) for individual products enclosed within the composition and 2) for serial products that enclose each other. The scores in Table 8.5are based on the information given in Table D.4.

| Product | Load-bearing connection | GPE Score |
|---|---|---|
| Compression layer | Hollow core slabs | 1.0 |
| Grout | Hollow core slabs | 0.4 |
| Hollow core slab | Steel beams | 0.4 |
| Perimeter ties | Grout | 0.1 |
| Peripheral ties | Grout | 0.1 |

**Table 8.5:** Geometry of product edge scores for floor system products

## 8.4. Disassembly potential of the product or element (DPp)

$$DP_p = \frac{2}{\frac{1}{DPc_n} + \frac{1}{DPcp_n}} \tag{8.4}$$

- $DP_p$ = disassembly potential of the product
- $DPc_n$ = disassembly potential of component $n$
- $DPcp_n$ = disassembly potential of complementary product $n$

## 8.5. Disassembly potential of the building (DPb)

$$DP_{bn} = \frac{1}{\sum_{i=1}^{l} ECIn} \left( \sum_{i=1}^{l} ECIn \cdot DPpn \right) \tag{8.5}$$

Where:

- $DP_{bn}$ = disassembly potential of building $n$
- $DPpn$ = disassembly potential of product or element $n$
- $ECIn$ = Environmental Cost Indicator of product or element $n$

For all scenarios, the disassembly scores have been calculated using the formulas given in the previous subsections. Calculations of the disassembly of the building potential can also be addressed as the disassembly potential of the system, as only a part of the building has been taken into account. However, due to the repetition in the building, the system can serve as a plausible representation for the entire building. The complete calculations for the scenarios can be found in Appendix D. The ECI has also been calculated for the different scenarios, and these extensive results can be found in Appendix C. The results of the disassembly score for the five scenarios can be found in Figure 8.3.

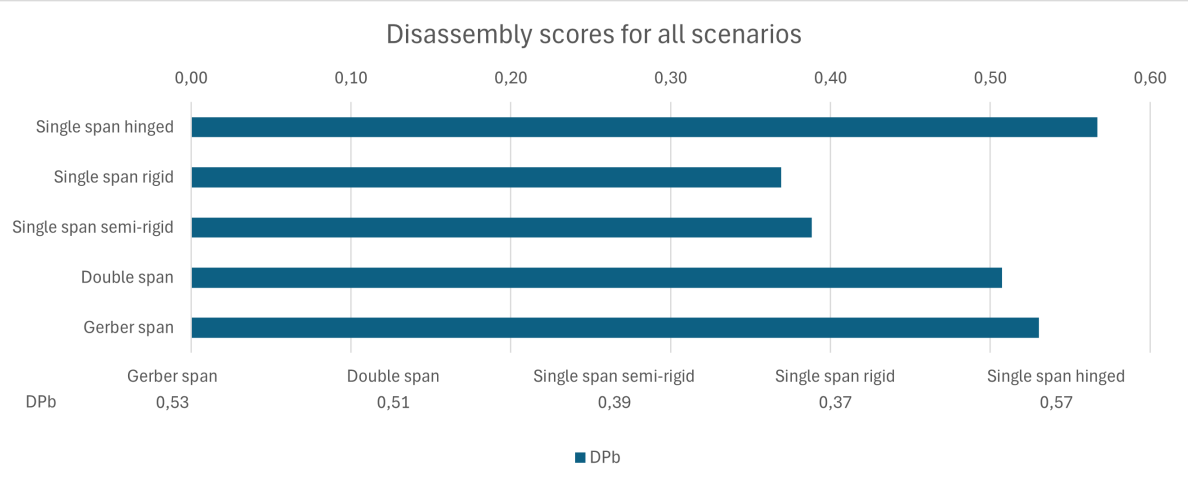


**Figure 8.3:** Disassembly score for all the scenarios

To calculate the total ECI (Environmental Cost Indicator), it is important to distinguish between different ECI values. The first value calculated is the total ECI of a building without considering the reusability of materials or products. The second calculation, in parentheses in Equation 8.6, multiplies the total ECI by the disassembly score. This can be seen as the ECI that can be subtracted from the total. The total ECI minus the ECI multiplied by the DP (Disassembly Potential) is the remainder of the ECI. This remaining ECI remains after the structure has been dismantled.

$$\text{Remaining ECI} = \text{ECI}_{\text{total}} - (\text{ECI}_{\text{total}} \times \text{DP}) \tag{8.6}$$

| Disassembly | ECI / m² | $ECI_{remaining}$ / m² |
|---|---|---|
| Single span hinged | € 10.14 | € 4.39 |
| Single span rigid | € 12.12 | € 7.64 |
| Single span semi-rigid | € 9.49 | € 5.80 |
| Double span | € 8.04 | € 4.05 |
| Gerber span | € 10.13 | € 4.26 |

**Table 8.6:** ECI Data

In Figure 8.4 below, the remaining ECI values of the five scenarios can be seen.

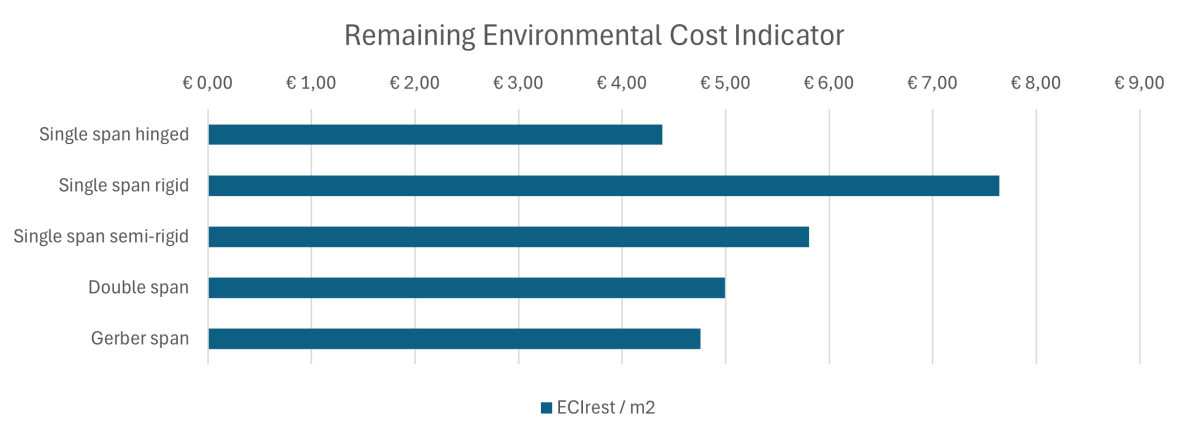


**Figure 8.4:** Remaining ECI for all scenarios

The disassembly potential of the different products in the case of a single-span hinged connection to a column can be seen in Figure 8.5. The hidden components in the grout, such as the ties and studs, have a relatively low disassembly potential. Steel beams that are connected by hinges have a high disassembly potential in this case, as well as the pre-cast concrete hollow core slabs.

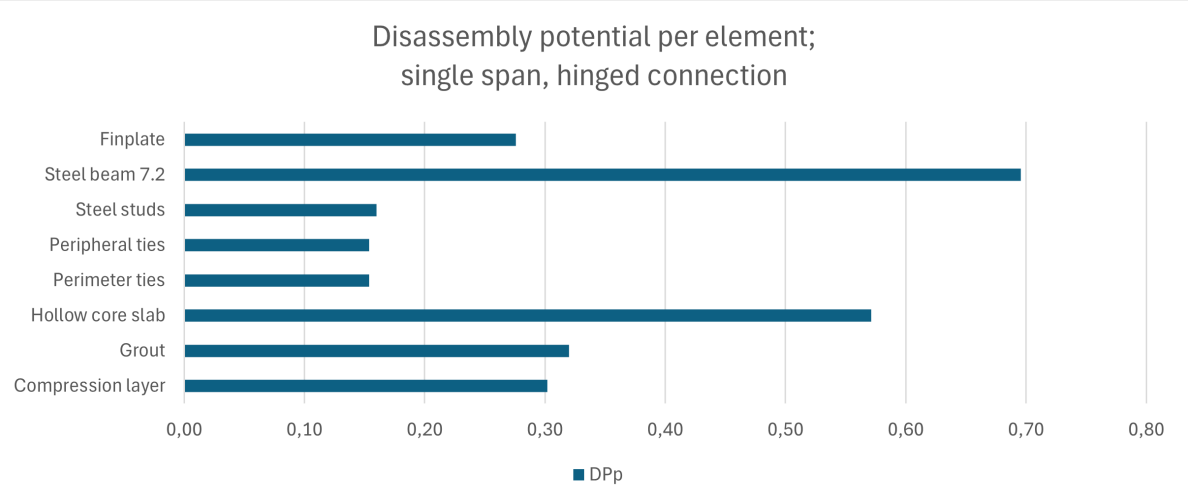


**Figure 8.5:** Disassembly potential per structural element

In Figure 8.6a, the disassembly potential of the different structural layers is shown. Figure 8.6b illustrates the share of each layer of brand in the total disassembly. The figures allow us to quickly see the contribution of each component to the DP. For example, it is evident that the beams in a single

hinged span contribute significantly to the DP. In the case of a rigid connection, this contribution is much smaller, and the connection to the column, which is fastened with 12 bolts, also plays a role. Furthermore, in the case of hinged connections (scenarios 1, 4, and 5), the beams make the largest contribution to the DP. To determine where improvements can be made, the maximum DP potential per element as a share of the whole should be considered first.

Based on Figure 8.6a, we can identify which elements score the lowest in terms of disassembly potential. It can be seen that, in the case of (semi-)rigid connections, there is still much room for improvement in the connections of the beam. Furthermore, improvements can be made in the scenarios on the floor ($DP_{\text{floor}} = 0.44$) for scenarios 1, 4, and 5. If these score below average, they reduce the disassembly potential. This is not the case for the rigid and semi-rigid connections, as the total disassembly potential there is below 0.4 (Figure 8.6b).

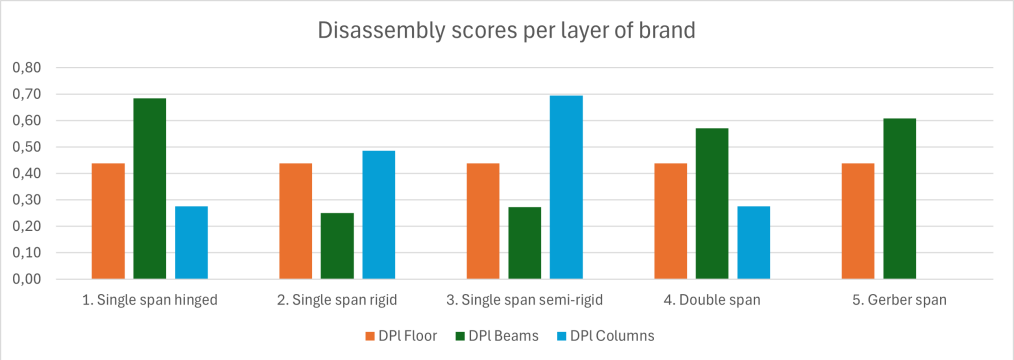


**(a)** Disassembly score per layer of brand

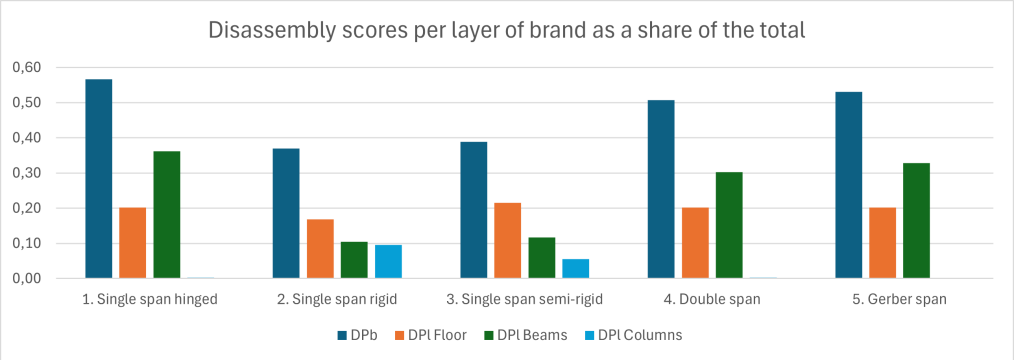


**(b)** Disassembly score per layer of brand as share of the total

**Figure 8.6:** Comparison of disassembly scores: (a) absolute values and (b) relative share of the total.

### 8.5.1. Influence of Connection Type

In the event that the steel structure is stiff enough that it does not have to support horizontal forces through the floor, a constructive compression layer is not needed. This is the case in case of a moment-resisting connection. Therefore, the connection between the compression layer and the channel plates must be changed from 0.1, hard chemical connection, to 1.0, dry connection. This subsequently leads to a change in the disassembly of the moment-resistant structure from 0.37 to 0.47. The updated graph can be seen in Figure 8.7a. Also, the ECI changes and drops from €7.64 to €6.38 per square meter, the renewed graph can be seen in Figure 8.7b.

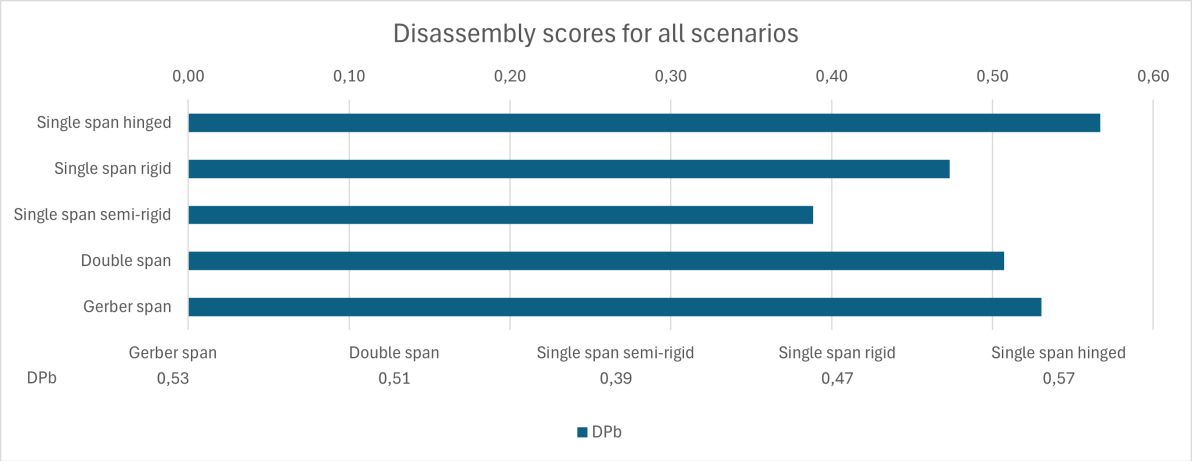


**(a)** Disassembly potential for all scenarios

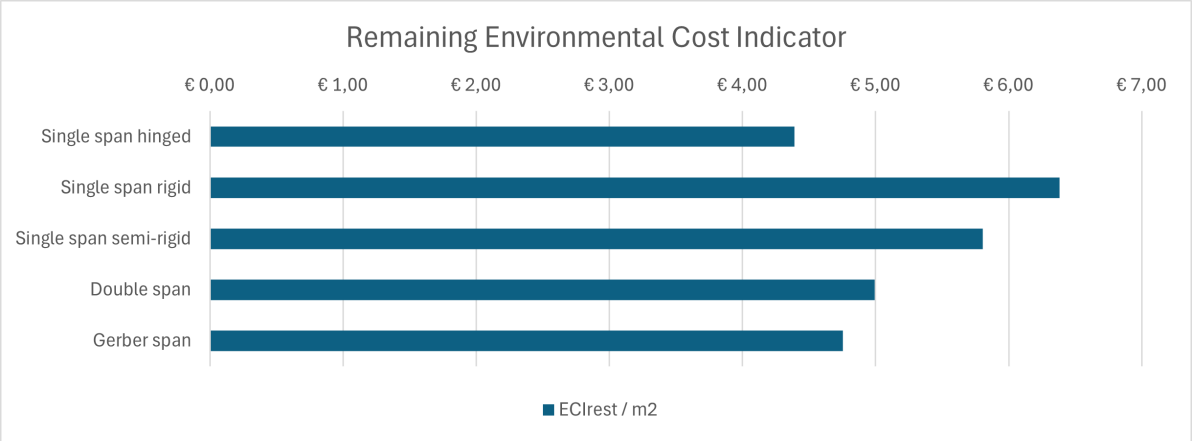


**(b)** Remaining ECI for all scenarios

**Figure 8.7:** Changed connection type of the compression layer in a rigid connections scenario, from 0.1 (hard chemical connection) to 1.0 (dry connection)

### 8.5.2. Influence of Connection Accessibility

The biggest difference between a single-span, double-span, and Gerber girder is the accessibility of the connections. In the case of a double-span, the connections are still equally accessible, but there are fewer connections. In the case of the Gerber girder, the connections are more accessible because they are not located near a node but at a certain distance from the columns. Due to the relatively high ECI of the girders compared to other components, the accessibility to these connections also greatly influences their disassembly. How accessibility affects the remaining ECI and disassembly can be seen in Figure 8.8. The difference between a non-accessible connection and a highly accessible connection increases the total disassembly score from 0.36 to 0.69, with the remaining ECI decreasing from €1674 to €804. This represents a doubling and halving, respectively.

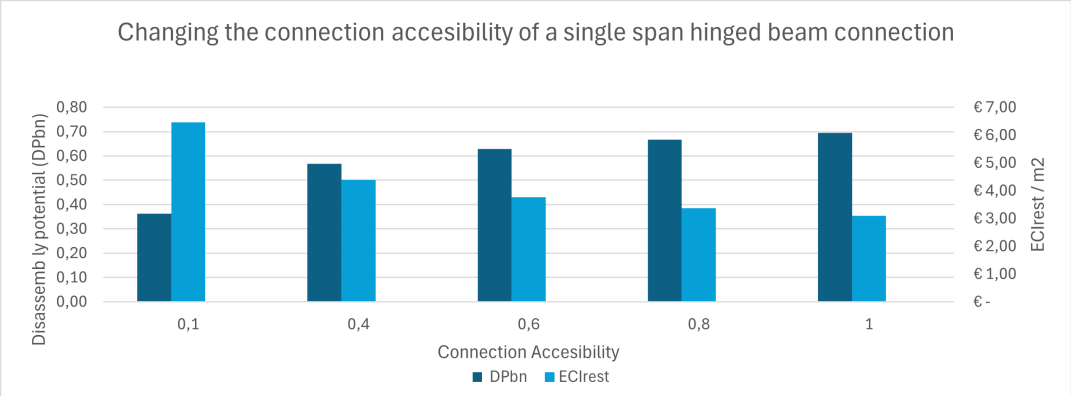


**Figure 8.8:** Remaining ECI and disassembly score change due to the connection accessibility

### 8.5.3. Adjusting the span and the cross-section of the beams

The force that can be absorbed depends on the span distance. In the standard scenarios, a column-to-column center distance of 7.2 meters has been considered. However, this distance may result in the inability to transfer forces in case of a (partially) hinged connection when a column is missing. One solution could be to reduce the span distance. Therefore, the disassembly potential of two alternative scenarios with spans adjusted to 3.6 and 5.4 meters has been assessed. This is compared to the original span of 7.2 meters.

Figure 8.9 shows the disassembly scores in case of changing or not changing the cross-section of the beam. When lowering the span, the disassembly potential of the situation where the cross section stays the same (HEB400) will increase, although more connections need to be demounted. The reason for this contradiction is that the disassembly potential depends on the ECI and, thus, the weight of the elements.

If the original disassembly potential is 0.59 and the disassembly potential of the columns (which amount doubles) is higher, the overall disassembly potential will increase if the weight of the columns increases with respect to the total construction. The downside of this situation is, however, that the remaining ECI also increases due to the extra columns. This can be seen in Figure 8.10.

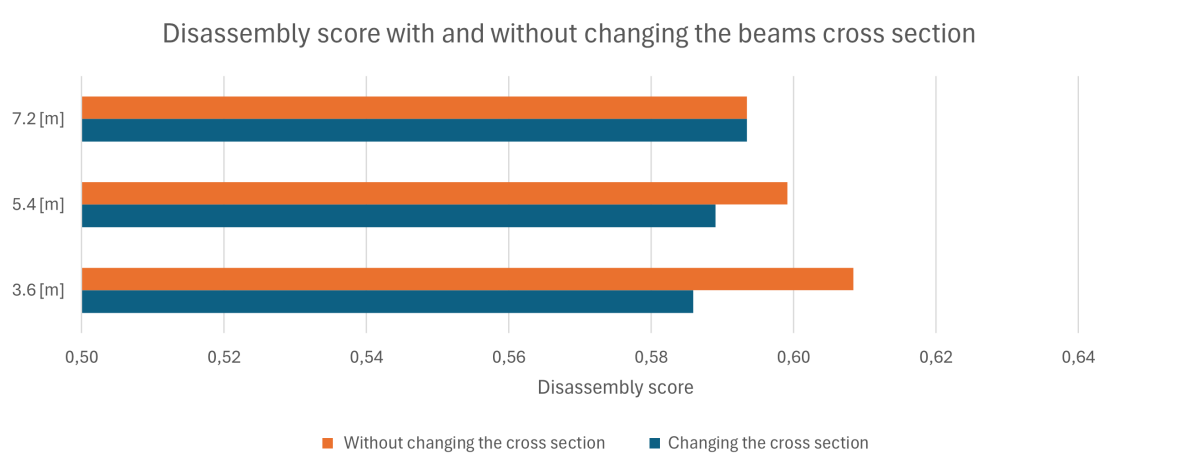


**Figure 8.9:** Disassembly potential for different column-to-column distances with and without changing the cross-sections of the beams

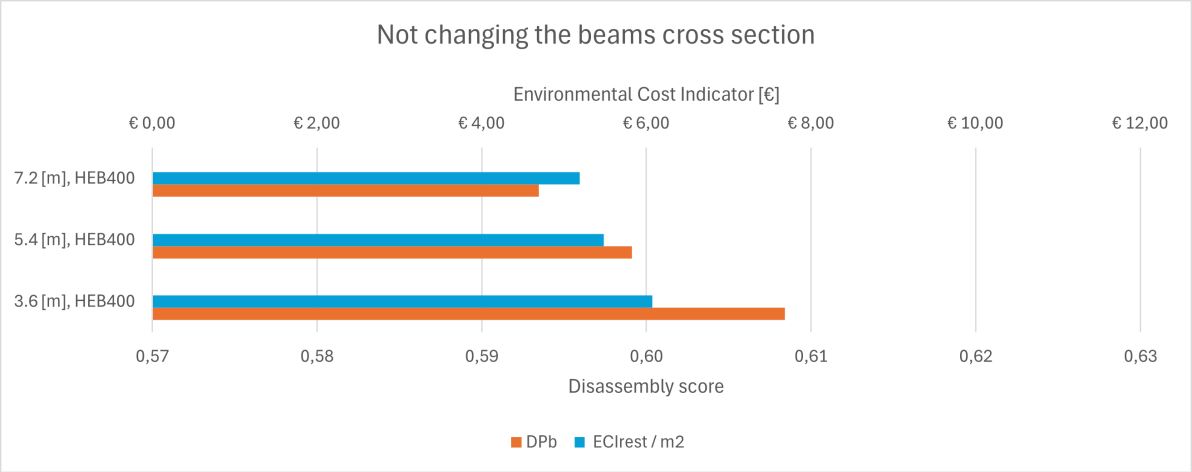


**Figure 8.10:** Changing the column to column distance but not the cross-section of the beams

In Figure 8.11, it can be seen how both the remaining ECI and the disassemble potential decrease as the span is reduced and the cross-section is also reduced. The disassemble potential decreases for two reasons:

- Shorter spans mean more connections, thus lower disassembly potential.
- Shorter spans and a smaller cross-section of the beams reduce the weight of the beam and thus its share in the total ECI.

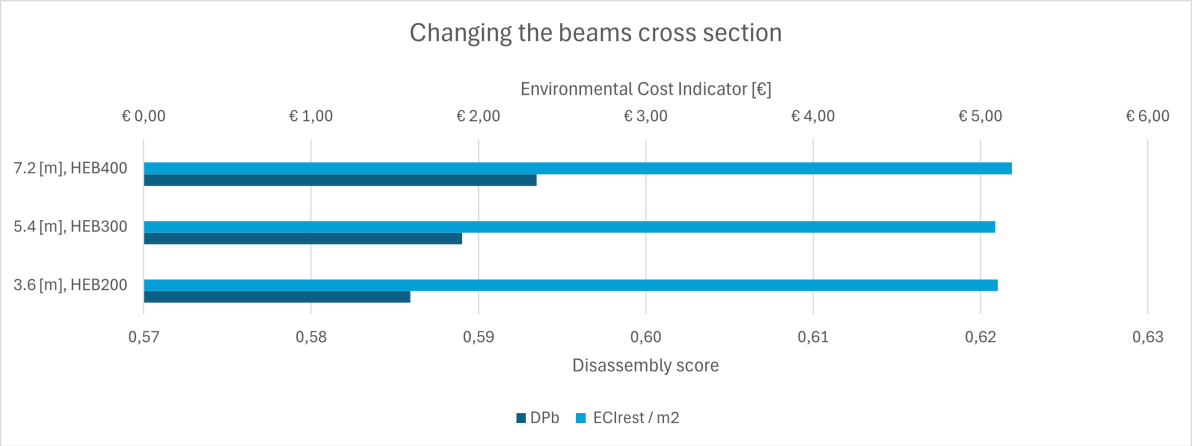


**Figure 8.11:** Changing the column to column distance and cross sections of the beams

Figure 8.12 shows that changing the cross-section and adding more columns and connections will decrease the disassembly ability. Additionally, a reduction in the ECI will contribute to a decreased disassembly score as long as the disassembly ability of the steel beams remains above average. This is because the weighting decreases. This can also be seen in Figure 8.11.

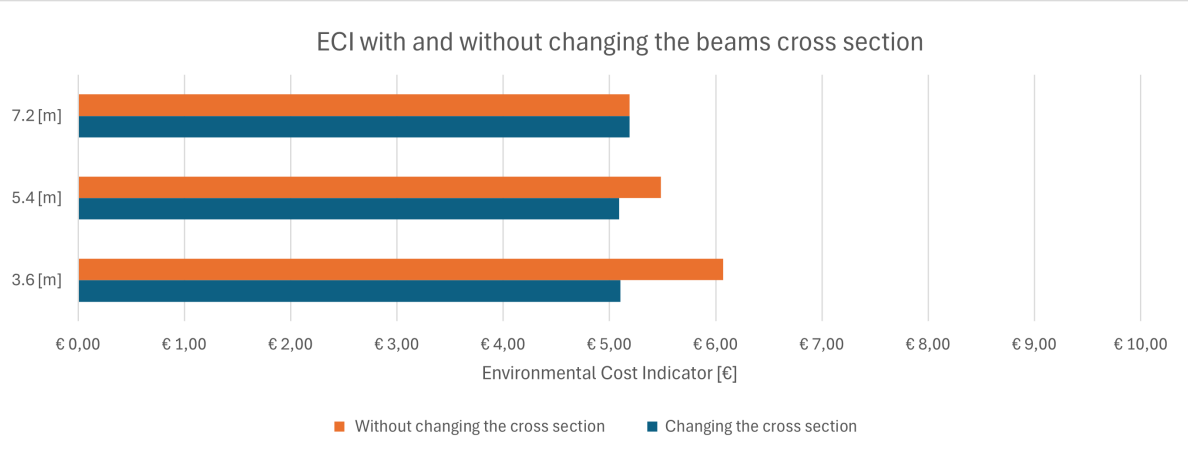


**Figure 8.12:** Remaining ECI comparison by (not) changing the cross-section of the beams

## 8.6. Conclusion

This chapter evaluated the disassembly potential of various structural configurations with regard to connection types, accessibility, and independence as factors affecting the ease of disassembling the structural part of a building. It became obvious from the results that demountability is highly sensitive to the number and type of connections; the more accessible and independent the connections are, the easier the disassembly will be. Key findings of the analysis are: a reduction in span and beam cross-sectional area is seen to have a negative effect on the disassembly potential as it increases the structural connections. On the other hand, smaller spans can reduce the ECI values due to material usage, but the complexity brought by extra connections makes the disassembly more laborious and, hence, less feasible. In addition, there was a clear effect due to the type of connection: the bolted ones generally scored higher in disassembly potential compared with welded or rigidly fixed connections. The Disassembly Index showed that optimization of connection traits like accessibility and modularity implies a much higher potential for reuse and circular construction.

# Part III

# Research outcome

# 9

# Discussion

In this chapter, first, the modeling approach and assumptions of the research are discussed. In addition, key findings and trade-offs between disassembly and robustness are discussed. The implications of these findings for the construction industry are also explored.

## 9.1. Modeling approach and assumptions

The research method applied in this study is based on a model building in which various scenarios were tested. In this study, the distances between the columns were kept constant, while the connection types and the length of the beams were adjusted. Although five scenarios were analyzed, this only provides a general view of the best option. In fact, many other possibilities could be investigated in more depth to better understand the overall behavior. Expanding and optimizing connection types will provide a better perspective, including hybrid connections with rigid properties, to enhance understanding and inform improvements in structure robustness and disassembly.

The prestressed hollow-core slab floor was adopted for the floor system because it is easily accessible for installation. There is little difficulty in dismantling this kind of floor compared to other floor systems. Therefore, it becomes an alternative where flexibility and material reuse are most valued. However, no research has been conducted on a dismountable steel-concrete composite floor with, for example, 'shear connectors.' Although this is a promising method, it requires a different approach and possibly other design and construction considerations. A steel-concrete composite floor could be more efficient than a hollow-core slab floor, especially in terms of structural performance and durability. Future research could focus on comparing these two types of floor system rather than steel beams to better understand the advantages and disadvantages of each system in terms of disassembly.

The research method using IDEAStatiCa is very time-consuming because each situation requires a new calculation. A simplified model in advance will be extremely helpful in speeding up the research method, especially in the case of many more adjustments to the connections. In this way, a comparison can be made even more efficiently, allowing variations in bolts, welds, and plate thicknesses.

### 9.1.1. 2D modeling

This report investigates the behavior of catenary action in a steel building using a two-dimensional (2D) frame modeling approach. A three-dimensional (3D) model was not utilized for two key reasons. First, the catenary action occurs when one-dimensional (1D) elements move within a 2D plane, and since the catenary in the structure deflects exclusively in the vertical direction, a 2D model is sufficient to capture the associated forces and deformations. Second, a 2D modeling approach simplifies the process of validating the results through analytical calculations, making it easier to refine and optimize the system.

### 9.1.2. IDeaStatiCa

In IDEAStatiCa, elements and connections are partly analyzed separately. This means that an element that meets the design requirements does not necessarily guarantee that the corresponding connection

will also comply. The joint should be checked separately for strength, stiffness, and stability. This makes it difficult to analyze a case in which the force on the structure is increasing.

One of the challenges in this analysis is to distinguish between flexural action and catenary action. The flexural action can lead to plastic deformations and ultimately to failure of the element due to bending. Catenary action can occur when an element fails due to bending, and then the forces are transferred by stress, which can lead to another type of failure.

For this reason, this research had to focus on the deflection under a point load at the element level. With significant changes in the vertical direction, the connection could be examined. In this way, it was still possible to analyze the connection, but it is time-consuming. However, a figure like Figure 5.1 is impossible because the connection calculation does not take the elements into account and vice versa.

#### Buckling

Due to vertical deformation at the location of the removed column, horizontal forces form in the beams, which causes horizontal forces on the columns of the structure. When a horizontal force occurs in the middle of a column, it can lead to buckling. This happens because the column is under stress, causing it to bend and eventually fail.

When the column bends due to tensile force, second-order effects can occur. This means that the deformations of the column further increase the internal forces in the construction. These effects arise because the deformed geometry of the column generates additional moments and forces, which can further reduce the stability of the construction. Therefore, it is important to include these second-order effects in the analysis to obtain an accurate assessment of structural integrity.

In the case of out-of-plane buckling, the column bends not in the direction of the load but perpendicular to it. This type of buckling can occur when the column lacks sufficient lateral support and the tensile force in the middle of the column causes it to bend outward. As a result, the column can severely deform and eventually fail, as happened with the WTC (subsection 2.1.3).

However, this mode of failure of the construction is not addressed in this report. The large force on top of the columns, combined with the horizontal forces, can lead to failure even if the construction does not collapse due to subsidence. The horizontal forces transferred in the concrete floor are partially addressed.

#### Beams in secondary direction

The use of beams in a second direction is not strictly necessary, since the floor of the channel slab is already used in that direction. These channel slab floors provide stability perpendicular to the direction of the main beam. However, in IDEAStatiCa, the use of these beams is useful to prevent columns from moving out of the plane in the lateral direction. By adding beams in a second direction, the overall stability of the structure is improved and the risk of deformation is reduced. Due to the dimension of IPE240 compared to HEB300 or HEB400 of the main beam and the hinge of the cross beams, this contributes negligibly to the final second load bearing path in the event of the loss of a column.

#### Dynamicac Amplification Factor

The Dynamic Amplification Factor (DAF) can be applied to structures under dynamic loads. A conservative DAF of 1.0, which was used in this research, may not adequately reflect the dynamic effects, resulting in a static approximation and an incomplete picture of the structural performance. The selection of the DAF is heavily dependent on how a column fails. A more realistic view of the structural dynamic response can be obtained by increasing the DAF to 2.0 [8]. This may, however, be an overdimensioning of the system. A brittle or sudden column failure mechanism may require a higher DAF than a plastic failure scenario to properly model the dynamic effects. The DAF can be taken as a value between 1 and 2 depending on the ductility of the connections.[14].

### 9.1.3. Shortcomings on the disassembly index

The Demountability Index created by ALBA Concepts is a tool to evaluate how easily a building or product can be disassembled, designed to support circular-economic practices in construction. However, it has several limitations that reduce its overall effectiveness.

One major drawback of the simplified scoring system is that it does not account for the number of bolts in a connection. This error can have a significant impact. For example, the more bolts in a connection, the more time it takes to disassemble the connection, directly impacting labor costs. In addition, the disassembly time and effort increase in such a way that the price on the market for the disassembled element increases. However, these subtleties are not captured by the simplified scoring system, therefore underestimating the actual disassembly effort and differences between, for example, a hinged or rigid connection.

Another shortcoming of the index is the secondary life of the elements. Although the index measures the ease with which components can be separated, it does not consider the environmental cost of recycling these materials or whether they can be reused in their original form. This omission is significant because reusability is a key factor in circular economy models. An example of this could be the use of beams in construction. The controversy about this is that short beams require more connections, but the length makes it easier to disassemble. The disadvantage may be that there is no demand for short beams, and therefore the market is negligible. Longer beams can be used on the other hand. These may require fewer connections, but they do require connections with more bolts. The length can then be a disadvantage when dismantling and transporting, but the demand for long beams, on the other hand, can be more significant; this is because the longer beams can be used more widely. A faster turnaround of elements can then lead to a price reduction.

In addition, connections can become tighter over time due to factors such as corrosion, vigorous expansion and contraction, and the accumulation of dirt and other contaminants. These factors can make loose connections difficult, even when proper methods are used. The index assumes that connections are easy to loosen, provided the correct methods are used.

Another aspect that can introduce subjectivity is the weighting factors applied to the formula to calculate the disassembly potential; the results are biased based on the interpretation of an assessor of the components that are most critical. Such subjectivity leads to inconsistent evaluations. Additionally, this index provides for ease of disassembly, but does not directly relate to time or cost. While a component may be technically easy to take apart, if it is time-consuming or costly to do so, it can ruin the overall feasibility of the approach, an impact that is not reflected in the index.

## 9.2. Discussing the results

The secondary load-bearing capacities of different types of connection and the potential to demount these connections were the two aspects influenced by structural connections that were analyzed in the previous two chapters (chapter 7 and chapter 8). The first goal of the study was to determine how different types of connection affect structural robustness. Secondly, to assess each connection's ease of construction, the demountability of each was computed. This section will use these findings by exploring the correlation between the structural robustness of the connections and the disassembly potential of those scenarios. The relationship between these characteristics will be evaluated to determine how strongly they influence each other. An overview of the scenarios and data is given in Table 9.1.

**Table 9.1:** Scenarios and Data

| Scenario | Connections [€/m$^2$] | $F_{max}$ [kN] | DPb | ECI [€/m$^2$] | $ECI_{rest}$ [€/m$^2$] |
|---|---|---|---|---|---|
| 1a | € 9.22 | 50 | 0.57 | 10.14 | 4.39 |
| 1b | € 64.62 | 400 | 0.37 | 12.12 | 7.64 |
| 1c | € 28.36 | 150 | 0.39 | 9.49 | 5.80 |
| 2 | € 5.53 | 350 | 0.51 | 10.09 | 4.96 |
| 3 | € 1.05 | 350 | 0.58 | 10.13 | 4.26 |

### 9.2.1. Correlation

The correlation can be calculated using the formula in Equation 9.1. This coefficient ranges from -1 to +1, where -1 indicates a strong negative correlation, and +1 indicates a strong positive correlation. From a value of 0.75, a strong correlation can be identified [40]. However, it is essential to remember that correlation does not imply causation. This means that even if two variables have a strong correlation,

it does not necessarily mean that one variable causes the other to change. Other factors or variables might influence the relation between the two factors as well.

$$r = \frac{\sum(X_i - \overline{X})(Y_i - \overline{Y})}{\sqrt{\sum(X_i - \overline{X})^2 \sum(Y_i - \overline{Y})^2}} \tag{9.1}$$

**Table 9.2:** Correlation Matrix

| | **Connections costs** | **$F_{max}$** | **DPb** | **ECI** | **$ECI_{rest}$** |
|---|---|---|---|---|---|
| **Connection costs** | 1.00 | 0.29 | **-0.87** | **0.77** | **0.98** |
| **$F_{max}$** | 0.29 | 1.00 | -0.21 | 0.57 | 0.41 |
| **DPb** | **-0.87** | -0.21 | 1.00 | -0.42 | **-0.91** |
| **ECI** | **0.77** | 0.57 | -0.42 | 1.00 | 0.75 |
| **$ECI_{rest}$** | **0.98** | 0.41 | **-0.91** | 0.75 | 1.00 |

- There is a strong negative correlation between **Total Cost of Connections** and **DPb** (**-0.87**). As the total cost of connections increases, DPb decreases (Figure 9.1a).
- There is a strong positive correlation between **Total Cost of Connections** and **ECI** (**0.77**). As the total cost increases, ECI also increases (Figure 9.1b).
- There is a strong positive correlation between **Total Cost of Connections** and **$ECI_{Rest}$** (**0.98**). As the total cost of connections increases, $ECI_{Rest}$ also increases (Figure 9.1c).
- There is a strong negative correlation between **DPb** and **$ECI_{Rest}$** (**-0.91**). As DPb increases, $ECI_{Rest}$ decreases.

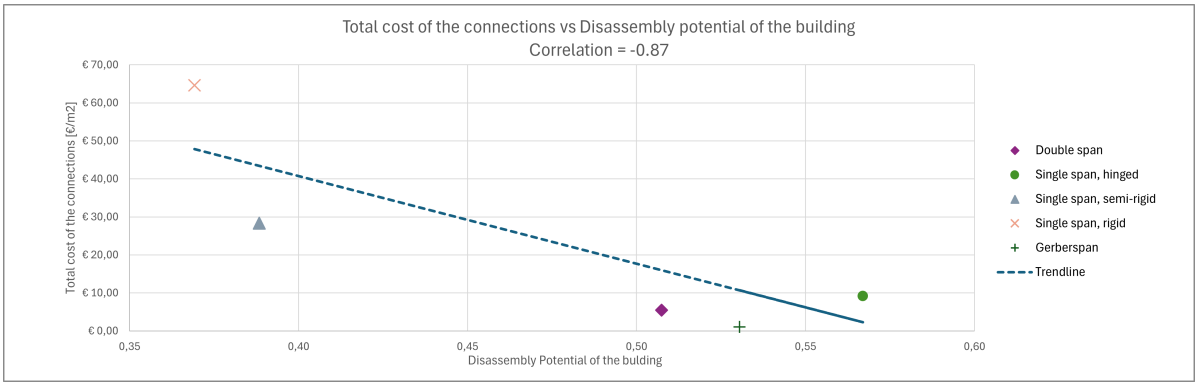


**(a)** Total Cost of Connections vs Disassembly potential

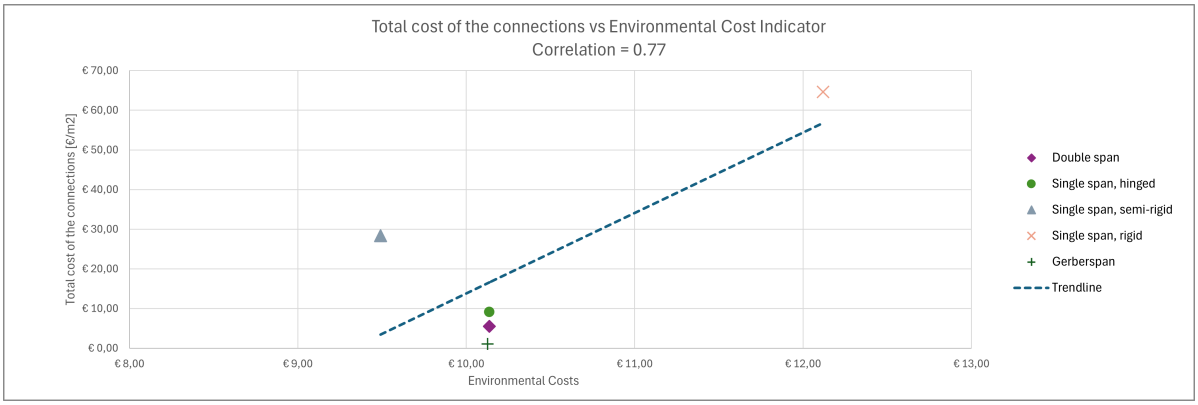


**(b)** Total Cost of Connections vs the total ECI

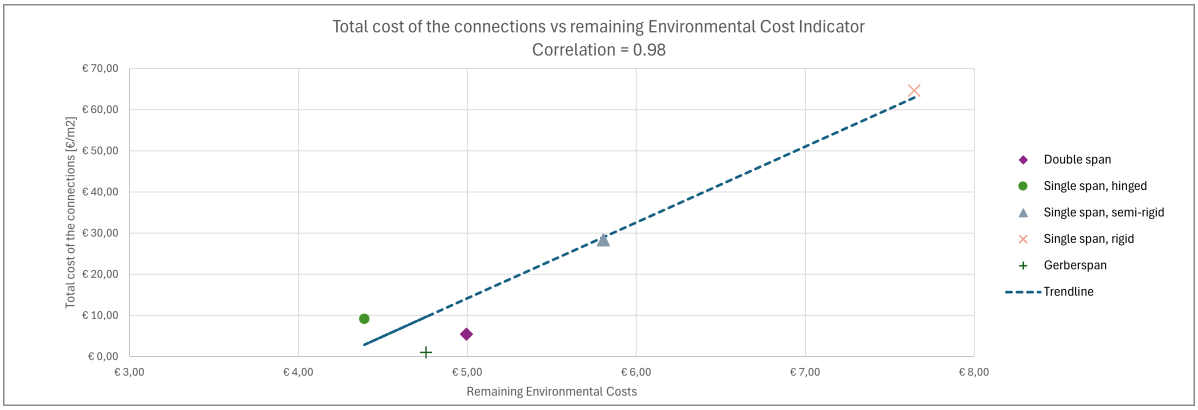


**(c)** Total cost of the connections vs the remaining ECI

**Figure 9.1:** Correlations between the total cost of Connections, DPb, the total ECI and the remaining ECI

According to Table 9.2, there is no strong correlation between the maximum force that can be applied to a structure. For that reason, it is impossible to maximize the link between robustness and demountability. However, there are some other interesting correlations.

There is a very high correlation between the total cost and the dismantling of a connection, namely 0.87 (see Figure 9.1a). Therefore, it could be said that the dismantling potential can be deduced from the cost of the connection. Independent calculations of the dismantling can be omitted, as conclusions can be drawn directly from the cost of the connection.

The correlation between the total cost and the ECI is 0.77 (Figure 9.1b), while the correlation between the total cost of the connections and the disassembly potential is -0.87, making the combined correlation close to 1. However, it is important to note that these ECI costs only account for materials, excluding transportation costs from this study's scope. Even if the disassembly potential is 1, resulting in a

remaining ECI of 0, the building is not entirely energy-neutral. Transportation costs and the energy required for the assembly and disassembling of all components must still be considered.

The total connection cost is closely linked to the remaining Environmental Cost Indicator (ECI), as shown in Figure 9.1c. The remaining ECI combines the DPb and the ECI.

However, it should be noted that the disassembly potential and the remaining ECI should be considered separately. A higher disassembly potential does not mean that the circularity is better, based of the remaining ECI, if the initial ECI is higher. This is illustrated in Figure 9.2. It shows how a disassembly potential of 0.5 and an initial total ECI of €10 results in a lower remaining ECI than, for example, a disassembly potential of 0.6 and an initial total ECI of €25. The remaining ECI for the case with the highest disassembly potential in this case, is twice that of the lower disassembly potential.

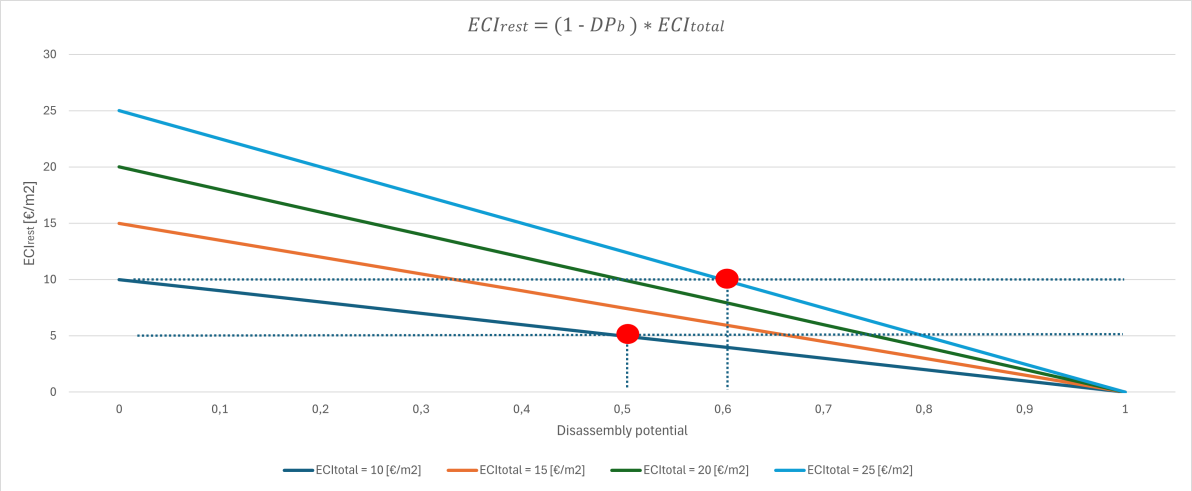


**Figure 9.2:** Varying the intitial total ECI

### Standard error

With only five measurements, there is a high likelihood that the correlation coefficient is unstable and has a wide confidence interval, which reduces the accuracy of the results. In addition, a standard error calculation can be performed to further assess the reliability of the correlation coefficient. The standard error of the correlation coefficient can be calculated using the following formula:

$$SE_r = \frac{1 - r^2}{\sqrt{n - 1}} \tag{9.2}$$

where $r$ is the correlation coefficient and $n$ is the number of measurements.

The formula for the margin of error (ME) is given by:

$$\text{ME} = z \times \text{SE} \tag{9.3}$$

where $z$ is the z-score corresponding to the desired confidence level, and SE is the standard error.

For a 95% confidence level, the z-score ($z$) is 1.96. Therefore, the margin of error for each correlation description and standard error can be calculated as follows:

$$\text{ME} = 1.96 \times \text{SE} \tag{9.4}$$

Table 9.3 below shows the correlation descriptions, correlation coefficients, standard errors, and calculated error margins.

| Correlation Description | Correlation Coefficient (r) | Standard Error (SE) | Margin of Error (ME) |
|---|---|---|---|
| Total Cost of Connections and DPb | -0.87 | 0.12 | 0.24 |
| Total Cost of Connections and ECI | 0.77 | 0.20 | 0.39 |
| Total Cost of Connections and $ECI_{Rest}$ | 0.98 | 0.02 | 0.04 |
| DPb and $ECI_{Rest}$ | -0.91 | 0.09 | 0.18 |

**Table 9.3:** Updated Correlations, Standard Errors, and Margins of Error

Based on the margin of error calculations for a 95% confidence level, the correlation between the total cost of connections and DPb has a margin of error of 0.24. This means that the true correlation coefficient is likely to fall within the range of -0.87 ± 0.24. Figure 9.3 below visualizes the correlation coefficients along with their respective margins of error.

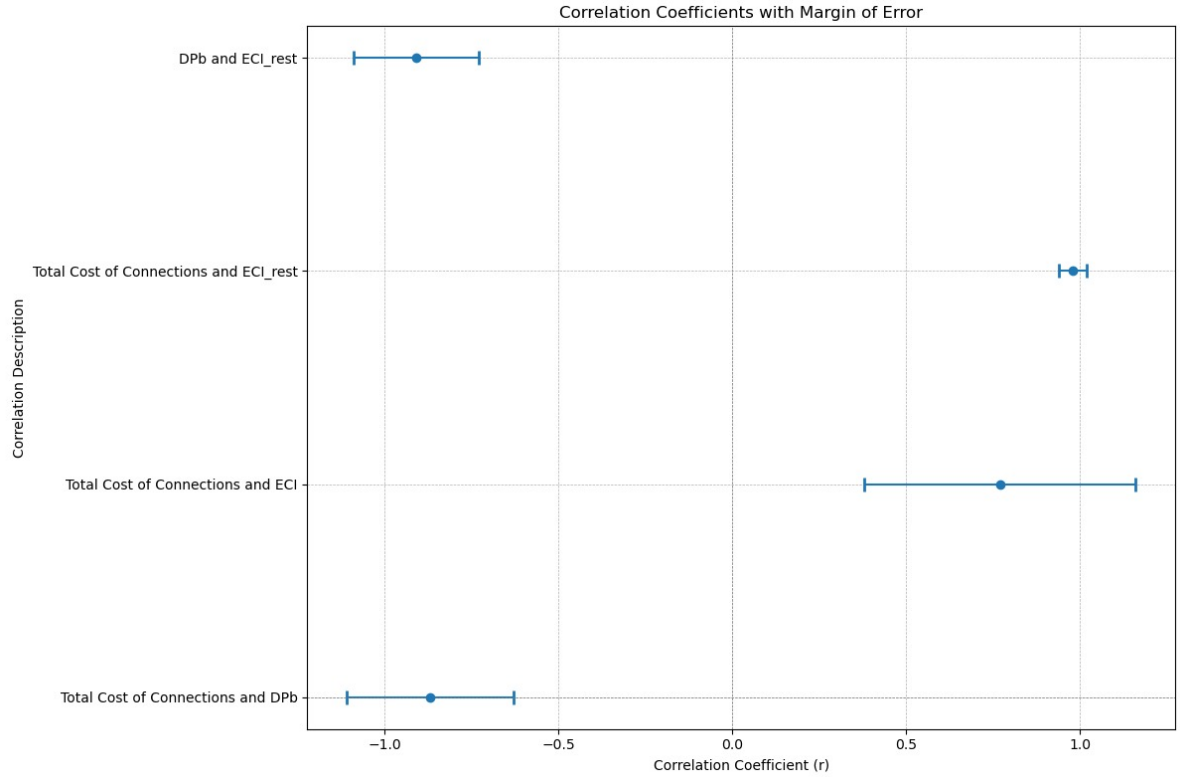


**Figure 9.3:** Correlation Coefficients with Margin of Error

### Fisher's Z transformation

The use of Fisher's Z-transformation is needed and more accurate when the correlation value is close to 1 (or -1), because the distribution of the sample correlation coefficient becomes very skewed. This skewness can lead to inaccurate confidence intervals when standard methods are used. Fisher's Z-transformation normalizes the distribution, making it more symmetric and allowing for more accurate estimation of confidence intervals. In this case. It will be used for the correlation between the Total cost of connections and the $ECI_{rest}$.

Transform the correlation coefficient (r) to Fisher's Z:

$$Z = \frac{1}{2} \ln \left( \frac{1+r}{1-r} \right) \tag{9.5}$$

Given $r = 0.98$:

$$Z = \frac{1}{2} \ln \left( \frac{1.98}{0.02} \right) = \frac{1}{2} \ln(99) \approx 2.298 \tag{9.6}$$

Calculate the standard error (SE) of Z:

$$SE_Z = \frac{1}{\sqrt{n-3}} \tag{9.7}$$

Given $n = 5$:

$$SE_Z = \frac{1}{\sqrt{2}} \approx 0.707 \tag{9.8}$$

Determine the Z-score for 95% confidence level: For a 95% confidence level, the Z-score is 1.96.

Calculate the margin of error for Z:

$$MOE_Z = Z \times SE_Z \tag{9.9}$$

$$MOE_Z = 1.96 \times 0.707 \approx 1.386 \tag{9.10}$$

Find the confidence interval for Z:

$$CI_Z = Z \pm MOE_Z \tag{9.11}$$

$$CI_{Z_{lower}} = 2.298 - 1.386 \approx 0.912 \tag{9.12}$$

$$CI_{Z_{upper}} = 2.298 + 1.386 \approx 3.684 \tag{9.13}$$

Transform the confidence interval back to the correlation scale:

$$r_{lower} = \frac{e^{2 \cdot CI_{Z_{lower}}} - 1}{e^{2 \cdot CI_{Z_{lower}}} + 1} \approx 0.722 \tag{9.14}$$

$$r_{upper} = \frac{e^{2 \cdot CI_{Z_{upper}}} - 1}{e^{2 \cdot CI_{Z_{upper}}} + 1} \approx 0.999 \tag{9.15}$$

So, the 95% confidence interval for the correlation coefficient using Fisher's Z transformation is approximately (0.722, 0.999). The results for the other correlations based on Fisher's Z transformation can be found in Table 9.4 and in Figure 9.4,

| **Correlation Description** | **Correlation Coefficient (r)** | **95% CI Lower** | **95% CI Upper** |
|---|---|---|---|
| Total Cost of Connections and DPb | -0.87 | -0.99 | 0.05 |
| Total Cost of Connections and ECI | 0.77 | -0.35 | 0.98 |
| Total Cost of Connections and $ECI_{Rest}$ | 0.98 | 0.72 | 1.00 |
| DPb and $ECI_{Rest}$ | -0.91 | -0.99 | -0.14 |

**Table 9.4:** 95% Confidence Intervals for Correlation Coefficients using Fisher's Z Transformation

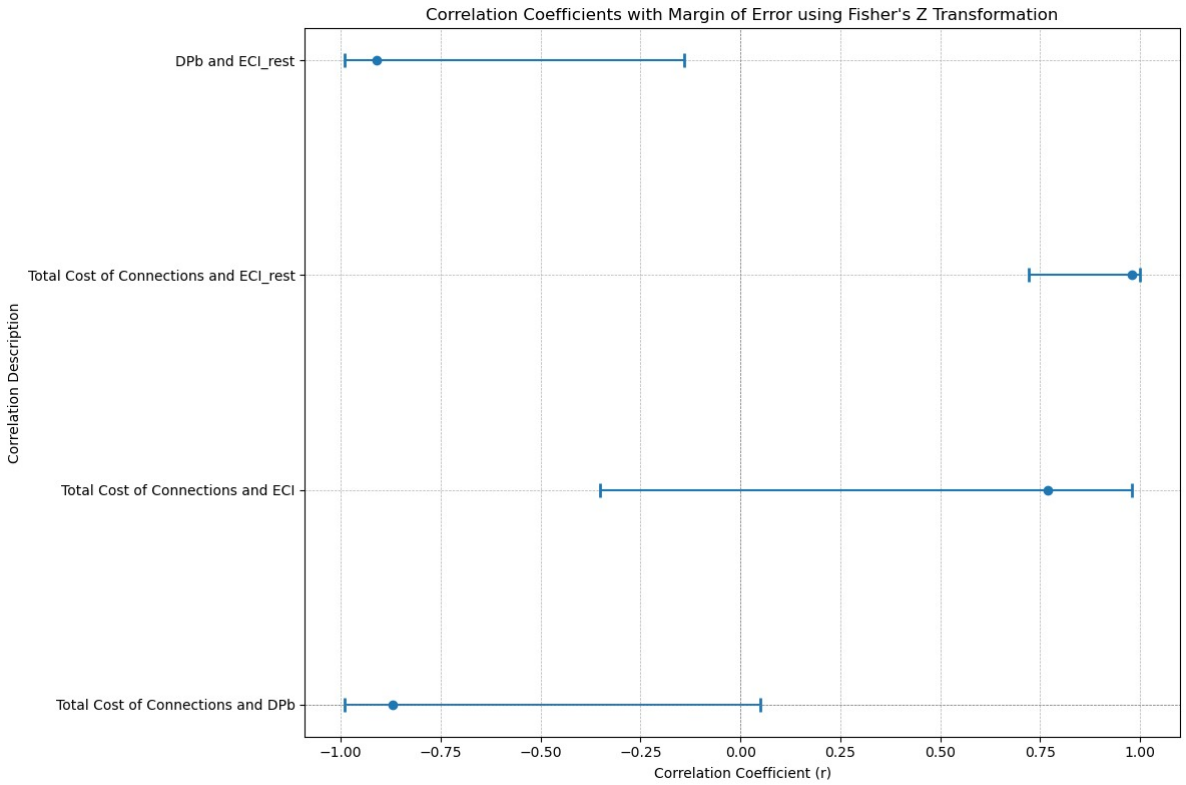


**Figure 9.4:** Correlation Coefficients with Margin of Error using Fisher's Z transformation

In summary, the smaller the margin of error, the more precise the estimate of the correlation coefficient. The correlation between Total Cost of Connections and $\text{ECI}_{\text{Rest}}$ has the smallest margin of error (0.72, 1.00), indicating a more precise estimate compared to the other correlations. A larger sample size helps to reduce the standard error and increase the reliability of the results.

### Hypothesis Test for Correlation

The objective is to test whether the sample correlation $r = 0.98$ is significantly stronger than 0.75. This corresponds to the following hypotheses:

- **Null Hypothesis ($H_0$):** $\rho = 0.75$

  The population correlation is equal to 0.75. This means there is no evidence that the correlation is stronger than 0.75.

- **Alternative Hypothesis ($H_A$):** $\rho > 0.75$

  The population correlation is greater than 0.75, indicating a stronger relationship between the variables.

This is a **one-tailed test**, as the interest lies in testing whether the correlation is stronger than 0.75.

The test statistic $z$ is calculated using the formula:

$$z = \frac{z' - z'_{\rho_0}}{SE} \tag{9.16}$$

Substituting the values:

$$z = \frac{2.298 - 0.973}{0.707} = \frac{1.325}{0.707} \approx 1.873 \tag{9.17}$$

For a one-tailed test at a 95% confidence level, the critical value of $z^*$ is:

$$z^* = 1.645 \tag{9.18}$$

The computed test statistic $z$ is compared to the critical value:

$$z = 1.873 > 1.645 \tag{9.19}$$

Since $z > z^*$, the null hypothesis $H_0$ is rejected.

Based on the sample correlation $r = 0.98$ and the sample size $n = 5$, it is concluded that the correlation is significantly stronger than 0.75 at the 95% confidence level. This indicates that the relationship between the variables is **very strong**.

### 9.2.2. Catenary action

Catenary action is an effective means of redistribution of loads after the failure of a structural member so that progressive collapse does not occur. This research has considered different beam configurations to determine how each would develop catenary action under accidental loading conditions.

The results indicate that single-span beams exhibit minimal catenary action because they are restricted in developing tensile forces in more than one span. Because catenary action depends upon a beam or slab's capacity to redistribute from bending action into axial tension, this action is inevitably weak at hinged or supported joints, where force redistribution cannot occur. Non-moment continuity prevents transferring forces to neighboring spans effectively, restricting the structure from resisting collapse. Therefore, single-span beam local failure occurs with quick progression, since there is no redundant load path for the forces to be picked up or redistributed.

Double-span beams are more ductile when forming a second load path because their continuity guarantees that the forces can be redistributed by tensile and flexural action. If a column is removed from the double-span beams, the surrounding beams can support loads through partial development of axial forces and moment transfer. In these cases, a second load path is achieved with ductile connections capable of accumulating large plastic deformations.

The Gerber beam design offers a compromise. Simple to disassemble and reassemble, its segmented nature avoids the production of tensile forces through the structure. Unlike monolithic beams or continuous steel members, which tend to stretch and produce considerable axial forces under loading, the Gerber system works with discrete plates and hinges, which are places of weakness in extreme loading conditions. The study indicates that changes in plate connection details, that is, increased bolt capacity, expanded hinge zones, or partial fixation of essential points, can increase the resistance to collapse while not sacrificing some demountability.

Finally, the primary barrier to complete catenary action in demountable structures is a deficiency of fully rigid or ductile connections to transfer forces. In conventional buildings, beams can resist tension by being welded or have moment-resisting frames, creating the continuous load paths needed to prevent collapse.

# 10

# Conclusion

## 10.1. Conclusions

The goal of this research was to find an answer to the following research question.

*"What strategies and design principles can be employed to maintain structural robustness while aiming for a high disassembly of connections in a building construction?"*

This chapter brings together the results of the literature review and case study and makes suggestions for future research and the building industry.

**• Conclusion - The type of connection is a determining factor in providing a second load path and in ensuring that the structure is demountable.**

Hinged connections provide free rotation but little moment resistance. In terms of disassembly, they can be easily removed. Still, because of their low moment resistance, they are inappropriate for retaining strength when columns are removed, mainly when the catenary action is activated. The structure is axially and shear-dominated in this mode, which is less efficient for load redistribution when a column is removed. The hinged connection can take up a load of only 50 kN which is approximately 14% of the required 350 kN (for the model building used), while the Disassembly Potential of the system is the highest at 0.57 (approximately 54% higher than that of rigid connections at 0.37).

Semi-rigid connections are neither fully resistant to moment transfer nor rotation; they offer a compromise between rigid and fully hinged connections. They are stronger than hinged connections, with increased structural integrity but reduced disassembly since more advanced disassembly is required. Moment capacity and rotational stiffness are significant if a column is being removed. The semi-rigid connection can take up 150 kN, three times as much as in the hinged situation, but it is still insufficient (43% of the 350 kN needed). Furthermore, the Disassembly Potential of the system of 0.39 is about 32% lower than the Disassembly Potential of the system of 0.57 of the hinged connection.

The rigid joints are almost fully resistant to moment and rotation, giving the structure the best possible performance to support loads and remain stable in the event of column removal. In addition, the structure can act as a Vierendeel system. This is at the expense of disassembly. disassembly requires additional labor or other mechanisms, which reduces reuse potential and affects the circular economy. Although the compression layer is not required in these connections, it greatly benefits in disassembly, and it still falls short compared to the others. The rigid connection can take up 400 kN, which is more than sufficient, but scores poorly in Disassembly Potential of the system compared to the hinged connection: 0.37 (about 35% lower). This can be increased to 0.47 (an improvement of 27%) if the floor is supported freely and does not function as a stability diagram.

**• Conclusion - Catenary action alone is insufficient to ensure structural robustness in single-span steel beams due to excessive stress on bolted connections.**

The test showed that reliance only on catenary action to produce column removal strength cannot be relied on. Although theoretically possible, high tension in this mechanism tended to overstress bolted connections, and premature bolt failure (zip-locker effect) was the norm. Only if the connection is rigid enough can a single span of a beam work.

**• Conclusion - Compared to single-span beams, double-span beams enhance load redistribution through flexural action and reduce the Disassembly Potential of the system due to having fewer connections.**

The added span length and the addition of a secondary support point made the double span strong enough to redistribute loads and remain intact despite the removal of the column. The double span can absorb the point load of 350 kN, as required. The increased strength of the structure is the result of the flexural resistance offered by the beam. There exists greater Disassembly Potential in the system with a value of 0.51, this is 38% higher than the rigid connection with a single span (0.37). The increased Disassembly Potential of the system results from the number of connections and the relatively smaller size of the connections to the rigid connection. This scenario also has a reduced ECI and a lower remaining ECI compared to the single-span options.

**• Conclusion - Gerber beams outperform double spans in providing a second load path and optimizing the Disassembly Potential of the system through strategic hinge placement.**

Gerber beams with strategically positioned hinges were a compromise between robustness and disassembly. The almost zero-moment hinges imposed less stress on the strength of the connection without compromising stability so much as to be unacceptable for normal loading. This solution necessitated more sophistication in moment redistribution and the capacity of the connection. This arrangement can also carry a design load of 350 kN with minor modifications. In addition, the Gerber beam is slightly better in disassembly than the double span, with a Disassembly Potential of the system of 0.53 instead of 0.51 for the double span (4% improvement). The ECI is also not much higher than the ECI of other scenarios.

Gerber beams with strategically positioned hinges were a compromise between robustness and disassembly. The almost zero-moment hinges imposed less stress on the strength of the connection without compromising stability so much as to be unacceptable for normal loading. This solution necessitated more sophistication in moment redistribution and the capacity of the connection. This arrangement can also carry a design load of 350 kN (100% of the requirement) with minor modifications. In addition, the Gerber beam is slightly better in disassembly than the double span, at a Disassembly Potential of the system of 0.53 instead of 0.51 for the double span. The ECI is also not much higher than the ECI of other scenarios.

**• Conclusion - The Environmental Cost Indicator (ECI) and the Disassembly Potential (DP) are interrelated, but must be assessed separately.**

The DP and the ECI are related but should be treated differently since the correlation is not always linear. A higher DP will have a lower rest ECI since better disassembly gives more material reuse, less construction waste, and less embodied carbon emissions. However, the correlation is not absolute. An increase in 20% in Disassembly Potential of the system can lead to a reduction 15% in environmental costs. One design solution, in particular, that is best for disassembly will have a higher indirect environmental burden. Bolted joint details are an example in that, in providing for easier disassembly than welded ones, they utilize more material in bolts and plates, adding to the overall environmental price of the building. Low-ECI materials such as mass timber, in turn, might encounter disassembly difficulties from using adhesives or composite bonding and thus be denied their reuse opportunity even with an initial lower environmental impact.

The main difference between the two measures is what they evaluate. DP measures how easy it is to take a building apart. This is different from material durability, where a material like steel can be easy

to disassemble but still have a high carbon footprint. The ECI quantifies the environmental footprints of the entire building lifecycle, from materials extraction to manufacturing, transport, and disposal. A building might be simple to dismantle (high DP) but environmentally resource intensive (high ECI), and vice versa.

**• Conclusion - Column spacing and beam cross-sections affect both robustness and the Disassembly Potential of the system, but their impact is secondary to the type of connection.**

Redesigning the structure to shorter spans in the main direction has little effect on the ECI. Shorter spans have lower cross-sectional areas on the one hand but more columns and connections on the other. Due to the reduced ratio of vertical to horizontal forces, structural robustness is easier to achieve.

In contrast, longer spans make disassembly easier by reducing the number of connections and columns, simplifying the removal and reuse of components. While longer spans increase the ECI because they require larger cross-sections and more material, they also reduce structural strength.

However, all these changes in ECI and DPb are not significant compared to the changes when the connection type of beam configuration is changed.

**• Conclusion - The overall cost of a system is strongly correlated with the Environmental Costs at the end of life.**

The $ECI_{rest}$ of a connection can be determined by looking at the cost of a connection. The increased material and assembly cost measures the challenge of assembling a connection and the value of the initial ECI. The total cost of a connection and the $ECI_{rest}$ have a correlation of 0.98 and the 95% confidence interval is within a margin of 0.72 and 1.00. This shows that the total cost of a connection gives good insight into the ECI at the end of the service life of a building.

**Final conclusion**

• The goal of this thesis was to investigate the rules and design strategies to achieve structural robustness and demountable connections in building constructions. The results confirm that the structural beam configuration significantly contributes to robustness and disassembly. Rigid joints in single spans provide the highest structural robustness, but are the least demountable, whereas hinged connections provide better disassembly compared to rigid connections. However, continuous beams offer a well-balanced compromise between these two critical aspects, making them a viable solution. Due to strategically placed hinges, the Gerber beam system scores the best overall.

• An overview of catenary action and how it can be used to achieve robustness was provided in this report. However, the study revealed that relying solely on catenary action in single-span steel beams is impractical due to excessive stress on connections and elements. Instead, robustness is best achieved through the flexural action of continuous beams or the strategic use of rigid connections.

• The correlation between the Disassembly Potential of a building and the Environmental Cost Indicator was successfully investigated, and it was found that although both indices contain different information on circularity and sustainability, they are inherently related. The Disassembly Potential of a building is a derivative of the ECI in that a higher DP implies improved reuse of materials and lower environmental impact. However, a high Disassembly Potential of a building does not imply a sustainable building.

## 10.2. Recommendations

This study indicates that there is a requirement for design solutions that balance structural robustness and disassembly in demountable buildings. This section discusses some recommendations for future research and the building industry.

### 10.2.1. Future research

In this subsection some recommendations for future research are given.

**I. Innovation in Connection Design**

Future research should be directed towards creating new connection systems that eliminate the inherent trade-off between disassembly and robustness. This includes studies of hybrid connection details, which achieve the strength of fixed connections and the disassembly convenience of hinged connections. Significant finite element analysis is needed to find the ideal connection shape and material choice for maximum load capacity and minimum stress concentration under regular and accidental loads. Furthermore, connection arrangements should provide easy disassembly access with less interference from other components and minimum effort and tools.

**II. Structural Optimization for Robustness and Disassembly**

Future designs may modify the structure to improve load transfer and strength in partial failure, based on research on double-span and Gerber beams. It is also important to consider adding additional load paths, but this must be done carefully to not compromise the disassembly. A study using advanced computer models that can simulate different failure modes is recommended to understand the behavior of potential structures. This should also include optimizing the beam length and cross-section design to balance strength and disassembly.

**III. Improved design tools and processes**

The current structural analysis and design software must be improved to enable the design of robust structures and demountable buildings. Software must have built-in explicit robustness and/or disassembly constraints so that engineers can contrast the performance of various connection types and structural systems under different loading conditions, including accidental ones. In addition, the software should enable systematic use of the DP and the ECI throughout the design phase to make decisions that optimize structural performance in addition to environmental sustainability.

**IV. Holistic Research and Testing:**

More research is needed to test the findings of this study and further improve design guidelines for demountable building construction. This involves rigorous experimental testing of new types of connections and structural systems for multiple failure modes under realistic loading conditions. Detailed investigation of material responses to different environmental and loading conditions can improve the precision of structural models. Lastly, a life cost evaluation based on the design cost of the whole life, initial building expenditure, maintenance, deconstruction costs, and environmental implications must be utilized to fully view the design options in perspective and stimulate genuinely sustainable and demountable building practice.

### 10.2.2. Building industry

In this subsection some recommendations are given for the building industry.

**I. Optimize the Length of Steel Beams**

Longer steel beams provide greater flexibility for reuse, as they can be cut and reused for other purposes. They also contribute to structural robustness by providing an efficient load distribution through the flexural action. The implementation of longer beams reduces the demand for new materials, aligning with sustainable construction practices.

**II. Use Gerber Beams to Increase Strength and Disassembly**

Gerber beams have proven to be the best method of structural robustness and disassembly. By strategically placing the connections, the disassembly can be increased. As long as the beams are not too

long to transport, it can also span multiple columns. An optimal solution could be achieved by reducing the column-to-column distance and allowing the beams to extend across multiple columns.

**III. Use More Bolted Connections**

Bolted connections make structures easily demountable, flexible, and efficient. It is important to use as few bolts as possible to conserve plates, bolts, and labor. Compared to hard chemical connections, such as welds, bolted connections allow components to be more easily reused. This supports the circular economy approach.

**IV. Use Disassembly Design Principles**

When designing a building, it should be considered in advance how easily it can be disassembled. Priority should be given to the elements with the highest shadow costs. A low disassembly potential does not lead to high sustainability but does help to achieve a low ECI after the building's service life. Calculating the disassembly potential is not necessarily important, but the design principles are good to consider during the design phase.

# References


[1] Council of the European Union. “Towards zero-emission buildings by 2050: Council adopts rules to improve energy performance”. In: (Apr. 2024). Accessed: 2024-05-21. URL: https://www.consilium.europa.eu/en/press/press-releases/2024/04/12/towards-zero-emission-buildings-by-2050-council-adopts-rules-to-improve-energy-performance/.

[2] M. Weir, A. Rempher, and R. Esau. “Embodied Carbon 101: Building Materials”. In: (Mar. 2023). URL: https://rmi.org/embodied-carbon-101/.

[3] “Do Not Underestimate the Danger of Explosion: Even Dust Can Destroy Equipment and Kill”. In: (2018). Accessed: June 4, 2024.

[4] M. N. Bussell and A. E. K. Jones. “Robustness and the relevance of Ronan Point today”. In: *The Structural Engineer* 88.23 (2010).

[5] Mark Juinio. “Progressive Collapse of Structures”. In: (July 2018). Accessed: 2024-06-25.

[6] National Institute of Standards and Technology (NIST). *Federal Building and Fire Safety Investigation of the World Trade Center Disaster: Final Report on the Collapse of World Trade Center Building 7*. Detailed investigation and findings on the collapse of WTC Building 7. 2008. URL: https://nvlpubs.nist.gov/nistpubs/Legacy/NCSTAR/ncstar1-6dv2.pdf.

[7] Olivier Berruyer. *Les tours jumelles du World Trade Center (5/10) – Les écroulements*. Accessed: 2025-03-13. 2017. URL: https://www.les-crises.fr/11-septembre-2001/.

[8] Stichting Koninklijk Nederlands Normalisatie Instituut. “NEN-EN 1991-1-7: Eurocode 1 - Actions on structures - Part 1-7: Accidental actions”. In: (2023). Available under license to TU Delft S.M.Mouw@student.tudelft.nl. Dutch version including Corrigendum C1:2010 and Amendment A1:2014. URL: www.nen.nl.

[9] Netherlands Standardization Institute. “NEN-EN 1991-1-7+C1+A1:2015 Eurocode 1: Actions on structures - Part 1-7: General actions - Accidental actions”. In: (Oct. 2015). Dutch version including Corrigendum C1:2010 and Amendment A1:2014.

[10] Konstantinos Voulpiotis, Styfen Schär, and Andrea Frangi. “Quantifying robustness in tall timber buildings: A case study”. In: *Engineering Structures* 265 (Aug. 2022), p. 114427. DOI: 10.1016/j.engstruct.2022.114427.

[11] Sherif El-Tawil. *Characterization of Catenary Action*. University of Michigan, College of Engineering, Civil & Environmental Engineering. Available online: URL of the webpage (Accessed on June 4, 2024). 2024.

[12] *Nationale bijlage bij NEN-EN 1992-1-1+C2 Eurocode 2: Ontwerp en berekening van betonconstructies - Deel 1-1: Algemene regels en regels voor gebouwen*. NEN-EN 1992-1-1+C2/NB+A1:2020. Feb. 2020. URL: https://www.nen.nl.

[13] Simon Wijte. “Eisen aan robuustheid”. In: *Thema* 42 (2015), pp. 15–22.

[14] Arup. “Review of international research on structural robustness and disproportionate collapse”. In: (Oct. 2011). Commissioned by the previous government. The views and analysis expressed in this report are those of the authors and do not necessarily reflect those of the Department for Communities and Local Government or the Centre for the Protection of National Infrastructure (CPNI).

[15] Johannes A. J. Huber et al. “Structural robustness and timber buildings – a review”. In: *Wood Material Science and Engineering* 14 (Mar. 2018), pp. 107–128. DOI: 10.1080/17480272.2018.1446052.

[16] Ellen MacArthur Foundation. *The circular economy in detail*. Accessed: 2025-02-14. 2019. URL: https://www.ellenmacarthurfoundation.org/the-circular-economy-in-detail-deep-dive.

[17] Alba Concepts and Technical University of Eindhoven. “Building Circularity Index: Assessing Circular Potential of Buildings”. In: *Journal of Circular Economy* 12 (2023), pp. 45–60. URL: https://www.albaconcepts.nl/bci.

[18] Stichting Koninklijk Nederlands Normalisatie Instituut. *NTA 8713: Hergebruik van constructiestaal*. Beschikbaar via: https://www.nen.nl/nta-8713-2021-nl-278153. 2021.

[19] Mike Van Vliet, Jip Van Grinsven, and Jim Teunizen. “Circular Buildings - Een Meetmethodiek Voor Losmaakbaarheid 2.0”. In: (2021). In opdracht van het Ministerie van Binnenlandse Zaken en de Transitieagenda Circulaire Bouweconomie.

[20] *Steel Beam To Concrete Slab Connection*. Accessed: 2024-06-28. 2016. URL: https://image.regimage.org.

[21] VBI. “Toekomstgericht bouwen met VBI kanaalplaatvloeren”. In: (2024). Available online: [URLofthewebpage].

[22] Unknown. “Principedetails Remontabel Bouwen”. In: (2023). Kanaalplaten in combinatie met staalconstructie. URL: URL%20of%20the%20web%20page.

[23] Ministerie van Binnenlandse Zaken en Koninkrijksrelaties. “Bouwbesluit Online 2012”. In: (2012). Accessed: 2023-05-29.

[24] Peter Musters. “Remontabel Bouwen: Een praktische weg naar CO2-reductie”. Version 2.0. In: (May 2024). Available at VBI (www.vbi.nl).

[25] Building Systems UK. *ComFlor® 51+ Composite Floor Deck*. https://www.tatasteeleurope.com/construction/products/flooring/composite-floor-deck/comflor-51plus. Accessed: 2024-06-07. Tata Steel Europe.

[26] Alfredo Romero and Christoph Odenbreit. “Experimental investigation on novel shear connections for demountable steel-timber composite (STC) beams and flooring systems”. In: *Engineering Structures* 304 (2024), p. 117620. ISSN: 0141-0296. DOI: https://doi.org/10.1016/j.engstruct.2024.117620. URL: https://www.sciencedirect.com/science/article/pii/S0141029624001822.

[27] Dr. Florentia Kavoura, Y. Zhang, and M. Veljkovic. “Structural Performance of Demountable Hybrid Floor Systems Under Monotonic and Cyclic Loading”. In: *TudRepo Institutional Repository* (2023), pp. 423–427. DOI: 10.1002/cepa.2755. URL: http://resolver.tudelft.nl/uuid:d8c433db-fb6c-4a6f-8021-ac5bd5ede50c.

[28] Ahmed Shamel Fahmy, Sherine Mostafa Swelem, and Mohamed Kamal Abdelaziz. “Behavior of high-strength demountable bolted shear connectors in steel-concrete girders with prefabricated slabs”. In: *Alexandria Engineering Journal* 70 (2023), pp. 247–260. ISSN: 1110-0168. DOI: https://doi.org/10.1016/j.aej.2023.02.041. URL: https://www.sciencedirect.com/science/article/pii/S1110016823001461.

[29] NEN. *Eurocode 3: Design of steel structures - Part 1-8: Design of joints*. NEN-EN 1993-1-8:2006 en. Delft, Netherlands: NEN, 2006.

[30] European Committee for Standardization (CEN). *EN 1993-1-8: Eurocode 3: Design of Steel Structures - Part 1-8: Design of Joints*. EN 1993-1-8. Brussels, Belgium: European Committee for Standardization, 2005.

[31] Steel Construction Institute. *Steel Construction: Composite Structures*. Accessed: 2025-02-21. 2023. URL: https://www.steelconstruction.info/images/d/d6/SCI_P102.pdf.

[32] Dick A. Hordijk and Jan W.B. Stark. “Column Base Plate Connections: The Dutch Approach”. In: *Eindhoven University of Technology and Adviesbureau Hageman, The Netherlands; Delft University of Technology and Stark Partners, The Netherlands* (2009). Accessed: 2024-05-29.

[33] *Eurocode 3: Design of steel structures - Part 1-1: General rules and rules for buildings*. EN 1993-1-1. Incorporating Corrigenda February 2006 and March 2009. Brussels: European Committee for Standardization (CEN), 2005.

[34] Xiaoyong Zhang et al. “Failure analyzes of high-strength bolted connection with over-preload tightening torque under double shear test”. In: *Structures* 72 (2025), p. 108249. ISSN: 2352-0124. DOI: https://doi.org/10.1016/j.istruc.2025.108249. URL: https://www.sciencedirect.com/science/article/pii/S2352012425000633.

[35] Feng Wei et al. “Fracture behaviour and design of steel tensile connections with staggered bolt arrangements”. In: *International Journal of Steel Structures* 15 (2015), pp. 863–879.

[36] Bo Yang and Kang Hai Tan. “Experimental tests of different types of bolted steel beam–column joints under a central-column-removal scenario”. In: *Engineering Structures* 54 (2013), pp. 112–130. ISSN: 0141-0296. DOI: https://doi.org/10.1016/j.engstruct.2013.03.037. URL: https://www.sciencedirect.com/science/article/pii/S0141029613001600.

[37] H.H. Snijder. “Trends in steel structures concerning materials, codes and applications”. English. In: *Stahlbau* 86.8 (Aug. 2017), pp. 666–673. ISSN: 0038-9145. DOI: 10.1002/stab.201710514.

[38] Structural Detailer. *Rules of Thumb*. Accessed: 2025-02-18. 2025. URL: https://structuraldetailer.com/rules-of-thumb/.

[39] Mark Spanenburg. “Robuustheid van horizontale trekbanden”. In: *Cement* (May 2024). Normbesef, Article 6. URL: https://www.arcadis.com/nl-nl/kennis/artikelen/robuustheid-van-horizontale-trekbanden.

[40] Zach Bobbitt. *What is Considered to Be a “Strong” Correlation?* Accessed: 2025-02-11. 2020. URL: https://www.statology.org/what-is-a-strong-correlation/.

# A

# Unity check calculations

This document provides unity check calculations for HEB400 and HEB300 beams under various support conditions: moment-resistant, partially fixed, hinged, and hinge-moment-resistant. Calculations are performed for both the Serviceability Limit State (SLS) and the Ultimate Limit State (ULS). The span of the beams is 7.2 meters. For four scenarios, it will be checked if an HEB300 is sufficient or if an HEB400 is required.

## A.1. Beam Dimensions and Properties

The dimensions for a beam of type HEB400 and HEB300 are given below.

### A.1.1. HEB400

- Height (H): 400 mm
- Width (B): 300 mm
- Web thickness (tw): 11 mm
- Flange thickness (tf): 21 mm
- Weight: 155.8 kg/m

### A.1.2. HEB300

- Height (H): 300 mm
- Width (B): 300 mm
- Web thickness (tw): 11 mm
- Flange thickness (tf): 19 mm
- Weight: 117 kg/m

## A.2. Load Calculations

The load calculation that are performed here are the SLS and the ULS.

### A.2.1. SLS (Serviceability Limit State)

$$\text{Permanent load} = 5.778 \times 7.2 = 41.6016\,\text{kN/m}$$
$$\text{Variable load} = 6 \times 7.2 = 43.2\,\text{kN/m}$$
$$\text{Total load (HEB400)} = 41.6016 + 43.2 + 1.526 = 86.3276\,\text{kN/m}$$
$$\text{Total load (HEB300)} = 41.6016 + 43.2 + 1.147 = 85.9486\,\text{kN/m}$$

### A.2.2. ULS (Ultimate Limit State)

$$\text{Permanent load} = 4.28 \times 7.2 = 30.816\,\text{kN/m}$$
$$\text{Variable load} = 4 \times 7.2 = 28.8\,\text{kN/m}$$
$$\text{Total load (HEB400)} = 30.816 + 28.8 + 1.526 = 61.142\,\text{kN/m}$$
$$\text{Total load (HEB300)} = 30.816 + 28.8 + 1.147 = 60.763\,\text{kN/m}$$

## A.3. Unity Check Calculations

The unity check involves comparing the applied loads to the design capacities of the beam. For S355 steel, the yield strength $f_y$ is 355 MPa.

### A.3.1. Bending Moment Capacity

$$\text{Section modulus (HEB400)} = 1.93 \times 10^6\,\text{mm}^3$$
$$\text{Section modulus (HEB300)} = 1.49 \times 10^6\,\text{mm}^3$$
$$M_{Rd} = \frac{f_y \times W}{\gamma_{M0}}$$
$$M_{Rd}(\text{HEB400}) = \frac{355 \times 1.93 \times 10^3}{1.0} = 685.15\,\text{kNm}$$
$$M_{Rd}(\text{HEB300}) = \frac{355 \times 1.49 \times 10^3}{1.0} = 529.95\,\text{kNm}$$

### A.3.2. SLS Unity Check

For a beam with a hinge on one side and a moment-resistant connection on the other side:

$$M_{Ed} = \frac{w \times L^2}{8}$$
$$M_{Ed}(\text{HEB400, SLS}) = \frac{86.3276 \times 7.2^2}{8} = 558.27\,\text{kNm}$$
$$M_{Ed}(\text{HEB300, SLS}) = \frac{85.9486 \times 7.2^2}{8} = 555.27\,\text{kNm}$$
$$\text{Unity Check (HEB400, SLS)} = \frac{558.27}{685.15} = 0.815$$
$$\text{Unity Check (HEB300, SLS)} = \frac{555.27}{529.95} = 1.048$$

### A.3.3. ULS Unity Check

For a beam with a hinge on one side and a moment-resistant connection on the other side:

$$M_{Ed} = \frac{w \times L^2}{8}$$
$$M_{Ed}(\text{HEB400, ULS}) = \frac{61.142 \times 7.2^2}{8} = 395.83\,\text{kNm}$$
$$M_{Ed}(\text{HEB300, ULS}) = \frac{60.763 \times 7.2^2}{8} = 393.43\,\text{kNm}$$
$$\text{Unity Check (HEB400, ULS)} = \frac{395.83}{685.15} = 0.578$$
$$\text{Unity Check (HEB300, ULS)} = \frac{393.43}{529.95} = 0.743$$

## A.4. Summary

| Beam Type | Scenario | SLS Unity Check | ULS Unity Check |
|---|---|---|---|
| HEB400 | Rigid | 0.54 | 0.39 |
| HEB400 | Semi-rigid | 0.68 | 0.48 |
| HEB400 | Hinged | 0.82 | 0.58 |
| HEB400 | Double span | 0.81 | 0.58 |
| HEB300 | Rigid | 0.70 | 0.50 |
| HEB300 | Semi-rigid | 0.88 | 0.62 |
| HEB300 | Hinged | 1.05 | 0.74 |
| HEB300 | Double span | 1.05 | 0.74 |

**Table A.1:** Unity Check results for HEB400 and HEB300 beams with different support conditions

# B

# Cost of the connections

This appendix displays the cost for the connections and how they are built up. The cost analysis is used in section 7.5. The values in Table B.1 are the standard IdeaStatiCa settings for the cost calculations.

| Component | Estimated Cost |
|---|---|
| Steel parts | €2.00 per kg |
| Welds | €40.00 per kg |
| Bolt assemblies | €5.00 per kg |
| Hole drilling | 30 percent of bolt assembly cost |

**Table B.1:** Standard Cost Estimates for Connections

The first cost will be that of the single span hinged connection and the double span hinged connection (Figure B.1). The second one is the rigid connection (Figure B.2). The third one is the semi-rigid connection (Figure B.3). The fourth is the Gerber connection (Figure B.4).

## Cost estimation

### Steel

| Steel grade | Total weight [kg] | Unit cost [€/kg] | Cost [€] |
|---|---|---|---|
| S 355 | 39,68 | 2,00 | 79,37 |

### Bolts

| Bolt assembly | Total weight [kg] | Unit cost [€/kg] | Cost [€] |
|---|---|---|---|
| M20 8.8 | 3,22 | 5,00 | 16,09 |

### Welds

| Weld type | Throat thickness [mm] | Leg size [mm] | Total weight [kg] | Unit cost [€/kg] | Cost [€] |
|---|---|---|---|---|---|
| Double fillet | 8,0 | 11,3 | 1,09 | 40,00 | 43,41 |
| Double fillet | 8,0 | 11,3 | 2,32 | 40,00 | 92,60 |

### Hole drilling

| Bolt assembly cost [€] | Percentage of bolt assembly cost [%] | Cost [€] |
|---|---|---|
| 16,09 | 30,0 | 4,83 |

### Cost summary

| Cost estimation summary | Cost [€] |
|---|---|
| Total estimated cost | 236,29 |

**Figure B.1:** Hinged connection costs, used for a single span and the double span scenario

## Cost estimation

### Steel

| Steel grade | Total weight [kg] | Unit cost [€/kg] | Cost [€] |
|---|---|---|---|
| S 355 | 214,63 | 2,00 | 429,26 |

### Bolts

| Bolt assembly | Total weight [kg] | Unit cost [€/kg] | Cost [€] |
|---|---|---|---|
| M24 8.8 | 15,19 | 5,00 | 75,96 |
| M20 8.8 | 1,23 | 5,00 | 6,16 |

### Welds

| Weld type | Throat thickness [mm] | Leg size [mm] | Total weight [kg] | Unit cost [€/kg] | Cost [€] |
|---|---|---|---|---|---|
| Double fillet | 18,0 | 25,5 | 8,96 | 40,00 | 358,52 |
| Double fillet | 15,0 | 21,2 | 19,09 | 40,00 | 763,59 |
| Double fillet | 8,0 | 11,3 | 0,40 | 40,00 | 16,08 |

### Hole drilling

| Bolt assembly cost [€] | Percentage of bolt assembly cost [%] | Cost [€] |
|---|---|---|
| 82,12 | 30,0 | 24,64 |

### Cost summary

| Cost estimation summary | Cost [€] |
|---|---|
| Total estimated cost | 1674,21 |

**Figure B.2:** Costs for the rigid connection

## Cost estimation

### Steel

| Steel grade | Total weight [kg] | Unit cost [€/kg] | Cost [€] |
|---|---|---|---|
| S 355 | 92,60 | 2,00 | 185,19 |

### Bolts

| Bolt assembly | Total weight [kg] | Unit cost [€/kg] | Cost [€] |
|---|---|---|---|
| M20 8.8 | 6,28 | 5,00 | 31,38 |
| M30 8.8 | 1,91 | 5,00 | 9,55 |

### Welds

| Weld type | Throat thickness [mm] | Leg size [mm] | Total weight [kg] | Unit cost [€/kg] | Cost [€] |
|---|---|---|---|---|---|
| Double fillet | 12,0 | 17,0 | 2,71 | 40,00 | 108,52 |
| Double fillet | 12,0 | 17,0 | 1,27 | 40,00 | 50,82 |
| Double fillet | 15,0 | 21,2 | 8,14 | 40,00 | 325,56 |
| Double fillet | 8,0 | 11,3 | 0,20 | 40,00 | 8,04 |
| Double fillet | 5,0 | 7,1 | 0,08 | 40,00 | 3,14 |

### Hole drilling

| Bolt assembly cost [€] | Percentage of bolt assembly cost [%] | Cost [€] |
|---|---|---|
| 40,94 | 30,0 | 12,28 |

### Cost summary

| Cost estimation summary | Cost [€] |
|---|---|
| Total estimated cost | 734,49 |

**Figure B.3:** Costs for the semi-rigid connection

## Cost estimation

### Steel

| Steel grade | Total weight [kg] | Unit cost [€/kg] | Cost [€] |
|---|---|---|---|
| S 355 | 20,64 | 2,00 | 41,28 |

### Bolts

| Bolt assembly | Total weight [kg] | Unit cost [€/kg] | Cost [€] |
|---|---|---|---|
| M20 8.8 | 3,97 | 5,00 | 19,86 |

### Welds

| Weld type | Total weight [kg] | Unit cost [€/kg] | Cost [€] |
|---|---|---|---|
| | | | |

### Hole drilling

| Bolt assembly cost [€] | Percentage of bolt assembly cost [%] | Cost [€] |
|---|---|---|
| 19,86 | 30,0 | 5,96 |

### Cost summary

| Cost estimation summary | Cost [€] |
|---|---|
| Total estimated cost | 67,09 |

**Figure B.4:** Costs for the Gerber span connection; beam to beam

# C

# ECI calculations

This Appendix contains the calculations for the Environmental Cost Indicator. The Environmental Cost Indicator (ECI) depends on various environmental effects. When calculating the ECI, the environmental effects of various substances (horizontal axis) are converted into a financial value by multiplying it by the weight (vertical axis). Environmental effects, such as global warming potential, acidification, eutrophication, and toxicity, are included in the calculation of the ECI.

| **Shadow prize (Euro) per kg equivalents** | | **0,16** | **0,05** | **30** | **0,09** | **0,03** | **0,0001** | **0,06** | **2** | **4** | **9** | |
|---|---|---|---|---|---|---|---|---|---|---|---|---|
| **Impact category** | **Unit [kg]** | **Abiotic depletion** | **Global warming (GWP100)** | **Ozone layer depletion (ODP)** | **Human toxicity** | **Fresh water aquatic ecotox.** | **Marine aquatic ecotoxicity** | **Terrestrial ecotoxicity** | **Photochemical oxidation** | **Acidification** | **Eutrophication** | |
| **Unit** | | kg Sb eq | kg CO2 eq | kg CFC-11 eq | kg 1,4-DB eq | kg 1,4-DB eq | kg 1,4-DB eq | kg 1,4-DB eq | kg C2H4 | kg SO2 eq | kg PO4--- eq | |
| **Pressure layer(7.2m*36m)** | | **3,05E-04** | **1,07E-01** | **4,88E-09** | **1,12E-02** | **2,28E-03** | **3,80E+00** | **2,01E-04** | **8,24E-06** | **2,44E-04** | **4,29E-05** | |
| Concrete C25/30 (CEM I-CEMIII) | 62208 | 3,03E+00 | 3,32E+02 | 9,12E-03 | 6,28E+01 | 4,25E+00 | 2,36E+01 | 7,50E-01 | 1,03E+00 | 6,08E+01 | 2,40E+01 | **€ 512,45** |
| **Hollow core slab (7.2m)** | | **3,05E-04** | **1,07E-01** | **4,88E-09** | **1,12E-02** | **2,28E-03** | **3,80E+00** | **2,01E-04** | **8,24E-06** | **2,44E-04** | **4,29E-05** | |
| Concrete C45/55 (CEM I-CEMIII) | 2549 | 1,24E-01 | 1,36E+01 | 3,74E-04 | 2,57E+00 | 1,74E-01 | 9,69E-01 | 3,07E-02 | 4,20E-02 | 2,49E+00 | 9,85E-01 | **€ 21,00** |
| **Grout (per joint of 7.2 meter)** | | **2,71E-04** | **9,33E-02** | **4,42E-09** | **1,03E-02** | **2,17E-03** | **3,57E+00** | **1,81E-04** | **7,40E-06** | **2,22E-04** | **3,94E-05** | |
| Concrete C12/15 (CEM III) | 144 | 7,03E-03 | 7,69E-01 | 2,11E-05 | 1,45E-01 | 9,84E-03 | 5,47E-02 | 1,74E-03 | 2,37E-03 | 1,41E-01 | 5,56E-02 | **€ 1,19** |
| **Steel beams HEB400** | | **1,56E-02** | **1,82E+00** | **5,66E-08** | **6,02E-01** | **4,57E-01** | **4,27E+02** | **1,08E-02** | **1,08E-03** | **6,16E-03** | **1,32E-03** | |
| 3.6 meter | 559 | 1,40 | 50,87 | 0,00 | 30,31 | 7,66 | 23,85 | 0,36 | 1,21 | 13,78 | 6,63 | **€ 136,07** |
| 7.2 meter | 1118 | 2,80 | 101,73 | 0,00 | 60,62 | 15,32 | 47,70 | 0,73 | 2,42 | 27,55 | 13,26 | **€ 272,14** |
| 9.0 meter | 1398 | 3,50 | 127,17 | 0,00 | 75,78 | 19,15 | 59,62 | 0,91 | 3,03 | 34,44 | 16,58 | **€ 340,17** |
| 10.8 meter | 1677 | 4,20 | 152,60 | 0,00 | 90,94 | 22,98 | 71,55 | 1,09 | 3,63 | 41,33 | 19,89 | **€ 408,20** |
| 14.4 meter | 2236 | 5,60 | 203,47 | 0,00 | 121,25 | 30,64 | 95,40 | 1,45 | 4,84 | 55,10 | 26,52 | **€ 544,27** |
| **Ties** | | **1,54E-02** | **1,79E+00** | **7,17E-08** | **3,81E+00** | **1,49E+00** | **1,32E+03** | **3,18E-02** | **9,27E-04** | **7,38E-03** | **1,34E-03** | |
| Perimeter ties | 341 | 8,38E-01 | 2,40E-01 | 2,76E-09 | 1,68E-09 | 4,00E-10 | 8,42E-08 | 4,29E-10 | 6,35E-14 | 7,51E-17 | 1,61E-20 | **€ 1,08** |
| Peripheral ties | 57 | 1,40E-01 | 4,00E-02 | 4,59E-10 | 2,80E-10 | 6,67E-11 | 1,40E-08 | 7,14E-11 | 1,06E-14 | 1,25E-17 | 2,69E-21 | **€ 0,18** |
| **Steel sheet** | | **1,57E-02** | **1,83E+00** | **7,84E-08** | **3,79E+00** | **1,48E+00** | **1,30E+03** | **3,16E-02** | **9,31E-04** | **7,61E-03** | **1,37E-03** | |
| Diagonals | 24 | 5,91E-02 | 2,15E+00 | 5,54E-05 | 8,02E+00 | 1,05E+00 | 3,07E+00 | 4,46E-02 | 4,38E-02 | 7,17E-01 | 2,91E-01 | **€ 15,45** |
| Finplate | 5 | 1,14E-02 | 4,15E-01 | 1,07E-05 | 1,55E+00 | 2,02E-01 | 5,91E-01 | 8,60E-03 | 8,45E-03 | 1,38E-01 | 5,61E-02 | **€ 2,98** |
| Endplate semi rigid | 30 | 7,57E-02 | 2,76E+00 | 7,09E-05 | 1,03E+01 | 1,34E+00 | 3,93E+00 | 5,71E-02 | 5,61E-02 | 9,17E-01 | 3,72E-01 | **€ 19,78** |
| Endplate rigid | 47 | 1,18E-01 | 4,31E+00 | 1,11E-04 | 1,60E+01 | 2,10E+00 | 6,14E+00 | 8,93E-02 | 8,77E-02 | 1,43E+00 | 5,82E-01 | **€ 30,90** |
| Gerber Finplate | 10 | 2,59E-02 | 9,44E-01 | 2,43E-05 | 3,52E+00 | 4,59E-01 | 1,34E+00 | 1,96E-02 | 1,92E-02 | 3,14E-01 | 1,27E-01 | **€ 6,77** |
| **Medium carbon steel** | | **1,00E-04** | **2,30E+00** | **1,50E-07** | **5,00E-02** | **2,00E-04** | **2,00E-02** | **1,00E-04** | **5,00E-05** | **1,00E-02** | **1,00E-03** | |
| Bolts M20 x 100 | 0,371 | 5,94E-06 | 4,27E-02 | 1,67E-06 | 1,67E-03 | 2,23E-06 | 7,42E-07 | 2,23E-06 | 3,71E-05 | 1,48E-02 | 3,34E-03 | **€ 0,06** |
| **Steel beams** | | **1,56E-02** | **1,82E+00** | **5,66E-08** | **6,02E-01** | **4,57E-01** | **4,27E+02** | **1,08E-02** | **1,08E-03** | **6,16E-03** | **1,32E-03** | |
| HEB200, 3,6 meter | 221 | 5,52E-01 | 2,01E+01 | 3,74E-04 | 1,20E+01 | 3,02E+00 | 9,41E+00 | 1,44E-01 | 4,78E-01 | 5,44E+00 | 2,62E+00 | **€ 53,71** |
| HEB300, 5.4 meter | 632 | 1,58E+00 | 5,75E+01 | 1,07E-03 | 3,43E+01 | 8,66E+00 | 2,70E+01 | 4,11E-01 | 1,37E+00 | 1,56E+01 | 7,49E+00 | **€ 153,77** |
| HEB300, 7.2 meter | 842 | 2,11E+00 | 7,66E+01 | 1,43E-03 | 4,57E+01 | 1,15E+01 | 3,59E+01 | 5,48E-01 | 1,82E+00 | 2,08E+01 | 9,99E+00 | **€ 205,02** |

## General

| | | |
|---|---|---|
| Length | 36 | m |
| Width | 7,2 | m |
| A_beam | 197,80 | cm2 |
| Beam volume | 0,71 | m3 |
| Bolt M20 x 100 | 31,42 | cm3 |

| Single span hinged | | |
|---|---|---|
| # connections | 10 | |
| Bolts\connections | 3 | |
| # bolts,total | 30 | |
| # finplates | 10 | |
| Finplate volume | 5,78E-04 | m3 |
| Bolts total volume | 9,42E-04 | m3 |
| Finplate total volume | 5,78E-03 | m3 |

| Single span semi rigid | | |
|---|---|---|
| # connections | 10 | |
| Bolts\connections | 8 | |
| # bolts,total | 80 | |
| # endplates | 10 | |
| Endplate volume | 3,84E-03 | m3 |
| Bolts total volume | 2,51E-03 | m3 |
| Endplate total volume | 3,84E-02 | m3 |

| Single span rigid | | |
|---|---|---|
| # connections | 10 | |
| Bolts\connections | 12 | |
| # bolts,total | 120 | |
| # endplates | 10 | |
| # diagonals | 20 | |
| V_endplate | 0,006 | m3 |
| V_diagonal | 0,003 | m3 |
| V_bolts,total | 3,77E-03 | m3 |
| V_endplate,total | 6,00E-02 | m3 |
| V_diagonal,total | 6,00E-02 | m3 |

| Double span | | |
|---|---|---|
| # connections | 6 | |
| Bolts\connections | 3 | |
| # bolts,total | 18 | |
| # finplates | 6 | |
| V_finplate | 5,78E-04 | m3 |
| V_bolts,total | 5,65E-04 | m3 |
| V_finplate,total | 3,47E-03 | m3 |

| Gerber span | |
|---|---|
| # connections | 4 |

# D

# Disassembly potential calculations

## D.1. Scores for connection properties

| Connection Type (CT) | Score |
|---|---|
| **Dry connection**<br>Loose (no fastening material)<br>Click connection<br>Velcro connection<br>Magnetic connection | 1.00 |
| **Connection with added elements**<br>Bolt and nut connection<br>Spring connection<br>Corner connections<br>Screw connection | 0.80 |
| **Connections with added connection elements**<br>Direct integral connection<br>Pin connections***<br>Nail connection | 0.60 |
| **Soft chemical connection**<br>Caulking connection<br>Foam connection (PUR) | 0.20 |
| **Hard chemical connection**<br>Adhesive connection<br>Dump connection<br>Weld connection<br>Cementitious connection<br>Chemical anchors | 0.10 |

**Table D.1:** Connection Types and scores [19]

| Connection Accessibility (CA) | Score |
|---|---|
| Freely accessible without additional actions | 1.00 |
| Accessible with additional actions that do not cause damage | 0.80 |
| Accessible with additional actions with fully repairable damage | 0.60 |
| Accessible with additional actions with partially repairable damage | 0.40 |
| Not accessible - irreparable damage to the product or surrounding products | 0.10 |

**Table D.2:** Connection Accessibility and scores [19]

| Independency (ID) | Score |
|---|---|
| No independency - modular zoning of products or elements from different layers | 1.00 |
| Occasional independency of products or elements from different layers | 0.40 |
| Full integration of products or elements from different layers | 0.10 |

**Table D.3:** Independency and scores [19]

| Geometry of Product Edge (GPE) | Score |
|---|---|
| Open, no obstacle to the (interim) removal of products or elements | 1.00 |
| Overlapping, partial obstruction to the (interim) removal of products or elements | 0.40 |
| Closed, complete obstruction to the (interim) removal of products or elements | 0.10 |

**Table D.4:** Geometry of Product Edge and scores [19]

## D.2. Calculations for the disassembly potential

This section provides an overview of the calculations on the disassembly of the various systems. The area considered in these calculations can be found in Figure 8.1

### D.2.1. Overview of the connections

This subsection prevents the overview of the connections including the number of the elements as listed in Table 8.1.

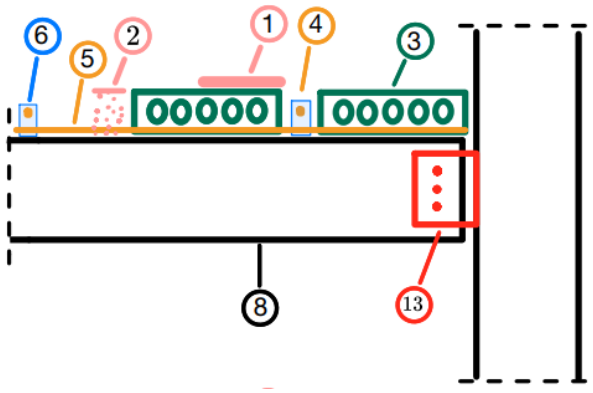


**Figure D.1:** Overview of the hinged connection

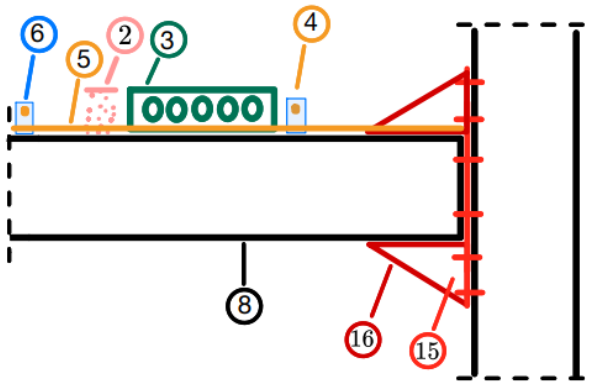


**Figure D.2:** Overview of the rigid connection

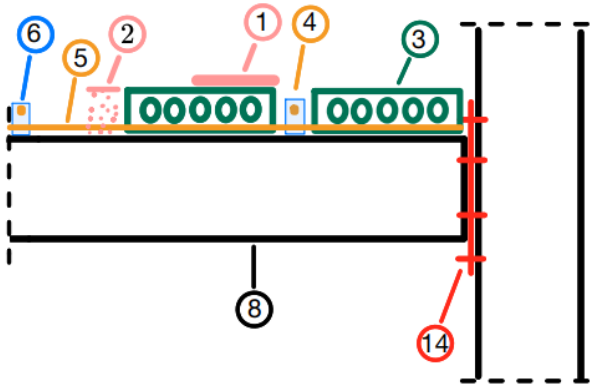


**Figure D.3:** Overview of the Semi-Rigid connection

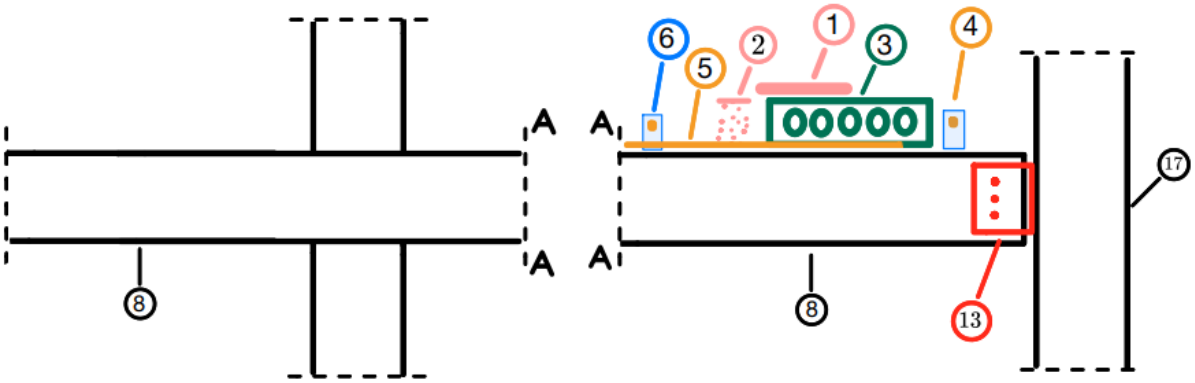


**Figure D.4:** Overview of the double span connections

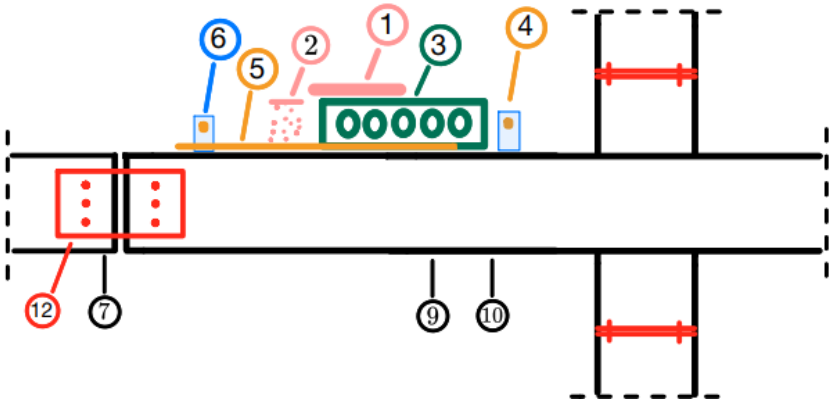


**Figure D.5:** Overview of the Gerber span connections

# D.2.2. Disassembly potential

## Disassembly potential calculation for the five scenarios.

| | |
|---|---|
| CT | Connection Type |
| CA | Connection Accesibility |
| DPc | Disassembly potential of the connection of n product or element |
| ID | Independency |
| GPE | Geometry product edge |
| DPcp | Disassembly potential of the composition |
| DPp | Disassembly potential of the product or element |
| ECI | Environmental Cost Indicator |
| DPb | Disassembly potential of the building |

### Single span

| Hinged | ID | Product | Load-bearing connection | Layer | CT | CA | DPc | ID2 | GPE | DPcp | DPp | ECI | number | ECI_tot | DPp*ECI_tot | | |
|---|---|---|---|---|---|---|---|---|---|---|---|---|---|---|---|---|---|
| Floor | 1 | Compression layer | Hollow core slabs | Structure | | 0,1 | 0,8 | 0,18 | 1,0 | 1,0 | 1,00 | **0,30** | € 512,45 | 1 | € 512,45 | € 154,70 | |
| | 2 | Grout | Hollow core slabs | Structure | | 0,2 | 0,4 | 0,27 | 0,4 | 0,4 | 0,40 | **0,32** | € 1,19 | 29 | € 34,40 | € 11,01 | |
| | 3 | Hollow core slab | Steel beams | Structure | | 1,0 | 0,4 | 0,57 | 1,0 | 0,4 | 0,57 | **0,57** | € 21,00 | 30 | € 629,89 | € 359,93 | |
| | 4 | Perimeter ties | Grout | Structure | | 0,2 | 0,1 | 0,13 | 1,0 | 0,1 | 0,18 | **0,15** | € 1,08 | 29 | € 31,28 | € 4,81 | 43,91% 0,20 |
| | 5 | Peripheral ties | Grout | Structure | | 0,2 | 0,1 | 0,13 | 1,0 | 0,1 | 0,18 | **0,15** | € 0,18 | 1 | € 0,18 | € 0,03 | |
| Beam | 6 | Steel studs | Finplate/endplate | Structure | | 0,1 | 0,4 | 0,16 | 0,4 | 0,1 | 0,16 | **0,16** | € 1,00 | 29 | € 29,00 | € 4,64 | 68,45% 0,36 |
| | 8 | Steel beam 7.2 | Finplate | Structure | | 0,8 | 0,4 | 0,53 | 1,0 | 1,0 | 1,00 | **0,70** | € 272,14 | 5 | € 1.360,68 | € 946,56 | |
| **Column** | 13 | Finplate | Column | Structure | | 0,1 | 0,4 | 0,16 | 1,0 | 1,0 | 1,00 | **0,28** | € 2,98 | 10 | € 29,77 | € 8,21 | 27,59% 0,00 |
| | | | | | | | | | | | | | | | **€ 2.627,64** | **€ 1.489,90** | 139,94% |
| | | | | | | | | | | | | | | | Disassembly potential | **0,57** | |
| | | | | | | | | | | | | | | | ECI remaining : (1 - DPp) * ECI_tot: | **€ 1.137,74** | |

| Rigid | ID | Product | Load-bearing connection | Layer | CT | CA | DPc | ID2 | GPE | DPcp | DPp | ECI | number | ECI_tot | DPp*ECI_tot | | |
|---|---|---|---|---|---|---|---|---|---|---|---|---|---|---|---|---|---|
| Floor | 1 | Compression layer | Hollow core slabs | Structure | | 0,1 | 0,8 | 0,18 | 1,0 | 1,0 | 1,00 | **0,30** | € 512,45 | 1 | € 512,45 | € 154,70 | |
| | 2 | Grout | Hollow core slabs | Structure | | 0,2 | 0,4 | 0,27 | 0,4 | 0,4 | 0,40 | **0,32** | € 1,19 | 29 | € 34,40 | € 11,01 | |
| | 3 | Hollow core slab | Steel beams | Structure | | 1,0 | 0,4 | 0,57 | 1,0 | 0,4 | 0,57 | **0,57** | € 21,00 | 30 | € 629,89 | € 359,93 | |
| | 4 | Perimeter ties | Grout | Structure | | 0,2 | 0,1 | 0,13 | 1,0 | 0,1 | 0,18 | **0,15** | € 1,08 | 29 | € 31,28 | € 4,81 | |
| | 5 | Peripheral ties | Grout | Structure | | 0,2 | 0,1 | 0,13 | 1,0 | 0,1 | 0,18 | **0,15** | € 0,18 | 1 | € 0,18 | € 0,03 | 43,91% 0,17 |
| Beam | 6 | Steel studs | Finplate/endplate | Structure | | 0,1 | 0,4 | 0,16 | 0,4 | 0,1 | 0,16 | **0,16** | € 10,00 | 29 | € 290,00 | € 46,40 | |
| | 8 | Steel beam 7.2 | Endplate/Finplate | Structure | | 0,1 | 0,4 | 0,16 | 1,0 | 1,0 | 1,00 | **0,28** | € 205,02 | 5 | € 1.025,11 | € 282,79 | 25,03% 0,10 |
| **Column** | 15 | Extended Endplate rigid | Column | Structure | | 0,8 | 0,4 | 0,53 | 1,0 | 1,0 | 1,00 | **0,70** | € 30,90 | 10 | € 309,00 | € 214,96 | |
| | 16 | Diagonal plate | Column | Structure | | 0,1 | 0,4 | 0,16 | 1,0 | 1,0 | 1,00 | **0,28** | € 15,45 | 20 | € 309,00 | € 85,24 | 48,58% 0,10 |
| | | | | | | | | | | | | | | | **€ 3.141,31** | **€ 1.159,88** | 117,51% |
| | | | | | | | | | | | | | | | Disassembly potential | **€ 0,37** | |
| | | | | | | | | | | | | | | | ECI remaining : (1 - DPp) * ECI_tot: | **€ 1.981,44** | |

| Semi-rigid | ID | Product | Load-bearing connection | Layer | CT | CA | DPc | ID2 | GPE | DPcp | DPp | ECI | number | ECI_tot | DPp*ECI_tot | | |
|---|---|---|---|---|---|---|---|---|---|---|---|---|---|---|---|---|---|
| Floor | 1 | Compression layer | Hollow core slabs | Structure | | 0,1 | 0,8 | 0,18 | 1,0 | 1,0 | 1,00 | **0,30** | € 512,45 | 1 | € 512,45 | € 154,70 | |
| | 2 | Grout | Hollow core slabs | Structure | | 0,2 | 0,4 | 0,27 | 0,4 | 0,4 | 0,40 | **0,32** | € 1,19 | 29 | € 34,40 | € 11,01 | |
| | 3 | Hollow core slab | Steel beams | Structure | | 1,0 | 0,4 | 0,57 | 1,0 | 0,4 | 0,57 | **0,57** | € 21,00 | 30 | € 629,89 | € 359,93 | |
| | 4 | Perimeter ties | Grout | Structure | | 0,2 | 0,1 | 0,13 | 1,0 | 0,1 | 0,18 | **0,15** | € 1,08 | 29 | € 31,28 | € 4,81 | |
| | 5 | Peripheral ties | Grout | Structure | | 0,2 | 0,1 | 0,13 | 1,0 | 0,1 | 0,18 | **0,15** | € 0,18 | 1 | € 0,18 | € 0,03 | 43,91% 0,22 |
| Beam | 6 | Steel studs | Finplate/endplate | Structure | | 0,1 | 0,4 | 0,16 | 0,4 | 0,1 | 0,16 | **0,16** | € 1,00 | 29 | € 29,00 | € 4,64 | |
| | 8 | Steel beam 7.2 | Endplate | Structure | | 0,1 | 0,4 | 0,16 | 1,0 | 1,0 | 1,00 | **0,28** | € 205,02 | 5 | € 1.025,11 | € 282,79 | 27,27% 0,12 |
| **Column** | 14 | Extended Endplate semi rigid | Column | Structure | | 0,8 | 0,4 | 0,53 | 1,0 | 1,0 | 1,00 | **0,70** | € 19,78 | 10 | € 197,76 | € 137,57 | 69,57% 0,06 |
| | | | | | | | | | | | | | | | **€ 2.460,07** | **€ 955,49** | 140,74% 0,39 |
| | | | | | | | | | | | | | | | Disassembly potential | **€ 0,39** | |
| | | | | | | | | | | | | | | | ECI remaining : (1 - DPp) * ECI_tot: | **€ 1.504,58** | |

### Double span

| Double span | ID | Product | Load-bearing connection | Layer | CT | CA | DPc | ID2 | GPE | DPcp | DPp | ECI | number | ECI_tot | DPp*ECI_tot | | |
|---|---|---|---|---|---|---|---|---|---|---|---|---|---|---|---|---|---|
| Floor | 1 | Compression layer | Hollow core slabs | Structure | | 0,1 | 0,8 | 0,18 | 1,0 | 1,0 | 1,00 | **0,30** | € 512,45 | 1 | € 512,45 | € 154,70 | |
| | 2 | Grout | Hollow core slabs | Structure | | 0,2 | 0,4 | 0,27 | 0,4 | 0,4 | 0,40 | **0,32** | € 1,19 | 29 | € 34,40 | € 11,01 | |
| | 3 | Hollow core slab | Steel beams | Structure | | 1,0 | 0,4 | 0,57 | 1,0 | 0,4 | 0,57 | **0,57** | € 21,00 | 30 | € 629,89 | € 359,93 | |
| | 4 | Perimeter ties | Grout | Structure | | 0,2 | 0,1 | 0,13 | 1,0 | 0,1 | 0,18 | **0,15** | € 1,08 | 29 | € 31,28 | € 4,81 | |
| | 5 | Peripheral ties | Grout | Structure | | 0,2 | 0,1 | 0,13 | 1,0 | 0,1 | 0,18 | **0,15** | € 0,18 | 1 | € 0,18 | € 0,03 | 43,91% 0,20 |
| Beam | 6 | Steel studs | Finplate/endplate | Structure | | 0,1 | 0,4 | 0,16 | 0,4 | 0,1 | 0,16 | **0,16** | € 1,00 | 29 | € 29,00 | € 4,64 | |
| | 8 | Steel beam 7.2 | Finplate | Structure | | 0,8 | 0,4 | 0,53 | 1,0 | 1,0 | 1,00 | **0,70** | € 272,14 | 1 | € 272,14 | € 189,31 | |
| | 11 | Steel beam 14.4 | Finplate | Structure | | 0,8 | 0,4 | 0,53 | 0,4 | 1,0 | 0,57 | **0,55** | € 544,27 | 2 | € 1.088,55 | € 600,58 | 57,17% 0,30 |
| **Column** | 13 | Finplate | Column | Structure | | 0,1 | 0,4 | 0,16 | 1,0 | 1,0 | 1,00 | **0,28** | € 2,98 | 10 | € 29,77 | € 8,21 | 27,59% 0,00 |
| | | | | | | | | | | | | | | | **€ 2.627,64** | **€ 1.333,22** | 128,67% 0,51 |
| | | | | | | | | | | | | | | | Disassembly potential | **€ 0,51** | |
| | | | | | | | | | | | | | | | ECI remaining : (1 - DPp) * ECI_tot: | **€ 1.294,42** | |

### Gerber span

| Gerber span | ID | Product | Load-bearing connection | Layer | CT | CA | DPc | ID2 | GPE | DPcp | DPp | ECI | number | ECI_tot | DPp*ECI_tot | | |
|---|---|---|---|---|---|---|---|---|---|---|---|---|---|---|---|---|---|
| Floor | 1 | Compression layer | Hollow core slabs | Structure | | 0,1 | 0,8 | 0,18 | 1,0 | 1,0 | 1,00 | **0,30** | € 512,45 | 1 | € 512,45 | € 154,70 | |
| | 2 | Grout | Hollow core slabs | Structure | | 0,2 | 0,4 | 0,27 | 0,4 | 0,4 | 0,40 | **0,32** | € 1,19 | 29 | € 34,40 | € 11,01 | |
| | 3 | Hollow core slab | Steel beams | Structure | | 1,0 | 0,4 | 0,57 | 1,0 | 0,4 | 0,57 | **0,57** | € 21,00 | 30 | € 629,89 | € 359,93 | |
| | 4 | Perimeter ties | Grout | Structure | | 0,2 | 0,1 | 0,13 | 1,0 | 0,1 | 0,18 | **0,15** | € 1,08 | 29 | € 31,28 | € 4,81 | |
| | 5 | Peripheral ties | Grout | Structure | | 0,2 | 0,1 | 0,13 | 1,0 | 0,1 | 0,18 | **0,15** | € 0,18 | 1 | € 0,18 | € 0,03 | 43,91% 0,20 |
| Beam | 6 | Steel studs | Finplate/endplate | Structure | | 0,1 | 0,4 | 0,16 | 0,4 | 0,1 | 0,16 | **0,16** | € 1,00 | 29 | € 29,00 | € 4,64 | |
| | 7 | Steel beam 3.6 | Gerber finplate | Structure | | 0,8 | 0,8 | 0,80 | 1,0 | 1,0 | 1,00 | **0,89** | € 136,07 | 2 | € 272,14 | € 241,90 | |
| | 9 | Steel beam 9.0 | Endplate/Finplate | Structure | | 0,8 | 0,4 | 0,53 | 0,4 | 1,0 | 0,57 | **0,55** | € 340,17 | 2 | € 680,34 | € 375,36 | |
| | 10 | Steel beam 10.8 | Finplate | Structure | | 0,8 | 0,4 | 0,53 | 0,4 | 1,0 | 0,57 | **0,55** | € 408,20 | 1 | € 408,20 | € 225,22 | |
| | 12 | Gerber Finplate | Steel beam (10.8/14.4) | Structure | | 0,8 | 0,4 | 0,53 | 0,4 | 1,0 | 0,57 | **0,55** | € 6,77 | 4 | € 27,08 | € 14,94 | 60,85% 0,33 |
| | | | | | | | | | | | | | | | **€ 2.624,95** | **€ 1.392,54** | 104,75% |
| | | | | | | | | | | | | | | | Disassembly potential | **0,53** | |
| | | | | | | | | | | | | | | | ECI remaining : (1 - DPp) * ECI_tot: | **€ 1.232,41** | |

| | | | | Scenario | | | | |
|---|---|---|---|---|---|---|---|---|
| Product | Number | Load bearing connection | Column2 | 1 | 2 | 3 | 4 | 5 |
| Compression layer | 1 | Hollow core slabs | | 0,30 | 0,30 | 0,30 | 0,30 | 0,30 |
| Grout | 2 | Hollow core slabs | | 0,32 | 0,32 | 0,32 | 0,32 | 0,32 |
| Hollow core slab | 3 | Steel beams | | 0,57 | 0,57 | 0,57 | 0,57 | 0,57 |
| Perimeter ties | 4 | Grout | | 0,15 | 0,15 | 0,15 | 0,15 | 0,15 |
| Peripheral ties | 5 | Grout | | 0,15 | 0,15 | 0,15 | 0,15 | 0,15 |
| Steel studs | 6 | Finplate/endplate | | 0,16 | 0,16 | 0,16 | 0,16 | 0,16 |
| Steel beam 3.6 | 7 | Gerber finplate | | | | | | 0,89 |
| Steel beam 7.2 | 8 | Endplate/Finplate | | 0,70 | 0,28 | 0,28 | 0,70 | |
| Steel beam 9.0 | 9 | Endplate/Finplate | | | | | | 0,55 |
| Steel beam 10.8 | 10 | Endplate/Finplate | | | | | | 0,55 |
| Steel beam 14.4 | 11 | Finplate | | | | | 0,70 | |
| Gerber Finplate | 12 | Steel beam (10.8/14.4) | | | | | | 0,55 |
| Finplate | 13 | Column | | 0,28 | | | 0,28 | |
| Extended Endplate semi rigid | 14 | Column | | | | 0,70 | | |
| Extended Endplate rigid | 15 | Column | | | | 0,70 | | |
| Diagonal plate | 16 | Column | | | | 0,28 | | |
| Column | 17 | Column | | | | | | |

## D.2.3. Changing the connection accessibility

**Changes in the accesibility of the beam** **Single span, hinged connection scenario**

| Hinged | ID | Product | Load-bearing connection | Layer | CT | CA | DPc | ID2 | GPE | DPcp | DPp | ECI | number | ECI_tot | DPp*ECI_tot |
|---|---|---|---|---|---|---|---|---|---|---|---|---|---|---|---|
| Floor | 1 | Pressure layer | Hollow core slabs | Structure | 0,1 | 0,8 | 0,18 | 1,0 | 1,0 | 1,00 | 0,30 | € 512,45 | 1 | € 512,45 | € 154,70 |
| | 2 | Grout | Hollow core slabs | Structure | 0,2 | 0,4 | 0,27 | 0,4 | 0,4 | 0,40 | 0,32 | € 1,19 | 29 | € 34,40 | € 11,01 |
| | 3 | Hollow core slab | Steel beams | Structure | 1,0 | 0,4 | 0,57 | 1,0 | 0,4 | 0,57 | 0,57 | € 21,00 | 30 | € 629,89 | € 359,93 |
| | 4 | Perimeter ties | Grout | Structure | 0,2 | 0,1 | 0,13 | 1,0 | 0,1 | 0,18 | 0,15 | € 1,08 | 29 | € 31,28 | € 4,81 |
| | 5 | Peripheral ties | Grout | Structure | 0,2 | 0,1 | 0,13 | 1,0 | 0,1 | 0,18 | 0,15 | € 0,18 | 1 | € 0,18 | € 0,03 |
| Beam | 6 | Steel studs | Finplate/endplate | Structure | 0,1 | 0,4 | 0,16 | 0,4 | 0,1 | 0,16 | 0,16 | € 1,00 | 29 | € 29,00 | € 4,64 |
| | 8 | Steel beam 7.2 | Finplate | Structure | 0,8 | 0,1 | 0,18 | 1,0 | 1,0 | 1,00 | 0,30 | € 272,14 | 5 | € 1.360,68 | € 410,77 |
| Column | 12 | Finplate | Column | Structure | 0,1 | 0,4 | 0,16 | 1,0 | 1,0 | 1,00 | 0,28 | € 2,98 | 10 | € 29,77 | € 8,21 |
| | | | | | | | | | | | | | | € 2.627,64 | € 954,11 |
| | | | | | | | | | | | | Disassembly potential | | | 0,36 |
| | | | | | | | | | | | | ECI remaining : (1 - DPp) * ECI_tot: | | | € 1.673,53 |

| Hinged | ID | Product | Load-bearing connection | Layer | CT | CA | DPc | ID2 | GPE | DPcp | DPp | ECI | number | ECI_tot | DPp*ECI_tot |
|---|---|---|---|---|---|---|---|---|---|---|---|---|---|---|---|
| Floor | 1 | Pressure layer | Hollow core slabs | Structure | 0,1 | 0,8 | 0,18 | 1,0 | 1,0 | 1,00 | 0,30 | € 512,45 | 1 | € 512,45 | € 154,70 |
| | 2 | Grout | Hollow core slabs | Structure | 0,2 | 0,4 | 0,27 | 0,4 | 0,4 | 0,40 | 0,32 | € 1,19 | 29 | € 34,40 | € 11,01 |
| | 3 | Hollow core slab | Steel beams | Structure | 1,0 | 0,4 | 0,57 | 1,0 | 0,4 | 0,57 | 0,57 | € 21,00 | 30 | € 629,89 | € 359,93 |
| | 4 | Perimeter ties | Grout | Structure | 0,2 | 0,1 | 0,13 | 1,0 | 0,1 | 0,18 | 0,15 | € 1,08 | 29 | € 31,28 | € 4,81 |
| | 5 | Peripheral ties | Grout | Structure | 0,2 | 0,1 | 0,13 | 1,0 | 0,1 | 0,18 | 0,15 | € 0,18 | 1 | € 0,18 | € 0,03 |
| Beam | 6 | Steel studs | Finplate/endplate | Structure | 0,1 | 0,4 | 0,16 | 0,4 | 0,1 | 0,16 | 0,16 | € 1,00 | 29 | € 29,00 | € 4,64 |
| | 8 | Steel beam 7.2 | Finplate | Structure | 0,8 | 0,4 | 0,53 | 1,0 | 1,0 | 1,00 | 0,70 | € 272,14 | 5 | € 1.360,68 | € 946,56 |
| Column | 12 | Finplate | Column | Structure | 0,1 | 0,4 | 0,16 | 1,0 | 1,0 | 1,00 | 0,28 | € 2,98 | 10 | € 29,77 | € 8,21 |
| | | | | | | | | | | | | | | **€ 2.627,64** | **€ 1.489,90** |
| | | | | | | | | | | | | Disassembly potential | | | **0,57** |
| | | | | | | | | | | | | ECI remaining : (1 - DPp) * ECI_tot: | | | **€ 1.137,74** |

| Hinged | ID | Product | Load-bearing connection | Layer | CT | CA | DPc | ID2 | GPE | DPcp | DPp | ECI | number | ECI_tot | DPp*ECI_tot |
|---|---|---|---|---|---|---|---|---|---|---|---|---|---|---|---|
| Floor | 1 | Pressure layer | Hollow core slabs | Structure | 0,1 | 0,8 | 0,18 | 1,0 | 1,0 | 1,00 | 0,30 | € 512,45 | 1 | € 512,45 | € 154,70 |
| | 2 | Grout | Hollow core slabs | Structure | 0,2 | 0,4 | 0,27 | 0,4 | 0,4 | 0,40 | 0,32 | € 1,19 | 29 | € 34,40 | € 11,01 |
| | 3 | Hollow core slab | Steel beams | Structure | 1,0 | 0,4 | 0,57 | 1,0 | 0,4 | 0,57 | 0,57 | € 21,00 | 30 | € 629,89 | € 359,93 |
| | 4 | Perimeter ties | Grout | Structure | 0,2 | 0,1 | 0,13 | 1,0 | 0,1 | 0,18 | 0,15 | € 1,08 | 29 | € 31,28 | € 4,81 |
| | 5 | Peripheral ties | Grout | Structure | 0,2 | 0,1 | 0,13 | 1,0 | 0,1 | 0,18 | 0,15 | € 0,18 | 1 | € 0,18 | € 0,03 |
| Beam | 6 | Steel studs | Finplate/endplate | Structure | 0,1 | 0,4 | 0,16 | 0,4 | 0,1 | 0,16 | 0,16 | € 1,00 | 29 | € 29,00 | € 4,64 |
| | 8 | Steel beam 7.2 | Finplate | Structure | 0,8 | 0,6 | 0,69 | 1,0 | 1,0 | 1,00 | 0,81 | € 272,14 | 5 | € 1.360,68 | € 1.107,00 |
| Column | 12 | Finplate | Column | Structure | 0,1 | 0,4 | 0,16 | 1,0 | 1,0 | 1,00 | 0,28 | € 2,98 | 10 | € 29,77 | € 8,21 |
| | | | | | | | | | | | | | | € 2.627,64 | € 1.650,33 |
| | | | | | | | | | | | | Disassembly potential | | | 0,63 |
| | | | | | | | | | | | | ECI remaining : (1 - DPp) * ECI_tot: | | | € 977,31 |

| Hinged | ID | Product | Load-bearing connection | Layer | CT | CA | DPc | ID2 | GPE | DPcp | DPp | ECI | number | ECI_tot | DPp*ECI_tot |
|---|---|---|---|---|---|---|---|---|---|---|---|---|---|---|---|
| Floor | 1 | Pressure layer | Hollow core slabs | Structure | 0,1 | 0,8 | 0,18 | 1,0 | 1,0 | 1,00 | 0,30 | € 512,45 | 1 | € 512,45 | € 154,70 |
| | 2 | Grout | Hollow core slabs | Structure | 0,2 | 0,4 | 0,27 | 0,4 | 0,4 | 0,40 | 0,32 | € 1,19 | 29 | € 34,40 | € 11,01 |
| | 3 | Hollow core slab | Steel beams | Structure | 1,0 | 0,4 | 0,57 | 1,0 | 0,4 | 0,57 | 0,57 | € 21,00 | 30 | € 629,89 | € 359,93 |
| | 4 | Perimeter ties | Grout | Structure | 0,2 | 0,1 | 0,13 | 1,0 | 0,1 | 0,18 | 0,15 | € 1,08 | 29 | € 31,28 | € 4,81 |
| | 5 | Peripheral ties | Grout | Structure | 0,2 | 0,1 | 0,13 | 1,0 | 0,1 | 0,18 | 0,15 | € 0,18 | 1 | € 0,18 | € 0,03 |
| Beam | 6 | Steel studs | Finplate/endplate | Structure | 0,1 | 0,4 | 0,16 | 0,4 | 0,1 | 0,16 | 0,16 | € 1,00 | 29 | € 29,00 | € 4,64 |
| | 8 | Steel beam 7.2 | Finplate | Structure | 0,8 | 0,8 | 0,80 | 1,0 | 1,0 | 1,00 | 0,89 | € 272,14 | 5 | € 1.360,68 | € 1.209,50 |
| Column | 12 | Finplate | Column | Structure | 0,1 | 0,4 | 0,16 | 1,0 | 1,0 | 1,00 | 0,28 | € 2,98 | 10 | € 29,77 | € 8,21 |
| | | | | | | | | | | | | | | € 2.627,64 | € 1.752,83 |
| | | | | | | | | | | | | Disassembly potential | | | 0,67 |
| | | | | | | | | | | | | ECI remaining : (1 - DPp) * ECI_tot: | | | € 874,81 |

| Hinged | ID | Product | Load-bearing connection | Layer | CT | CA | DPc | ID2 | GPE | DPcp | DPp | ECI | number | ECI_tot | DPp*ECI_tot |
|---|---|---|---|---|---|---|---|---|---|---|---|---|---|---|---|
| Floor | 1 | Pressure layer | Hollow core slabs | Structure | 0,1 | 0,8 | 0,18 | 1,0 | 1,0 | 1,00 | 0,30 | € 512,45 | 1 | € 512,45 | € 154,70 |
| | 2 | Grout | Hollow core slabs | Structure | 0,2 | 0,4 | 0,27 | 0,4 | 0,4 | 0,40 | 0,32 | € 1,19 | 29 | € 34,40 | € 11,01 |
| | 3 | Hollow core slab | Steel beams | Structure | 1,0 | 0,4 | 0,57 | 1,0 | 0,4 | 0,57 | 0,57 | € 21,00 | 30 | € 629,89 | € 359,93 |
| | 4 | Perimeter ties | Grout | Structure | 0,2 | 0,1 | 0,13 | 1,0 | 0,1 | 0,18 | 0,15 | € 1,08 | 29 | € 31,28 | € 4,81 |
| | 5 | Peripheral ties | Grout | Structure | 0,2 | 0,1 | 0,13 | 1,0 | 0,1 | 0,18 | 0,15 | € 0,18 | 1 | € 0,18 | € 0,03 |
| Beam | 6 | Steel studs | Finplate/endplate | Structure | 0,1 | 0,4 | 0,16 | 0,4 | 0,1 | 0,16 | 0,16 | € 1,00 | 29 | € 29,00 | € 4,64 |
| | 8 | Steel beam 7.2 | Finplate | Structure | 0,8 | 1,0 | 0,89 | 1,0 | 1,0 | 1,00 | 0,94 | € 272,14 | 5 | € 1.360,68 | € 1.280,64 |
| Column | 12 | Finplate | Column | Structure | 0,1 | 0,4 | 0,16 | 1,0 | 1,0 | 1,00 | 0,28 | € 2,98 | 10 | € 29,77 | € 8,21 |
| | | | | | | | | | | | | | | € 2.627,64 | € 1.823,98 |
| | | | | | | | | | | | | Disassembly potential | | | 0,69 |
| | | | | | | | | | | | | ECI remaining : (1 - DPp) * ECI_tot: | | | € 803,66 |

# E

# IDeaStatiCa code settings

This appendix contains the settings that were used in the analysis of IDeaStatiCa.

## E.1. IDeaStatiCa code settings for the member calculations

### Code settings

| | | |
|---|---|---|
| Stop at limit strain | No | |
| Pretension force factor k | 0,70 | - |
| Friction coefficient in slip-resistance | 0,30 | - |
| γ M2 | 1,00 | - |
| Anchor length for stiffness calculation [d] | 8 | |
| Limit plastic strain | 1500,0 | 1e-4 |
| Division of surface of the biggest circular hollow member | 64 | |
| Division of arc of rectangular hollow member | 3 | |
| Number of elements on biggest member web or flange | 8 | |
| Number of elements on biggest web of RHS member | 16 | |
| Number of elements on individual plates | 20 | |
| Number of analysis iterations | 25 | |
| Divergent iterations count | 6 | |
| Minimal size of element | 10 | mm |
| Maximal size of element | 50 | mm |
| Number of buckling modes | 6 | |

### Software info

| | |
|---|---|
| Application | IDEA StatiCa Member |
| Version | 23.1.0.4061 |
| Developed by | IDEA StatiCa |

# E.2. IDeaStatiCa code settings for the connection calculations

## Code settings

| Item | Value | Unit | Reference |
|---|---|---|---|
| Safety factor $\gamma_{M0}$ | 1,00 | - | EN 1993-1-1: 6.1 |
| Safety factor $\gamma_{M1}$ | 1,00 | - | EN 1993-1-1: 6.1 |
| Safety factor $\gamma_{M2}$ | 1,00 | - | EN 1993-1-1: 6.1 |
| Safety factor $\gamma_{M3}$ | 1,00 | - | EN 1993-1-8: 2.2 |
| Safety factor $\gamma_{C}$ | 1,00 | - | EN 1992-1-1: 2.4.2.4 |
| Safety factor $\gamma_{Inst}$ | 1,00 | - | EN 1992-4: Table 4.1 |
| Joint coefficient βj | 0,67 | - | EN 1993-1-8: 6.2.5 |
| Effective area - influence of mesh size | 0,10 | - | |
| Friction coefficient - concrete | 0,25 | - | EN 1993-1-8 |
| Friction coefficient in slip-resistance | 0,30 | - | EN 1993-1-8 tab 3.7 |
| Limit plastic strain | 0,05 | - | EN 1993-1-5 |
| Detailing | Yes | | |
| Distance between bolts [d] | 2,20 | - | EN 1993-1-8: tab 3.3 |
| Distance between bolts and edge [d] | 1,20 | - | EN 1993-1-8: tab 3.3 |
| Concrete breakout resistance check | Both | | EN 1992-4: 7.2.1.4 and 7.2.2.5 |
| Use calculated αb in bearing check. | Yes | | EN 1993-1-8: tab 3.4 |
| Cracked concrete | Yes | | EN 1992-4 |
| Local deformation check | Yes | | CIDECT DG 1, 3 - 1.1 |
| Local deformation limit | 0,03 | - | CIDECT DG 1, 3 - 1.1 |
| Geometrical nonlinearity (GMNA) | Yes | | Analysis with large deformations for hollow section joints |
| Braced system | No | | EN 1993-1-8: 5.2.2.5 |

# F

# IDeaStatiCa output documents

In this Appendix, the outcomes of the IDeaStatiCa report are provided in the following order:

- section F.1: Single spans, hinged connections
- section F.2: Single spans, rigid connections
- section F.3 Single spans, semi-rigid connections
- section F.4: Double spans
- section F.5: Gerber spans

# F.1. Single span hinged

This section displays the output of the IDeaStatica calculations for the single-span hinged scenario.

## F.2. Single span rigid

This section displays the output of the IDeaStatica calculations for the single-span rigid scenario.

## F.3. Single span semi-rigid

This section displays the output of the IDeaStatica calculations for the single-span semi-rigid scenario.

## F.4. Double span

This section displays the output of the IDeaStatica calculations for the double-span scenario.

**Project:**
**Project no:**
**Author:**

IDEA StatiCa
Calculate yesterday's estimates

# Project data

| | |
|---|---|
| Project name | |
| Project number | |
| Author | |
| Description | |
| Date | 18/10/2024 |
| Design code | EN |

# Geometry

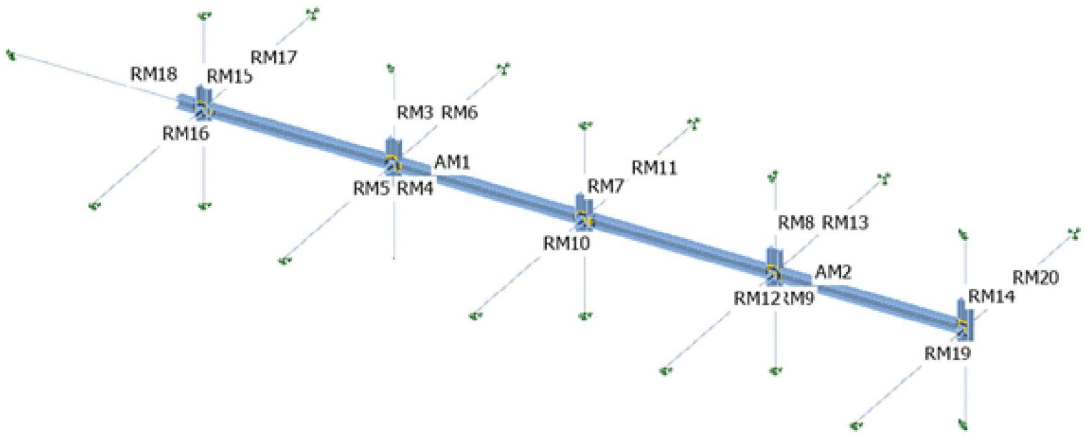


**Project:**
**Project no:**
**Author:**

## Analyzed members

### AM1

| Property | Value |
|---|---|
| Name | AM1 |
| Members | M1 |
| Cross-section | HEB400 |
| Length | 14,40 m |
| ey | 0 mm |
| ez | 0 mm |
| Begin | (0,00; 0,00; 0,00) m |
| End | (14,40; 0,00; 0,00) m |

### AM2

| Property | Value |
|---|---|
| Name | AM2 |
| Members | M2 |
| Cross-section | HEB400 |
| Length | 14,40 m |
| ey | 0 mm |
| ez | 0 mm |
| Begin | (14,40; 0,00; 0,00) m |
| End | (28,80; 0,00; 0,00) m |

## Related members

### RM3

| Property | Value |
|---|---|
| Name | RM3 |
| Members | M3 |
| Cross-section | HEB450 |
| Length | 3,60 m |
| ey | 0 mm |
| ez | 0 mm |
| Begin | (7,20; 0,00; 3,60) m |
| End | (7,20; 0,00; 0,00) m |
| Support | ■ X \| ■ Y \| □ Z \| □ Rx \| □ Ry \| □ Rz |

**Project:**
**Project no:**
**Author:**

IDEA StatiCa®
Calculate yesterday's estimates

## RM4

| Property | Value |
|---|---|
| Name | RM4 |
| Members | M4 |
| Cross-section | HEB450 |
| Length | 3,60 m |
| ey | 0 mm |
| ez | 0 mm |
| Begin | (7,20; 0,00; -3,60) m |
| End | (7,20; 0,00; 0,00) m |
| Support | □ X \| □ Y \| □ Z \| □ Rx \| □ Ry \| □ Rz |

## RM5

| Property | Value |
|---|---|
| Name | RM5 |
| Members | M5 |
| Cross-section | IPE240 |
| Length | 7,20 m |
| ey | 0 mm |
| ez | 0 mm |
| Begin | (7,20; -7,20; 0,00) m |
| End | (7,20; 0,00; 0,00) m |
| Support | ■ X \| ■ Y \| ■ Z \| □ Rx \| □ Ry \| □ Rz |

## RM6

| Property | Value |
|---|---|
| Name | RM6 |
| Members | M6 |
| Cross-section | IPE240 |
| Length | 7,20 m |
| ey | 0 mm |
| ez | 0 mm |
| Begin | (7,20; 7,20; 0,00) m |
| End | (7,20; 0,00; 0,00) m |
| Support | ■ X \| ■ Y \| ■ Z \| □ Rx \| □ Ry \| □ Rz |

**Project:**
**Project no:**
**Author:**

## RM7

| Property | Value |
|---|---|
| Name | RM7 |
| Members | M7 |
| Cross-section | HEB450 |
| Length | 7,20 m |
| ey | 0 mm |
| ez | 0 mm |
| Begin | (14,40; 0,00; -3,60) m |
| End | (14,40; 0,00; 3,60) m |
| Support Begin | ■ X \| ■ Y \| ■ Z \| □ Rx \| □ Ry \| □ Rz |
| Support End | ■ X \| ■ Y \| ■ Z \| □ Rx \| □ Ry \| □ Rz |

## RM8

| Property | Value |
|---|---|
| Name | RM8 |
| Members | M8 |
| Cross-section | HEB450 |
| Length | 3,60 m |
| ey | 0 mm |
| ez | 0 mm |
| Begin | (21,60; 0,00; 3,60) m |
| End | (21,60; 0,00; 0,00) m |
| Support | ■ X \| ■ Y \| ■ Z \| □ Rx \| □ Ry \| □ Rz |

## RM9

| Property | Value |
|---|---|
| Name | RM9 |
| Members | M9 |
| Cross-section | HEB450 |
| Length | 3,60 m |
| ey | 0 mm |
| ez | 0 mm |
| Begin | (21,60; 0,00; -3,60) m |
| End | (21,60; 0,00; 0,00) m |
| Support | ■ X \| ■ Y \| ■ Z \| □ Rx \| □ Ry \| □ Rz |

**Project:**
**Project no:**
**Author:**

IDEA StatiCa®
Calculate yesterday's estimates

## RM10

| Property | Value |
|---|---|
| Name | RM10 |
| Members | M10 |
| Cross-section | IPE240 |
| Length | 7,20 m |
| ey | 0 mm |
| ez | 0 mm |
| Begin | (14,40; -7,20; 0,00) m |
| End | (14,40; 0,00; 0,00) m |
| Support | ■ X \| ■ Y \| ■ Z \| □ Rx \| □ Ry \| □ Rz |

## RM11

| Property | Value |
|---|---|
| Name | RM11 |
| Members | M11 |
| Cross-section | IPE240 |
| Length | 7,20 m |
| ey | 0 mm |
| ez | 0 mm |
| Begin | (14,40; 7,20; 0,00) m |
| End | (14,40; 0,00; 0,00) m |
| Support | ■ X \| ■ Y \| ■ Z \| □ Rx \| □ Ry \| □ Rz |

## RM12

| Property | Value |
|---|---|
| Name | RM12 |
| Members | M12 |
| Cross-section | IPE240 |
| Length | 7,20 m |
| ey | 0 mm |
| ez | 0 mm |
| Begin | (21,60; -7,20; 0,00) m |
| End | (21,60; 0,00; 0,00) m |
| Support | ■ X \| ■ Y \| ■ Z \| □ Rx \| □ Ry \| □ Rz |

**Project:**
**Project no:**
**Author:**

## RM13

| Property | Value |
|---|---|
| Name | RM13 |
| Members | M13 |
| Cross-section | IPE240 |
| Length | 7,20 m |
| ey | 0 mm |
| ez | 0 mm |
| Begin | (21,60; 7,20; 0,00) m |
| End | (21,60; 0,00; 0,00) m |
| Support | ■ X \| ■ Y \| ■ Z \| □ Rx \| □ Ry \| □ Rz |

## RM14

| Property | Value |
|---|---|
| Name | RM14 |
| Members | M14 |
| Cross-section | HEB450 |
| Length | 7,20 m |
| ey | 0 mm |
| ez | 0 mm |
| Begin | (28,80; 0,00; -3,60) m |
| End | (28,80; 0,00; 3,60) m |
| Support Begin | ■ X \| ■ Y \| ■ Z \| □ Rx \| □ Ry \| □ Rz |
| Support End | ■ X \| ■ Y \| ■ Z \| □ Rx \| □ Ry \| □ Rz |

## RM15

| Property | Value |
|---|---|
| Name | RM15 |
| Members | M15 |
| Cross-section | HEB400 |
| Length | 7,20 m |
| ey | 0 mm |
| ez | 0 mm |
| Begin | (0,00; 0,00; -3,60) m |
| End | (0,00; 0,00; 3,60) m |
| Support Begin | ■ X \| ■ Y \| ■ Z \| □ Rx \| □ Ry \| □ Rz |
| Support End | ■ X \| ■ Y \| ■ Z \| □ Rx \| □ Ry \| □ Rz |

**Project:**
**Project no:**
**Author:**

IDEA StatiCa®
Calculate yesterday's estimates

## RM16

| Property | Value |
|---|---|
| Name | RM16 |
| Members | M16 |
| Cross-section | IPE240 |
| Length | 7,20 m |
| ey | 0 mm |
| ez | 0 mm |
| Begin | (0,00; -7,20; 0,00) m |
| End | (0,00; 0,00; 0,00) m |
| Support | ■ X \| ■ Y \| ■ Z \| □ Rx \| □ Ry \| □ Rz |

## RM17

| Property | Value |
|---|---|
| Name | RM17 |
| Members | M17 |
| Cross-section | IPE240 |
| Length | 7,20 m |
| ey | 0 mm |
| ez | 0 mm |
| Begin | (0,00; 7,20; 0,00) m |
| End | (0,00; 0,00; 0,00) m |
| Support | ■ X \| ■ Y \| ■ Z \| □ Rx \| □ Ry \| □ Rz |

## RM18

| Property | Value |
|---|---|
| Name | RM18 |
| Members | M18 |
| Cross-section | HEB400 |
| Length | 7,20 m |
| ey | 0 mm |
| ez | 0 mm |
| Begin | (-7,20; 0,00; 0,00) m |
| End | (0,00; 0,00; 0,00) m |
| Support | ■ X \| ■ Y \| ■ Z \| □ Rx \| □ Ry \| □ Rz |

**Project:**
**Project no:**
**Author:**

IDEA StatiCa
Calculate yesterday's estimates

## RM19

| Property | Value |
|---|---|
| Name | RM19 |
| Members | M19 |
| Cross-section | IPE240 |
| Length | 7,20 m |
| ey | 0 mm |
| ez | 0 mm |
| Begin | (28,80; -7,20; 0,00) m |
| End | (28,80; 0,00; 0,00) m |
| Support | ■ X \| ■ Y \| ■ Z \| □ Rx \| □ Ry \| □ Rz |

## RM20

| Property | Value |
|---|---|
| Name | RM20 |
| Members | M20 |
| Cross-section | IPE240 |
| Length | 7,20 m |
| ey | 0 mm |
| ez | 0 mm |
| Begin | (28,80; 7,20; 0,00) m |
| End | (28,80; 0,00; 0,00) m |
| Support | ■ X \| ■ Y \| ■ Z \| □ Rx \| □ Ry \| □ Rz |

## Cross-section

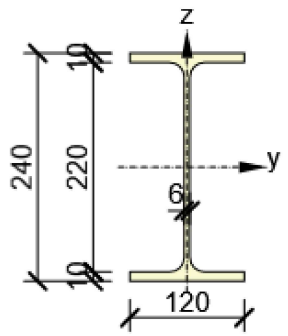


*IPE240, Material: S 355*

**Project:**
**Project no:**
**Author:**

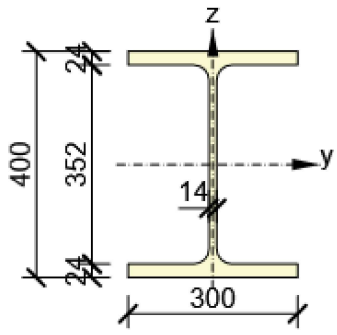


*HEB400, Material: S 355*

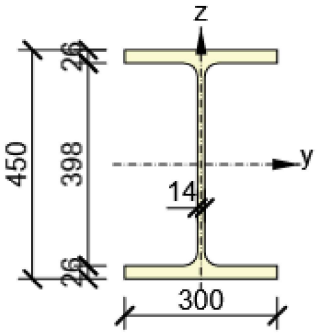


*HEB450, Material: S 355*

## Loading

### LE1 – Type ULS

**Line load**

| Member | Begin [m] | End [m] | X [kN/m] | Y [kN/m] | Z [kN/m] | Location | Width [mm] | Ey [mm] |
|---|---|---|---|---|---|---|---|---|
| AM1 | 0,00 | 14,40 | 0,0 | 0,0 | 0,0 | Top | 0 | 0 |
| AM2 | 0,00 | 14,40 | 0,0 | 0,0 | -60,0 | Top | 0 | 0 |
| RM18 | 0,00 | 7,20 | 0,0 | 0,0 | -60,0 | Member axis | 0 | 0 |

**Point load**

| Member | N [kN] | Vy [kN] | Vz [kN] | Mx [kN] | My [kN] | Mz [kN] |
|---|---|---|---|---|---|---|
| RM3 / Begin | 0,0 | 0,0 | 0,0 | 0,0 | 0,0 | 0,0 |
| RM4 / Begin | 0,0 | 0,0 | 0,0 | 0,0 | 0,0 | 0,0 |
| RM5 / Begin | 0,0 | 0,0 | 0,0 | 0,0 | 0,0 | 0,0 |
| RM6 / Begin | 0,0 | 0,0 | 0,0 | 0,0 | 0,0 | 0,0 |
| RM7 / Begin | 0,0 | 0,0 | 0,0 | 0,0 | 0,0 | 0,0 |
| RM7 / End | 0,0 | 0,0 | 0,0 | 0,0 | 0,0 | 0,0 |
| RM8 / Begin | 0,0 | 0,0 | 0,0 | 0,0 | 0,0 | 0,0 |
| RM9 / Begin | 0,0 | 0,0 | 0,0 | 0,0 | 0,0 | 0,0 |
| RM10 / Begin | 0,0 | 0,0 | 0,0 | 0,0 | 0,0 | 0,0 |
| RM11 / Begin | 0,0 | 0,0 | 0,0 | 0,0 | 0,0 | 0,0 |
| RM12 / Begin | 0,0 | 0,0 | 0,0 | 0,0 | 0,0 | 0,0 |
| RM13 / Begin | 0,0 | 0,0 | 0,0 | 0,0 | 0,0 | 0,0 |
| RM14 / Begin | 0,0 | 0,0 | 0,0 | 0,0 | 0,0 | 0,0 |
| RM14 / End | 0,0 | 0,0 | 0,0 | 0,0 | 0,0 | 0,0 |
| RM15 / Begin | 0,0 | 0,0 | 0,0 | 0,0 | 0,0 | 0,0 |
| RM15 / End | 0,0 | 0,0 | 0,0 | 0,0 | 0,0 | 0,0 |
| RM3 / 0,50 | 0,0 | 0,0 | -350,0 | 0,0 | 0,0 | 0,0 |
| RM16 / Begin | 0,0 | 0,0 | 0,0 | 0,0 | 0,0 | 0,0 |
| RM17 / Begin | 0,0 | 0,0 | 0,0 | 0,0 | 0,0 | 0,0 |
| RM18 / Begin | 0,0 | 0,0 | 0,0 | 0,0 | 0,0 | 0,0 |
| RM19 / Begin | 0,0 | 0,0 | 0,0 | 0,0 | 0,0 | 0,0 |
| RM20 / Begin | 0,0 | 0,0 | 0,0 | 0,0 | 0,0 | 0,0 |

# Results

## Materially non-linear analysis (MNA)

### Summary

| Load | Applied loads [%] |
|---|---|
| LE1 | 100,0 |

**Project:**
**Project no:**
**Author:**

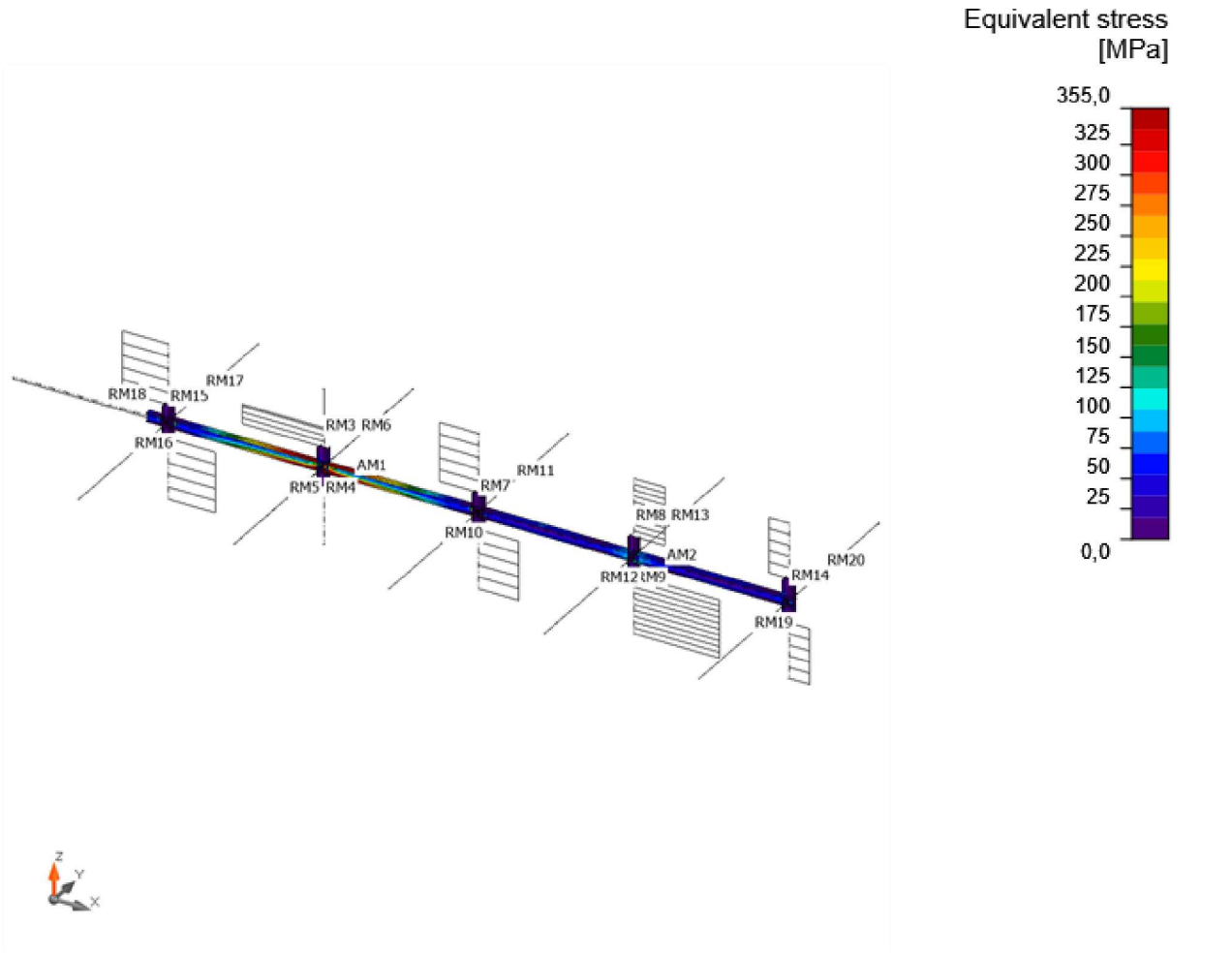


*Eq. stress ,LC1*

**Project:**
**Project no:**
**Author:**

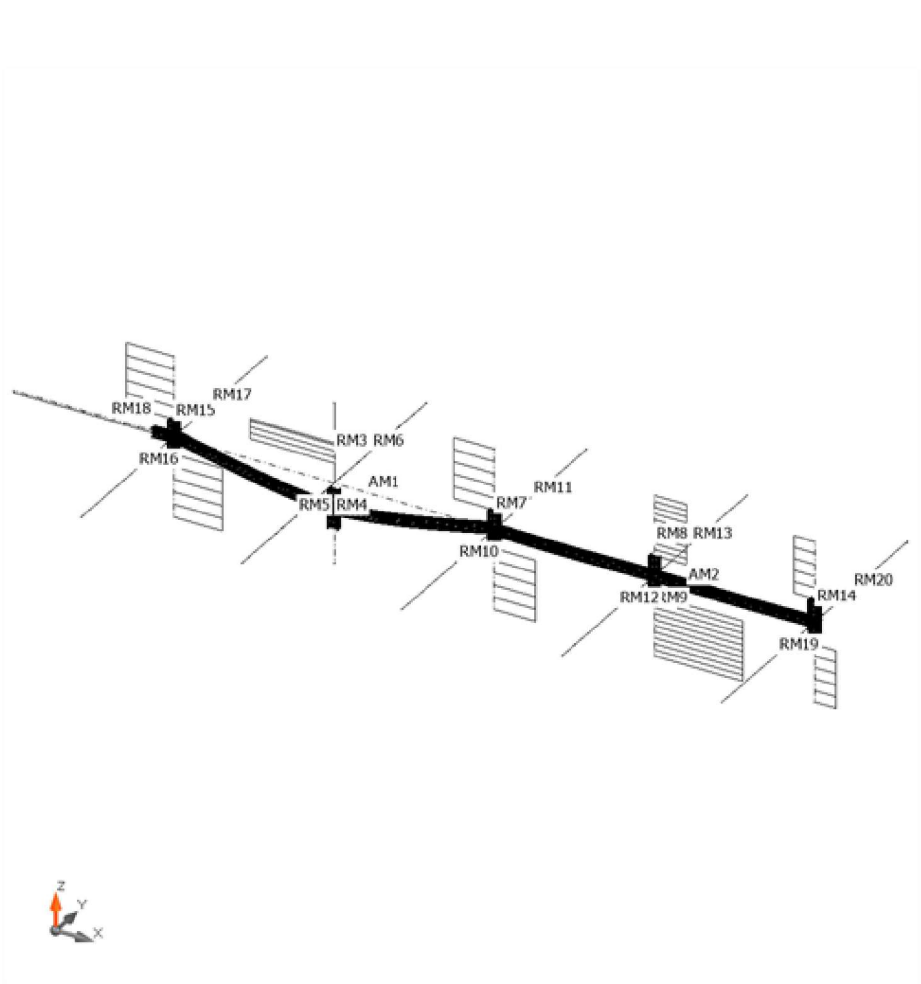


*Plastic strain ,LC1*

## Design data

| Material | $f_y$ [MPa] | $\varepsilon_{lim}$ [%] |
|---|---|---|
| S 355 | 355,0 | 15,0 |

## Symbol explanation

| Symbol | Explanation |
|---|---|
| $f_y$ | Yield strength |
| $\varepsilon_{lim}$ | Limit of plastic strain used in 2D plate element check |

## F.5. Gerber span

This section displays the output of the IDeaStatica calculations for the Gerber-span scenario.